Synthesis and analysis of conformationally restricted ceramide analogs

(Synthese und Untersuchung konformativ fixierter Ceramidanaloga)

Dissertation

zur

Erlangung des Doktorgrades (Dr. rer. nat.)

der

Mathematisch-Naturwissenschaftlichen Fakultät

der

Rheinischen Friedrich-Wilhelms-Universität Bonn

vorgelegt

von

Jennifer Wirtz

aus Mönchengladbach

Bonn 2008

Die vorliegende Arbeit wurde in der Zeit vom Mai 2004 bis März 2008 unter der Leitung von Herrn Priv. Doz. Dr. Thomas Kolter am Life and Medical Sciences Center (LIMES), Program Unit Membrane Biology and Lipid Biochemistry, der Rheinischen Friedrich-Wilhelms-Universität Bonn angefertigt.

Angefertigt mit Genehmigung der Mathematisch-Naturwissenschaftlichen Fakultät der Rheinischen Friedrich-Wilhelms-Universität Bonn

1. Referent: Priv. Doz. Dr. Thomas Kolter
2. Referent: Prof. Dr. Konrad Sandhoff

Tag der Promotion: 04.07.2008

Hiermit versichere ich, dass ich diese Arbeit selbstständig und ohne jede unerlaubte Hilfe angefertigt habe, dass diese oder eine ähnliche Arbeit noch keiner anderen Stelle zur Prüfung vorgelegen hat.

---	---
Ort, Datum	Jennifer Wirtz

Wissenschaftliche Beiträge

Publikationen

M. Wendeler, J. Wirtz, and T. Kolter
Sphingolipids as emerging drug targets
Drug Design Reviews – Online **2005**, 2, 53-65

A. Dommisse, J. Wirtz, K. Koch, W. Barthlott, and T. Kolter
Synthesis of (S)-Nonacosan-10-ol, the Major Component of Tubular Plant Wax Crystals
Eur. J. Org. Chem. **2007**, 3508-3511

J. Wirtz and T. Kolter
Novel tools for the proteomic identification of acylated proteins
ChemBioChem **2007**, 24, 1631-1635

Posterbeiträge

J. Wirtz, P. Sawatzki, M. Wendeler, and T. Kolter
Synthesis and properties of heterocyclic ceramide mimics
ORCHEM **2004**, Bad Nauheim

J. Wirtz, P. Sawatzki, and T. Kolter
Synthesis of conformationally rigid ceramide analogs and their effect on glycolipid metabolism
Glyco XVIII, **2005**, Florenz

J. Wirtz and T. Kolter
Synthetic ceramide analogs as modulators of glycosphingolipid biosynthesis
EUROCARB 14, **2007**, Lübeck

Dank

Herrn Priv. Doz. Dr. Thomas Kolter danke ich für die Ermöglichung dieser Arbeit, sowie für die außergewöhnlich gute und intensive Betreuung.

Herrn Prof. Dr. Konrad Sandhoff möchte ich ganz herzlich für seine Anregungen sowie für die Finanzierung dieser Arbeit danken.

Herrn Prof. Dr. Heinrich Wamhoff und Herrn Priv. Doz. Dr. Hans-Hubert Kirch danke ich für ihre Bereitschaft, zusammen mit Herrn Priv. Doz. Dr. Kolter und Herrn Prof. Dr. Sandhoff die Aufgaben der Promotionskommission zu übernehmen.

Besonders Christine Oeste und Martina Domgörgen danke ich für ihr freundliches und hilfsbereites Wesen, das über die Oberflächlichkeit des Laboralltags hinausreicht. Sie haben durch ihre Assistenz bei der Synthese und der Lipidanalytik einen großen Teil zu dieser Arbeit beigetragen.

Bei Andrea Raths möchte ich mich für ihre liebevolle Betreuung in der Zellkultur bedanken.

Bei Heike Hupfer möchte ich mich für die Aufnahme der ESI-Massenspektren und bei Dr. Katu Bernardo für die massenspektrometrische Analyse der Lipidextrakte bedanken.

In besonderem Maße zur guten Atmosphäre haben durch ihre unverwechselbare Art Dr. Alina Tenea und Bettina Kircharz beigetragen. Für ihre stets gutgelaunte Hilfbereitschaft möchte ich mich bei ihnen bedanken.

Herrn Dr. Peter Sawatzki und Dr. Hany Farwanah danke ich für die effektive Zusammenarbeit.

Herrn Dr. Günther Schwarzmann möchte ich für die Bereitstellung des C_6-NBD-ceramide/BSA Komplexes danken.

Ich danke ausserdem Dr. Ute Schepers, Nicole Brunnett, Albina Cryns und Martina Schmidt für die Hilfestellungen bei den molekularbiologischen Experimenten.

Herrn Dr. Hichem Gallala und Manuela Fandel möchte ich für die Korrekturen danken.

Susi, Janna, Tobi, Rainer, Katja und Vanessa danke ich für die lustige Zeit in Bonn während meines Studiums.

Papa und Marita, Thomas und Claudia, Patrick, meinen Großeltern und ganz besonders Giorgio danke ich für die Unterstützung, ihre Kraft und ihre Liebe, die mich durch meine Promotion begleitet haben.

Allen Kollegen und Institutsangehörigen der chemischen Institute der Universität Bonn sowie den Praktikanten, die direkt oder indirekt zum Gelingen dieser Arbeit beigetragen haben und nicht namentlich erwähnt wurden, sei mein Dank ausgesprochen.

Für den Jonathan

Content **page**

1. Summary 1

2. Introduction 4
2.1. Sphingolipids 4
2.1.1. Structure, metabolism and function 4
2.2. Glycosphingolipids 8
2.2.1. Function 8
2.2.2. Biosynthesis of glycosphingolipids 9
2.2.3. Catabolism and sphingolipid storage diseases 11
2.3. Conformational restriction of ceramide 14

3. Aim and Concept of the present study 17

4. Results 18
4.1. Strategy for the synthesis of ceramide analogs 18
4.2. Substituted cyclic carbamates as ceramide analogs 19
4.2.1. Synthesis 19
4.2.2. Analysis of the oxazolidinone **5b** in primary cultured neurons 21
4.2.3. Analysis of the oxazolidinone **5b** in cultured fibroblasts 23
4.3. Determination of GalNAc-transferase activity in the presence of oxazolidinone **5b** *in vitro* 26
4.4. Analysis of metabolites derived from carbamates **5a** and **5b** 27
4.4.1. Analysis of metabolites of oxazinanone **5a** by thin layer chromatography (TLC) 28
4.4.2. Analysis of metabolites of oxazolidinone **5b** by mass spectrometry 29
4.4.3. Attemps for the radiolabeling of **5a** and **5b** 33
4.4.4. ω-azido-group as chemical reporter for the determination of metabolites 35
4.5. Influence of oxazolidinone **5b** on intracellular membrane flow 38
4.6. Requirement of the iodine-atom in **5a** for the mechanism of action 40
4.6.1. Synthesis 40
4.6.2. Effect of oxazinanones on glycolipid biosynthesis 42
4.7. Synthesis and investigation of structurally modified carbamates 44
4.7.1. Synthesis of an 1'C Methyl oxazinanone **23a** 44
4.7.2. Effect of 1'C Methyl oxazinanone **23a** on sphingolipid biosynthesis 45
4.8. Analysis of a Benzazepinone as conformational restricted ceramide analog 47
4.8.1. Synthesis of *N*-Phenylacetalceramide **25** 47
4.8.2. Investigation of ceramide derivatives **24** and **25** in cultured granule cells 48
4.9. Investigation of the influence of **5b** and **24** on PKC activity 50
4.10. Synthesis of internal standards for glycolipid quantification by mass spectrometry 52

4.11.1. Synthesis of C_6-GM3 **30** 52
4.11.2. Synthesis of C_{17}-sulfatide **34** 54

5. Discussion 56
5.1. General Remarks 56
5.2. Halogen containing oxazinanones as conformnationally restricted ceramide derivatives 56
5.2.1. Synthesis 56
5.2.2. Investigation of ceramide derivatives in cultured cells 58
5.2.3. Investigation of oxazolidinone **5b** *in vitro* 59
5.2.4. Analysis for putative metabolites of **5b** 60
5.2.5. Relevance of iodine of **5b** for its activity towards inhibition of GSL biosynthesis 62
5.2.6. Effect of oxazolidinone **5b** on Golgi morphology 63
5.3. A Benzazepinone as conformationally restricted ceramide derivative 68

6. Material and Methods 69
6.1. Material 69
6.1.1. Analytical Techniques and Instruments 69
6.1.2. Consumables and Chemicals 70
6.1.3. Radiolabeled Chemicals 71
6.2. Biological materials 71
6.2.1. Cells and Additives 71
6.3. Methods 72
6.3.1. General conditions for the synthesis 72
6.3.2. Chromatographic methods 72
6.4. Instrumental Analytic 72
6.5. Biological experiments 73
6.5.1. Cell culture 73
6.5.2. Metabolic studies with cultured fibroblasts and cerebellar granule cells 74
6.5.3. Protein determination 74
6.5.4. Extraction 74
6.5.5. Anion-exchange chromatography 75
6.5.6. Alkaline hydrolysis 75
6.5.7. Reversed-Phase Chromatography (RP18) 75
6.5.8. Thin layer chromatography 76
6.5.9. Preparation of lipidextract for quantification by mass spectrometry 76
6.5.10. Expression and membrane preparation of GM2 synthase 76
6.5.11. Glycosyltransferase Assay 77
6.5.12. Fluorescence microscopy studies 77
6.5.13. PKC activity assay 78
6.5.14. Agarose Gel 78

6.5.15. Quantification by Spectrophotometry 78

7. Synthetic section 79
7.1. Synthesis of Garner aldehydes **2a** and **2b** 79
7.2. Synthesis of iodine-containing oxazinones **5a**, **5b** and **8a** 81
7.3. Synthesis of bromine-containing oxazinones **7a** and **7b** 85
7.4. Synthesis of alkyne oxazinones **10.2a-c** and **11** 86
7.5. Synthesis of ω-azido-oxazinanone **12** 92
7.7. Synthesis of 1'C methyl-oxazinones **23.2a** and **23.2b** 97
7.8. Synthesis of oxazinanones **18a** and **18b** 101
7.9. Synthesis of *N*-phenylacetylsphingosine **25** 105
7.10. Synthesis of lipid standards **30** and **34** 107

8. References 111

9. Abbreviations 126

10. Nomenclature of glycosphingolipids 128

1. Summary

Ceramide (e.g. (2*S*,3*R*,4*E*)-2-Octadecanoylamino-octadec-4-en-1,3-diol) is a structural component of membrane glycosphingolipids and sphingomyelin, and occurs in free form as well as bound to proteins in the human skin (Kolter and Sandhoff, 1999). Certain conformationally rigid analogs of this lipid, such as **5b** and **24** (figure 1.1), showed an unexpected interference with the biosynthesis of complex glycosphingolipids such as that of ganglioside GM2 (GalNAcβ1,4-(NeuAcα2,3)Galβ1,4Glcβ1Cer; Figure 1.2).

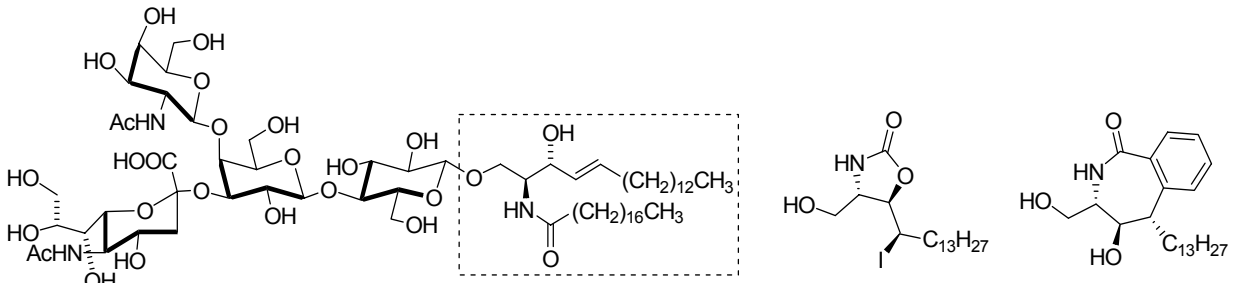

Figure 1.1: Structures of ganglioside GM2 and selected synthetic ceramide analogs that have been prepared and investigated during this work.

To get insight into the molecular mechanism of this apparent inhibition, a series of experiments have been carried out in this work:

1) New structural analogs of the halogenated oxazinanone (**5a**) and oxazolidinone (**5b**) have been prepared, and analysed in cultured cells.

1a) The preparative route that gave access to these compounds (Fig. 4.2) was used for the preparation of the brominated compounds **7.2a** and **7.2b** (Fig. 4.4). At least in cultured fibroblasts, the biosynthetic incorporation of 3-[^{14}C]L-serine into cellular glycosphingolipids in the presence of **5b** and **7.2b** were similar.

1b) To further address the role of the halogen atom, oxazinanones bearing a hydroxyl group instead of a halogen (**18a,b**) were prepared from phytosphingosine (Fig. 4.18). As has been shown before, these substances were not accessible on the route used otherwise (Fig. 4.2) due to a competing rearrangement reaction (Fig. 5.2). **18a** and **18b** showed entirely different lipid labelling patterns, when glycosphingolipid biosynthesis is analysed in cultured neurons. These data indicate a vital role of the halogen atom for the observed effects.

1c) Other structural analogs of **5a** and **5b** were prepared and analyzed: Title compounds bearing an additional methyl group in the head group were prepared from L-threonine (**23.2a,b**; Fig. 4.20). **23.2a** behaved similar to **5a** when analysed in cultured fibroblasts, indicating that the substituent does not hinder the molecular interaction leading to the observed effects.

2) An appropriate way to investigate metabolism of **5a** or **5b**, was well as to address the question, if these substances are covalently bound to certain cellular proteins, is the incorporation of a suitable radioisotope into these substances. In model experiments, conditions for two reactions (Fig. 4.11) were found, under which incorporation of a tritium atom into newly synthesized suitable precursor substances should be possible, at least in low yields.

3) Oxazinanone **12** (Fig. 4.13) with an azide group within the alkyl chain was prepared. This substance should allow the identification of potential metabolites via Staudinger ligation, together with the identification of putative protein targets after affinity purification.
4) Initially, **5a** and **5b**, as well as potential glycosidated metabolites, have been investigated on their effect of ganglioside GM2 synthase, a membrane bound *N*-acetylgalactosaminyltransferase of the Golgi-apparatus. Baculovirus-infected insect cells overexpressing this enzyme were used as enzyme-source to investigate **5b** in a liposomal assay system, since alteration of membrane properties caused by the compound has to be excluded as reason for the observed effects. Due to the instability of the enzyme in the proteoliposome preparation, no conditions could be found to analyse this possibility. Also a micellar GalNAc transferase assay in the presence of lipid extracts derived from fibroblast cells incubated with **5b** showed no inhibition (Chapter 4.3).
5) Metabolites of **5b** were searched for by thin layer chromatography (Chapter 4.4.1) and mass spectrometry. For this purpose, fragmentation pattern of **5a**, **5b**, and a glucosylated potential metabolite were recorded and used for parent ion- and neutral loss-scans in the lipid extract of cultured fibroblasts (Chapter 4.4.2). No metabolites could be found by this method. For glycolipid quantification and analysis of molecular species distribution in the lipid extract of cells by electrospray (ESI) and atmospheric pressure chemical ionisation (APCI) mass spectrometry, a ganglioside GM3 and a sulfatide derivative were prepared as glycolipid standards with appropriate alkyl chain lengths for further investigation (Chapter 4.10).
6) It could be demonstrated by fluorescence microscopy, that the Golgi apparatus is fragmented in response to **5b** in cultured human fibroblasts. Although it cannot be distinguished at the moment, if this is cause or effect of altered sphingolipid metabolism induced by **5b**, this observation points to a protein target of **5a** and **5b** that is required for vesicular transport through the Golgi apparatus.
7) To investigate the role of the benzene substituent in another conformationally rigid ceramid analogue, the benzazepinone **24** (Fig. 1), phenylacetylsphingosine was prepared as an open-chain analog (Chapter 4.8.1) and analyzed in cultured murine granule cells and human fibroblasts. Since the ganglioside patterns in the presence of both compounds are similar, glycosyltransferase inhibition by this substance is not caused by conformational restriction, but by the presence of the benzene moiety. Analysis of the substances in fibroblasts indicated a higher toxicity of the open chain compound, which is in agreement with the current view on cytotoxicity of cell-permeable ceramide analogs.
8.) In chapter 4.9, a direct influence of **5b** and **24** on protein kinase C as another potential mediator of the indirect effect on glycosphingolipid metabolism has been ruled out experimentally.

Although the molecular target of **5a,b** could not been identified, novel tools to address this question have been prepared in this work, several possibilities have been ruled out, and the integrity of the Golgi apparatus has been shown to be affected by these substances.

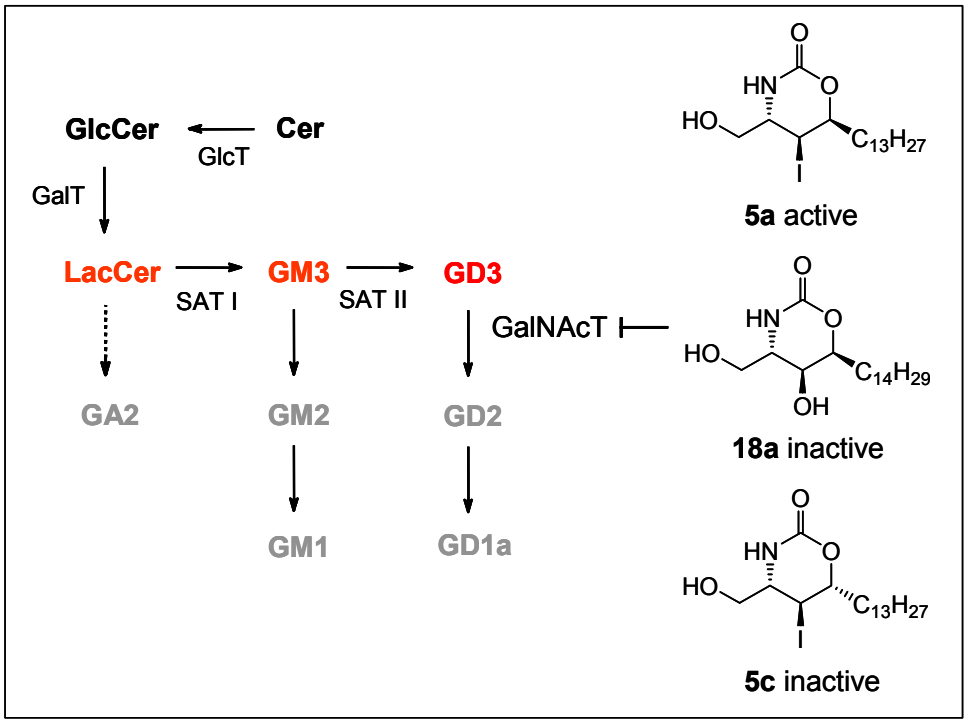

Figure 1.2: Early steps in combinatorial ganglioside biosynthesis (Kolter et al., 2002) together with selected ceramide analogs (Sawatzki, 2003a). Glycolipids accumulating in cultured cells treated with **5a** (10 µM in the medium) are marked in red. For abbreviations, compare chapter 9 and 10.

2. Introduction

2.1. Sphingolipids

2.1.1. Structure, metabolism, and function

Sphingolipids, including ceramide, sphingomyelin, and glycosphingolipids, are components of the outer leaflet of eukaryotic plasma membranes (Kolter and Sandhoff, 1999). Ceramide (Figure 2.1) consists of a long chain 2-amino-1,3-diol, which is *N*-acylated with a fatty acid. Most of the long chain bases contain an *E*-configured $\Delta^{4,5}$-double bond. Especially in the human epidermis, the sphingoid base can also be saturated, 4-hydroxylated, and/or modified in other ways (Holleran et al., 2006). In mammalian tissues, the most common sphingoid base is D-*erythro*-C18-sphingosine. In vertebrates, the *N*-acyl group normally consists of 16-24 carbon atoms, wereas much longer acyl chains up to 36 carbon atoms are present in ceramides of the human skin to form the epidermal water barrier (Coderch et al., 2003; Holleran et al., 2006).

The *de novo* biosynthesis of ceramide is catalyzed by membrane-bound enzymes that are localized on the cytosolic leaflet of the endoplasmic reticulum (ER) (Mandon et al., 1992). The first step is the condensation of the amino acid L-serine with Palmitoyl-CoA to 3-Ketosphinganine, catalyzed by the pyridoxal phosphate-dependent enzyme serine palmitoyltransferase (Braun and Snell, 1968; Stoffel et al., 1968; Hanada, 2003). Subsequent steps are the reduction to D-*erythro*-sphinganine catalyzed by 3-Ketosphinganine reductase in the presence of NADPH, followed by acylation to dehydroceramide. The acylation is catalyzed by enzymes encoded by different genes (longevity assurance genes). They control by which fatty acids the spingoid bases are *N*-acylated to generate different dihydroceramide species (Pewzner-Jung et al., 2006). Insertion of the 4,5-trans-double bond of ceramide is introduced by a dihydroceramide desaturase (Rother et al., 1992). From the ER, ceramide is transferred to the Golgi apparatus or the trans-Golgi network (TGN) with the aid of a transfer protein, CERT (Hanada, 2006).
At the cytosolic leaflet of the Golgi apparatus, ceramide can be transformed to glucosylceramide (GlcCer), while galactosylceramide (GalCer) is formed on the lumenal site of the Golgi and the phospholipid sphingomyelin (SM) is formed in the TGN and the plasma membrane (Huitema et al., 2004). The glucosyltransferase and galactosyltransferase transfer a hexose residue from the nucleotide-activated sugar (UDP-Glc, UDP-Gal) to the 1-OH-group of ceramide. These glycolipids are precursors of a number of complex glycolipids (chapter 2.2.2). The lipid-binding protein FAPP2 (four-phosphate adaptor protein) is reported to be required for the non-vesicular transport of glucosylceramide to the distal Golgi compartments (D'Angelo et al., 2007), and plays are role for the biosynthesis of glycosphingolipids (Halter et al., 2007). Sphingomyelin is synthesized by the transfer of phosphorylcholine from phosphatidylcholine to ceramide liberating diacylglycerol through the action of the sphingomyelin synthase (review: Tafesse et al., 2006). Another metabolite of ceramide, ceramide-1-phosphate (C1P), is formed by phosphorylation catalyzed by the ceramide kinase (Bajjalieh and Batchelor, 2000).

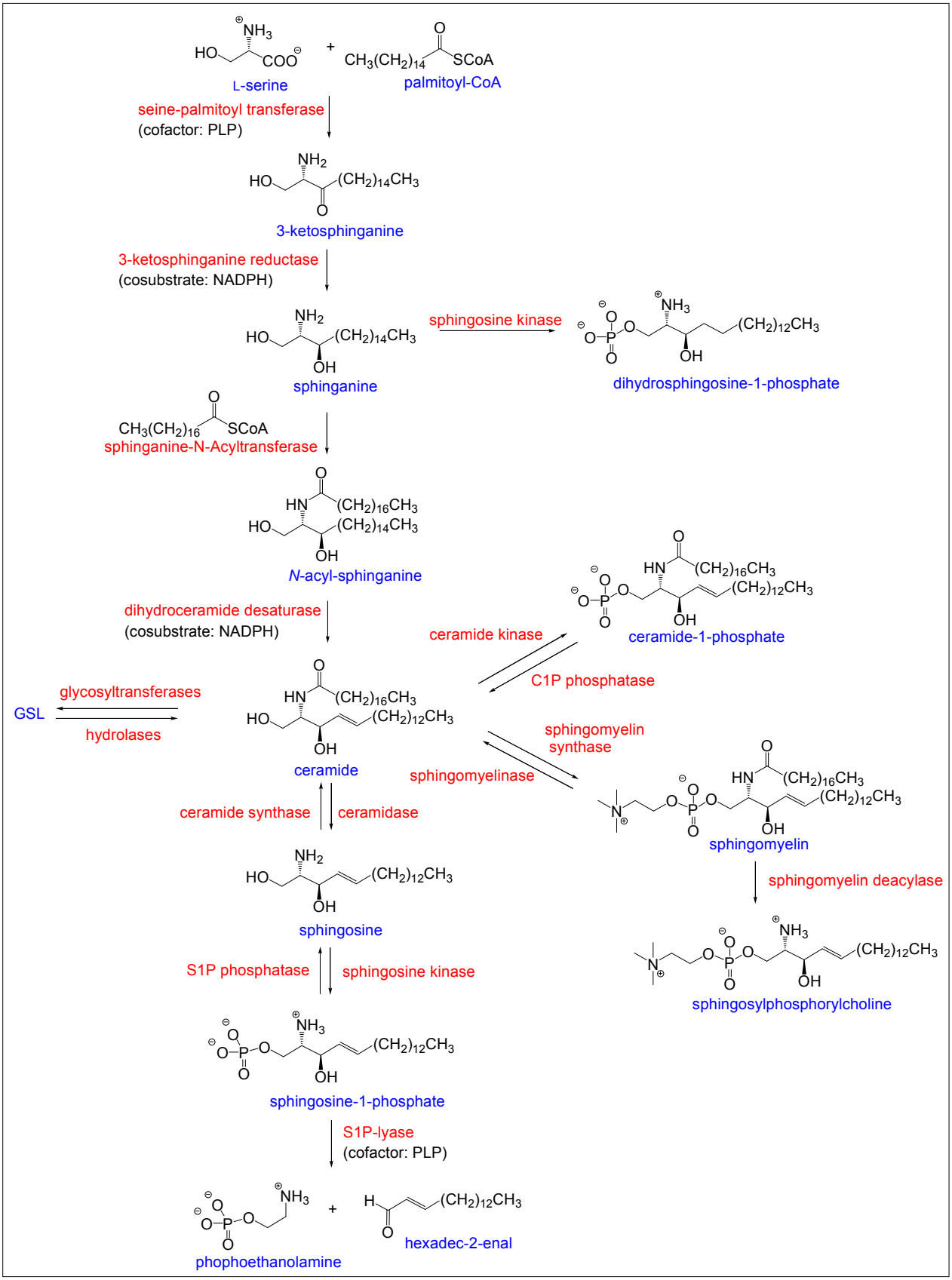

Figure 2.1: Sphingolipid metabolism. Abbreviations: GSLs = glycosphingolipids, PLP = pyridoxalphosphate, NADPH = nicotine adenine dinucleotide phosphate, C1P = ceramide-1-phosphate, S1P = sphingosine-1-phosphate.

The major pathway for the catabolism of ceramide is its deacylation by ceramidases to sphingosine, which in turn can be phosphorylated at the 1-position to sphingosine-1-phosphate (S1P). S1P can be cleaved by a pyridoxal phosphate dependent lyase to phosphoethanolamine and hexadec-2-enal, or it can be transformed to sphingosine by the action of phosphatases. Another sphingolipid is sphingosylphosphorylcholine (SPC, lysosphingomyelin), which can be formed by deacylation of sphingomyelin by a sphingomyelin deacylase. SPC occurs naturally in plasma and is a consituent of lipoproteins. Several studies indicated that SPC can act as a mitogen in several different cell types and in certain circumstances may also be a pro-inflammatory mediator (Review: Nixon et al., 2008), but there are no exact information of the mechanisms involved available. In addition, SPC is discussed to be potentially involved in neurotoxicity in Niemann-Pick type A (NP-A) disease (Chiulli et al., 2007). This lysosomal storage disease is characterized by the genetically determined absence of acidic sphingomyelinase activity and accumulation of sphingomyelin and also SPC in various tissues, including the brain.
In the salvage pathway, ceramide can be generated by acylation of sphingosine by the ceramide synthase. In addition, sphingomyelin and glycosphingolipids can be degraded to ceramide through the action of sphingomyelinases (Goni and Alonso, 2002) and glycosidases, specially in the lysosomes.

Sphingolipids are structural components of the plasma membrane of eukaryotic cells. In this context, it is suggested that GSLs and sphingomyelin together with cholesterol and GPI-anchored proteins form organized microdomains on the plasma membrane (Simons ans Ikonen, 1997). These so-called “rafts” are believed to take part in processes such as protein sorting, cell adhesion, signal transduction or cell resistance towards viral infection (Hanzal-Bayer and Hancock, 2007; van Meer and Sprong 2004, Sangiorgio et al, 2004). However, the raft-concept is an extrapolation of *in vitro*-results (Brown and London, 2000), and most of the biological studies of the domain organization of membranes are carried out using detergents (e. g. Triton, CHAPS) to extract detergent resistance membranes (DRMs), or with the aid of antibodies. There is no evidence that the composition of DRMs correlates with that of native lipid rafts in cell membranes (Heerklotz et al., 2003). Until now, the existence of these rafts has not been demonstrated experimentally and is still controversially discussed (Munro, 2003; Shaw 2006).
In addition to their structural roles, sphingolipids attracted attention as bioactive mediators in a variety of biological processes, including the regulation of apoptosis (Ruvolo, 2003), cellular transformation, differentiation and proliferation, as well as other cell signaling processes (Figure 2.2; Liu et al., 1999; Fernandis and Wenk, 2007; Hannun and Obeid, 2008). In response to diverse extracellular stimuli, including tumor necrosis factor α, platelet-activating factor, and stress factors such as heat and UV radiation, ceramide is formed by the hydrolysis of sphingomyelin by sphingomyelinases or by enhanced biosynthesis. In most cell types, ceramide and its deacylated form (sphingosine) are mediators of cell-cycle arrest, cell differentiation, and apoptosis. The saturated form (dihydroceramide) is apparently not proapoptotic, indicating a functional role of the C4-C5 double bond for the induction of apoptosis (Bielawska et al., 1993). It has been suggested that ceramide mediates this action through binding and regulation of intracellular effectors such as protein kinases PKCα and PKCζ (Mathias et al., 1991; Wang et al., 2005), serine/threonine protein phosphatase-1 and –2A (Chalfant et al., 2004), and the cysteine protease cathepsin D (Heinrich et al., 2000). In addition, alteration of membrane properties (Goni and Alonso, 2006) have to be considered. Also the formation of ceramide-pores in mitochondria have been proposed to occur in apoptosis (Siskind et al., 2006) Recent studies support the notion that changes within ceramide

metabolism are critically involved in human diseases, such as neurological disorders, Wilson`s disease, lung injury, cancer, allergies, and infections (Schenk et al., 2007). The deacylated form of ceramide, sphingosine, is generated by the action of ceramidases and mediates cell cycle-arrest and apoptosis (Suzuki et al., 2004). Unlike ceramide and sphingosine, S1P is a mediator of cell growth and survival in most cell types (Milstien et al., 2007). S1P acts as ligand of extracellular receptors of the EDG family, now termed S1P receptors (Spiegel and Milstien, 2003). Furthermore, S1P acts as an intracellular second messenger to control calcium mobilization, although its intracellular target is not known. In contrast to S1P, little is known about its corresponding saturated form, dihydrosphingosine-1-phosphate (dhS1P), which is formed from dihydrosphingosine by the action of sphingosine kinase. Ceramide-1-phosphate is generated by phosphorylation of ceramide catalyzed by ceramide kinase (Bajjalieh and Batchelor, 2000). C1P stimulates DNA synthesis and promotes cell division. Phytosphingosine (PHS) and phytoceramide (PHC) are abundant in fungi and plants, and are also found in eukaryotic cells. Compared to other sphingosine-derivatives, they possess a hydroxyl-group at C-4 in the sphingoid long-chain base instead of a trans double bond. It has been reported that PHS inhibits cell growth in a specific manner differing from that of other sphingolipids (Chung et al., 2001). In summary, the interconnected network of sphingolipid metabolism regulates the formation of diverse sphingolipids that function as critical determinants of membrane structure, as well as a source of bioactive molecules involved in various signalling mechanisms and cell regulatory pathways (Sims et al., 2007).

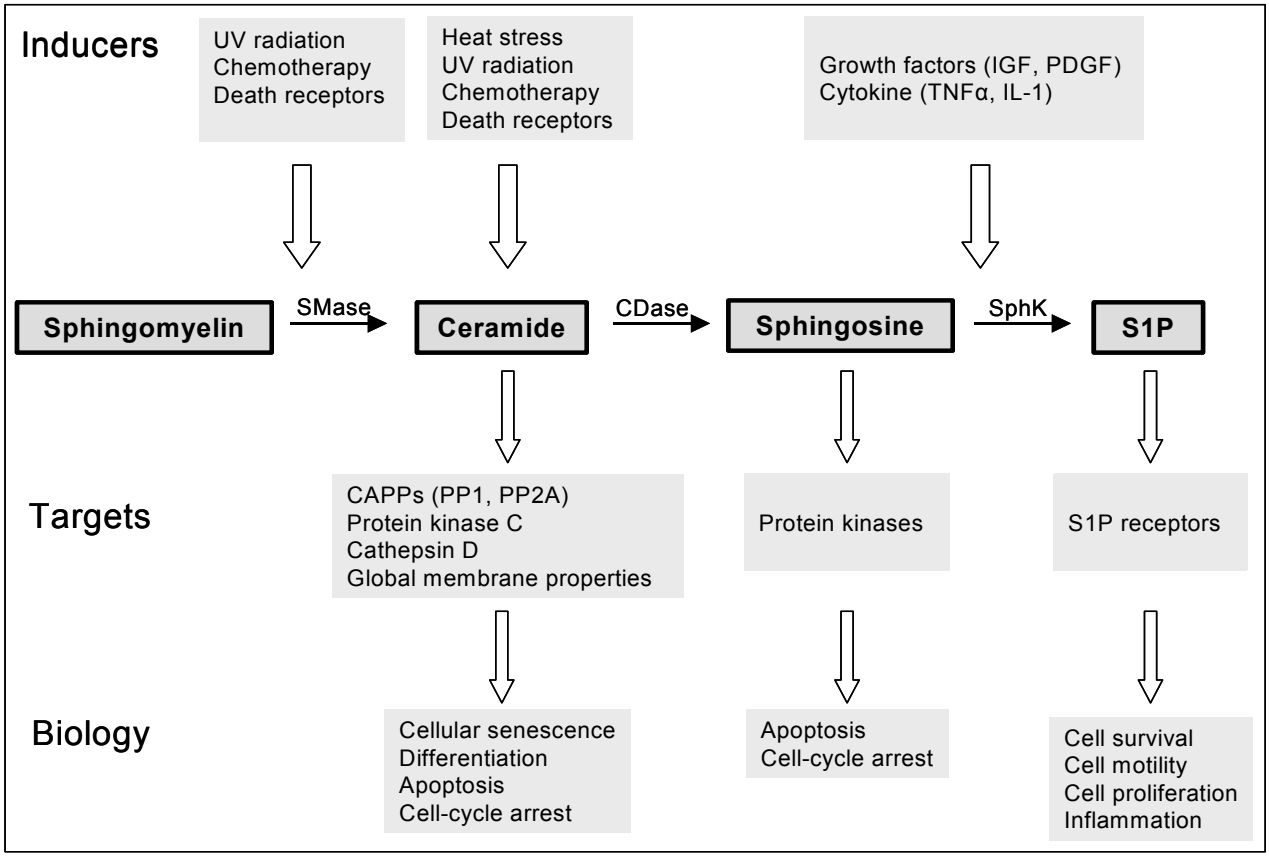

Figure 2.2: Potential participations of ceramide and its metabolites as putative coordinators in cell biological responses (modified from Hannun and Obeid, 2008). Abbreviations: CAPP = ceramide activated Ser-Thr phosphatase; CDase = ceramidase; IGF = insulin-like growth factor; IL-1 = interleukin-1; PDGF = platelet-derived growth factor; TNFα = tumor necrosis factor α; SMase = sphingomyelinase; S1P = sphingosine-1-phosphate; SphK = sphingosine kinase.

2.2. Glycosphingolipids

2.2.1. Function

Glycosphingolipids (GSLs) are components of eukaryotic cell membranes. They consist of ceramide and an oligosaccharide chain. The hydrophilic oligosaccharde moiety is exposed to the extracellular space, while their hydrophobic ceramide part is embedded in the outer leaflet of the plasma membrane (Kolter and Sandhoff, 1999; Sonnino et al., 2006). Variation in type, number, and linkage of carbohydrate residues, and additional modifications of the lipid moiety of glycosphingolipids, give rise to a large number of naturally occurring GSL structures. On cellular surfaces, GSLs form complex patterns, which are cell-type-specific and change during cell differentiation, or viral and oncogenic transformation. The function of these complex GSL patterns is not entirely clear, and only relatively few GSLs have been shown to control cellular functions (Review: Hakomori, 2005).

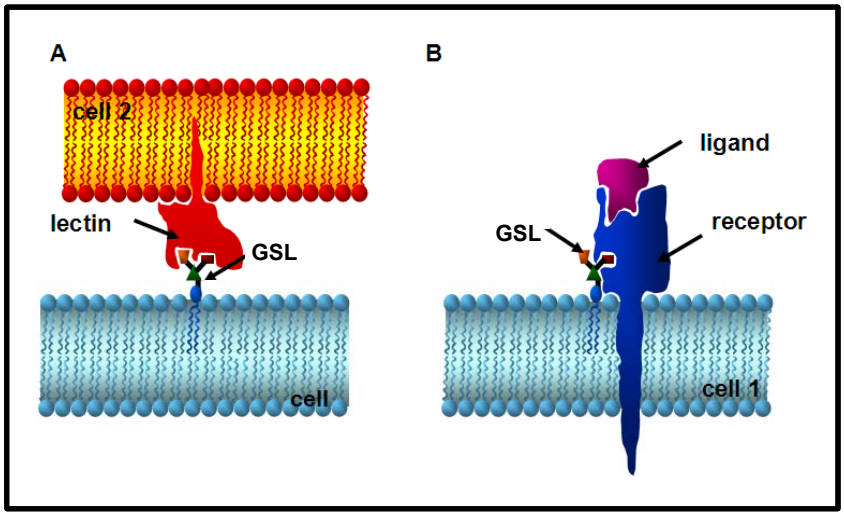

Figure 2.3: Interactions between GSLs and proteins. **A**: Glycolipid-mediated cell-cell recognition; **B**: regulation of receptor activity

They can interact with soluble or membrane-bound lectins outside the cell (Figure 2.3. A), and thus serve as binding sites for bacteria, viruses, and toxins (Heung et al., 2006; Hanada, 2005), and mediate cell adhesion processes (Schnaar, 2004). An example is the axon-myelin-interaction mediated by binding of complex gangliosides such as GD1a and GT1b to the myelin-associated glycoprotein (Pan et al., 2005). Furthermore, GSLs can regulate the function of proteins present in the same membrane (Fig. 2.2, B). This has been demonstrated for the downregulation of insulin receptor activity by ganglioside GM3 in genetically engineered mice, lacking GM3 synthase (Yamashita et al., 2003). These animals did not develop insulin-resistance when fed on a high-fat diet, suggesting that ganglioside GM3 is a potential therapeutic target in type 2 diabetes (Zhao et al., 2007).

There is also evidence that GSLs can influence the conformation of several proteins. Recent studies showed that various gangliosides have a high affinity to the pathological conformers of the Alzheimer amyloid peptide and the prion proteins (Ariga et al., 2001). Additionaly, Galactosylceramide and sphingomyelin were detected in highly purified preparations of prion rods, and the composition of these lipids correlates inversely with the infectiveness of the material (Klein et al., 1998).

2.2.2. Biosynthesis of glycosphingolipids

The synthesis of gangliosides and other GSLs starts with the formation of glucosylceramide (GlcCer) at the cytosolic leaflet of the Golgi apparatus which undergoes a transversal membrane translocation to the lumen of the Golgi apparatus (De Rosa *et al.* 2003), where membrane-resident glycosyltransferases transfer nucleotide activated sugars and sialic acids to the carbohydrate chain (Uliana et al., 2006). In has been shown that the transfer of GlcCer for the synthesis of GSLs requires the action of the lipid-binding protein FAPP2 (D'Angelo et al., 2007). A new model suggests that GlcCer, which is formed at the cytosolic leaflet of the Golgi apparatus is transported back to the ER via FAPP2, translocates across the ER membrane and enters the vesicular membrane flow to the Golgi (Halter et al., 2007).

The formation of complex ganglioside patterns on the cell surface is based on a combinatorial synthesis (see figure 2.3), which is now better understood through the analysis of animal models (Review: Kolter et al., 2002) and is coupled to the exocytotic vesicle flow through the Golgi apparatus to the plasma membrane. At least for GSLs of the ganglio series, it has been shown that in the early compartiments of the Golgi, glycosyltransferases control the generation of precursors (LacCer, gangliosides GM3, GD3, and GT3) of several series of gangliosides and are the branching point of ganglioside biosynthesis. Expression and activity of the glycosyltransferases influences the final pattern of glycolipids at the cell surface. The GM3 synthase (ST3Gal V; SAT I) and the GD3 synthase (ST8Sia I; SAT II) have a high specificity for the glycosyl acceptor, while the sialyltransferase IV (ST8Sia IV; SAT IV) and the sialyltransferase V (ST8Sia V, SAT V) use different substrates (Pohlentz et al., 1988). Pohlentz et al. and Iber et al. showed that the sequential glycosylation of the precursor GSLs to the complex 0, -a, -b, and –c ganglioside series is catalyzed by unspecific glycosyltransferases (Pohlentz et al., 1988; Iber et al., 1991). For example, the *N*-acetyl-galactosaminyl-transferase catalyzes not only the reaction from GM3 to GM2, but also from GD3 and GT3 to GD2 and GT2, and *in vitro* and in SAT-1-deficient mice also from LacCer to GA2. The heterogeneity in the expression pattern of ganglioside synthase genes during mouse development shows that the transcriptional regulation of transferases and translocators is the most important level of control of glycolipid biosynthesis (Yamamoto et al., 1996). The activity of glycolipid glycosyltransferases can also be regulated by post-translational modifications like phosphorylation. Bieberich and co-workers reported that ganglioside compositional changes accompanying differentiation may be specifically induced by activation and inhibition of, respectively, GalNAc-T and Sial-T2 by protein kinase A- and protein kinase C-related phosphorylation systems of these cells (Bieberich et al., 1998).

Specific transporters translocate the nucleotide sugars from the cytosol to the lumen of the Golgi-apparatus and can be rate-limiting e.g. in the supply of UDP-galactose into the Golgi lumen (Review: Csala et al., 2007; Brändli et al. 1988; Perez and Hirschberg 1985). Experiments with mutant polarized epithelial cells deficient in the UDP-Gal-transporter showed that the levels of the sugar nucleotide play a regulatory role in determining the composition of galactose-containing glycosphingolipids (Toma et al., 1996).

The activity of glycosyltransferases can also be affected by the pH value of their environment. Labeling studies in primary cultured murine cerebellar cells showed the influence of the pH value of the medium on the biosynthesis of glycolipids (Iber et al., 1990). After lowering the pH of the culture medium from 7.4 to 6.2, the pattern of gangliosides changed in a reversible manner from the a- to the b-series.

Other studies indicate a regulation of glycosphingolipid biosynthesis by feedback control either by their respective reaction product or by an end product of the respective glycosphingolipid series (Yusuf et al., 1987; Review: Kolter et al., 2002). Sphingosine, as degradation product of GSLs, downregulates the serine palmitoyltransferase which catalyses the first step of sphingolipid biosynthesis (Mandon et al., 1991). Furthermore, the formation of multi enzyme complexes from glycosyl- and sialyltransferases was demonstrated by coimmunoprecipitation (Bieberich et al., 2002; Giraudo et al, 2003), after it has been postulated by Roseman many years ago (Roseman, 1970). The enzyme complex of GalNAc-transferase and galactosyltransferase II may accept ganglioside GM3, and finally releases ganglioside GM1. This might explain why the brain contains large amounts of gangliosides GM1 and GD1a, but little amounts of ganglioside GM2 (Review: Kolter et al., 2002).

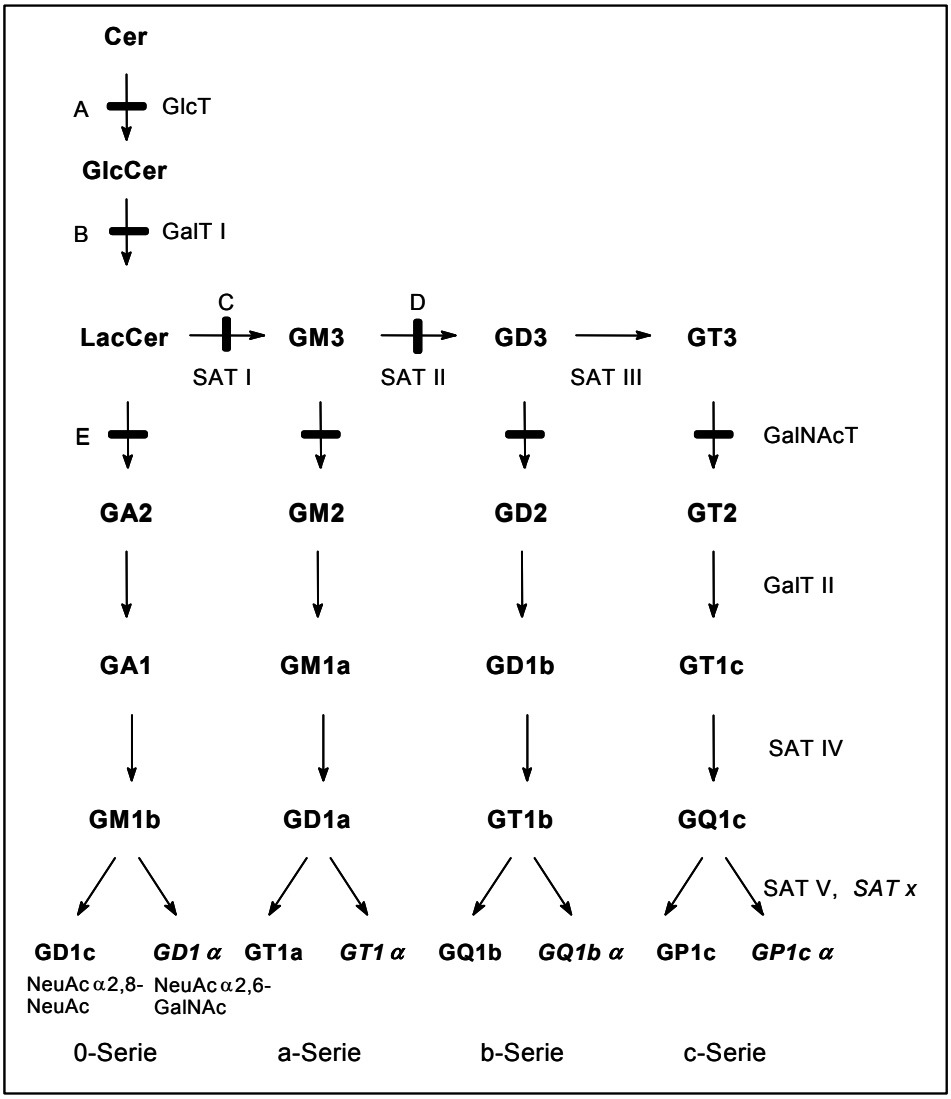

Figure 2.4: **Ganglioside biosynthesis** (Pohlentz, 1988; Kolter et al., 2002). Enzyme defects in knockout mice are indicated. A: ceramide glycosyltransferase -/-, B: galactosyltransferase -/-, C: sialyltransferase I -/-, D: sialyltransferase II -/-, E: GalNAc transferase -/-, 'GM3-only' mice have enzyme defects D+E.

To date, only a few human diseases are known to be associated with sphingolipid biosynthesis. A deficiency of a biosynthetic enzyme associated with a human disease is reported for lactosylceramide 2,3

sialyltransferase (GM3-synthase). Deficiency of this enzyme causes an autosomal recessive infantile-onset symptomatic epilepsy syndrome (Simpson et al., 2004). Another human disease is caused by alteration of a biosynthetic enzyme in the biosynthesis of ceramide. In hereditary sensory neuropathy, type 1, there is an increased activity of serine palmitoyltransferase, which results in increased de novo ceramide synthesis and triggers apoptosis of neural cells (Dawkins et al., 2001).

2.2.3. Catabolism and sphingolipid storage diseases

The constitutive degradation of sphingolipids and GSLs occurs in the acidic subcellular compartments, the endosomes and lysosomes, at the surface of intra-endosomal and intra-lysosomal membrane structures (Fuerst and Sandhoff, 1992; Kolter and Sandhoff, 1999). During endocytosis, parts of the plasma membrane are internalized and transported via the endosome to the lysosomal compartment. The inner leaflet of the lysosomes is covered with a thick glycocalix made of sugar chains (mostly lactosamine structures) of LIMPs (lysosomal intergral membrane proteins) and LAMPs (lysosomal associated membrane proteins) (Eskelinen et al., 2003). This glycocalix protects the membrane from enzymatic attack, but is also involved in the targeting of soluble lysosomal enzymes (Griffiths, 2007). Along the endocytic pathway, the luminal pH value of these organelles steadily decreases from 6.0 to 4.0 to reach optimal conditions for the action of lysosomal enzymes. The carbohydrate residues of GSLs are sequentially cleaved off by the action of watersoluble exohydrolases. Membrane-bound glycosphingolipids with less than four carbohydrate residues require the additional presence of activator proteins and negatively charged lysosomal lipids such as BMP for degradation (Wilkening et al., 1998; Fürst and Sandhoff, 1992). Sphingolipid activator proteins (SAPs) solubilize membranes and mediate the interaction between the membrane-bound substrate and the enzyme.

In humans, inherited defects of glycosphingolipid and sphingolipid catabolism give rise to lysosomal storage diseases, the sphingolipidoses. For almost all of the steps of the constitutive degradation of sphingolipids, an inherited disorder is known (Gieselmann, 1995; Futerman and van Meer, 2004; Kolter and Sandhoff, 2006). These storage disorders are generally caused by genetic defects of enzymes or activator proteins acting in the degradation pathway (Figure 2.4). To these belong GM1- and GM2 gangliosidoses, Niemann-Pick-disease, type a and b, Gaucher-, Farber-, and Krabbe disease, as well as metachromatic leucodystrophy. With the exception of Fabry disease, which exhibits an X- chromosomal mode of inheritance, the sphingolipidoses are inherited in an autosomal recessive mode.

The GM2 gangliosidoses are caused by the deficiency of one of the polypeptide chains required for degradation of ganglioside GM2. β-Hexosaminidase α-chain deficiency is known as Tay-Sachs disease, β-chain deficiency as Sandhoff disease, and deficiency of the GM2 activator protein as AB-variant of the GM2-gangliosidoses. The accumulation of nondegradable enzyme substrates damages cells and organs that synthesize the relevant lipid by only partially clarified mechanisms. Due to their cell-type specific expression, the dysfunction in the metabolism of gangliosides leads primarily to the degeneration of the CNS.

The correlation between lipid storage and cellular dysfunction is not fully understood (Silence and Platt, 2003). The accumulation of morphogenetically active compounds (Purpura and Suzuki, 1976) such as toxic lysoglycolipids (Neuenhofer et al., 1985; Suzuki, 1998) and cholesterol, which modulates the endocytotic

membrane flow (Puri et al., 1999) and induces Golgi vesiculation (Grimmer et al., 2005), are among the factors that are considered to be relevant for the pathogenesis.

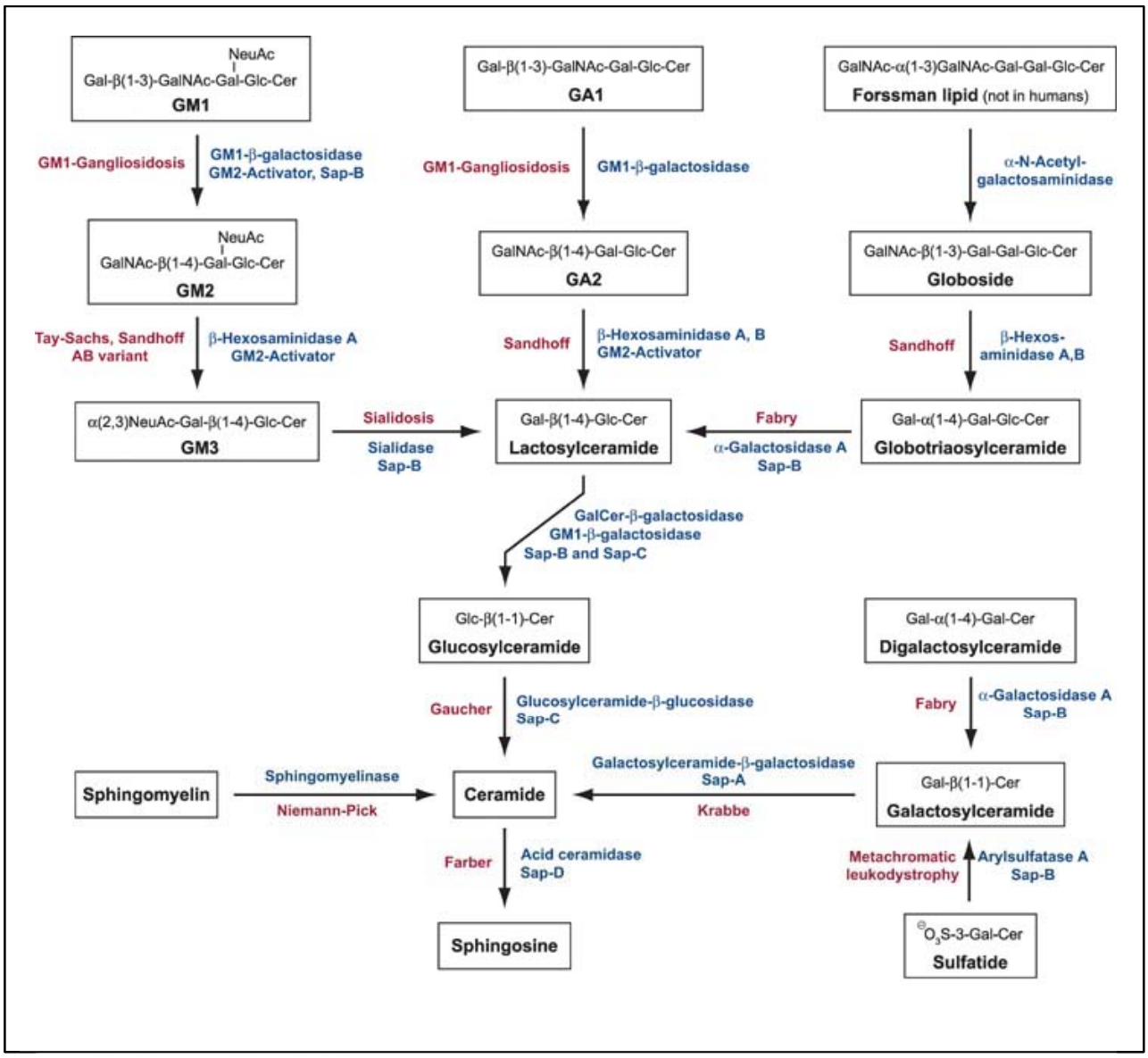

Figure 2.5: Pathways for lysosomal glycosphingolipid metabolism (Kolter and Sandhoff, 2005). Degradative enzymes and activator proteins and corresponding storage diseases are shown.

The aim of most causal therapies of sphingolipidoses is the restauration of the defective degradation capacity within the lysosome. A causal therapy for sphingolipidoses exists only for the adult forms of Gaucher and Fabry disease. In these cases, the degradation capacity can be enhanced by intravenous application of the recombinant intact enzyme (enzyme replacement therapy; Barranger and O'Rourke, 2001; Brady, 1997). A new concept is the so-called enzyme-enhancement therapy with the aid of "chemical chaperones" (Tropak and Mahuran, 2007; Fan and Ishii, 2007; Yu et al., 2007). This strategy aims to enhance the fraction of correctly folded, and thus active, enzyme by binding to an inhibitor. Radin (1996) suggested an additional strategy for the treatment of sphingolipidoses, the substrate reduction therapy. The treshold theory (Conzelmann and Sandhoff, 1983/84; Leinekugel et al., 1992) explains how the ratio of substrate influx into the lysosomes and degradation capacity determines the course of a sphingolipid

storage disease like the GM2-gangliosidoses or metachromatic leukodystrophy. The substrate reduction therapy consists in the reduction of substrate influx into the lysosomes. This can be achieved by inhibition of biosynthetic enzymes (Platt et al., 1997) or in genetic model animals (Liu et al., 1999). A necessary condition for this treatment is the existence of residual activity of the defective enzyme in the lysosome. Two classes of sphingolipid derivatives have been investigated as inhibitors of ceramide glucosyltransferase and used for substrate reduction therapy of sphingolipidoses: imino sugar derivatives such as *N*-Butyldeoxynojirimycin and compounds like D-threo-(1R,2R)-1-phenyl-2-decanoyl-amino-3-morpholino-1-propanol (Abe et al., 1992; Platt and Butters, 2000; Tifft and Proia, 2002).

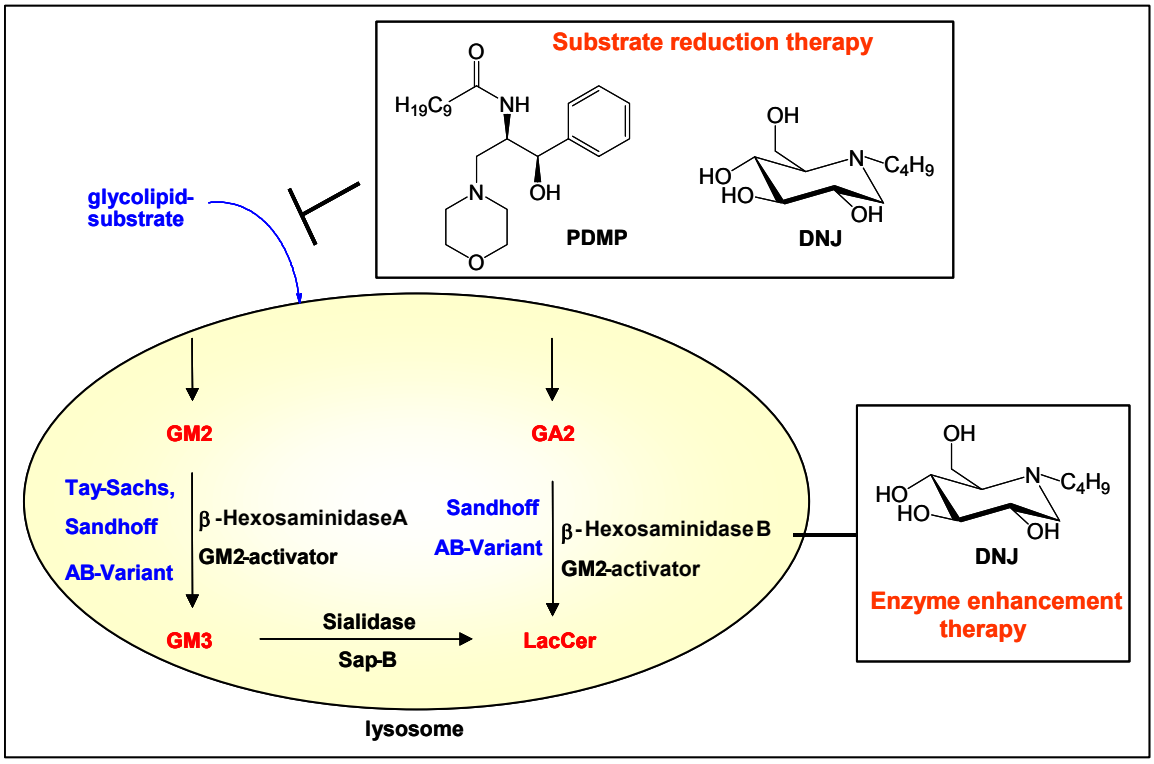

Figure 2.6: Pharmacologic strategies for the treatment of glycosphingolipid storage diseases. Abbreviations: DNJ = *N*-Butyldeoxynojirimycin; PDMP = D-threo-(1R,2R)-1-phenyl-2-decanoyl-amino-3-morpholino-1-propanol

2.3. Conformational restriction of ceramide

Conformationally flexible compounds can adopt a variety of conformations, which may make it possible for them to bind to different proteins, sometimes via different conformations (Figure 2.7), basing on the “lock and key rationale” proposed by Emil Fischer many years ago (Fischer, 1894). Restriction of conformational flexibility is a commonly used technique in the design of biologically active compounds and is a widely used approach in drug development (Review: Harrold, 1996; Mann, 2003).

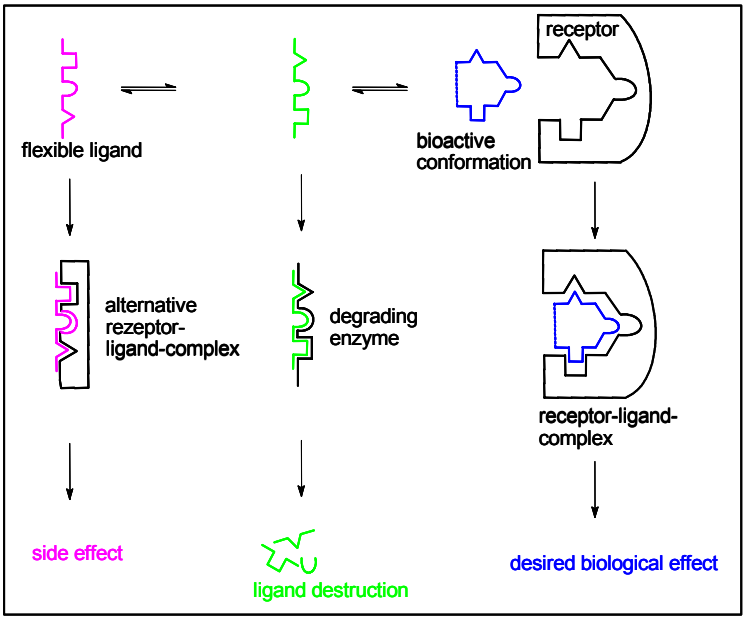

Figure 2.7: Conformational equilibrium of a flexible ligand (Kolter, 2004)

The conformational restriction strategy can lead to analogs with enhanced affinity (1), selectivity (2), and metabolic stability (3) compared to the parent compound (King, 1995).

(1) The energy required to change a drug molecule from its most energetically preferred conformation in solution to its receptor-bound active conformation enzyme can be obtained experimentally. The contribution of the different types of interactions to the change of free enthalpy on ligand binding are loss of translational and rotational entropy, formation of hydrogen bonds, ionic interactions, lipophilic contact, and arrest of rotatable bonds (Review: Kolter, 2004). The conformational restriction of a molecule reduces entropy loss on receptor binding and contributes in this way to receptor affinity. Many examples of this concept are represented in Medical Chemistry, e. g. the development of enzyme inhibitors of HMG-CoA reductase for the treatment of hypercholesterolemia (Pfefferkorn et al., 2007) or inhibitors of tubulin polymerization for the treatment of cancer (Mateo et al., 2007). Other examples from the lipid field are phorbol esters and bryostatin, which can be regarded as conformationally rigid natural analogs of 1,2-diacylglycerol (DAG). DAG binds to and activates protein kinase C (PKC), and thus initiates biological processes such as signal transduction, cell regulation and, tumor promotion (Ron et al., 1999). The binding affinity of phorbol esters to PKC are 3-4 orders of magnitude higher than those of DAGs and they have been used as lead compounds in the development of analogs of more simple structures (Kang et al., 2004).

(2) Also binding selectivity toward receptor subtypes can be enhanced when alternative receptors recognize alternative conformations, which are not accessible for the restricted system. For example, the selective binding of histamine derivatives to the H_3 receptor, which is one of four receptor subtypes for the neurotransmitter histamine (Watanabe et al., 2006). Antagonists of the H_3 receptor are considered to be potential drugs for diseases such as Alzheimer's disease, dementia, and epilepsy (Leurs, 1998).
(3) Also Drug metabolizing enzymes can recognize distinct conformations of their substrates, which can differ from those bound by other receptors. Therefore, conformational restriction can also be used to enhance the biological half life of a ligand and improve its pharmacokinetic properties. In this context, DAG is metabolized immediately through phosphorylation or hydrolysis, while phorbol esters persistently activate PKC because there is no natural mechanism to terminate their action.

With the exception of sterols, most membrane lipids including sphingolipids are conformationally flexible molecules. The question arises, whether the concept of conformational restriction can be extended to the field of sphingolipids (Review: Kolter, 2004). Ceramide and ceramide analogs exogenously applied to cultured cells can induce a variety of complex effects, including metabolic transformation and apoptotic responses, which complicates the analyses of their function. Ceramides with selectivity for one of the putative ceramide binding proteins or metabolizing enzymes are potential means to characterize the proteins involved and to influence their respective pathways. To date, only a few conformationally constrained sphingolipid analogs have been characterized (Figure 2.8).
The sphingosine analog Penazetidine A, bearing an azetidine ring as structural component, was isolated from *Penares sollase* (Shier and Shier, 2000). Penazetidine A inhibits proteinkinase C (PKC) with an IC_{50} of 1 µM and has been considered as an anticancer agent (Alvi et al., 1994). A synthetic pyrrolidine-derivative (Figure 2.8) can be regarded as a conformational restricted analog of 1-deoxy-5-hydroxysphinganine, which showed cytotoxic effects against HT-29 cells (human colon adenocarcinoma; Dougherty et al., 2006). Examples for conformationally restricted ceramide-derivatives are the synthetic Uracil- and Thiouracil-derivatives that showed moderate effects in terms of toxicity and anti-tumor activity *in vitro* and *in vivo* (Maccia et al., 2001). Isoquinoline-derivatives were investigated as ligands of protein phosphatase 2A, a ceramide binding protein involved in the transmission of the ceramide-mediated signal into the cell (Leoni et al., 1998). Oxazolidinone-derivatives were shown to exhibit cytotoxity in human cancer cell lines (Ha et al., 2006). The lactone-derivative can also be regarded as a conformationally rigid ceramide derivative. They have been reported as potent and selective inhibitors of neutral sphingomyelinase (Wascholowski and Giannis, 2006).

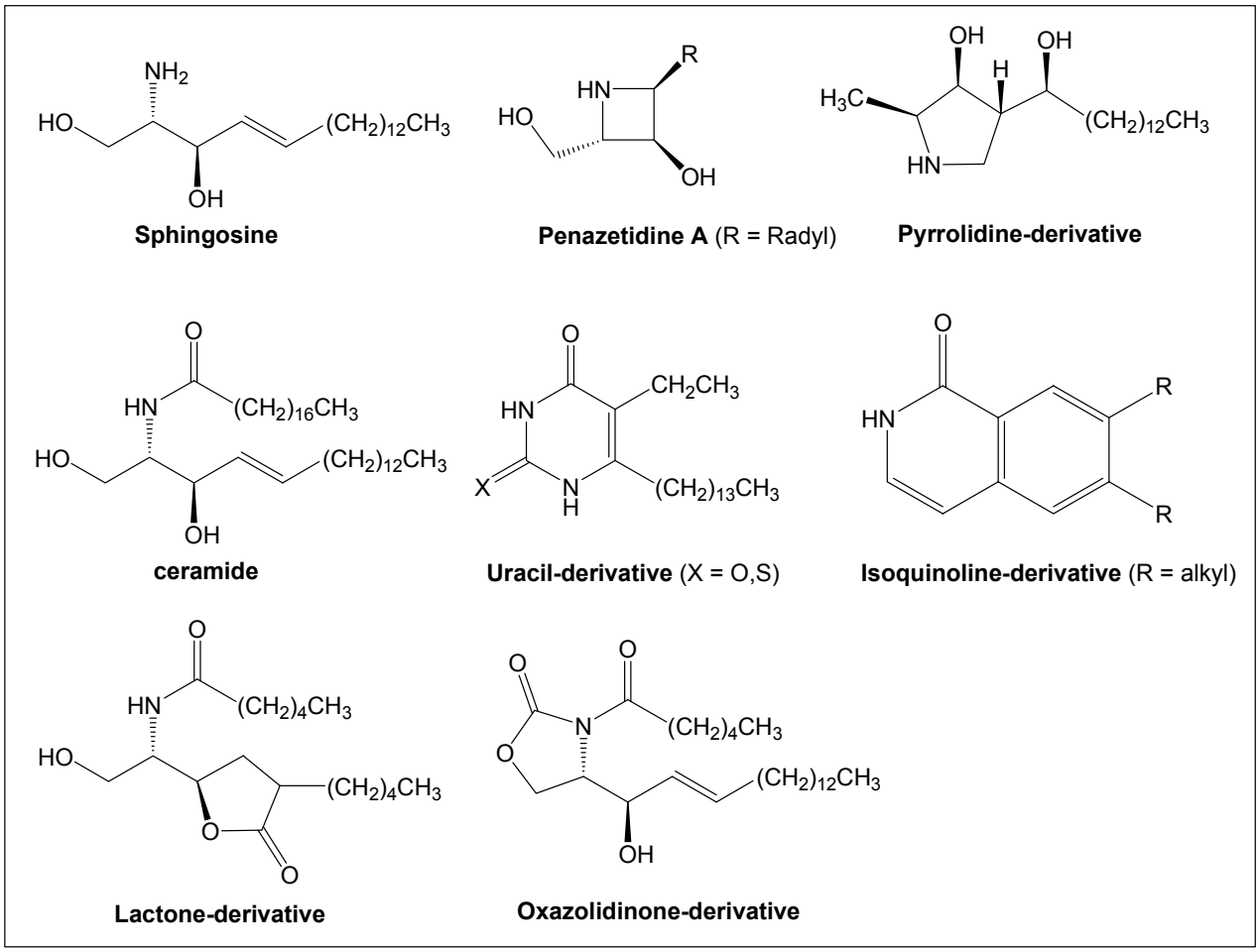

Figure 2.8: Structures of sphingosine, ceramide, the natural sphingolipid derivative Penazetidine A, and other synthetic heterocyclic sphingolipid derivatives

3. Aim and Concept of the present study

Ceramide can be metabolized to a series of sphingolipids that play a role in a number of cellular events. The exogenous application of ceramide analogs to cells leads to a variety of effects (van Blitterswijk, 2003), including metabolic transformation and apoptotic responses, thus complicating the analysis of sphingolipid function. The initial aim of the present study was to reduce the multitude of ceramide-mediated effects using synthetic ceramide analogs. The restriction of biologically active, conformationally flexible ligands is a widely used approach in drug development, especially in the area of peptide mimetics (Giannis A. et al., 1993). Extrapolation of this concept, from peptides to lipids we designed and synthesized ceramide derivatives and investigated their effect on the biosynthesis of complex GSLs. Following questions arised from the observation, that ceramide analogs such as **5a** and **5b** (Figure 4.2) can interfere with the biosynthesis of complex GSLs in cultured cells:

1) **Which molecular mechanism underlies the modulation of GSL biosynthesis in cultured cells incubated with halogenated ceramide derivatives?**
   Exogenous addition of **5a** and **5b** to cultured cells led to the accumulation of ganglioside GM2-synthase-substrates. However, no inhibition of the recombinant enzyme could be detected *in vitro*. It was therefore necessary to clarify the exact mechanism of action.

2) **What is the function of the iodine atom in the ceramide derivatives?**
   The ceramide derivatives **5a** and **5b** bear an iodine atom, which distinguishes them from most other ceramide derivatives that have been applied to cultured cells. To investigate, if the presence of a halogen atom is required for the biological activity, ceramide derivatives like **18a** and **18b** (Figure 4.18) had to be synthesized for structure-activity analysis.

3) **How are ceramide derivatives 5a and 5b metabolized after added to cultured cells?**
   To investigate if a metabolite of the exogenously added compounds mediates the effect on GSL biosynthesis, the lipids of cultured fibroblasts incubated with the active compounds had to be analyzed for putative metabolic products derived from the exogenously added substances.

4. Results

4.1. Strategy for the synthesis of ceramide analogs

Ceramide analogs are potential inhibitors of pharmacologically relevant enzymes or ligands of putative ceramide binding proteins. In addition, they might be metabolically incorporated into glycosphingolipids and sphingomyelin and alter membrane function. Several preparative approaches to sphingolipids have been reported, which can be modified for the synthesis of sphingolipid analogs. Ceramides are long chain 2-amino-1,3-diols, which are *N*-acylated with a fatty acid. The long chain base has an *E*-configured $\Delta^{4,5}$-double bond, but can also be saturated, 4-hydroxylated, and/or modified in other ways (Futerman and Hannun, 2004). In mammalian tissues, the most common sphingoid base is D-erythro-C_{18}-sphingosine, and the typical *N*-acyl group has chain lengths of 16-24 carbon atoms, although much longer acyl chains are present in ceramides of the skin (Holleran et al., 2006). For the synthesis of the ceramide analogs prepared in this work, the amino acid L-serine, and in the case of ceramide analogs with an additional methyl group in the 1-position, also L-threonine, has been chosen as starting material.

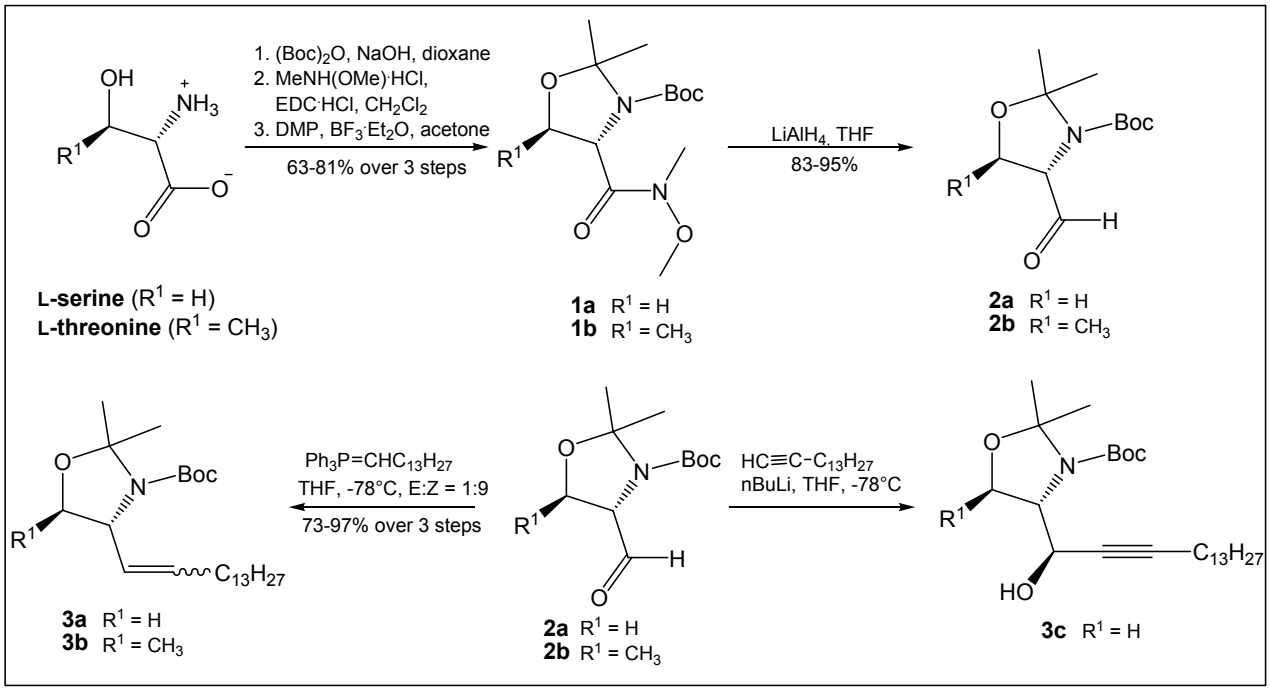

Figure 4.1: Transformation of protected α–amino aldehydes (**2a,b**) derived from L-serine and L-threonine with organometallic (R^1 = H, CH_3) or Wittig reagents.

These amino acids carry the functional groups at C1 and C2 of the sphingoid backbone including the configuration of naturally occurring sphingosine at C2. They allow elongation at C3 (Fig. 4.1) by alkylation or olefination, and, in the first case, the establishment of a defined configuration at C3 (Review: Kulkarni et al., 1999). The alkyl chain was introduced by reaction of Garner's aldehyde **2a** or the corresponding aldehyde derived from L-threonine (**2b**). These intermediates were derived from the natural amino acids in 4 steps. The resulting compounds **3a-c** were further modified as described in chapters 4.2.1, 4.2.3, 4.4.2, 4.4.3, 4.7.1,and 4.8.1.

4.2. Substituted cyclic carbamates as ceramide analogs

4.2.1. Synthesis

The conformationally restricted ceramide analogs **5a** and **5b** (Fig 4.2) have been prepared in a sequence of 3 reaction steps according to (Sawatzki, 2003a). These structures are of great interest, because previous studies in cultured cells showed that oxazinanone **5a** and oxazolidinone **5b,** but not oxazinanone **5c** (Figure 1.2), led to a reduction of ganglioside biosynthesis on the stage of GM2-synthase (Sawatzki, 2003a).

The synthesis started with the preparation of Weinreb-amide **1a** from L-serine. This was reduced to Garner's serine aldehyde (**2a**) by treatment with $LiAlH_4$ according to a modified procedure (Campbell et al. 1998) of the original route (Garner, 1984). The amino aldehyde was elongated by a Wittig reaction, which leads to a mixture of (*Z*)- and (*E*)-isomers (*Z:E* = 8:1) of **3a** in 73 % combined yield. The two products were isolated by column chromatography with silica gel using the solvent system cyclohexane/ethyl acetate (9:1 by vol.) to afford pure *Z*-alkene (43 % of total product) and a mixture of both compounds that could be further resolved by repeated chromatography. The treatment of (*Z*)-allylic carbamate **3a** with *N*-iodosuccinimide (NIS) in dichloromethane according to (Casado-Bellver et al., 2002) leads to the formation of the bicyclic products **4a** and **4b** in 52 % combined yield with the oxazolidinone-derivative **4b** as major product. The two products were purified by column chromatography with silica gel using the solvent system cyclohexane/ethyl acetate (9:1 by vol.), but the separation of **4a** and **4b** was quite difficult, which explains the low isolated yields.

The relative configuration of the products was determined from the coupling constants of the ring-protons in the ^{1}H-NMR-spectra. The coupling constants in the spectrum of compound **4a** ($J_{4,5}$ = 4.5 Hz, $J_{5,6}$ = 11.3 Hz) agree with the expected values and with those of related compounds (Jorda-Gregori *et al.*, 2000). Deprotection of the bicyclic compounds **4a** and **4b** by acidic treatment lead to the compounds **5a** and **5b**. The ring size of the cyclic carbamates was also confirmed by IR absorption of the C=O stretch vibration. The strain in cyclic carbamates rises from the 6-membered system to the 5-membered system and causes a shift of the C=O stretch absorption to higher frequencies in the infrared spectra. The absorption for oxazinanone **5a** at 1634 cm^{-1} and the absorption for the oxazolidinone **5b** at 1698 cm^{-1} are in agreement with those of related compounds (Kemp et al., 1996). Treatment of the (*E*)-isomer of **3a** with NIS and deprotection leads to the formation of the oxazinanone **5c** (Figure 1.2; Sawatzki, 2003a). This reaction was not followed, since previous studies showed that the oxazinanone **5c** has no influence on sphingolipid metabolism as described above (Sawatzki, 2003a).

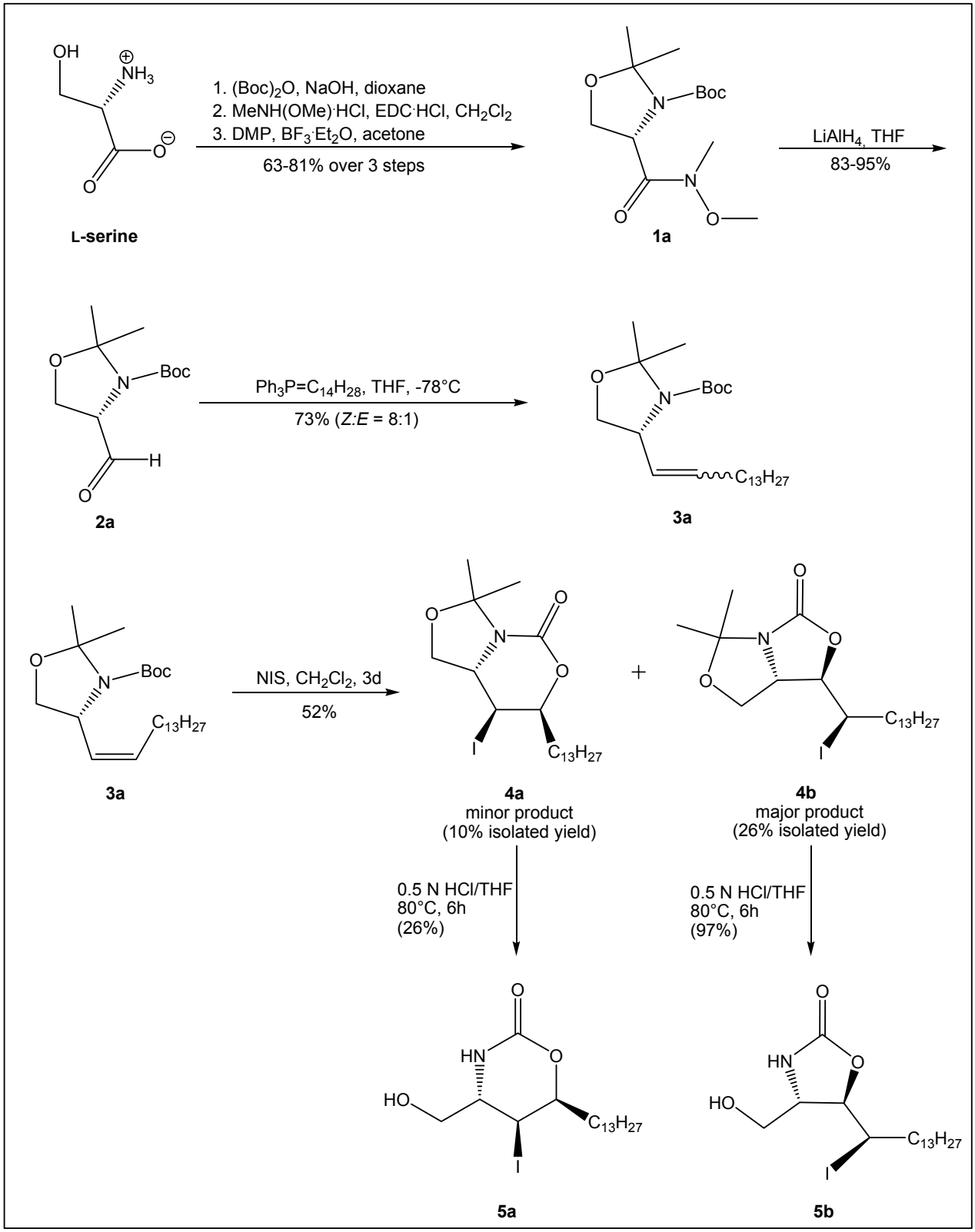

Figure 4.2: Synthesis of compounds **5a** and **5b** (modified from Sawatzki, 2003a). Abbreviations: EDC·HCl = *N*-(3-Dimethylaminopropyl)-*N'*-ethylcarbodiimide Hydrochloride; DMP = 2,2,-Dimethoxypropane; NIS = *N*-iodosuccinimide

4.2.2. Analysis of oxazolidinone 5b in primary cultured neurons

Previous studies in cultured cells showed that oxazinanone **5a** and oxazolidinone **5b,** but not oxazinanone **5c**, led to a reduction of ganglioside biosynthesis on the stage of GM2-synthase (Sawatzki, 2003a). This has been demonstrated by metabolic labeling experiments in cultured murine granule cells using the radioactive precursor D-[^{14}C]galactose, and in the case of **5a** and **5c** additionally using L-[3-^{14}C]serine. Labelling with L-[3-^{14}C]serine is a measure for *de novo* biosynthesis, while labelling with D-[^{14}C]galactose additionally reflects the contribution of the salvage pathway, which accounts for the majority of biosynthetically formed glycosphingolipids in neurons.

In previous experiments (Sawatzki, 2003a), the influence of **5b** on incorporation of L-[3-^{14}C]serine into sphingomyelin could not be unambiguously quantified. To proof, if the previous data are reproducible, and to analyze the influence of the ceramide-derivative **5b** on the biosynthesis of sphingomyelin the target compound **5b** was investigated again in primary cultured neurons on their effect on sphingolipid metabolism. Figure 4.3 illustrates the effect of oxazolidinone **5b** on glycosphingolipid biosynthesis. Granule cells were prepared from the cerebellum of 6 days old mice. In this case, the cells display time-stable glycolipid-patterns. They were incubated with 50 µM **5b** in the culture medium for 24 h. L-[3-^{14}C]serine was added to the culture medium and its incorporation into newly synthesized sphingolipids was analyzed after labelling for 24h. Cells were harvested, lipids were extracted, sphingolipids and GSLs were separated into acidic and neutral fractions. After the glycerolipids were removed by mild alkaline hydrolysis the lipid extracts were desalted, separated by thin layer chromatography (TLC) and visualized by phosphoimaging. In the presence of **5b** the incorporation of radioactivity into sphingolipids is 85 % reduced (0.19 µCi/mg protein) compared to control (0.22 µCi/mg protein). Cells incubated in the presence of 50 µM **5b** and L-[3-^{14}C]serine (Fig 4.4) accumulate large quantities of radioactively labelled ganglioside GM3 (up to 500% of control) and GD3 (to 630% of control). The decrease of glucosylceramide (112% of control) and lactosylceramide (125% of control) is not as drastic. The levels of higher gangliosides like GD1a and GT1b are reduced compared to the control. Taken together, these data indicate an inhibition of GM2-formation. The glycosphingolipid pattern obtained by L-[3-^{14}C]serine labeling in the presence of 50 µM compound **5b** shown in figure 4.3 is similar to those obtained previously (Sawatzki, 2003a). In addition, the separation into neutral and acidic sphingolipids allowed closer examination of SM-levels, which were not significantly altered. This indicates that **5b** is not recognized by SM-synthase. Also the steady state concentration of GlcCer are not significally altered, which might be a result of accumulation of GlcCer as a lipid species proximal to the metabolic block, and inhibition of GlcCer formation, which might be expected for a ceramide analog.

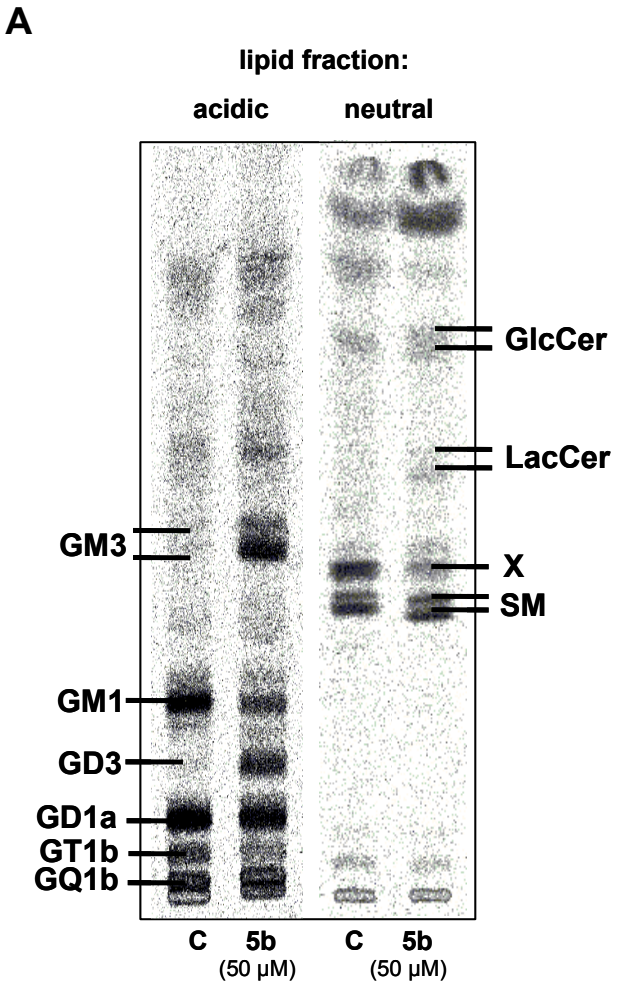

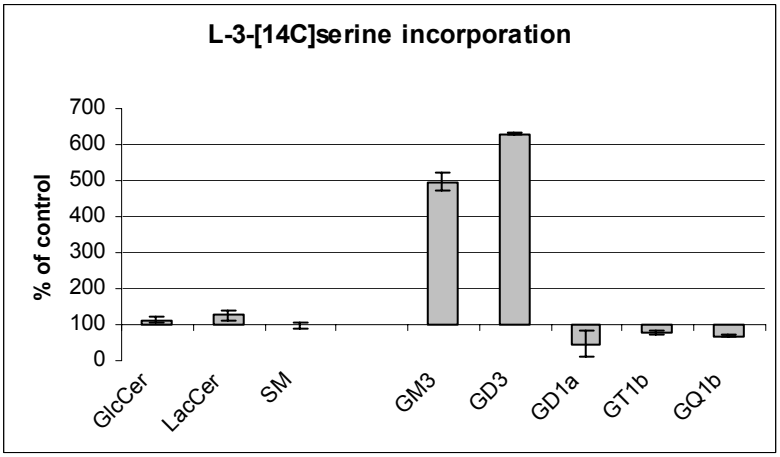

Figure 4.3: **Effect of oxazolidinone 5b on the incorporation of L-[3-^{14}C]serine into sphingolipids of murine granule cells.** Cells were treated with 50 µM lipid **5b** in the culture medium for 24h. Then, cells were fed with L-[3-^{14}C]serine in the presence of the tested compound for 24h. Lipids were extracted, separated into acidic and neutral fractions, and glycerolipids were removed by alkaline treatment.
A: Sphingolipids were separated by thin layer chromatography using the solvent system: $CHCl_3$/MeOH/0.22% aqueous $CaCl_2$ 60:35:8 by vol. Radioactive bands were visualized by phosphoimaging. (C = control; X = the nature of this band is not known). **B**: Radioactivity found in the TLC spots of untreated cells were set equal 100 %. The results of 2 experiments are given. Radioactivity was analyzed by phosphoimager analysis. Data are expressed as percentages of control values that were obtained by labelling cells with L-[3-^{14}C]serine in the presence of methanol. All data are given as mean values of two different experiments.

4.2.3. Analysis of the oxazolidinone-derivatives (5b, 6 and 7.2b) in cultured fibroblasts

Because of the low availability of cell material and time consuming preparations of primary granule cells, compounds were also tested in cultured human fibroblasts. The use of these cells has the advantage of the easy preparation of the cells and their availability from patients or animal models of various different diseases. Therefore, the target compounds were investigated in L-[3-^{14}C]serine labeling experiments in cultured human fibroblasts. To address the role of the iodine atom in oxazolidinone **5b** for the alteration of lipid pattern in cultured cells, oxazolidinones **6** and **7.2b** (see figure 4.5 (A)) were testet. Oxazolidinone **6** was synthesized and provided by Sawatzki (2003a). The Bromine derivative **7.2b** was prepared in a manner similar to the synthesis of the iodine derivative with NBS (*N*-Bromosuccinimide) instead of NIS (Fig. 4.4). The bicyclic products **7.1a** and **7.1b** were obtained in 68 % combined yield, but the separation of both products by column chromatography with silica gel using the solvent system cyclohexane/ethyl acetate (5:1 by vol.) was difficult. The oxazolidinone-derivative **7.1b** was isolated in 21 % yield, while the oxazinanone-derivative **7.1b** was obtained only in a mixture with **7.1a**. Deprotection of **7.2b** by acidic treatment afforded the oxazolidinone **7.2b** in 63% yield. The oxazinanone **7.2a** was obtained by deprotection of the mixture of **7.1a** and **7.1b**. Purification by column chromatography on silica gel using the solvent system chloroform/methanol = 10:1 yielded **7.2a** in 5% over two steps.

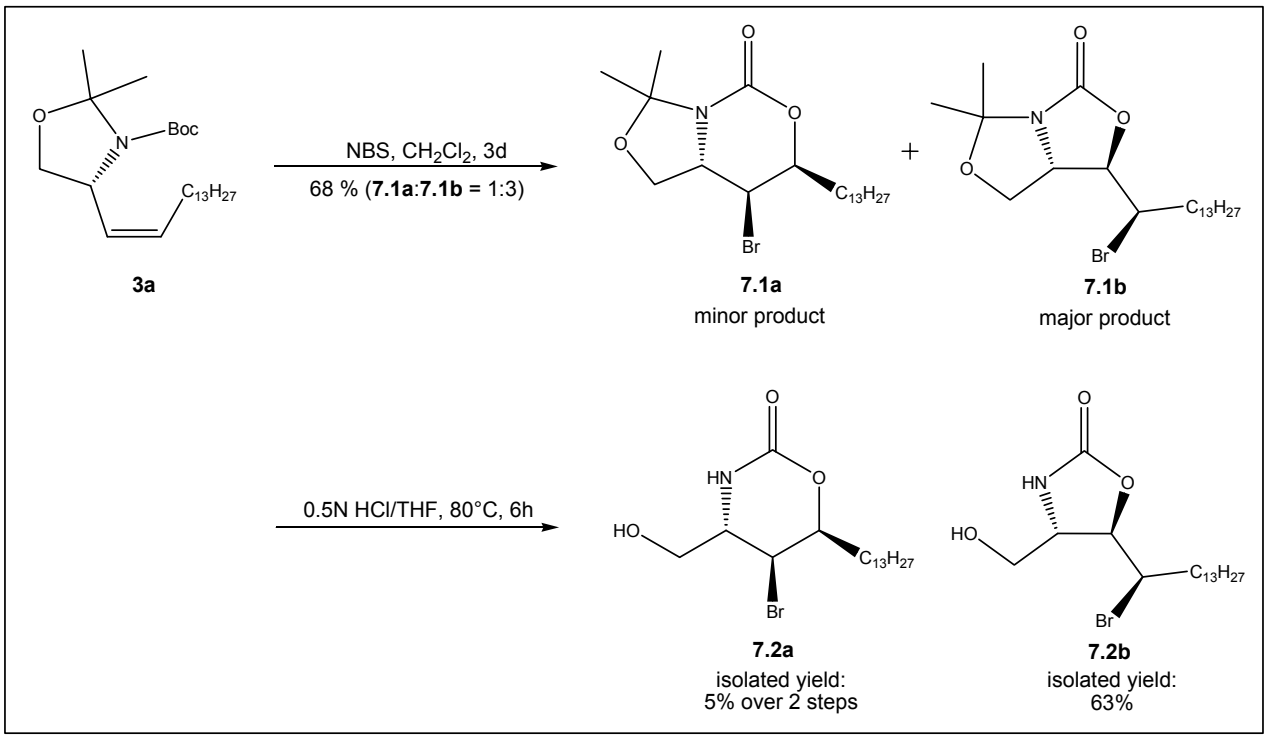

Fig. 4.4: Synthesis of Bromocarbamates **7.2a** and **7.2b**

Cultured fibroblasts were incubated with 25 µM **5b**, **6** and **7.2b** in the culture medium for 24 h. L-[3-^{14}C]serine was added to the culture medium and its incorporation into newly synthesized sphingolipids was analyzed after labelling for 24h. Lipid extracts were prepared as described above, separated by thin layer chromatography (TLC), and visualized by phosphoimaging (Figure 4.5 (A)).

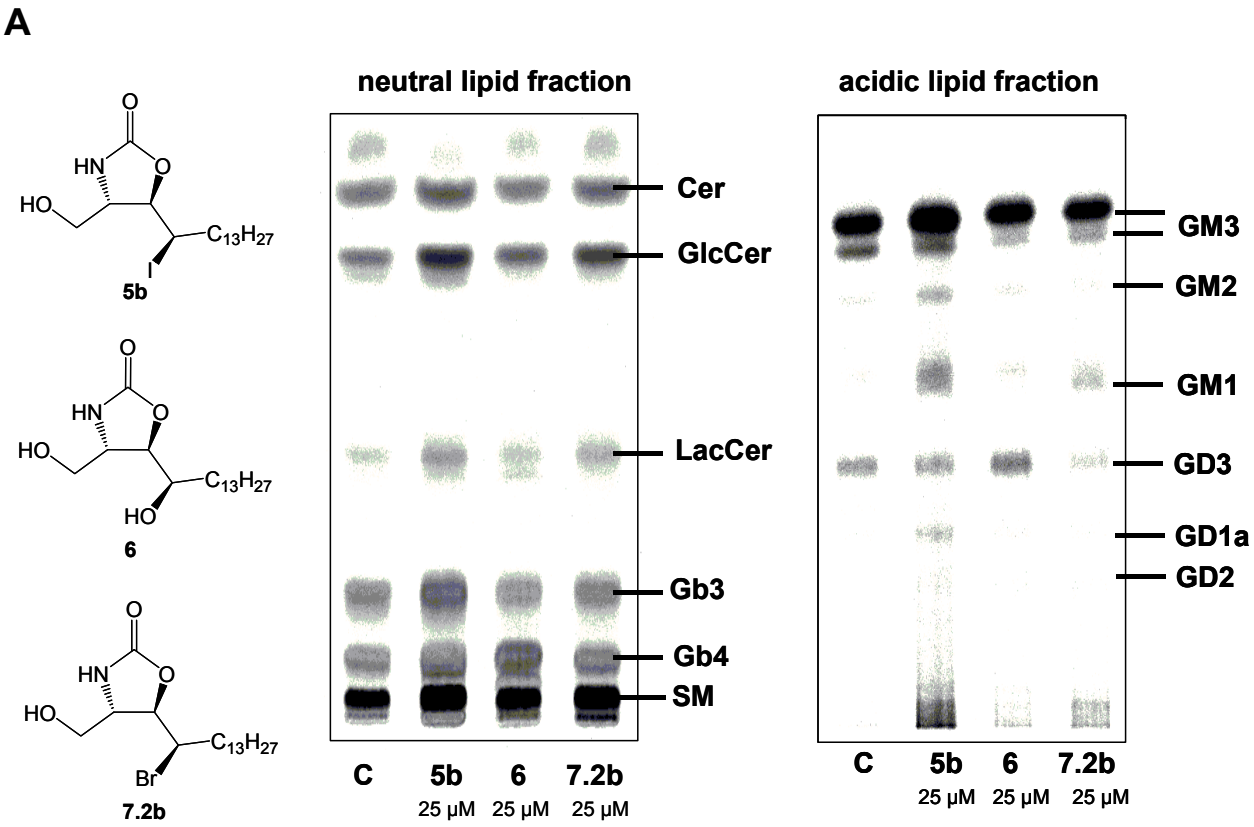

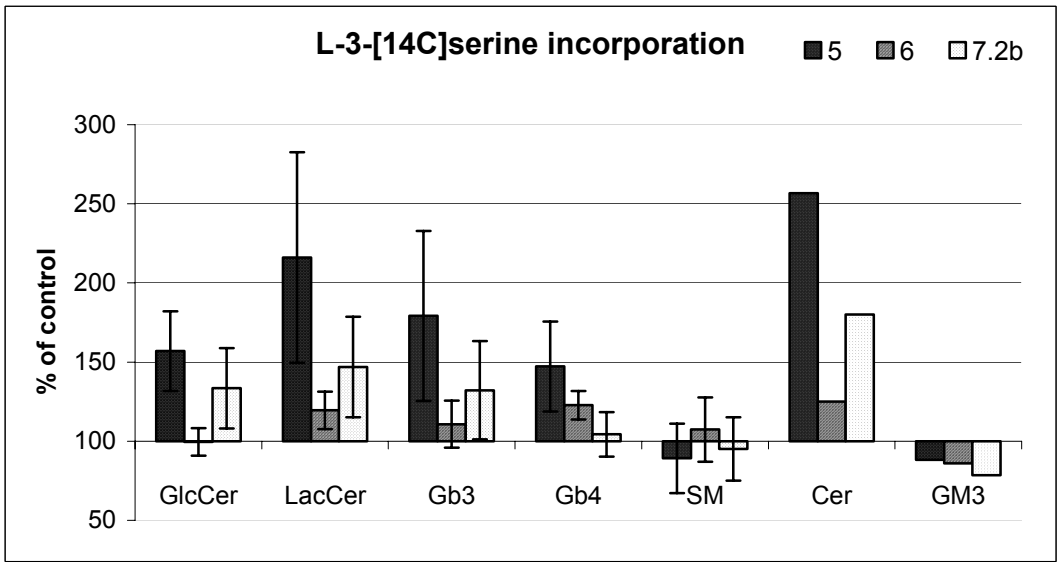

Figure 4.5: **Effect of oxazolidinones 5b, 6 and 7.2b on the incorporation of 3-[^{14}C]serine into neutral sphingolipids of human fibroblasts.** Cells were treated with 25 µM target compounds in the culture medium for 24h. Then, cells were fed with L-3-[^{14}C]serine in the presence of the tested compound for 24h. Lipids were extracted, separated into acidic and neutral fractions, and glycerolipids were removed by alkaline treatment. **A**: Sphingolipids were separated by thin layer chromatography by threefold development (as decribed in the material and method section; chapter 6.3.2) Radioactive bands were visualized by phosphoimaging. (X = the nature of this band is not known). **B**: Data are normalized to the total radioactivity found in each lane and radioactivity of each TLC spot of untreated cells was set equal 100%. Data for neutral lipids are given as mean values of two different experiments.

The experiments with fibroblasts were complicated by the fact that they contain additional neutral glycolipids, $GbOse_3$ and $GbOse_4$, compared to murine granule cells. No solvent system suitable for the separation of all neutral sphingolipids from fibroblasts by TLC was described in the literature. The standard solvent system chloroform/methanol/water (60:35:8 by vol.) does not provide sufficient separation of sphingomyelin and $GbOse_4$. In addition, in order to analyse cholesterol and ceramide, a separate analysis (using the solvent system chloroform/methanol/glacial acetic acid 190:9:1 by vol.) is required. The lipid analysis of fibroblasts by TLC required the development of a new solvent system. Therefore, a threefold development was used with progressively increasing migration distances (chapter 7.3.8, Farwanah et al., in preparation). For the separation of neutral lipids, the tlc plate was developed two times using the solvent system chloroform/methanol/glacial acetic acid (70:30:8 by vol.), and the solvent front was allowed to migrate to about two-thirds of the planned migration distance. This separates the polar sphingolipids (SM, $GbOse_3$, $GbOse_4$, LacCer and GlcCer), while the less polar lipids (ceramide, cholesterol) are migrating with the solvent front without being separated. In the third stage, ceramide and cholesterol are separated over the total migration distance by using the solvent chloroform. The polar lipids do not migrate on the plate in this mobile phase and remain in their original position.

In the presence of 25 µM of the oxazolidinone-derivatives **5b**, **6** and **7.2b** in the medium of cultured fibroblasts, the incorporation of L-[3-^{14}C]serine into sphingolipids was increased. Compared to untreated control cells (2.33 µCi/mg protein), the incorporation of L-[3-^{14}C]serine into sphingolipids increased in the presence of **5b** by 178 % (4.15 µCi/mg protein), in the presence of **6** by 106 % (2.47 µCi/mg protein), and in presence of **7.2b** by 141 % (3.2 µCi/mg protein). This is in contrast to the results obtained from the experiments in cultured neurons (chapter 4.2.2, figure 4.3). We observed, that in the presence of the halogenated oxazolidinones **5b** and **7.2b**, the incorporation of radioactivity into ceramide drastically increased, whereas the incorporation of radioactivity into sphingomyelin was slightly reduced. It has been shown in human keratinocytes, that the expression rates of several enzymes involved in ceramide metabolism, including serine palmitoyl transferase, increase in the presence of ceramide-derivatives (Brodesser and Kolter, in preparation). In addition, the authors showed, that the transcription of the gene encoding acid sphingomyelinase, that cleaves sphingomyelin into ceramide and phosphocholine, is also increased. In order to clarify, if the accumulation of ceramide and the decreased level of sphingomyelin brought about by **5b**, are a consequence of an inhibition of the ceramide metabolizing enzyme sphingomyelin synthase, or are a consequence of an increased expression or of acid sphingomyelinase, we have to make further experiments, including the quantification of mRNA levels and activity assays of ceramide metabolizing enzymes. In terms of the influence on GSL biosynthesis the iodine substituted oxazolidinone **5b** has the effect on the L-[3-^{14}C]serine incorporation. In the presence of 25 µM **5b** in culture medium, levels of neutral GSLs (GlcCer, LacCer, $GbOse_3$ and $GbOse_4$) were elevated up to 200 % compared to control cells. In addition, in the presence of **5b** we observed an increased L-[3-^{14}C]serine incorporation into all gangliosides. However, we did not observe a specific accumulation of ganglioside GM3. The ganglioside content, pattern, and, in particular, the molar ratio of GM3 and GD3 of cultured fibroblasts have been shown to be very variable (Sciannamblo et al., 2003; Colombo et al., 2000). The influence of ceramide derivative **5b** on ganglioside biosynthesis was analyzed in only one experiment yet. Therefore, the results should not be used for any conclusions, and have the to be confirmed by further experiments.

4.3. Determination of GalNAc-transferase (GM2-synthase) activity in the presence of oxazolidinone 5b *in vitro*

The glycolipid pattern generated by exogenous addition of compounds **5a** and **5b** to cultured murine neurons are qualitatively identical to those obtained from cells derived from the GM2-synthase ko-mice (Yamashita et al., 2003).

To determine whether oxazolidinone **5b** inhibits GalNAc-transferase directly, **5b** was tested *in vitro* with murine recombinant GM2-synthase in a micellar assay. GalNAc-T was isolated as membrane fraction from Baculovirus-transfected insect cells overexpressing murine GalNAc-transferase, as described in the Material and Methods section. The assay was conducted under conditions described by Wendeler et al., 2003, with some modifications. Samples of the enzyme were incubated with 200 µM **5b** in the assay buffer, radiolabeled UDP-[^{3}H]GalNAc, and different concentrations of ganglioside GM3 under micellar conditions for 30 min at 37°C. Glycolipids were separated by reversed phase chromatography (Kyrklund, 1987), the flow-through containing watersoluble UDP-[^{3}H]GalNAc was discarded, and radiolabeled ganglioside GM2 was eluted and measured by scintillation counting. The ratio of transferred [^{3}H]GalNAc on the acceptor ganglioside GM3 was determined by quantification of radioactivity incorporated into the lipid substrate.

For the determination of enzyme activity, the assay was conducted in the absence of **5b** (Figure 4.6). In the presence of 200 µM **5b**, incorporation of [^{3}H]GalNAc is increased compared to control. This indicates a low activation of the enzyme, or a higher availability of the substrate in the presence of the oxazolidinone **5b**. In conclusion, no inhibition of the enzyme by **5b** could be obtained *in vitro* under micellar conditions. Also a micellar GalNAc transferase assay in the presence of lipid extracts derived from fibroblast cells incubated with **5b** showed no inhibition.

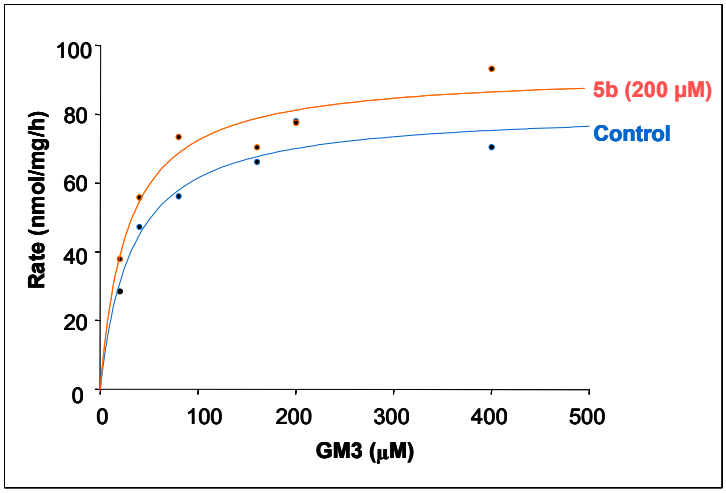

Figure 4.6: **Effect of compound 5b on activity of recombinant GM2-synthase in a micellar assay.** The incorporation of [^{3}H]GalNAc into lipids is shown in dependence of GM3 concentration. Test series have been carried out in the presence and absence of **5b.**

Micelles composed of detergents such as *N*-Octyl-beta-D-glucopyranoside represent a quite simplified but unphysiological model of biological membranes. Nevertherless, the preparation of micelles is rapid and straightforward and they are widely used in activity assays of membrane-bound enzymes. Compared to micelles, unilamellar liposome modelsystems resemble biological membranes more closely. To test the influence of the oxazolidinone **5b** on GalNAc-transferase activity under more physiological conditions, we planned to test the ceramide-derivative in a detergent-free liposomal assay according to Wendeler (2004). Up to now, our attemps were not successful. The composition of the liposomes (45 mol% PC, 20 mol% cholesterol, 15 mol% GM3, 10 mol% PE, 10 mol% PG) was based on the described content of lipids in Golgi membranes (van Meer, 1998). Through sonication, the exchange or fusion of the GalNAc-transferase preparation with GM3-containing liposomes was stimulated and the samples were then incubated for 30 min at 37°C. The specific activity of the GM2-synthase determined in the liposomal assay system was only 3% compared to the activity determined in a micellar testsystem. For further experiments, we have to optimize the fusion of GM3-containing liposomes and enzyme-containing membranes.

4.4. Analysis of potential metabolites derived from carbamates 5a and 5b

Since the effect of substances like **5b** on GSL biosynthesis is an indirect one, we investigated if a metabolite of **5b** might be the inhibitor of the GalNAc-transferase. Synthetic ceramide derivatives exogenously added to cultured cells can be metabolized to various compounds. In contrast to most other drugs, ceramide analogs added to cells can undergo anabolic reactions similar to those of the parent compound. They can be metabolized like endogenous ceramide by the enzymes that catalyze the formation of glucosylceramide, sphingomyelin, or ceramide-1-phosphate. Several strategies were followed to monitor metabolism of the synthetic ceramide derivatives. In one approach, it was attempted to incorporate a radioisotope into the substance. This could be followed by the analysis of lipid extracts from cells incubated with the labeled compound by thin layer chromatography and quantification by phosphoimaging. Attemps to introduce a radiolabel into **5a** and **5b** by different strategies were not successful (chapter 4.4.2).

Metabolite identification requires high recovery and a sensitive detection method. In cellular lipid extracts, gangliosides coexist as minor components with phospholipids and other lipid species, which can hinder metabolism studies. In most cell types, the content of glycolipids is in the range of only a few mol% of total lipids. In the case of fibroblasts, the glycosphingolipids constitute about 3% of the total lipid (Dawson et al., 1972).

Although the effect of oxazolidinone **5b** on GSL biosynthesis in cultured neurons is different than that in cultured fibroblasts, metabolism studies of the oxazinones **5a** and **5b** (chapter 4.3) and other experiments (chapter 4.5) were conducted in cultured fibroblasts.

4.4.1. Analysis of metabolites of oxazinanone 5a by thin layer chromatography (TLC)

As mentioned above, the effect of oxazolidinone **5b** on GSL biosynthesis in cultured neurons is different than that in cultured fibroblasts. It can be expected that the cell type specifity of this effect derived from a different metabolism of the ceramide derivatives in cultured fibroblasts and neurons. Because of the higher amounts required for lipid analysis, we startet with the analysis in fibroblasts. Therefore, the lipids of cultured fibroblasts incubated with the ceramide derivatives **5a** and **5b** were analyzed by thin layer chromatography for putative metabolic products derived from the exogenously added substance. Cells were incubated with 25 µM compound **5a** in the culture medium for 10 days. Lipids were extracted, separated into acidic and neutral lipids and desalted. Analyzed lipids were normalized on protein content, separated by thin layer chromatography, and were visualized by staining with Kägi-Miescher (Material and Methods section; figure 4.7).

Before tlc-separation, glycerolipids are usually removed by mild alkaline treatment of the lipid extract. Because of the lability of iodine-containing metabolites, the samples could not be treated with an alkaline solution in this case. The high amounts of phospholipids and endogenous lipids prevented the detection of lipid bands derived from **5a**. In figure 4.10, the tlc of the neutral lipid extract from untreated cells (lane 2) and incubated cells (lane 3) is shown. Lane 1 shows standard bands corresponding to **5a**, and the chemically synthesized neoglucosylceramide and neolactosylceramide derivatives derived from **5a** (Wirtz, 2004). As expected, the neoglycolipids derived from **5a** have a lower retention factor than the native glycolipids with the same head group derived from ceramide.

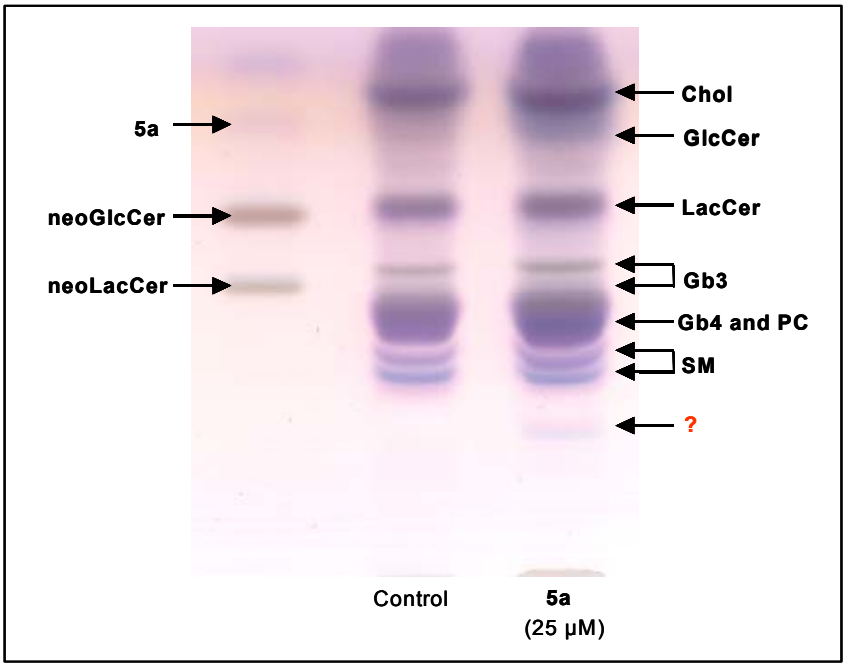

Figure 4.7: Analysis of metabolites: cultured fibroblasts were incubated with 25 µM compound **5a** in culture medium for 10 d, harvested and extracted. Neutral lipid fractions were separated by tlc using the solvent system: $CHCl_3$/MeOH/0.22% aqueous $CaCl_2$ 60:35:8 by vol. The lipids were visualized by staining with Kägi-Miescher (see Material and Method section). The assignment of lipid class structures to the separated bands is based on comparison of their R_f values with those of commercially available standards.

In the lipid extract of the incubated cells, only one weak new band could be visualized by staining with Kägi-Miescher. The characteristic blue staining indicates the formation of a sphingomyelin-derivative. Attemps to extract this band to proof the assigment by a more sensitive method like mass spectrometry were not successful, because the extract contained large amounts of impurities derived from the chromatography material and the solvent. To avoid this kind of contaminations, we made several analyses of the crude lipid extracts derived from cells incubated with the ceramide derivatives **5a** and **5b** by mass spectrometry (chapter 4.4.2).

4.4.2. Analysis of metabolites of oxazolidinone 5b by mass spectrometry

In the study of the lipid metabolome (Lipidomics), electrospray ionization mass spectrometry (ESI-MS) has become increasingly popular. Methods for lipid analysis of crude cell extracts ("shotgun" analysis) have been published for the analysis of phospholipids, sphingolipids, and cerebrosides (Watson, 2006; Houjou et al., 2004; Han and Cheng, 2005). On the other hand, in the lipid extracts of cells treated with exogenously added lipid analogs, possible metabolites coexist as minor components with phospholipids and other endogenous lipid species, which can hinder metabolism studies. As mentioned above, the separation of sphingolipids from glycerolipids by mild alkaline treatment was not possible in the case of metabolism studies of the carbamate **5b** due to the base-lability of the iodine-group. The mass spectrometric profile (full scan method) of lipids derived from lipid extracts of fibroblasts contains a large number of ions in the mass range of *m/z* 700-900 (data not shown). These signals originate predominatly from phospholipids. Signals of other lipids like ceramide, glycolipids, and metabolites of the exogenously added ceramide analogs can be overlaid or can be suppressed.

In mass spectrometry, different scan techniques are known that allow the specific detection of molecular ions from complex mixtures. The collision-induced dissociation (CID) of compounds through collision with neutral gas molecules like argon generate characteristic daughter ions (Ekroos 2003). In a precursor ion scan (PIS), those parent masses are identified that yield the specific daughter ion with chosen *m/z*. In a neutral loss experiment, only those masses are detected, which originate from the cleavage of a defined neutral molecule.

To profile metabolites containing **5a** or **5b**, characteristic fragment ions of oxazinanone **5a** and oxazolidinone **5b** had to be found. Therefore, purified **5a** and **5b** were analyzed by ESI-MS/MS in positive ion mode as shown in figure 4.8 (A). Fragmentation of oxazolidinone **5b** generates a fragmentation pattern similar to **5a**.

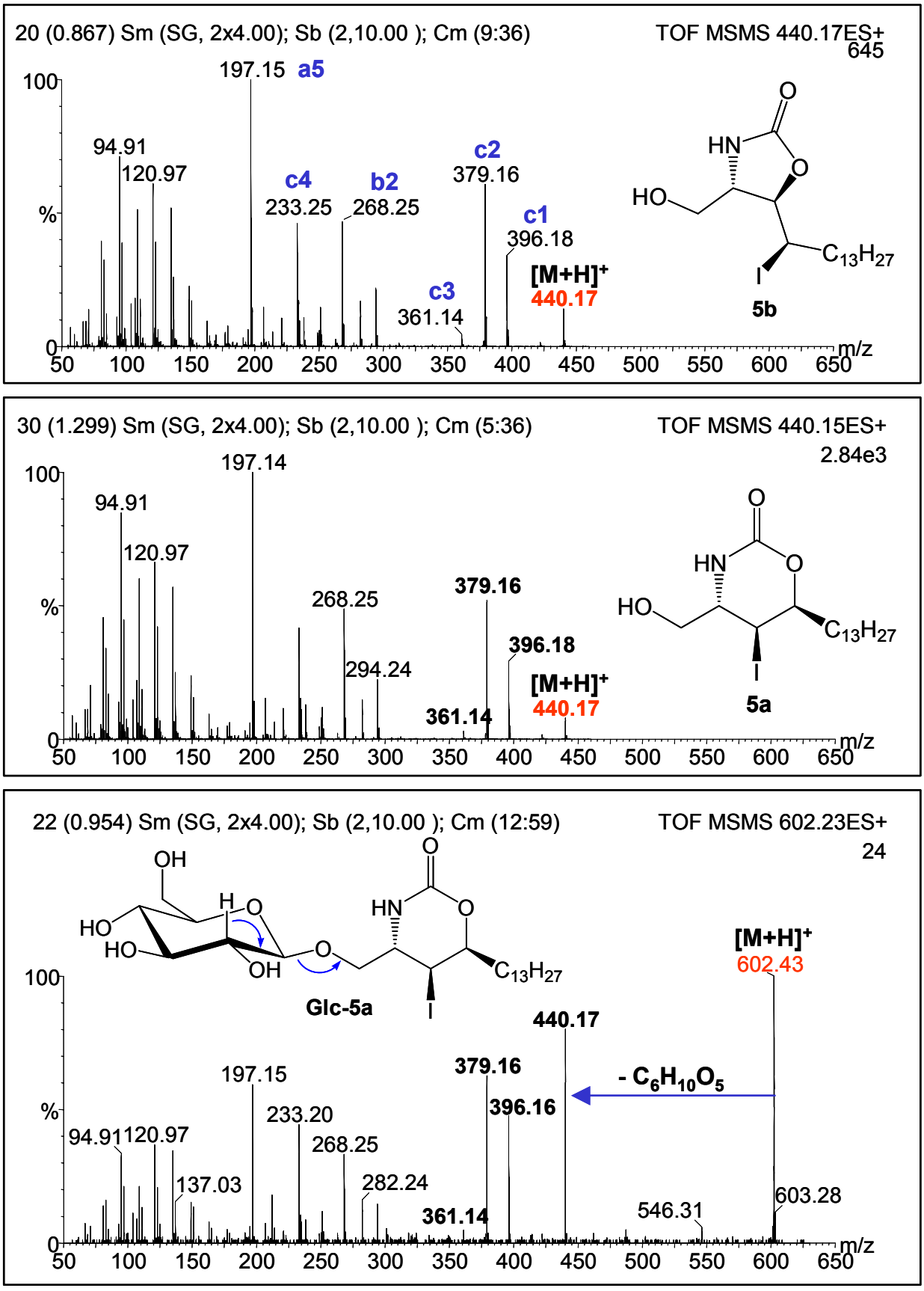

Figure 4.8: ESI-MS/MS-spectra (positive ion scan) of **5a, 5b** and **Glc-5a**, scan range: 50-650, cycle time: 1.1s, CID: 20-22 eV.

In figure 4.9, possible pathways for the formation of characteristic fragments are given. For each molecular ion, only one of several possible structures is given. The elimination of one water molecule from the parent ion $[M+H]^+$ can result in the formation of a terminal double bond in the fragment ion at *m/z* 422.13 (see **a1**). A neutral loss of carbon dioxide, hydrogen iodide and ammonia can yield an allene product ion at *m/z* 235.24 (see **a4**). The cleavage of the C3-C4 bond in the resulting ion **a4** yields an aliphatic ion **a5** at *m/z* 197.15, which is the most prominent fragment in the spectrum. Alternatively, HI can be eliminated from the parent ion to form a fragment at *m/z* 312.13 (see **b1**). Then, loss of CO_2, NH_3, and H_2O leads to the formation of product ion allene **c4** at *m/z* 233.20. On the other hand, the product ion **c4** can be formed by the neutral loss of one CO_2 molecule from the parent ion, followed by loss of NH_3, H_2O, and HI. In addition, the glycosylated oxazinanone (**Glc-5a**), as representative metabolite was analyzed by ESI-MS/MS (Figure 4.8, C). Fragmentation of **Glc-5a** leads to neutral loss of glucose and to the formation of **5a** as product ion *m/z* 440.17. In addition, we detected several fragments with masses that are similar to fragments derived from **5a**. For example, fragments at m/z 396, 379, and 361 appear in the spectra of the MS/MS-spectrum of **Glc-5a** as well as in the spectrum of **5a**. This allowed us to analyse the crude lipid extracts by parent ion scans for these specific fragments.

For the profiling of metabolites of lipid **5a and 5b**, cultured human fibroblasts were incubated with **5a** or with **5b** respectively for 48h, harvested, and lipids were extracted with chloroform/methanol/water (1:2:0.8 by vol.). Then the dried lipid extract was redissolved in chloroform/methanol/water (1:2:0.8 by vol.) and upon changing the solvent system to chloroform/methanol/water (2:2:1.8 by vol.), two phases separated following the method of Bligh and Dyer (1959). The upper aqueous layer containing gangliosides and sphingosine was removed for further purification by reverse-phase chromatography. The chloroform (organic) phase contained glycerolipids, glycolipids, ceramide, sphingomyelin, and cholesterol. Both extracts were dried under a stream of nitrogen, redissolved in chloroform/methanol (1:2 (v/v)), and analyzed by ESI-MS/MS experiments. The spectra for precursor ion scan of iodine (*m/z* 126) contained signals that originate from ion adducts of **5b** (*m/z* 438.6 for $[M-H]^-$, *m/z* 498.6 for $[M+CH_3COO]^-$, and *m/z* 474.3 for $[M+Cl]^-$), but no other signals corresponding to iodine-containing metabolites could be detected. In addition, the neutral loss analysis of carbon dioxide (*m/z* 44) gave no indication for the presence of metabolites of **5b**.

In addition, we calculated the theoretical mass of metabolites like **SM-5b**, **Glc-5b**, **LacCer-5b**, and **GM3-5b**, and their adducts and searched for them in the lipid extracts by scan techniques that are used in the identification of sphingomyelins (parent ion scan *m/z* 184) and glycosphingolipids (neutral loss scan 162). Also the parent ion scans for the fragments *m/z* 440.2, 396.2 and 379.2 gave no indication for the presence of such metabolites.

In summary, we could not find any metabolites of **5a** and **5b** by different approaches, including the described mass-spectrometical techniques. From this, we may conclude that the synthetic ceramide derivatives are metabolically stable under the chosen conditions and that therefore their indirect effect on ganglioside biosynthesis is not mediated by a metabolite. However, we cannot exclude the possibility that putative metabolites are present in concentrations lower that the detection limit of the applied methods.

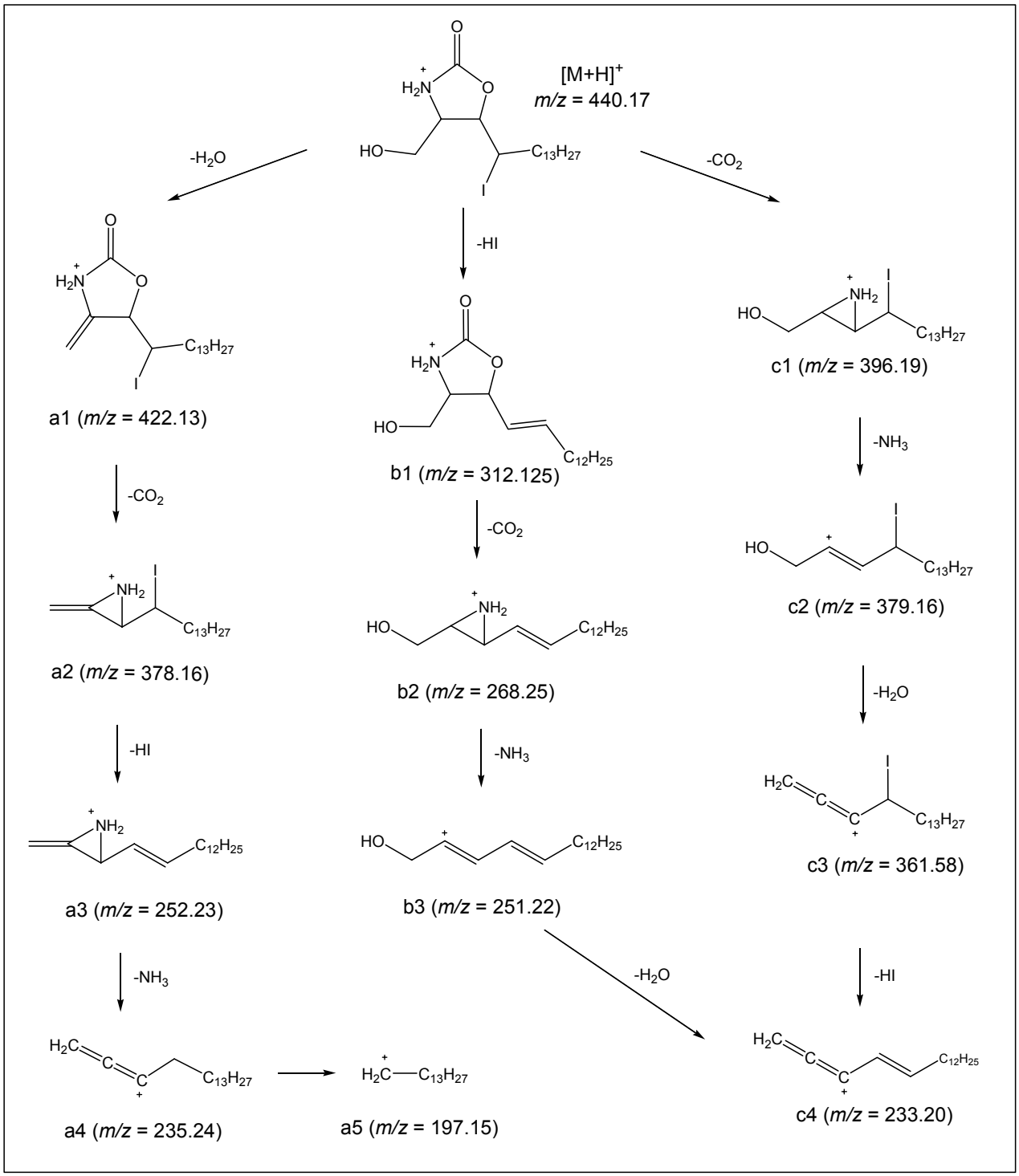

Fig.4.9: Suggested pathways for the formation of characteristic fragment ions by means of collision induced dissociation (CID) of synthetic ceramide analog **5b**.

4.4.3. Attemps for the radiolabeling of 5a and 5b

Detection of a metabolite of **5a** and **5b** by tlc turned out to be unsuccessful, due to the limited separation of endogenous lipids and of metabolites derived from the exogenously added substance by this method (chapter 4.4.1). In addition, the detection of metabolites of compound **5a** and **5b** by thin-layer chromatography was prevented by the low sensitivity of the method. Radiolabeling of **5a** or **5b** should facilitate the detection of their metabolites. In addition, radiolabeling should also be a suitable method for the detection of putative interacting proteins that might undergo covalent attachment to the substance by substitution of the iodine, in the case of a sufficiently high specific radioactivity. Therefore, various attempts were undertaken to prepare one of the active compounds **5a** and **5b** in radiolabeled form. The incorporation of a radioisotope requires a suitable method that uses one of the commercially available sources of ^{3}H or ^{14}C. These isotopes were selected, although their low specific radioactivity might not be high enough for the detection of low-abundant proteins. Two strategies to introduce the radioisotope in the last synthetic step were followed. Figure 4.10 shows the strategy and the results of preliminary experiments. Here, the alcohol function of the iodolactones should be oxidized to the aldehyde, and subsequently reduced to the alcohol by reaction with tritium-labeled sodium borohydride.

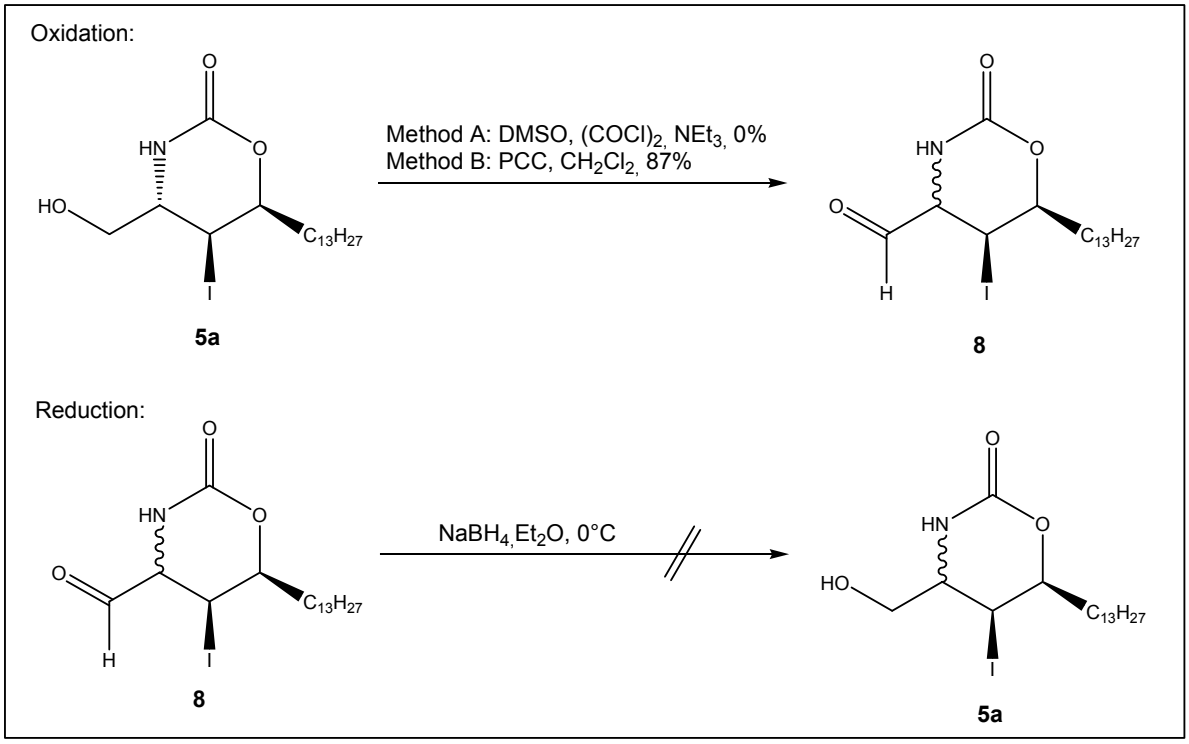

Figure 4.10: Synthetic strategy for the preparation of radiolabeled lipid **5a**

Attemps to oxidize the alcohol function in the oxazolidinone **5b** by Swern oxidation (Kobayashi and Kobayashi, 2000) did not result in the desired compound. Insolubility of the alcohol in dichloromethane at low temperatures prevents Pfitzner-Moffatt conditions (Pfitzner and Moffatt, 1963). Also the reaction with pyridinium chlorochromate (PCC) in dichloromethane did not lead to the formation of the target compound. However, oxidation of oxazinanone **5a** with PCC yielded aldehyde **8** in 87% yield. However, preliminary experiments to reduce the aldehyde **8** with sodiumborohydride did not result in the formation of alcohol **5a**.

It also has to be considered that, tritiated sodiumborohydride can only be handled in solutions of high pH values. TLC control showed the formation of many by-products, which were not characterized. The α-amino aldehydes are known for their chemical instability and configurational lability (Jurczak and Golebrowsky, 1989; Reetz, 1991). We had to conclude, that due to the reactivity of the intermediate (**8**) and the lability of the iodine-group towards reducing reagents and basic conditions, this strategy is not suitable for the introduction of a radiolabel.

In a second strategy, we tried to introduce the radioisotope by hydrogenation of an unsaturated alkyl chain (Figure 4.11). Therefore, the iodolactones with unsaturated alkyl chains had to be synthesized. The synthesis followed the scheme for the synthesis of lipid **5a-c** (chapter 4.2.1).

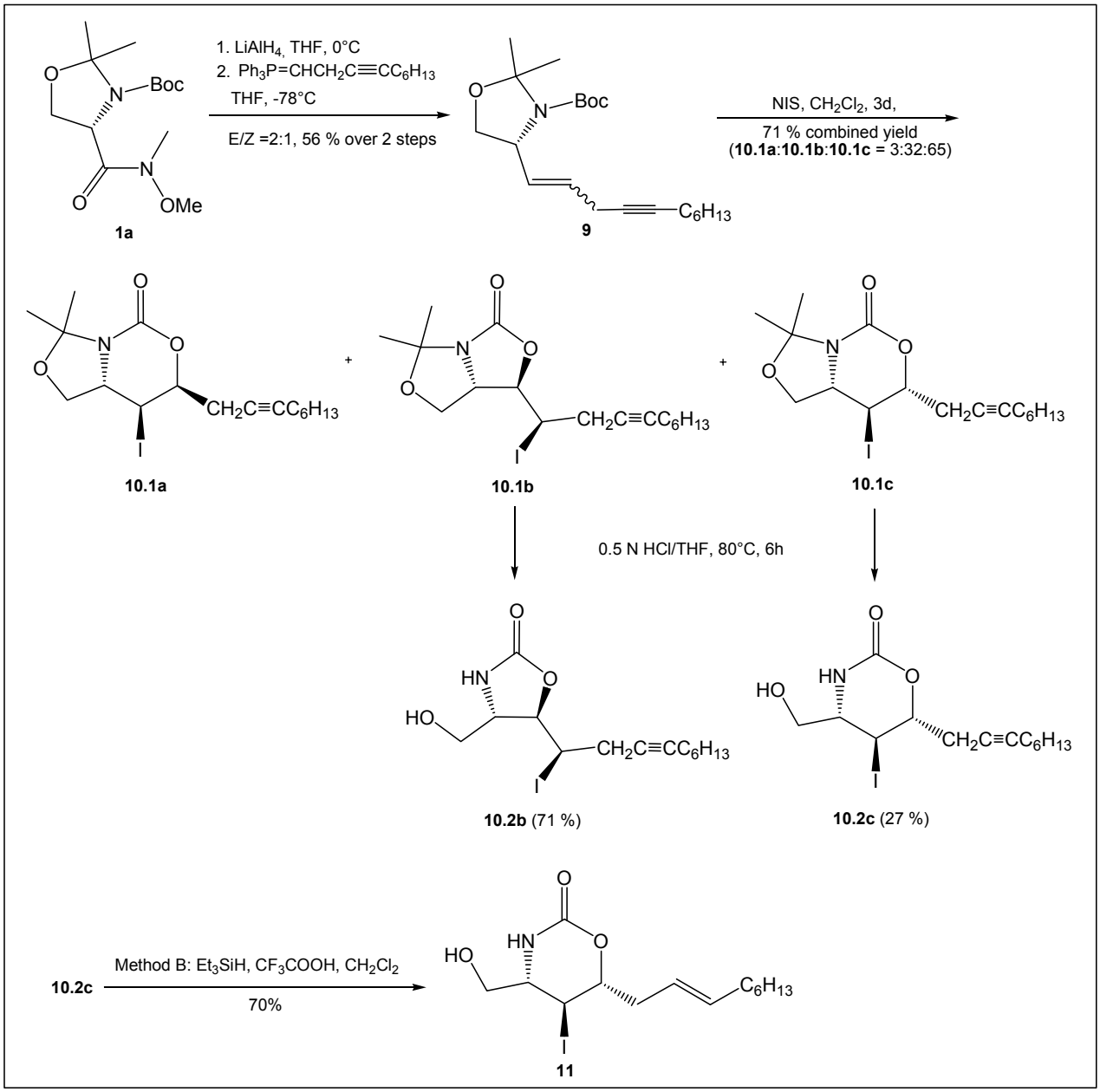

Figure 4.11: Strategy and results of preliminary experiments for the preparation of precursors of radiolabeled form of lipid **5a** and **5b**.

The phosphonium salt required for the elongation by a Wittig reaction was synthesized starting from 3-alkyne-1-ol in a yield of 87% over 3 steps. Wittig reaction of Garner's aldehyde with the ylide derived from the phosphonium salt afforded the *Z*-alkene **9** in a lower ratio than that expected for nonstabilized ylides. For the synthesis of the active compound, the *Z*-configured alkene is required. After iodolactonization with NIS, all three isomers could be separated by column chromatography, and deprotected to the carbamates **10.2a-b** in good yield.

The iodolactone **10.2c** with the configuration of the biologically inactive compound **5c** was preliminary used to control the conditions for mild and effective hydrogenation of the triple bond. First, the solvent system, reaction time, and temperature were varied. Reaction conditions for catalytic hydrogenation with Pd-C as catalyst in ethanol at room temperature yielded small amounts alkene **11** in a mixture with alkyne **10.2c**. Longer reaction time resulted in the loss of the iodine. We had to conclude that the introduction of a radiolabel by this strategy is difficult under the investigated conditions. To avoid the loss of the iodine-group, we tried to hydrogenate the triple bond by ionic hydrogenation (Kursanov et al., 1974). Treatment of alkyne **10.2c** with triethylsilane and trifluoracetic acid in dichloromethane for 16h resulted in the formation of the *E*-alkene **11**. The structure was confirmed by the coupling constant of $^{3}J_{HH}$ = 18.0 Hz in the ^{1}H-NMR spectrum. The alkene **11** could not be fully separated from the alkyne **10.2c** by column chromatography with silica gel using the solvent system chloroform/methanol (10:1 by vol.). The ratio of alkene and alkyne was 9:1. Both methods described above, offer the possibility to obtain at least small amounts of radiolabelled substance.

For the second method, we have to prepare the reagents ((Et_3Si^3H or CF_3COO^3H) in tritiated form, and have to carry out the hydrogenation reaction of **10.2b** with these radiolabeled reagents. [^{3}H]Trifluoroacetic acid can be obtained by hydrolysis of trifluoroacetic acid anhydride with [^{3}H]water (Dugger and Schwarz, 1967), and [^{3}H]triethylsilane (Et_3Si^3H) can be prepared by reduction of triethylsilylchloride with LiB^3H_4 (Guillerm et al., 1977).

4.4.4. ω-Azido-group as chemical reporter for the determination of metabolites

As a new and non-radioactive alternative for the detection of metabolites, we attempted the introduction of an azido-group as chemical reporter. Alkyl azides are functional groups of sufficiently high chemical reactivity to be easily and selectively modified. The alkyl azides have several features that make them well suited for the tagging of biological molecules. An azido-group incorporated into the hydrocarbon chain of a ceramide analog provides a minimal structural change due to its small size and nonpolar nature. Moreover, it is not present in any known naturally occuring molecule and relatively inert within the cellular milieu. Azide- modified molecules can be selectively tagged to a fluorescent group or to a biotin residue by chemoselective ligation reactions developed by the Bertozzi-group: Staudinger ligation, Cu(I)-catalyzed azide-alkyne cycloaddition, or the strain-promoted [3+2] cycloaddition (Agard et al. 2006). The chemical properties of azides should make them suitable as tool to analyze metabolites of synthetic ceramide derivatives. This approach should consist of three steps (figure 4.12). First, the synthetic ceramide analog (**12**) is applied to cells, were it is metabolized. Second, after cell harvesting and lipid extraction, the azido-group containing metabolites in the lipid extract are selectively conjugated with a fluoresceine phosphine

capture reagent (**13**) by means of the Staudinger conjugation reaction (Saxon and Bertozzi, 2000), in which the nucleophilic aza-ylide can be captured by Staudinger reaction and intramolecular cyclization. Finally, the conjugated lipids can be separated by TLC and detected by fluorescence.

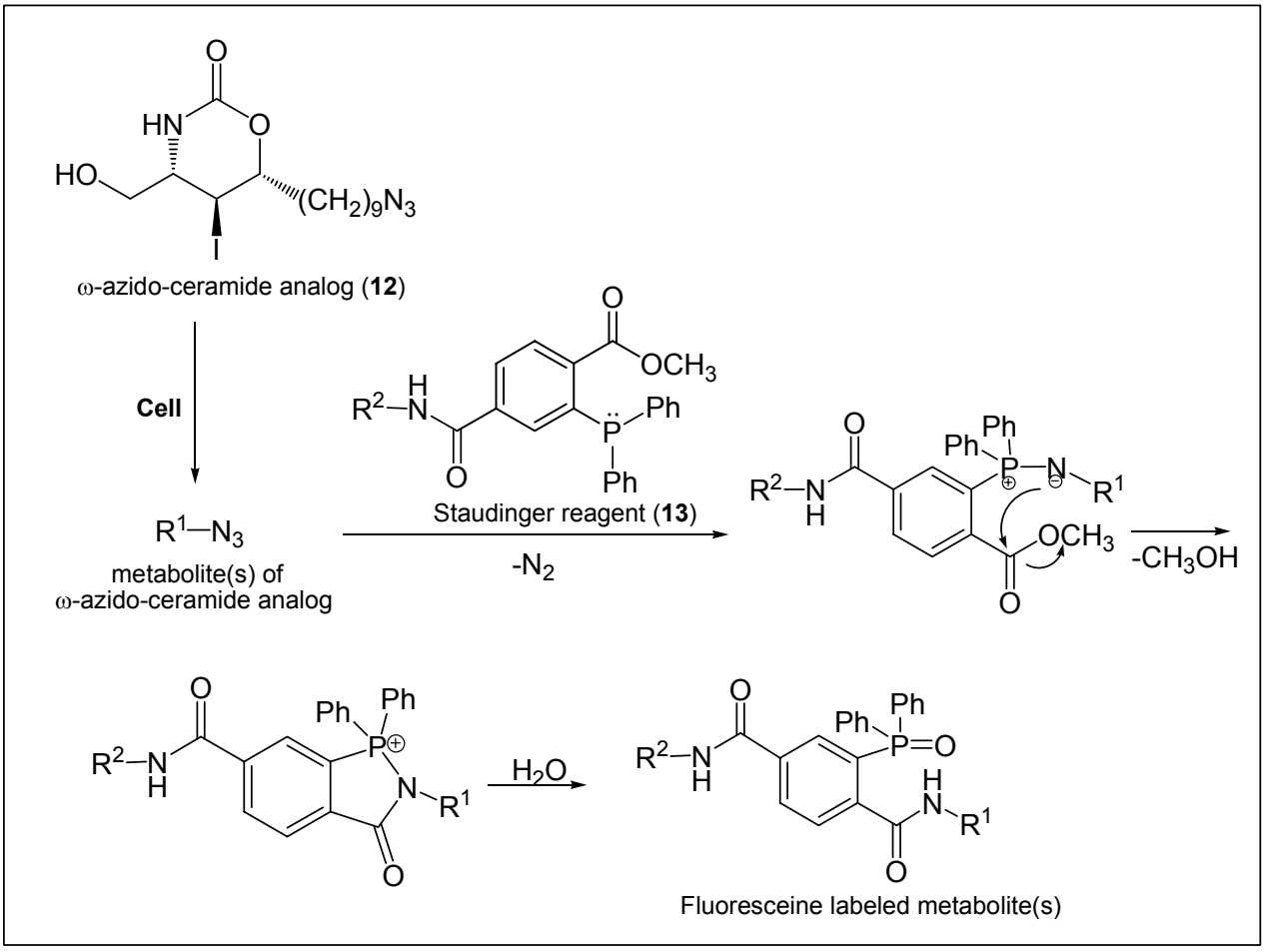

Scheme 4.12. Strategy for the detection of metabolites in cells with ω-azido-ceramides (modified from Wirtz and Kolter, 2007) based on Staudinger ligation (Saxon and Bertozzi, 2000). Cells are incubated with azido-containing ceramide derivatives, followed by bioorthogonal labeling with a phosphine-fluorescein reagent via a modified Staudinger ligation. Resulting labelled ceramide derivatives should be separated by tlc and visualized with UV (R^1 = metabolites of ω-azido-ceramide, R^2 = fluorescein).

For this approach, oxazinanone **12**, bearing an ω-azido-group in the alkyl chain was prepared (Figure 4.13). The synthesis started with the Wittig reaction of **2a** with the methyltriphenylphosphonium ylide generated from methyltriphenylphosphonium bromide with potassium bis(trimethylsilyl)amide (Campbell et al., 1998). The vinyl-derivative **14** was obtained in 92% yield. The terminal azido-group was introduced by two different strategies. In method A, first the alkyl chain was elongated via cross metathesis with undec-10-en-1-ol to give **15**, then the alcohol function was converted to the methanesulfonate and substituted with an azide by reaction with sodium azide in acetone. The desired product **16** was obtained from **15** in 23 % yield over 2 steps. Within the second strategy (**B**), the ω-azidoalkene was generated from undec-10-en-1-ol and the following cross metathesis with head group equivalent **14** generated **16** in 54 % yield. The iodocyclization was performed as described for **4b** (chapter 4.2.1) and led to **17** in 35 % yield. The oxazinanone **12** could be obtained in 71 % yield by acidic treatment of **17**. It has been reported that the Wittig reaction of the α-

amino aldehydes **2a** under the conditions used in this work, should provide the alkene **14** without loss of optical purity (McKillop et al., 1994). Since the enantiomeric purity of this **14** cannot be taken for granted, we still have to determine the optical purity. This can be done by cleavage of the isopropylidene group and converting the alcohol function into the Mosher ester, followed by NMR analysis. In the following steps, we have to synthesize the capture reagent (**13**) according to Saxon et al. (2007) and we have to test this approach in lipid extracts of fibroblasts.

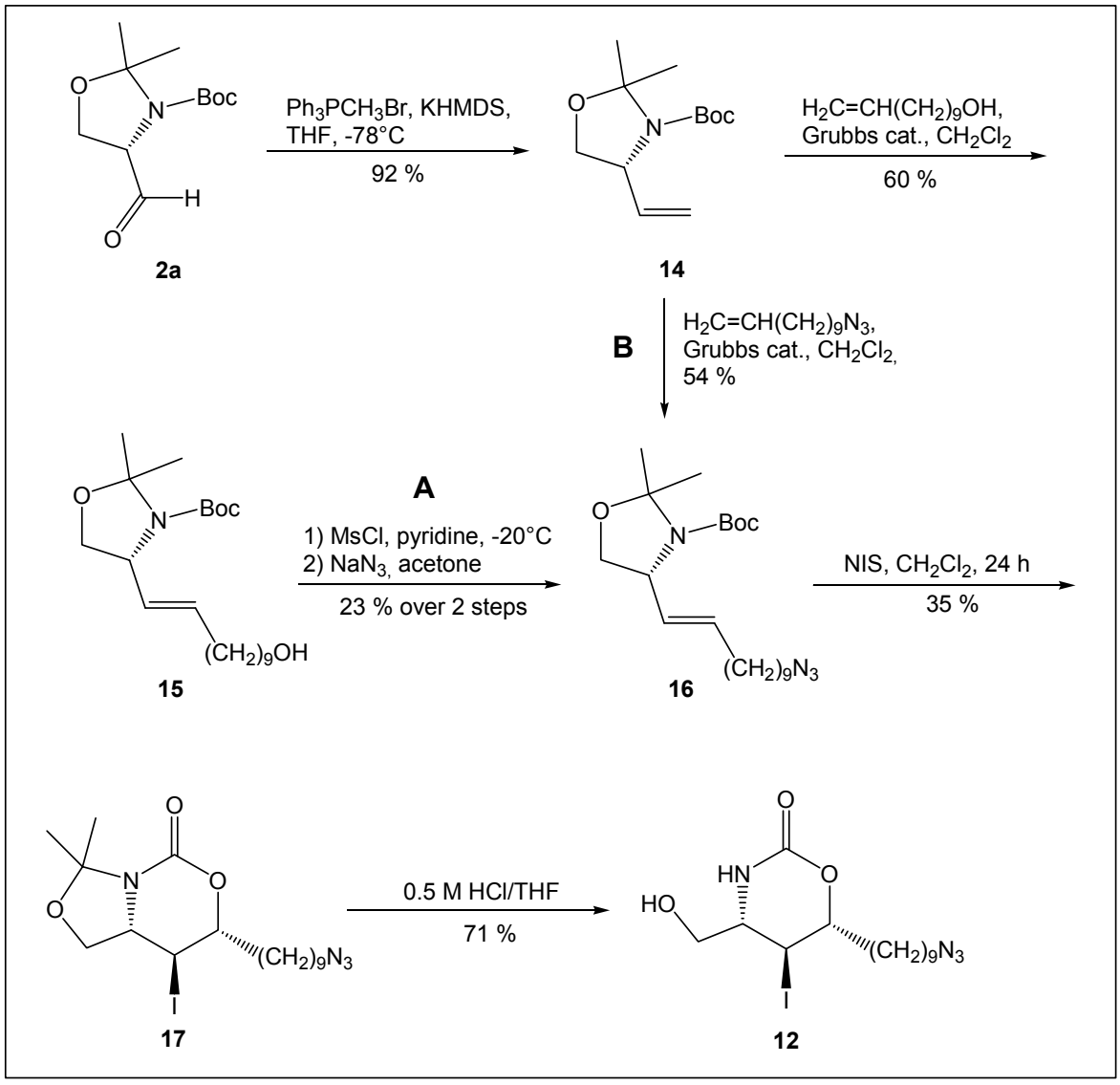

Figure 4.13: Synthesis of ω-azido-oxazinanone **12** (Abbreviations: KHMDS = Potassium hexamethyldisilamide; MsCl = Methanesulfonyl chloride; NIS = *N*-iodosuccinimide; Grubbs cat. 2nd generation = $C_{46}H_{65}Cl_2N_2PRu$.

4.5. Influence of oxazolidinone 5b on intracellular membrane flow

The major intracellular transport pathway coupled to the biosynthesis of membrane lipids, glycoproteins, and secreted proteins is exocytotic vesicle flow from the Endoplasmic Reticulum (ER) via the Golgi apparatus to the plasma membrane. Effects of different drugs that interfere with this intracellular membrane flow on GSL biosynthesis have been studied before (van Echten and Sandhoff, 1989). Brefeldin A (BFA), a fungal metabolite, disrupts the integrity of the Golgi apparatus by preventing the binding of small GTP-binding proteins, ADP-ribosylation factors (ARFs), and the coatomer coat proteins to Golgi membranes (Renault et al., 2003). Monensin, a cationic ionophore, interferes with vesicular processing between cis-and trans-cisternae of the Golgi apparatus (Tartakoff, 1983).

Previous studies (van Echten et al., 1990, van Echten and Sandhoff, 1989) have shown that treatment of cultured cerebellar granule cells with BFA or monensin result in a block of glycolipid biosynthesis on the stage of GlcCer, LacCer, gangliosides GM3, and GD3. These obtained pattern are qualitatively similar to the lipid patterns that are obtained in the presence of the cyclic carbamates **5a** and **5b**. In addition, it has been reported that some cell-permeable ceramide derivatives accumulate in the Golgi apparatus (Lipsky and Pagano, 1985), lead to an inhibition of protein transport on the level of the trans-Golgi (Rosenwald and Pagano, 1993), and lead to the fragmentation of the Golgi apparatus (Hu et al., 2005; Nakamura et al., 2002; Fukunaga et al., 2000).

To proof, if the synthetic ceramide derivatives **5a** and **5b** disrupt the integrity of the Golgi apparatus like BFA or C_6-ceramide and produce the altered lipid pattern by this mechanism, cultured cells were incubated with oxazolidinone **5b** and analyzed by fluorescence microscopy. Although the oxazolidinone **5b** showed no drastic alterations of GSL-pattern in fibroblasts as in neurons, we started with the analysis in cultured fibroblasts. The Golgi apparatus was stained with NBD-C_6-ceramide (see figure 4.15), according to (Pütz and Schwarzmann, 1995).

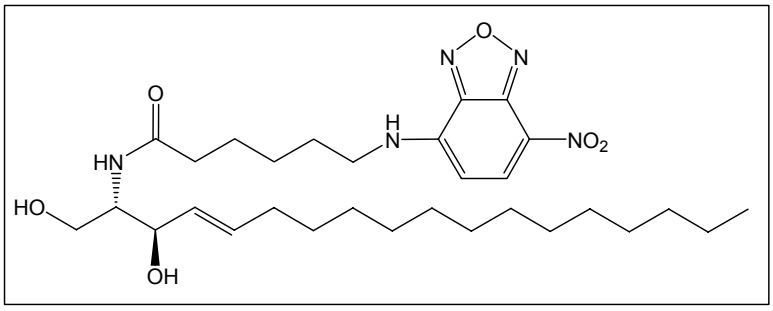

Figure 4.15. Structure of NBD-C_6-ceramide (*N*-[7-(4-Nitrobenz-2-oxa-1,3-diazole)]-6-aminohexanoyl sphingosine)

After addition to the culture medium of fibroblasts, NBD-C_6-ceramide can diffuse through the cytosol to the ER and the Golgi apparatus due to its short apolar acyl chain. In the Golgi apparatus, the fluorescent analog is metabolized to the sphingomyelin and glucosylceramide analogs, which cannot diffuse across membranes and are to some extent trapped at the site of their synthesis. C_6-NBD-ceramide is therefore a useful tool for labeling of the Golgi apparatus and to investigate morphological changes of the Golgi by fluorescence microscopy (Lipsky and Pagano, 1985).

The effect of **5b** on the Golgi membranes is shown in Figure 4.16. Cells treated with derivative **5b** underwent extensive Golgi vesiculation (Figure 4.16b), and reproduced the morphological phenotype of cells incubated with Brefeldin A (Figure 4.16c). We cannot conclude that the vesiculation of the Golgi-apparatus is responsible for or a consequence of the observed reduction of the biosynthesis of higher gangliosides in neuronal cells. Further experiments are required to clarify the mechanism of action that leads to the observed effects in cell culture.

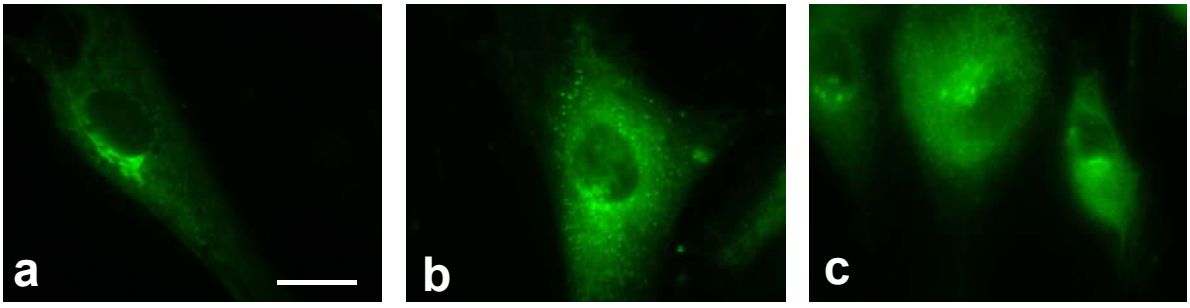

Figure 4.16: Effect of carbamate **5b** and Brefeldin A on the morphology of the Golgi apparatus in cultured cells. Human skin fibroblasts (a) were incubated with 25 µM of **5b** (b) for 24h and 1 µg/ml Brefeldin A (c) for 2h, stained with C_6-NBD-ceramide-BSA complex, and examined in the fluorescence microscope (scale bar: 20 µm).

4.6. Requirement of the iodine atom in 5a for the mechanism of action

To address the role of the iodine atom in oxazinanone **5a** at position C-5 for the alteration of lipid pattern in cultured cells, derivatives **18a** and **18b** were synthesized, in which the iodine is substituted by a hydroxyl-group. These compounds are conformationally restricted ceramide analogs with a higher structural similarity to the parent compound (ceramide) than **5a**.

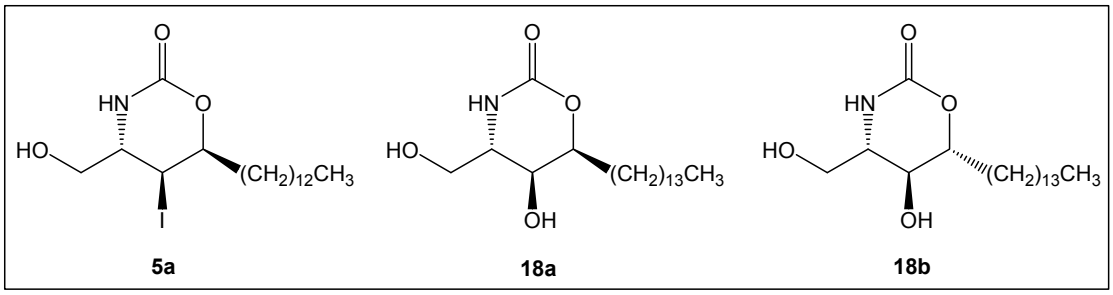

Figure 4.17

4.6.1. Synthesis

We decided to prepare the oxazinanones starting from phytosphingosine with selective protection of the 1,3-diol and intramolecular ring formation as key steps. Commercially available D-*ribo*-Phytosphingosine (figure 4.18) with a purity of 80% was the starting material in the syntheses of both oxazinanones. The synthesis started with the protection of the amino function of phytosphingosine by treatment with di-*tert*-butyl dicarbonate in 75% yield. The 1,3-diol in the *N*-Boc protected phytosphingosine (**19**) was protected by silylation with di-*tert*-butylsilyl ditrifluoromethanesulfonate (Hoberg, 1997), resulting in the silyl-derivative **20** in 62% yield. The 4-OH-group of compound **20** was then sulfonated by treatment with methanesulfonyl chloride in pyridine to give the methanesulfonate **21**. Key step in the synthesis of the desired compound is the intramolecular ring close reaction (Kemp *et al.*, 1996). The use of tetrahydrofurane as solvent and reflux reaction conditions resulted in the formation of compound **22a** in 75% isolated yield. Desilylation with tetrabutylammonium fluoride afforded **18a** in nearly quantitative yield (Corey and Hopkins, 1982).
Treatment of the silyl-derivative **21** with lithiumdiisopropylamide and intramolecular attack of the resulting oxyanion on the carbonyl group afforded **22b** in 82% yield. The silyl group was cleaved by treatment with a solution of *tert*-butylammoniumfluoride in THF at 0°C to afford the desired oxazinanone **18b** in 26% yield.
The absorption of the C=O stretch vibration in the infrared spectrum at 1654 cm^{-1} of **18a** and 1682 cm^{-1} of **18b** agree with those of related compounds in literature (Kemp et al., 1996). The trans,trans-relationship of the protons in compound **18b** is reflected by the values of the coupling constant ($J_{4,5} = J_{5,6} = 9.2$ Hz). On the other hand, the smaller coupling constant of the protons in trans,cis-relationship ($^3J_{5,6} = 2.4$ Hz) reflects the configuration of stereoisomer **18a**.

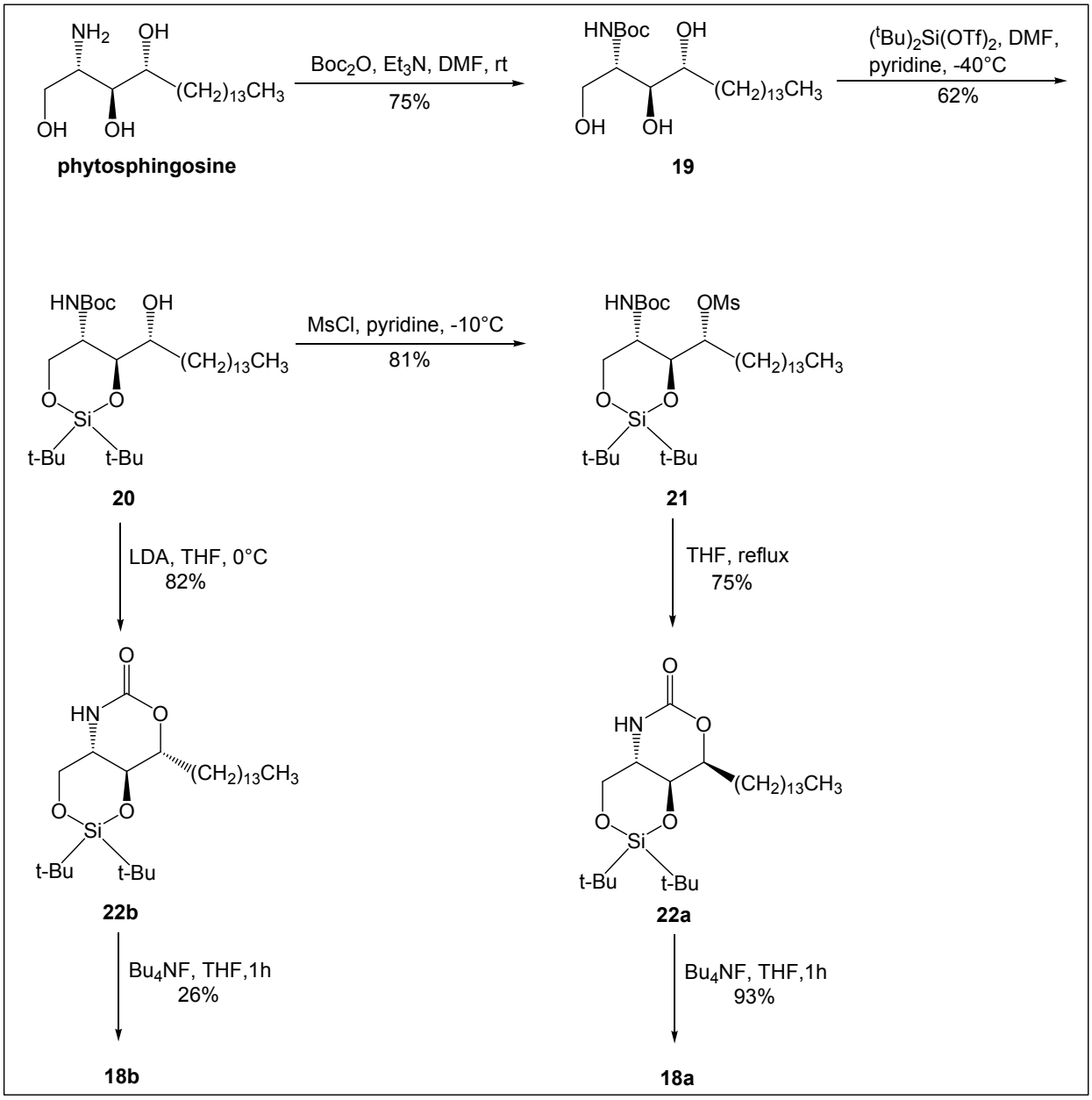

Figure 4.18: Synthesis of oxazinanone **18a** and **18b** starting from phytosphingosine

4.6.2. Effect of oxazinanones on glycolipid biosynthesis

To determine the influence of the iodine atom in compound **5a** on glycosphingolipid biosynthesis, the oxazinanones **5a**, **18a** and **18b** were tested in cultured murine cerebellar granule cells. Cells were pre-incubated with 50 µM target compounds in the culture medium for 24 h. L-[3-^{14}C]serine was added to the culture medium, and its incorporation into newly synthesized sphingolipids was analyzed after labelling for 24 h. Lipids were extracted, separated into acidic and neutral fractions, and glycerolipids were removed by mild alkaline hydrolysis. Desalted lipid extracts were separated by thin layer chromatography (TLC) and visualized by phosphoimaging.

Figure 4.19 shows the L-[3-^{14}C]serine incorporation into acidic glycolipids of control cells and of cells incubated with the heterocycles. In the presence of all tested compounds, the incorporation of L-[3-^{14}C]serine into SM was reduced. In the presence of **5a**, the formation of glucosylceramide (112% of control) and lactosylceramide (300% of control) is increased. Cells incubated with the iodine derivatives (**5a,b**), gangliosides GM3 and GD3 are clearly labelled compared to control cell (5 times higher), while the formation of higher gangliosides like GD1a, GT1b and GQ1b is reduced. Differences in the labeling profile between **5a** and **5b** might be due to inhibition of GalNAc-transferase by both compounds, which formation of GM3 and GD3 appears also to be reduced in the presence of **5a**. The influence of the hydroxy-derivative (**18a**) on serine-incorporation into these gangliosides is negligible. In the presence of oxazinanone **18a** an additional band (X_2) with a smaller retention factor that SM is found in the neutral lipid fraction. The nature of this band could not identified yet.

Together with the results from L-[3-^{14}C]serine labeling in cultured fibroblasts (chapter 4.2.3, Figure 4.5), these data indicate that the presence of a halogen atom (iodine, bromine) plays an important role for the biological effect on GSL biosynthesis.

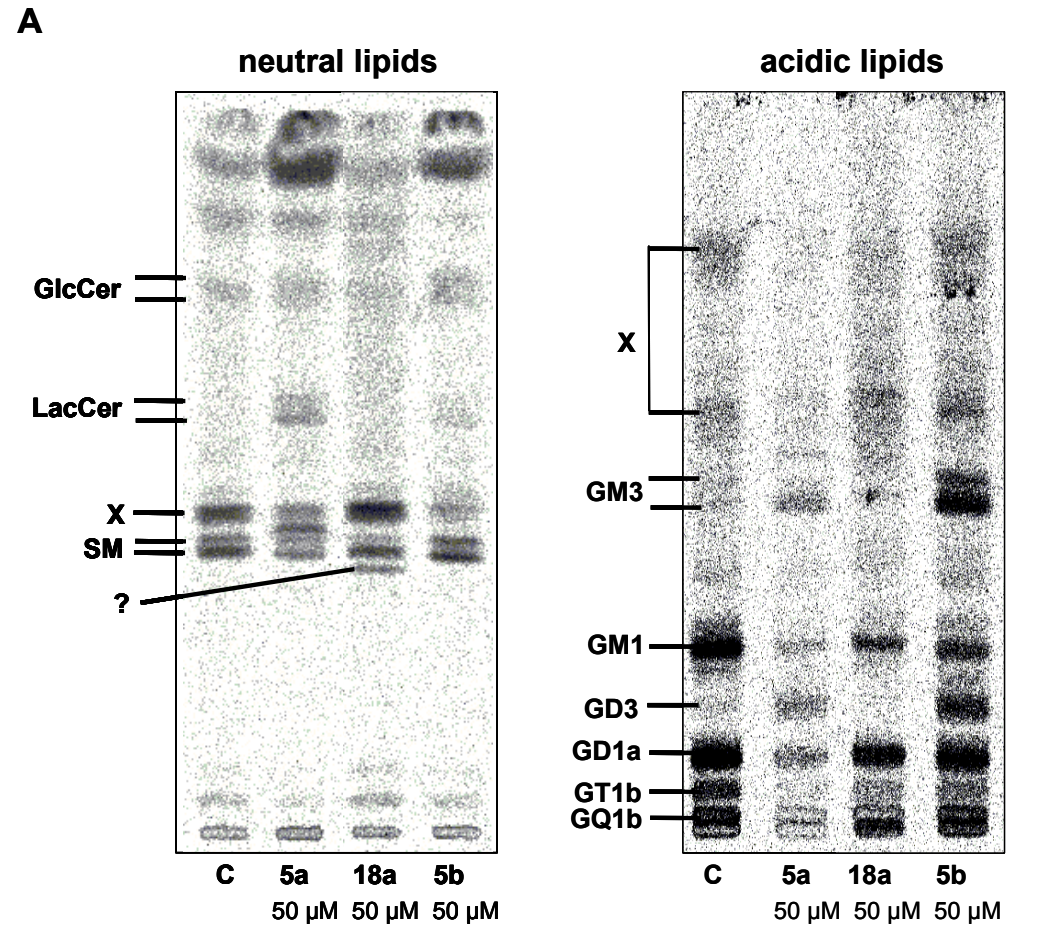

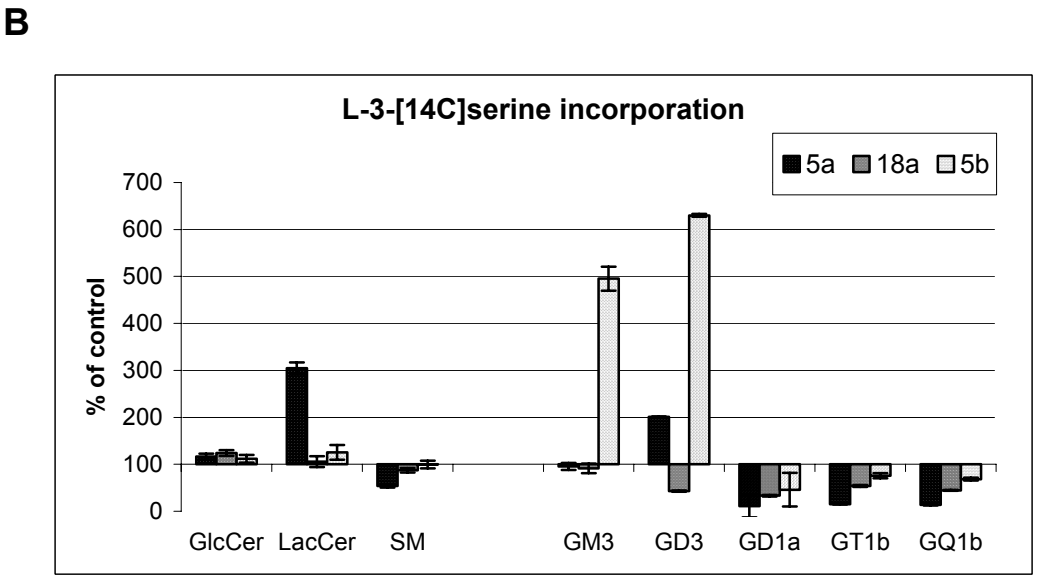

Figure 4.19: **Effect of oxazinanones on ganglioside biosynthesis in primary cerebellar neurons.** Cells were pre-incubated with 50 µM **5a**, **5b** and **18a** in culture medium for 24 h and pulse-labeled with L-[3-^{14}C]serine. After 24h, cells were harvested and subjected to lipid analysis. **A**: Total lipids were separated by tlc using the solvent system chloroform/methanol/0.22 % aqueous $CaCl_2$ 60:35:8 by volume (C = control). **B**: Radioactivity found in the TLC spots of untreated cells were set equal 100 %. The results of 2 experiments are given. Radioactivity was analyzed by phosphoimager analysis. Data are expressed as percentages of control values that were obtained by labelling cells with L-[3-^{14}C]serine in the presence of methanol. All data are given as mean values of two different experiments.

4.7. Synthesis and investigation of structurally modified cyclic carbamates

4.7.1. Synthesis of an 1'C-Methyl oxazinanone

A principle problem in the analysis of ceramide derivatives exogenously added to cells is their metabolic interconversion with other signaling molecules. The substitution of a proton by a methyl group in the head group of ceramide analogs can have consequences for the molecular recognition and the metabolic procession of the substance. Binding to specific proteins can be enhanced due to additional hydrophobic interactions, or binding can be reduced because of sterical hinderence in the binding pocket of the protein. Exogenously added ceramide derivatives can be modified to various metabolites in cultured cells. Modification of the 1-C should hinder the way by which the substances are metabolized, so that enhanced metabolic stability could be achieved.

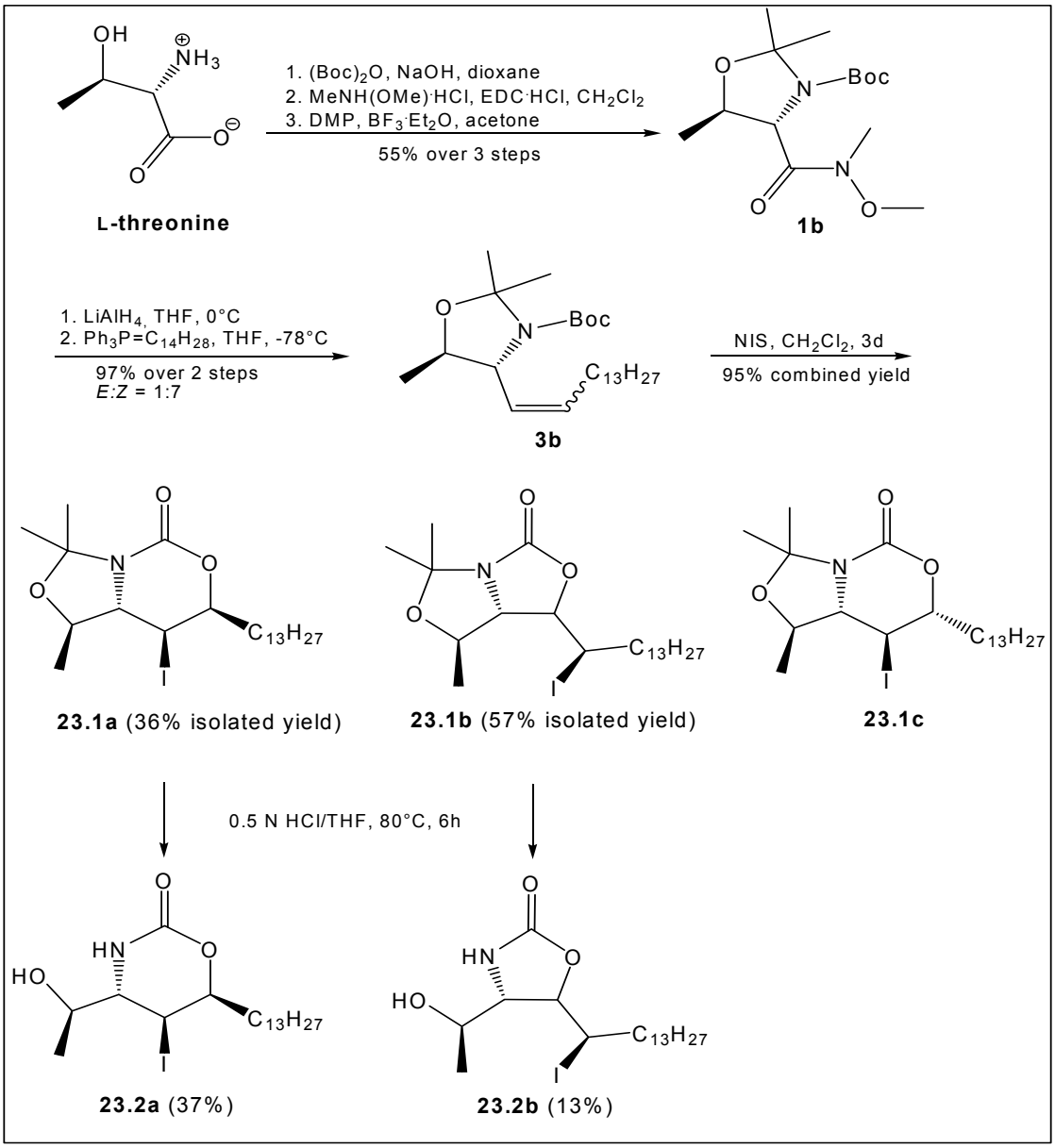

Figure 4.20: Synthesis of compounds **23a,b** starting from L-threonine. Abbreviations: EDC·HCl = *N*-(3-Dimethylaminopropyl)-*N'*-ethylcarbodiimide hydrochloride; DMP = 2,2-dimethoxypropane; NIS = *N*-iodosuccinimide

The synthetic route for the formation of target compounds **23.2a** and **23.2b**, which follows the preparation of the other iodolactones (**5a,b**), is shown in figure 4.20.
Weinreb amide **1b** was prepared from L-threonine in a yield of 55 % over 3 steps. The protected allylamine **3b** was prepared from the aldehyde derived from **1b** followed by a Wittig reaction in 97 % yield and selectivity of *E*:*Z* = 1:7. The bicyclic products from the cyclization reaction could be isolated by column chromatography in 36 % (for **23.1a**) and 57% (for **23.1b**). The desired products **23.2a** and **23.2b** were obtained by acidic treatment with hydrochloric acid in THF.

4.7.2. Effect of 1'C-Methyl oxazinanone 23.2a on sphingolipid biosynthesis

The properties of oxazinanone **23.2a** were investigated in cultured human fibroblasts. Cells were preincubated with **23.2a** for 24 h in concentrations of 5, 10, and 25 µM in the culture medium. L-[3-^{14}C]serine was added to the culture medium, and its incorporation into newly synthesized sphingolipids was analyzed after labelling for 24 h. Lipids were extracted, and glycerolipids were removed by mild alkaline hydrolysis. The desalted lipid extracts were separated by thin layer chromatography (TLC) and visualized by phosphoimaging (Figure 4.21 A). In the presence of the oxazinanone-derivatives **5a** and **23.2a** in the culture medium, the incorporation of L-[3-^{14}C]serine into sphingolipids was increased. This is in agreement with the results obtained from labeling experiments in fibroblasts in the presence of oxazolidinone-derivatives **5b** and **6** (chapter 4.2.3, Figure 4.5). The substitution of the proton by a methyl group leads to a more potent compound in regard to L-[3-^{14}C]serine incorporation into lactosylceramide. At concentration of 25 µM, the effect of **23.2a** is two-fold higher than that of **5a**. There is no explanation described in literature, why the biosynthesis of sphingolipids is increased in the presence of synthetic ceramide-derivatives. In following studies, we have to investigate the 1'C-Methyl derivatives **23.2a** and **23.2b** in cultured neuronal cells.

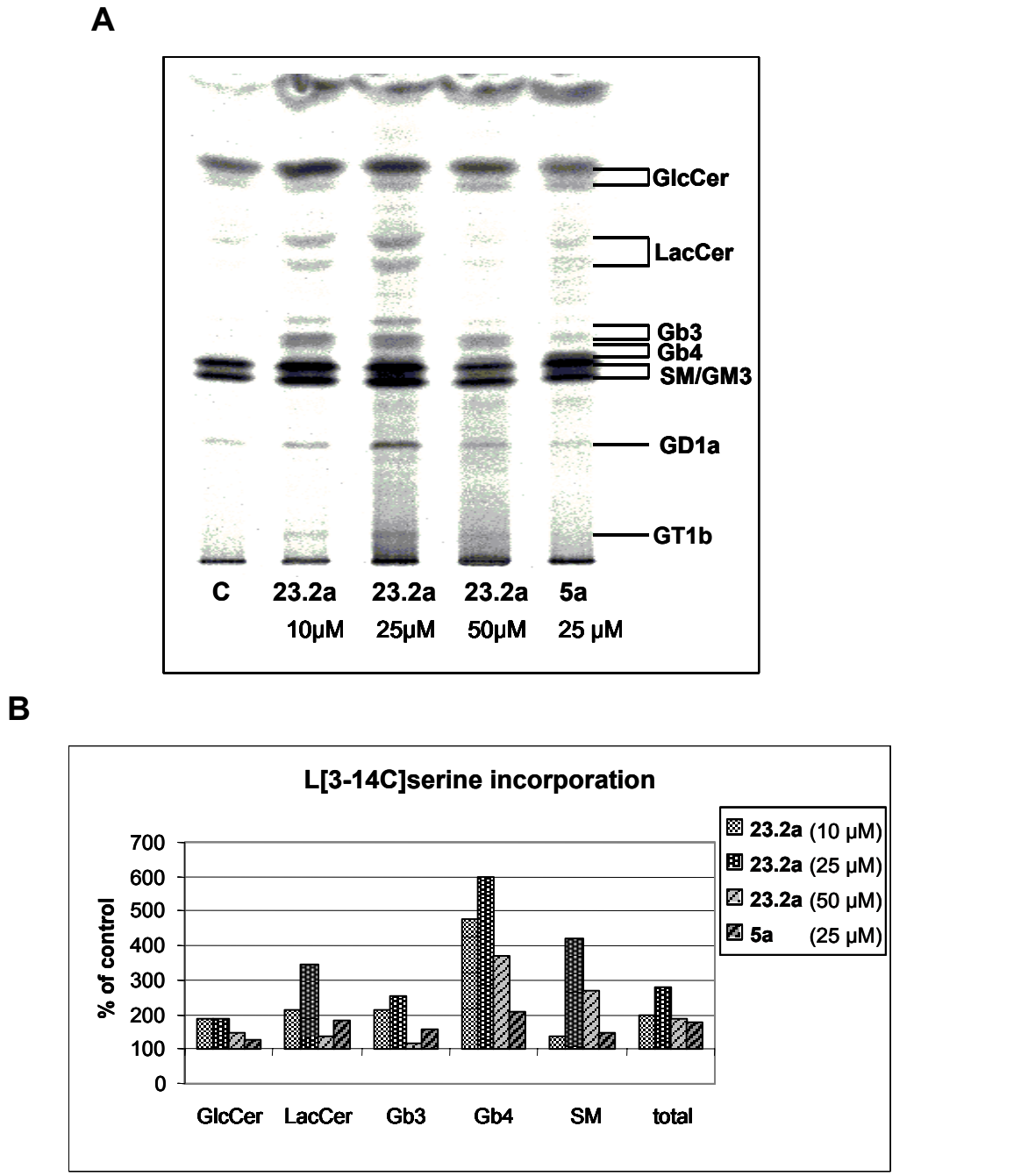

Figure 4.21: **Effect of oxazinanones 23.2a and 5a on the incorporation of L-[3-^{14}C]serine into sphingolipids of human fibroblasts.** Cells were treated with target compounds **23.2a** (10, 25 and 50 µM) and **5a** (25 µM) in the culture medium for 24h. Then, cells were fed with L-[3-^{14}C]serine in the presence of the tested compounds for 24h. Lipids were extracted, and glycerolipids were removed by alkaline treatment.
A: Sphingolipids were separated by thin layer chromatography using the solvent system: $CHCl_3$/MeOH/0.22% aqueous $CaCl_2$ 60:35:8 by vol. Radioactive bands were visualized by phosphoimaging. **B**: Radioactivity found in the TLC spots of untreated cells were set equal 100 %. Radioactivity was analyzed by phosphoimager analysis. Data are expressed as percentages of control values that were obtained by labelling cells with L-[3-^{14}C]serine in the presence of methanol.

4.8. Analysis of a Benzazepinone as a conformationally restricted ceramide analog

The Benzazepinone has been **24** (Figure 4.22) has been prepared in further studies (Sawatzki, 2003a) as a conformationally restricted ceramide analog. Previous labeling experiments with D-[^{14}C]galactose in the presence of **24** in primary neurons indicated an inhibition of sialyltransferase II at concentrations of 10 µM, and at higher concentrations (25 µM) inhibition of GalNAc-transferase.

To decide, if the conformational restriction or the presence of the bulky aromatic group within the benzazepinone is responsible for the observed effects in cell culture, the open chain analog **25** was prepared as described in chapter 4.8.1. It was tested in cultured neuronal cells on its influence of glycosphingolipid biosynthesis.

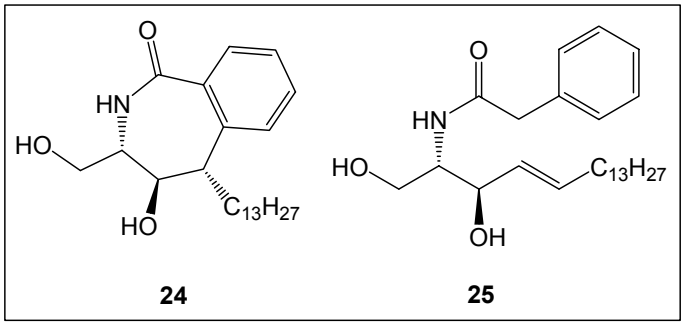

Figure 4.22: Benzazepinones **24** and *N*-Phenylacetylceramide **25**

4.8.1. Synthesis of *N*-Phenylacetylceramide (25)

To determine whether the conformation of the ceramide head group fixed in **24** or the aromatic ring inhibits the biosynthesis of glycosphingolipids, compound **25** was synthesized as open chain analog of **24**. The synthetic route is summarized in figure 4.23.

The sphingosine part of the molecule was prepared starting with alkynylation of Garner's protected aldehyde **1a** with a lithium alkyde to give a mixture of the diastereomers in a ratio of erythro:threo = 7:1 in 55% combined yield. The erythro-isomer **3c** was isolated by column chromatography with silica gel using the solvent system petroleum ether/ethylacetate (7:1 by vol.) in 24 % yield and was reduced with RedAl® to the alkene **26**. Although the transformation of the intermediate **3c** to **26** has been described to be efficient (65% yield by Herold, 1988; 71% by Sawatzki, 2003a). However, in our hands the transformation was less efficient, and the separation of the alkene **26** from the alkyne **3c** by column chromatography with silica gel, using the solvent system cyclohexane/ethyl acetate (5:1, by volume), yielded 8% of pure alkene **26**. After the protecting groups were cleaved off by acidic treatment, the amino group was acylated with phenylacetyl chloride in methanol. Although, the reaction procedure was not optimized, the target compound, *N*-Phenylacetylceramide, could be isolated in 11% over two steps.

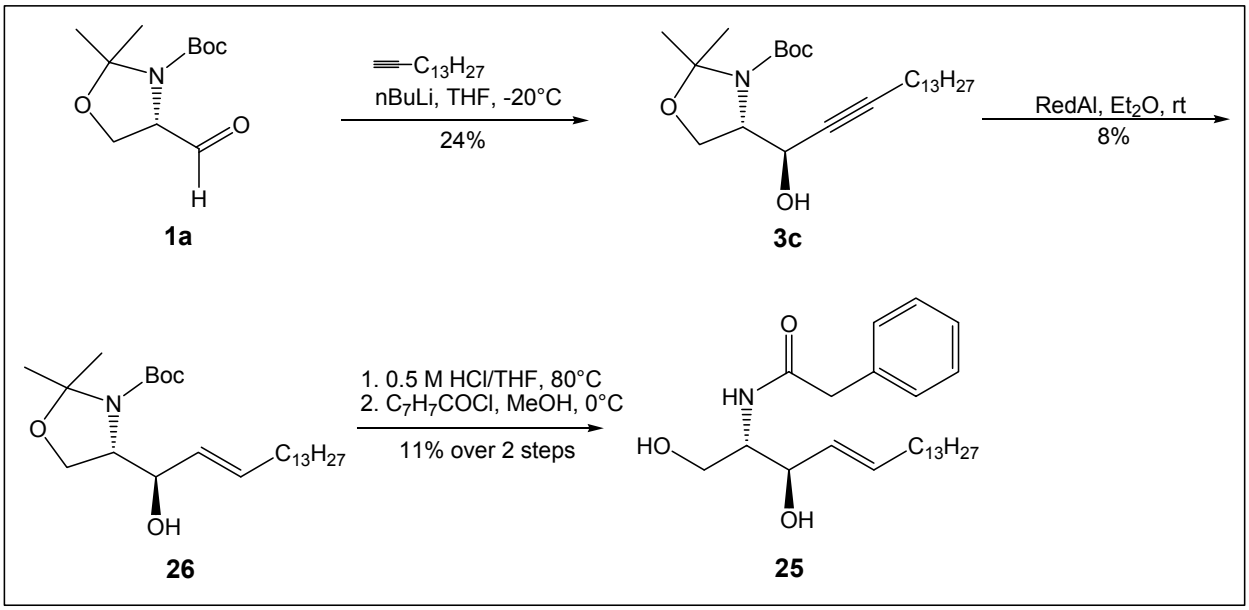

Figure 4.23: Synthetic route to compound **25** (RedAl® **=** Sodium bis(methoxyethoxy) aluminium hydride)

4.8.2. Investigation of ceramide derivatives 24 and 25 in cultured granule cells

The influence of the synthetic ceramide analogs **24** and **25** on GSL-biosynthesis was examined in cultured primary murine granule cells. Figure 4.24 shows the glycolipids of primary granule cells after labeling with D-[^{14}C]galactose in the presence of 25 µM synthetic ceramide analogs in the culture medium. Data are quantified in figure 4.24 B. In the presence of **25**, the incorporation of D-[^{14}C]galactose is increased in glucosylceramide (by 30% compared to control) and lactosylceramide (by 70% compared to control), as well as in gangliosides GM3 (by 60%), GM2 (by 40%) and GM1 (by 20%). At the same time, a reduction of labeling in gangliosides GD3 and GT1b is observed. These data indicate an inhibition of SAT-II and confirm with data obtained previously with the compound **24** by Sawatzki (2003a). A weaker effect on glycolipid biosynthesis is observed in the presence of the cyclic benzazepinone **24**. The patterns obtained in the presence of both synthetic ceramide analogs are comparable. This indicates that the hydrophobic phenyl ring plays a key role for the observed effects and appears to be more important than the conformational rrestriction. The nature of the lipid bands indicated as X1 and X2 could not be elucidated. X1 shows the same retention factor like sphingomyelin. Labeling of this lipid may result from degradation of galactose and the subsequent biosynthetic incorporation of radiolabeled fatty acids into sphingomyelin.

The influence of the synthetic ceramide derivative **25** has also been tested in cultured human fibroblasts. 25 µM *N*-Phenylacetylceramide (**25**) in the culture medium showed cytotoxic effects after incubation of the cells for 24 h. This might be due to the higher membrane content and apoptotic protection of neurons. It can be expected, that compound **25** behaves like a short-chain ceramide (C_2- and C_6-ceramide). It has been described, that exogenous addition of short-chain ceramides to cultured cells leads to apoptotic responses, while the saturated form dihydroceramide has no effect (Bielawska et al., 1993). It can be expected that hydrogenation of the double bond in **25** should lead to a less toxic compound that should be more compareable compound to **24**.

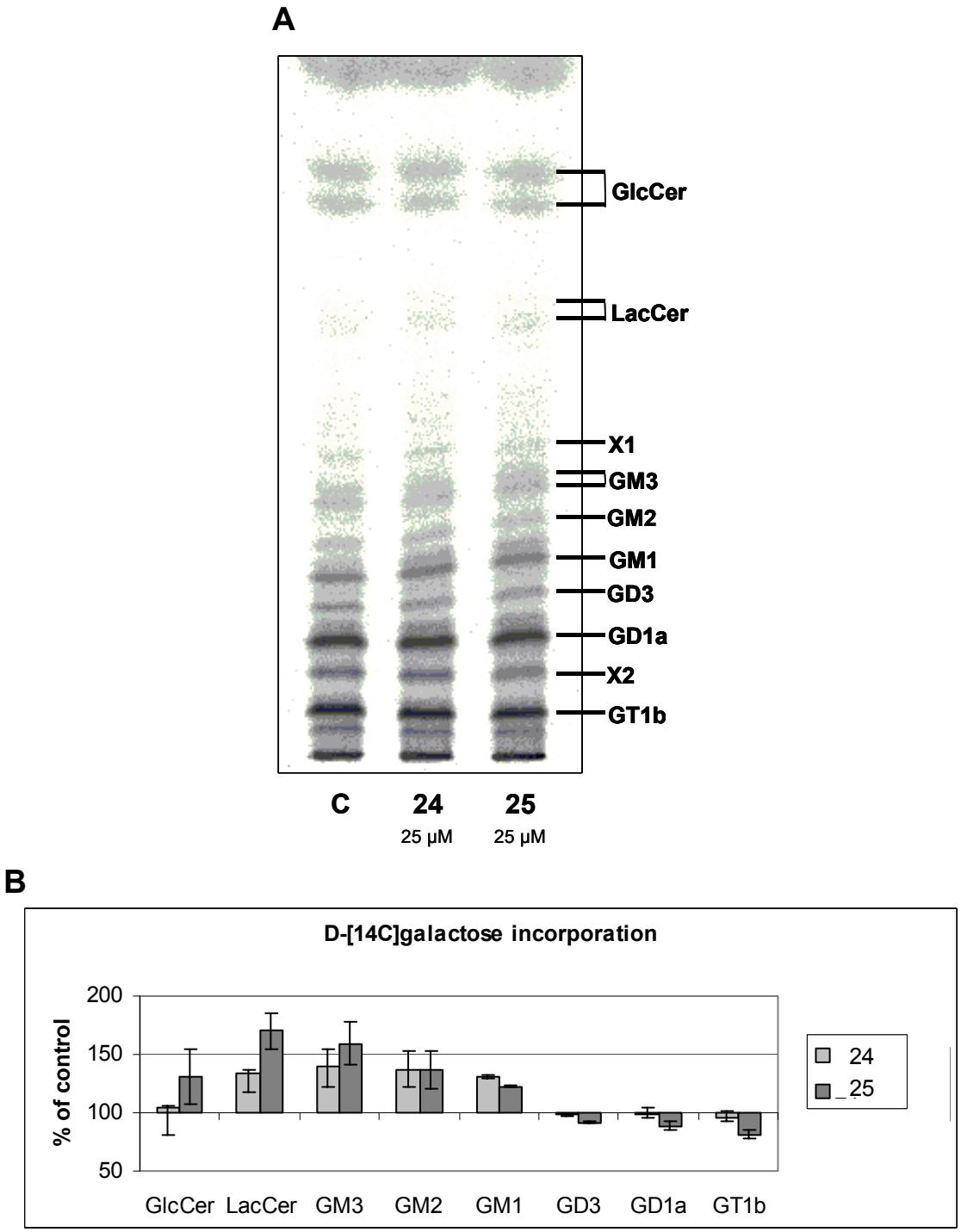

Figure 4.24: **Effect of benzazepinone 24 and *N*-Phenylacetylceramide 25 on the incorporation of D-[^{14}C]galactose into glycolipids of cerebellar cells.** Cells were treated for 24h with 25 µM test compounds. Then cells were fed with D-[^{14}C]galactose in presence of the test compounds for 24h. Lipids were extracted, separated into acidic and neutral fractions, and glycerolipids were removed by alkaline treatment. **A**: Lipids were separated by thin layer chromatography using the solvent system: $CHCl_3$/MeOH/0.22% aqueous $CaCl_2$ 60:35:8 by vol. The lipids were visualized by autoradiography. (X1 and X2 = identity of this bands was not analyzed). **B**: Radioactivity found in TLC spots of untreated cells was set equal 100%. All data are given as means ± range of two experiments.

4.9. Investigation of the influence of 5b and 24 on PKC activity

Ceramide is known to bind to and to regulate the activity of specific isoforms of Proteinkinase C (Huwiler et al., 1998, Wang et al., 2005, Bourbon et al., 2000). Proteinkinase C (PKC) represents a family of 12 serine/threonine kinase isoforms that differ in structure, substrate specificity, expression, and localization. PKC is involved in the regulation of several cellular functions such as cell growth and proliferation, gene transcription, and protein synthesis. Many of PKC target substrates are components of signal transduction pathways and include proteins that regulate ion channels, structural and regulatory proteins of the cytoskeleton, and many other proteins. The activity of two glycolipid glycosyltransferases, GalNAc-T and Sia-T2, are regulated by protein kinase A- and protein kinase C-related phosphorylation systems (Bieberich et al., 1998). Bieberich and co-workers examined the effect of exogenous applied protein phosphatase inhibitors (okadaic acid and orthovanadate) and protein kinase activators (phorbol ester and forskolin) on GalNAc-transferase activity. By metabolic labeling studies in NG108-15 (mouse/rat, neuroblastoma-glioma hybrid cells), they could show that stimulation of intracellular phosphorylation leads to an enhancement of the relative amount of a-series gangliosides derived from ganglioside GM3. It can be expected that exogenously added ceramide derivatives might lead to modulation of cellular kinase systems and in this way influence glycosyltransferase activities.

To analyse if the synthetic ceramide analogs **5b** and **24** have a regulatory effect on protein kinase activity, *in vitro*-experiments were performed with PKC isolated from rat brain. The enzyme used in this assay was obtained from Promega and consists primarily of PKC-α, β and γ isoforms with lesser amounts of δ and ξ isoforms. The micellar assay is based on a rhodamine-labeled fluorescent peptide that is phosphorylated by PKC according to a literature protocol (Isbell et al., 1995). In agarose gel electrophoresis (0.8% agarose in 50 mM Tris-HCl, pH 8.0), the phosphorylated peptide migrates toward the anode, while the non-phosphorylated peptide migrates toward the cathode. PKC activity was quantified by analysis of the relative fluorescence intensity of the spots in the photograph of the gel estimated under UV-light (λ = 365 nm) and additionally by excision of the fluorescent bands and measuring their relative fluorescence. To minimize diffusion of the bands, the photograph and the spectrofluorimetric analysis were performed as rapidly as possible after electrophoresis. Figure 4.25 (A) is a photograph of an agarose gel with samples from different experiments. Two bands were separated by electrophoresis. Substrate alone (lane 1) migrated to the cathode, while addition of PKC (lane 2) resulted in the migration of phosphorylated substrate towards the anode. Lanes 3 to 5 represent assays, which were made in the presence of 200 nM PMA (phorbol-12-myristate-13-acetate, lane 5), 50 µM ceramide derivative **5b** (lane 3), and 50 µM ceramide derivative **24** (lane 4) in the assay buffer. Phorbol esters like PMA are described as specific activators of PKC (Ryves et al., 1991). The increase of PKC activity in the presence of 200 nM PMA in the assay buffer (140 % of control) is in agreement with reported data (Isbell et al., 1995). In the presence of ceramide derivative **5b**, a minimal inhibitory effect on PKC activity (95 % of control) was observed, while in the presence of **24** no significant change of PKC activity could be observed. From these results we conclude that PKC is not activated by the synthetic ceramide derivative, but we cannot exclude that the protein kinase A- and protein kinase C-related phosphorylation systems in the cell are indirectly activated.

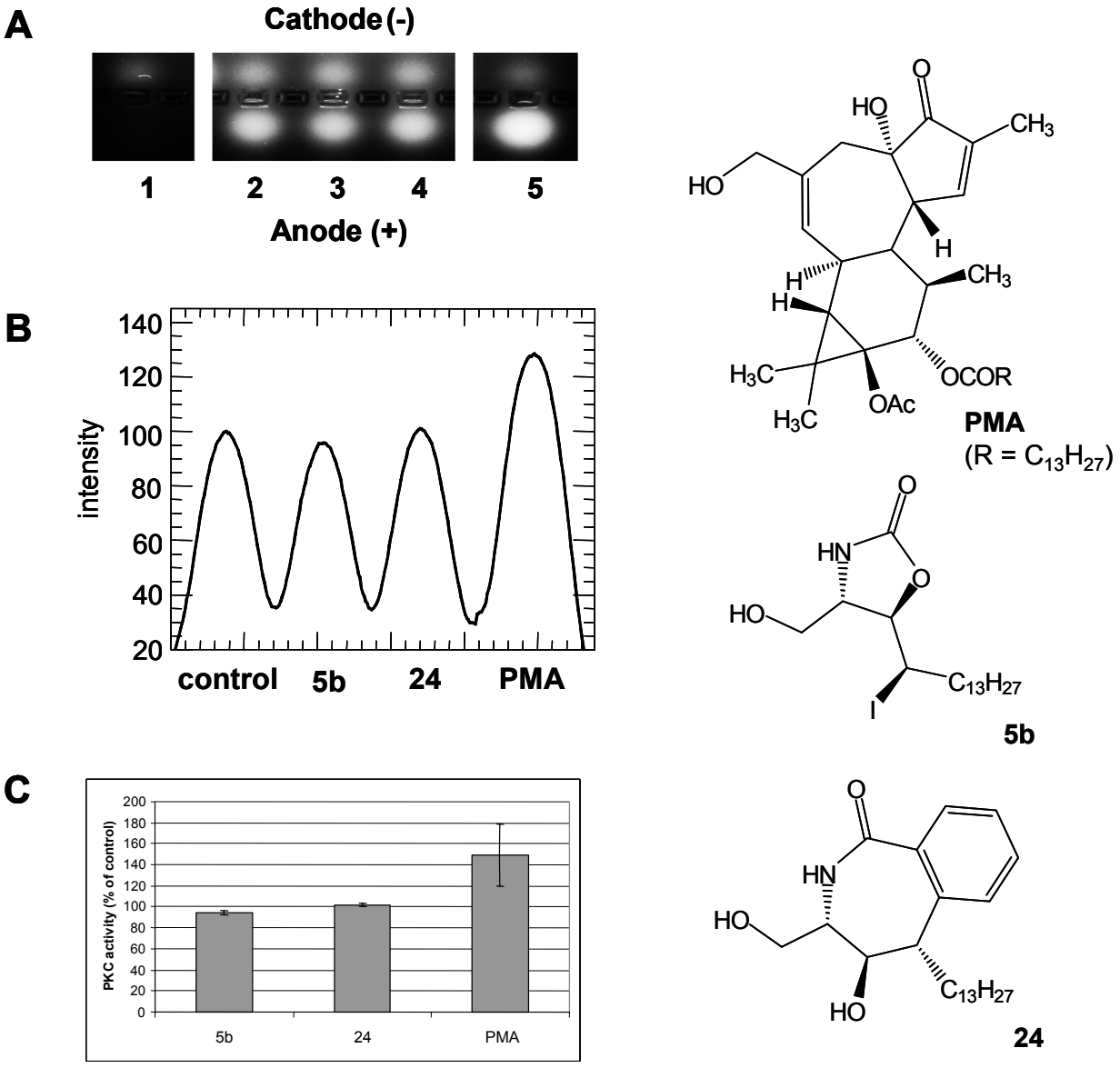

Figure 4.25. **Influence of PMA (phorbol-12-myristate-13-acetate) and ceramide derivatives (5b and 24) on PKC activity.** (**A**) Photograph of an agarosegel. Bands were visualized under UV-light (λ = 365 nm) and photographed. Well 1 and 2 represent control samples containing no PKC (1, negative control) and containing 0.25 µg PKC (2, positive control). Wells 3-5 represent samples containing 0.25 µg PKC and **5b** (50 µM, well 3), **24** (50 µM, well 4), and **PMA** (200 nM, well 5) in the assay buffer. (**B**) Relative intensity of the product bands that moved towards the anode were determined using X-software. (**C**) Fluorescent bands were excised, solubilized, and fluorescence measured by spectrofluorometry (as described in the material and methods section, chapter 6.5.15). Measured intensity of positive control (lane 2) was set equal 100 %. The results of 2 independent experiments are given.

4.10. Synthesis of internal standards for glycolipid quantification by mass spectrometry

4.10.1. Synthesis of C_6-GM3 (30)

The metabolic labeling experiments (chapter 4.2.2, 4.2.3, 4.6.2, and 4.8.3) gave no information on changes of the total content of cellular sphingolipids in response to exogenously added ceramide analogs. For pharmacological applications, it is important to know how differences in sphingolipid biosynthesis translate into alterations in the total content of certain GSL species. Mass spectrometric quantification gives more detailed information about the quantitative ceramide composition of individual GSL species, which could vary between different samples. To quantify the amount of ganglioside GM3, a standard substance of closely related structure is required that is not occurring in the investigated cell type. As an internal ganglioside standard for the quantification of GM3/GM2 levels in lipid extracts, we chose ganglioside GM3 with a capronic acid in the ceramide moiety (**30**). It was synthesized following the reaction scheme outlined in figure 4.28. In this work, only the last step was carried out.

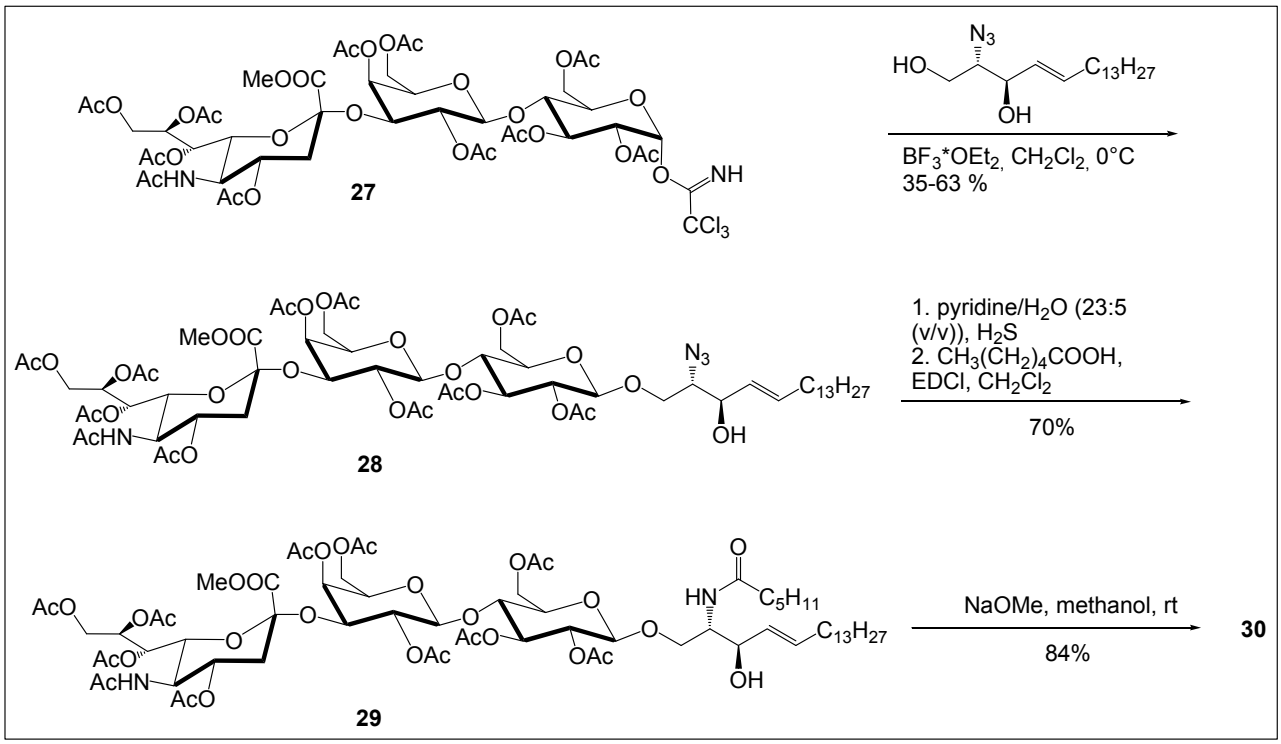

Fig. 4.28: Synthesis of a ganglioside GM3 derivative **30** as standard substance for the determination of GM3-levels in cultured cells by mass spectrometry. Peracetylated C_6-GM3 (**29**) was prepared and kindly provided by Karl Clasen (1994).

The synthesis started with the condensation of azidosphingosine (Zimmermann et al., 1988) with the peracetylated 1-O-trichloroacetimidate of 3'-Sialyllactose methyl ester (**27**). The azide function was reduced with hydrogen sulfide in pyridine (Zimmermann and Schmidt, 1988), and the resulting amine was acylated

with capronic acid and EDCI to give **29**, which was kindly prepared by K. Clasen. Cleavage of the O-Acetyl groups with sodium methanolate and purification by reverse-phase chromatography yielded the ganglioside derivate **30** in 84% yield.

The synthetic ganglioside C_6-GM3 (**30**) was analyzed by Nano-ESI-MS/MS to determine its suitability as internal standard for mass spectrometric analysis of ganglioside levels in lipid extracts. The product ion spectra of ganglioside C_6-GM3 (**30**) is shown in figure 4.29. Cleavage of the glycosidic bonds of the $[M-H]^-$ ion of **30** produce fragments corresponding to C_6-lactosylceramide (*m/z* 720), C_6-glucosylceramide (*m/z* 558), and C_6-ceramide (*m/z* 396). The most abundant fragment in the spectra is the ion of *m/z* 290, which corresponds to *N*-acetyl dehydroneuraminic acid. This fragmentation pattern is in agreement with those described for natural gangliosides (Whitfield et al., 2000).

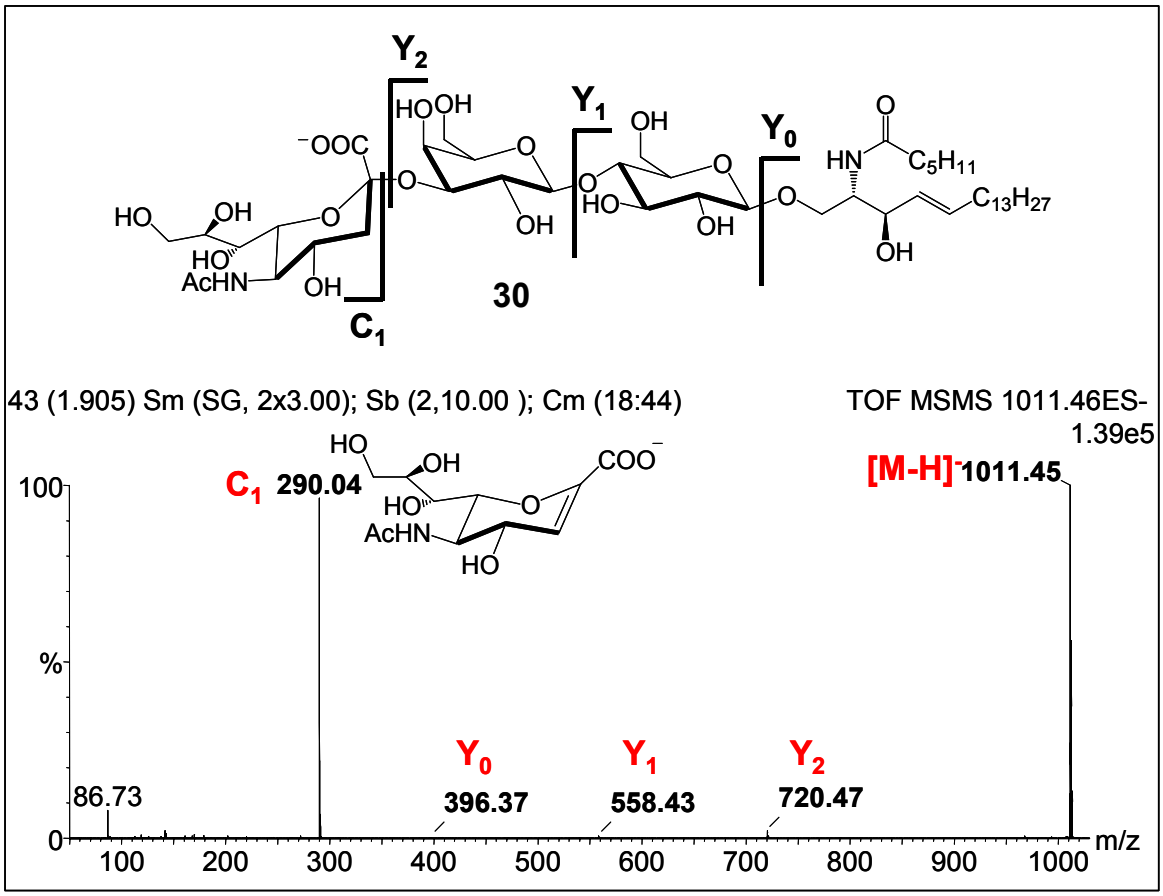

Figure 4.29: ESI-MS/MS spectrum of the $[M-H]^-$ ion of gangliosideC_6-GM3 (**30**).

4.10.2. Synthesis of C_{17}-sulfatide (34)

During this work, a C_{17}-sulfatide derivative was synthesized for the determination of sulfatide levels in biological samples. Sulfatide (galactosylceramide-3-sulfate) is a glycolipid found in high concentrations in the myelin sheats in the white matter of the brain as well as Schwann cells of the peripheral nervous system and in the kidney. In lower concentrations, it is also found in serum, granulocytes, and red blood cells. Sulfatide is implicated in diverse biological processes including the regulation of insulin secretion (Buschard et al., 2005), neuronal development, modulation of blood coagulation, and tumor cell metastasis (Ishizuka, 1997). Alterations in sulfatide metabolism are present in Alzheimer's disease and are associated with metachromatic leukodystrophy (von Figura et al., 2001).

The C_{17}-sulfatide derivative was already synthesized by Kim et al., 2004 as described in figure 4.30. The synthesis started with the deacylation of natural bovine brain sulfatide with sodium hydroxide in ethanol to form the lysosulfatide in 14% yield. C_{17}-Sulfatide (**34**) was obtained by a base-mediated reacylation of the lyso-sulfatide (**32**) using the *N*-hydroxysuccinimide ester **33** and was isolated by column chromatography in 17% yield. The intermediate **33** was prepared from reaction of C_{17}-fatty acid with *N*-hydroxysuccinimide in the presence of EDC (1-ethyl-3-(3-dimethylaminopropyl) carbodiimide) following the method by Lapidot et al., 1967.

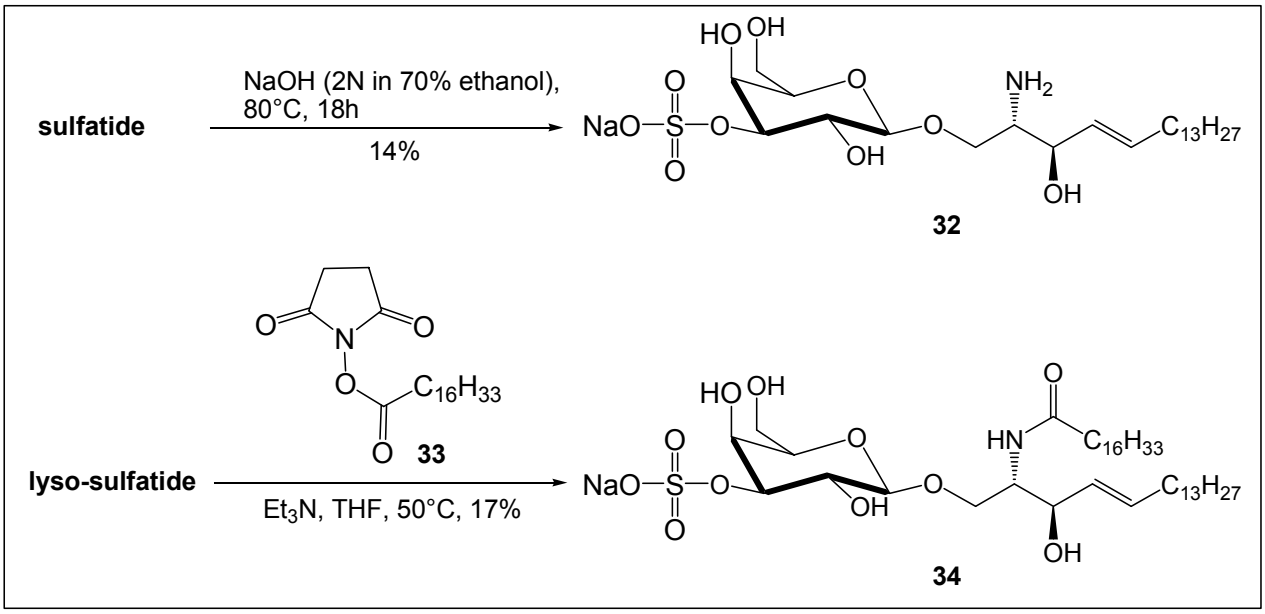

Figure 4.30: Synthesis of a sulfatide derivative **34** as standard substance for the determination of sulfatide-levels in cultured cells by mass spectrometry.

The synthetic C_{17}-sulfatide was analyzed by ESI-MS/MS in negative ion mode (Figure 4.31). The $[M-H]^-$-ion forms two characteristic fragment ions. The cleavage of the glycosidic bond forms a fragment of *m/z* 240 (C_2-H_2O), and cleavage of the sulphate group forms a fragment ion of *m/z* 96 (C_1). The fragmentation pattern is in agreement with previous data published for natural forms of sulfatide (Whitfield et al., 2000).

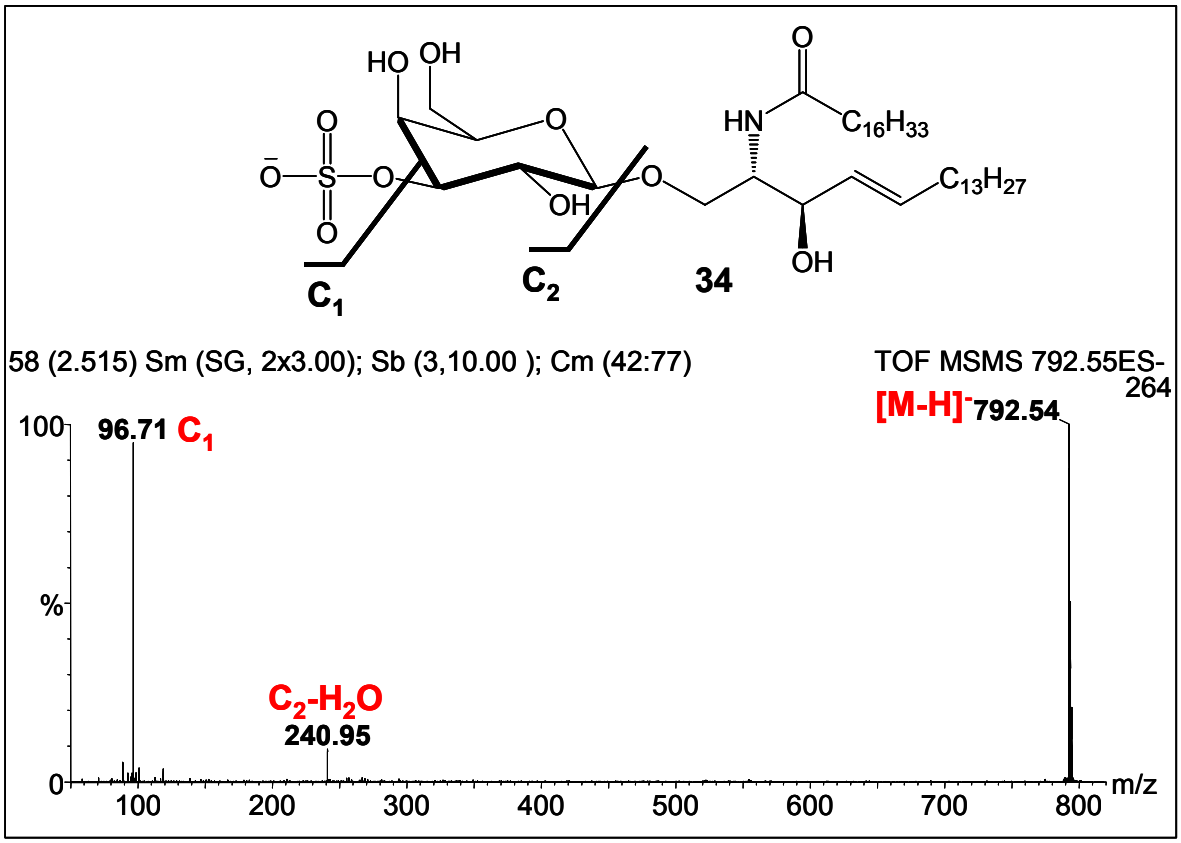

Figure 4.31: ESI-MS/MS spectra of the $[M-H]^-$ ion of C_{17}-cerebroside sulfate (**34**).

5. Discussion

5.1. General

Sphingolipids comprise an important group of structurally diverse biomolecules. They are structural components of the plasma membrane of eukaryotic cells and are thought to play a role in the regulation of various cell functions. In order to gain further insights into the biological and biophysical functions of sphingolipids, genetically engineered mice have been generated that have defined defects in certain steps of sphingolipid metabolism. In addition, also efforts have been made to design synthetic ceramide analogs as chemical tools to alter intracellular sphingolipid levels (Brodesser et al., 2003; Degaldo et al., 2007). Several ceramide analogs have been investigated as potential enzyme inhibitors or as ligands of putative ceramide binding proteins that are of pharmacological relevance (Wendeler et al., 2005). Ceramide and ceramide analogs exogenously applied to cultured cells can induce a variety of complex effects, including metabolic transformation and apoptotic responses, that complicate the analyses of their function. Ceramides with selectivity for one of the putative ceramide binding proteins are potential means to characterize the proteins involved, and to influence their respective pathways. In addition, for pharmacological application of ceramide derivatives it is important to reduce side-effects. A substantial aim of this work was to analyze the effect of conformationally restricted ceramide analogs on cellular lipid metabolism. Several heterocyclic ceramide derivatives were designed, synthesized, and tested in cultured neurons, which express complex gangliosides. The major effect of these ceramide derivatives was their unexpected interference with the biosynthesis of complex glycosphingolipids. These data could not have been arisen from *in vitro*-experiments with ceramide-metabolizing enzymes, since their potent and unexpected effects are indirect and require a cellular environment. As it will be discussed below, some of the observed effects were specific for nerve cells, and did not occur, at least to the same extent, in the much more easily cultured fibroblasts. The investigated substances are of particular importance, since there are still no inhibitors available for enzymes that catalyze the formation of complex gangliosides. The availability of such substances would permit the evaluation of new types of substrate reduction therapy of sphingolipidoses (chapter 5.2.2) and might serve as pharmacological equivalents to glycosyltransferase knockout mice.

5.2. Halogen-containing oxazinanones as conformationally restricted ceramide derivatives

5.2.1. Synthesis

The conformationally restricted ceramide analogs **5a** and **5b** (chapter 4.2.1, figure 4.2) represent scaffolds that present the 1-OH-group, the amide group, and one of the alkyl chains of ceramide in a defined conformation. However, the 3-OH-group of ceramide has been replaced by an iodine atom, which turned out to be crucial for their effect on GSL metabolism in cultured cells. They have been prepared in a

sequence of 3 reaction steps starting from Garner's aldehyde. Key steps in the synthesis were the Wittig reaction and an iodocyclization reaction. The synthetic route permits the preparation of structurally related compounds like the alkyne-derivatives **10.2a** and **10.2b** (chapter 4.4.3, figure 4.11), the 1-methyl-derivatives **23a** and **23b** (chapter 4.7.1, figure 4.20), the azido-derivative **12** (chapter 4.4.3, figure 4.13), and the bromo-derivatives **7.2a** and **7.2b** (chapter 4.2.3, figure 4.4) for structure-activity analysis. The bromine derivative **7.2b** was prepared in a manner similar to the synthesis of the iodine derivative, but using NBS (*N*-Bromosuccinimide) instead of NIS (*N*-Iodosuccinimide). We observed that treatment of the *N*-Boc-protected allylic carbamates (**3a**, **3b**, **9** and **21**) with NIS resulted predominantly in the formation of the corresponding oxazolidinone-derivatives (**4b**, **10.1b**, **22b**, **7.1b**) by a 5-exo cyclization. Generally, the regioselectivity of the iodocyclization can be influenced by the substitution pattern of the alkene, the choice of the *N*-carbamate (Boc or Cbz), and the choice of the electrophile (NIS or I_2). The isolated yield of the bicyclic products was limited due to the difficulties in the separation of the isomers by column chromatography with silica gel. Only isolated yield of pore substances were given. The relative stabilities of the isopropylidene groups towards hydrolysis changed with the structure of the ring system. The oxazolidinone-derivatives were cleaved under acidic conditions at room temperature, while the oxazinanone-derivatives were unaffected by treatment under the same reaction conditions. In this case, the reaction mixture had to be heated to 80°C. Longer reaction times and increasing reaction temperature were accompanied by an increase in the amount of side-products, e. g. by the elimination of hydrogen iodide and the formation of compound **35** (Figure 5.1), which was reflected in the lower isolated yield of the desired deprotected products (Figure 5.1). The oxazolidinone-derivatives could be isolated in 37% - 97% yield, the oxazinanone-derivatives only in 13% - 26% yield.

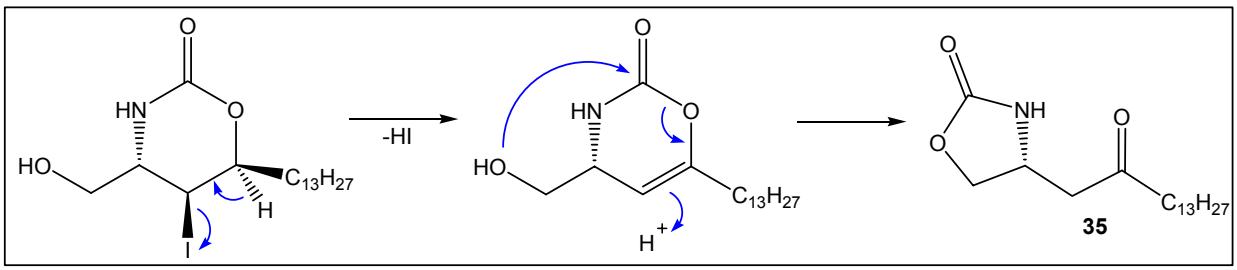

Figure 5.1

To evaluate the role of the iodine-group in compound **5a** for the observed effects, the hydroxylated compounds **18a** and **18b** (chapter 4.6) were synthesized for structure-activity analysis. In previous experiments, the hydroxylated oxazinanone should have been prepared by substitution of the iodine in **4a** by an oxygen-nucleophile (Sawatzki, 2003a; Figure 5.2). However, treatment of **4a** with silver acetate in acetic acid resulted in the formation of compound **36** by an anionotropic 1,2-rearrangement-like reaction (Hüsken, 2005). Therefore, we elaborated an alternative strategy and synthesized the oxazinanones starting from commercially available phytosphingosine (chapter 4.6.1, figure 4.18), with selective protection of the 1,3-diol and intramolecular ring formation as key steps. By this strategy, we obtained the oxazinanone **18a** in 26 % yield over 5 steps, and the oxazinanone **18b** in 10 % yield over 4 steps.

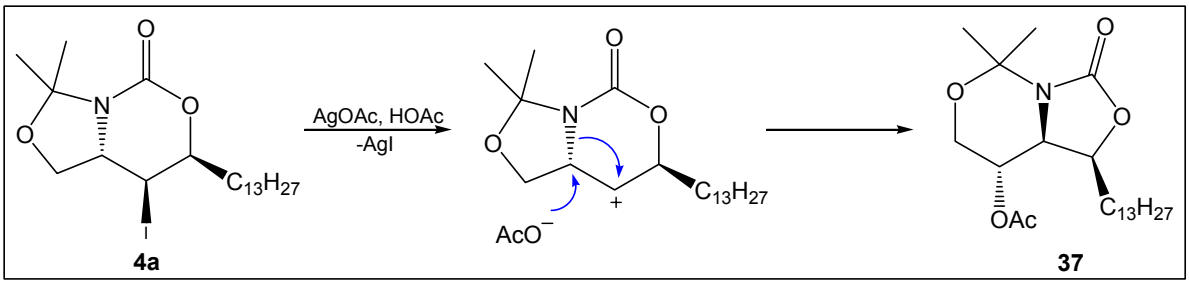

Figure 5.2

5.2.2. Investigation of ceramide derivatives in cultured cells

Prior studies described oxazinanone **5a** and oxazolidinone **5b** as cell-permeable apparent inhibitors of the GalNAc-transferase (Sawatzki, 2003a). This was demonstrated by labeling experiments with D-[^{14}C]galactose and L-[3-^{14}C]serine in cultured murine granule cells, which are rich in complex gangliosides. Labelling with L-[3-^{14}C]serine is a measure of *de novo* biosynthesis of glycosphingolipids, while labelling with D-[^{14}C]galactose additionally reflects the contribution of the salvage pathway, which accounts for the majority of biosynthetically formed glycosphingolipids in neurons. The glycosphingolipid pattern obtained in this work by L-[3-^{14}C]serine labeling in the presence of 50 µM compound **5a** and **5b** were similar to that obtained previously (Sawatzki, 2003a). Cells incubated with iodocarbamates **5a** and **5b** (50 µM in culture medium) and L-[3-^{14}C]serine accumulated radioactively labeled LacCer, ganglioside GM3, and GD3, compared to controls. On the other hand, cellular levels of complex gangliosides such as GM1, GD1a, and GT1b were decreased. The separation into neutral and acidic sphingolipids allowed a closer examination of SM-levels, which were not significantly altered. Due to the low availability of cell material, the need to sacrifice animals, and the time consuming preparation of primary granule cells, compounds were additionally tested in cultured human fibroblasts. These cells are easy to prepare and are available in larger quantities. Furthermore, cells from patients with different diseases, like the GM2-gangliosidoses are available. A disadvantage of this cell type was that it expresses only low amounts of ganglio series-GSLs. In addition, we could show that the results obtained from exogenous addition of the ceramide-derivatives **5a** and **5b** to fibroblasts (chapter 4.2.3 and 4.7.2) differ from the results obtained with murine granule cells (chapter 4.2.2 and 4.6.2). The specificity of this effect for nerve cells can result from several factors, especially from differences in protein expression between both cell types. The major one is that the ganglio-series of GSLs is much more expressed in neurons. Another one is, that the concentration of ceramide-derivative in both cell types is different due to a different metabolism of the ceramide-derivative. It can also be expected that experimental factors contribute to the different results. It might be possible that even the different supplements of the culture medium, e. g. horse serum for nerve cells and calf serum for fibroblasts, that differ in their composition, can influence the results.

In fibroblasts, we also analyzed the effect of ceramide derivative **5b** on incorporation of L-[3-^{14}C]serine into ceramide. In the presence of 25 µM **5b** in culture medium, the ceramide level increases two-fold higher compared to control cells, whereas the incorporation of radioactivity into sphingomyelin was slightly reduced. This can be explained by competition of the substrate analog for the substrate binding side. Mass spectrometry indicated that 5b is no substrate of the enzyme. It has been shown in human keratinocytes,

that the expression rates of several enzymes involved in ceramide metabolism, including serine palmitoyl transferase, increase in the presence of ceramide-derivatives (Brodesser and Kolter, in preparation). In addition, the authors showed, that the transcription of the gene encoding acid sphingomyelinase, that cleaves sphingomyelin into ceramide and phosphocholine, is also increased in keratinocyte cells that do not form sphingolipids with 4,5-double bond. Therefore, it cannot be excluded that enhanced sphingomyelin degradation in the presence of **5b** accounts for the observed effects. In order to clarify, if the accumulation of ceramide and the decreased level of sphingomyelin brought about by **5b**, are a consequence of an inhibition of the ceramide metabolizing enzyme sphingomyelin synthase, or are a consequence of an increased expression of acid sphingomyelinase, we have to make further experiments, including the quantification of mRNA levels and activity assays of ceramide metabolizing enzymes.

As the compounds **5a**, **5b** and **7b** turned out to be effective inhibitors of ganglioside GM2-formation in neurons, the question arises, if these compounds are suitable for the substrate reduction therapy of Tay-Sachs and Sandhoff disease. The advantage of these substances would be that glucosylceramide and lactosylceramide are still biosynthesized, while only the biosynthesis of the storage compounds is inhibited. The limitations of GalNAc-transferase inhibition as a therapeutical approach for GM2-gangliosidoses have been demonstrated by the genetic model of substrate reduction (Liu et al., 1999) in mice, were the accumulation of enzyme substrates of non-lipid nature were determined. For a pharmacological application, it is important to understand how differences in sphingolipid biosynthesis translate into alterations of the total content of certain GSL species. The metabolic labeling experiments give no information on changes of the total content of cellular sphingolipids in response to exogenously added ceramide analogs. The quantification of ganglioside levels in lipid extracts from fibroblasts by thin layer chromatography and densitometric analysis showed no significant change of the total content of gangliosides after 48h (data not shown). To quantify the amount and molecular species distribution on of gangliosides GM3 and GM2 by mass spectrometry, we synthesized a standard substance with a closely related structure that does not occur in the investigated cell type. We chose ganglioside C_6-GM3 as internal ganglioside standard for the quantification of GM3/GM2 levels in lipid extracts. In this work, the last step of a partial synthesis was carried out; the key step was the condensation of azidosphingosine with the peracetylated 1-O-trichloroacetimidate of 3'-Sialyllactose, which has been isolated from colostrum (Clasen, 2004). After reduction of the azido-group, the amine was acylated with capronic acid. The lysoform of gangliosides can also be prepared in a multistep sequence by deacylation of native gangliosides through alkaline treatment (Neuenhofer et al., 1985). However, this method has a drawback: alkaline treatment releases *N*-acyl residues in both, ceramide and sialic acid in the carbohydrate moiety. Thus, the amine residues in the carbohydrate moiety need to be selectively reacetylated. A second possibility consists in the use of a sphingolipid ceramide deacylase (SCDase, Kurita et al., 2000). The synthesized C_6-GM3, prepared during this work will be used as an internal standard for the determination of GM3/GM2 levels in lipid extracts from nerve cells.

5.2.3. Investigation of oxazolidinone 5b *in vitro*

To determine, to which extent oxazolidinone **5b** inhibits GalNAc-T directly, the substance was tested *in vitro* with murine recombinant GM2 synthase. The enzyme has been expressed as a glycoprotein in insect cells, using the baculovirus expression system according to Wendeler et al. (2003). Surprisingly, no inhibition occurred up to a concentration of 200 µM **5b** in the assay buffer (chapter 4.3). The micellar assay system contained *N*-Octyl-beta-D-glucopyranoside. Micelles composed of detergents represent a simplified, but unphysiological model of biological membranes. However, reconstitution of transmembrane enzymes in liposomes is usually accompanied by a loss of activity, which prevented such inhibition studies, also in our hands. In addition, the preparation of micelles is rapid and straightforward and they are widely used in enzyme activity assays. Attempts to test the ceramide-derivative in a detergent free liposomal assay according to Wendeler (2004) did not work, because the specific activity of the GM2-synthase, determined in the liposomal assay system was only 3 % compared to the activity determined in micellar test systems. Further experiments are required to optimize the fusion of GM3-containing liposomes and enzyme-containing membranes. From the results of the micellar assay, we concluded that the inhibitory effect in cell culture is not through direct interaction with the enzyme, but appears to be mediated by a more complex mechanism.

GalNAc-T is a type II membrane protein that can be cleaved by a cathepsin D-like protease to form a soluble species that is released from the Golgi membrane (Jaskiewicz et al., 1996). The cleaved catalytically active soluble domain shows a lower activity towards their membrane-bound substrate (2-dimensional enzyme kinetics; Scheel et al., 1982), which results in an accumulation of its substrates like LacCer, GM3 and GD3. Studies in murine liver cells have shown that during acute-phase response (secretion of acute-phase reactants from the cells in reponse to inflammation), sialyltransferases are cleaved from the Golgi membrane by the action of a cathepsin D-like protease (McCaffrey and Jamieson, 1993; Richardson and Jamieson, 1995). Cathepsin D is lysosomal aspartatic pretease that is synthesized in the ER as an 51-kDa inactive pre-proenzyme (Gieselmann et al., 1983). After transport through the Golgi into the lysosomes, it is processed via a 44-kDa intermediate to the active 31-kDa species. It has been described that in the presence of Golgi disturbing agents, the transport of Cathepsin D from the Golgi to lysosomes is inhibited and that Cathepsin D accumulates in the Golgi vesicles (Scheel et al., 1990). In addition, experiments with the Golgi disturbing agent Brefeldin A in CHO cells overexpressing myc-tagged GalNAc-transferase show higher amounts of a soluble form of GalNAc-T in the medium compared to control cells (Young et al., 1999). We have to consider that the accumulation of GalNAc-transferase substrates in the presence of **5b** in nerve cells might result from the cleavage of the enzyme by Cathepsin D. Recent studies have shown that ceramide binds to Cathepsin D and stimulates the formation of the active 31-kDa form (Heinrich et al., 2000). The activity of Cathepsin D within the cell can be reduced by the addition of agents such as desipramine, methylamine, and chloroquine to the culture medium (Lammers and Jamieson, 1989; Heinrich et al., 2000). These compounds are well known as lysosomotropic agents that raise the pH of endosomal and lysosomal compartments, and affect the processing and activity of proteins such as Cathepsin D (Braulke et al., 1987). Other lysosomal proteins like acid sphingomyelinase (Hurwitz et al., 1994; Kölzer et al., 2004) and acid ceramidase (Elojeimy et al., 2006) are released from internal membranes by desipramine and are subsequently degraded. Pretreatment of cells with desipramine, should

prevent the effect of compound **5b**, if ganglioside accumulation is due to the mechanism as described above. Activity assays with Cathepsin D in the presence of the ceramide derivatives **5a** and **5b** should answer the question, if the derivatives can enhance the activity of Cathepsin D directly, or if the effect is indirect through the increased ceramide levels in the cell caused by **5b**.

5.2.4. Analysis for putative metabolites of 5b

It has been demonstrated in cultured cells that some exogenously added ceramide derivatives can be metabolized to various compounds. In contrast to most drugs, they undergo anabolic reactions similar to those of the parent compound. For example, short chain ceramide derivatives (C_6-ceramide) applied to cultured cells are transformed to long chain ceramides (Ogretmen et al., 2002). In addition, they can be transformed like endogenous ceramides by enzymes that catalyze the formation of glucosylceramide or sphingomyelin (Pütz and Schwarzmann, 1995; Brodesser, 2007). It is possible that the observed effects of **5a** and **5b** result from a metabolite of these ceramide-derivatives. We followed several strategies to monitor the metabolism of the bioactive synthetic ceramide derivatives **5a** and **5b**. One problem in the identification of metabolites in crude lipid extracts was the high concentration of endogenous sphingolipids and glycerolipids compared to the low concentration of putative metabolites. A sample preparation to remove glycerolipids by alkaline treatment was not possible, due to the base-lability of the iodine-group. The analysis of the neutral lipid fraction derived from fibroblasts incubated with **5a** by thin layer chromatography (chapter 4.3.1) using the solvent system chloroform/methanol/water (60:35:8, by volume) revealed a spot that does not occur in the lipid extract from control cells. The spot has the same retention factor as lysophosphatidylcholine and disappears in lipid extract that underwent alkaline treatment. Lysophosphatidylcholine is a neutral phosphoglycerolipid that is formed from phosphatidylcholine by the action of phospholipase A1 or A2. Attemps to extract this spot from tlc and to proof the assignment by mass spectrometry were not successful up to now. In order to overcome the disadvantage of the tlc-procedure, we analyzed the neutral lipid extract by using normal phase LC (Liquid Chromatography) interfaced with APCI (Atmospheric Pressure Chemical Ionization) according to Farwanah et al. (in preparation, data not shown). However, phosphoglycerolipids, including lysophosphatidylcholine, are not accessible to APCI-MS methods (H. Farwanah, personal communication). Therefore, we plan to optimize procedures for the analysis of lipid extracts using LC/ESI-MS.

The analysis of the lipid extracts derived from fibroblasts incubated with **5a** by tlc and mass spectrometry (chapter 4.4.4) revealed no metabolites, but we cannot exclude that the sensitivity of the choosen methods was not high enough. Therefore, strategies were established to introduce a radiolabel in **5b** (chapter 4.4.3). Two strategies were followed to introduce the radioisotope in the last synthetic step: In the first strategy, the aminoaldehyde **8** (Figure 4.10) should be reduced by reaction with tritium-labeled sodium borohydride. Various attempts to prepare one of the active compounds on this strategy failed. The most severe problems of this strategy were the reactivity of the intermediate **8** and the reduction of the aldehyde under mild reaction conditions without loss of the iodine atom by elimination or hydrogenolysis.

In a second strategy, the introduction of the radiolabel was attempted by hydrogenation of a derivative of **5b** with an unsaturated alkyl chain (Figure 4.11). In preliminary experiments we were able to transform the

alkyne into the alkene by ionic hydrogenation, but further experiments are necessary to optimize the reaction conditions. In the following steps, it would be necessary to prepare the tritiated reagents ((Et_3Si^3H or CF_3COO^3H) and to carry out the hydrogenation reaction of **10.2b** with this them. [^{3}H]trifluoroacetic acid can be obtained by hydrolysis of trifluoracetic anhydride with [^{3}H]-water (Dugger and Schwarz, 1967), and [^{3}H]triethylsilane (Et_3Si^3H) can be prepared by reduction of triethylsilylchloride with LiB^3H_4 (Guillerm et al., 1977).

A strategy that was not followed to introduce the radiolabel before the introduction of the iodine-atom, is shown in figure 5.3. The radiolabel might be introduced using the Wittig reaction of Garner's aldehyde with a radiolabeled ylide. The corresponding phosphonium salt can be derived from commercially available [1-^{14}C]tetradecanol in a one pot reaction, as decribed by Lee and Kim (2000), or by the transformation of the alcohol into an alkyl halide (bromide or iodide), followed by reaction with triphenylphosphane (Beaulieu et al., 1990). The corresponding *N*-Boc allylamine can be transformed to the iodo-oxazolidinones by treatment with NIS in CH_2Cl_2. One drawback of this pathway is the very low substance amounts, with which the reactions in the presence of radiolabel have to be carried out. The yield is usually drastically reduced due to the presence of small traces of water, and multistep syntheses are usually not suitable with radioactive intermediates. Although all isomers (**5a**, **5b** and **5c**) might be obtained in radiolabeled form by this approach, the disadvantages make it not attractive.

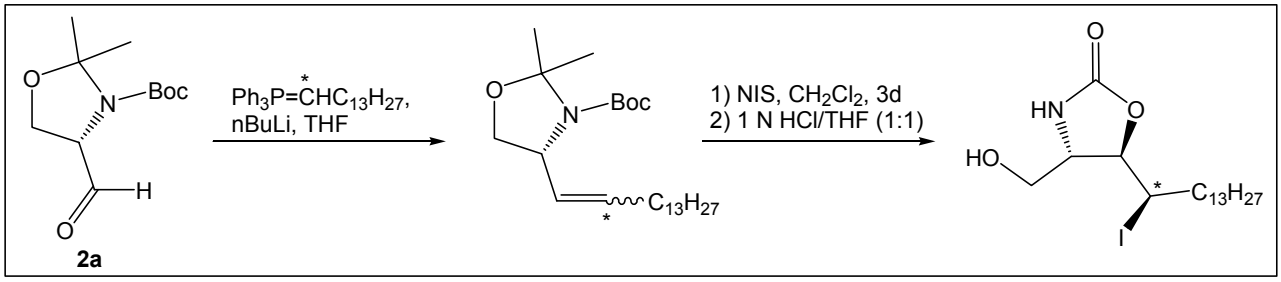

Figure 5.3: An alternative strategy to introduce a radiolabel in bioactive synthetic ceramide analog **5b**

As an alternative, non-radioactive strategy, we prepared substances with an azido-group in the ω-position of the alkyl chain in oxazinanone **12 (**Figure 4.10) instead of a radioactive isotope (^{3}H, ^{14}C) as chemical reporter. This strategy has been successfully applied in the field of proteomics (Review: Wirtz and Kolter, 2007) and functional glycomics (Toshinori et al., 2007, Saxon et al., 2002). When the ω-ceramide derivative **12** is exogenously added to cells and metabolized, the putative metabolical products are bearing the azido-group. In the cell lysate, such compounds can be usually selectively conjugated with a biotinylated phosphine capture reagent (Figure 4.10, compound **13**) by means of the Staudinger conjugation reaction (Saxon and Bertozzi, 2000).

5.2.5. Relevance of iodine of 5b for its activity towards inhibition of GSL bioynthesis

It can be expected that the iodine atom present in **5a** and **5b**, plays a role for the observed effects. L-[3-^{14}C]serine labeling experiments in granule cells (chapter 4.6.2) and fibroblasts (chapter 4.2.3) indicate that the presence of a halogen atom (iodine or bromine) is required for the mechanism of action. Iodine

represents a good leaving group in nucleophilic substitution reactions. It is well known that alkyl halides behave as electrophils in a cellular environment and are trapped e.g. by the action of Glutathiontransferases (Guengerich, 2005). It is therefore not unlikely that the covalent modification of an unknown target molecule by the halogenated ceramide derivatives **5a** and **5b** might account for the observed effect.

To analyze putative interacting proteins that might undergo covalent attachment to the ceramide derivatives **5a** and **5b** by substitution of the iodine, we want to analyze the cell lysate of fibroblasts and neurons that were incubated in the presence of ω-azido oxazinanone **12**. Proteins that are covalently bound to **12** can be selectively conjugated to a biotinylated Staudinger reagent (Saxon and Bertozzi, 2000), separated by SDS-PAGE and visualized with strepatvidin horse-dish peroxidase. This strategy was successfully in the identification of fatty-acylated proteins (Hang et al., 2007) and farnesylated proteins (Kho et al., 2004). In addition, taken advantage of the strong interaction between biotin and streptavidin, putative proteins can be concentrated from the cell lysate by the use of streptavidin-conjugated materials (e.g. beads). Alternatively, proteins covalently bound to **12** can also be isolated by the reduction of the azido-group to the amine, and the conjugation to *N*-hydroxysuccinimide activated material (e. g. AffiGel® 10, Biorad).

5.2.6. Effect of oxazolidinone 5b on Golgi morphology

The major intracellular transport pathway coupled to the biosynthesis of membrane lipids, glycoproteins, and secreted proteins, is the exocytotic vesicle flow from the ER via the Golgi apparatus to the plasma membrane. It has been shown that several drugs such as Brefeldin A, monensin, and vinblastine, which interfere with this intracellular membrane flow (Nakamura et al., 2003), can also reduce GSL biosynthesis (Townsend et al., 1984; van Echten and Sandhoff, 1989; van Echten et al., 1990). Using fluorescence microscopy, we showed that fibroblasts treated with 25 µM **5b** in the culture medium underwent extensive Golgi vesiculation and reproduced the morphological phenotype of cells incubated with Brefeldin A (chapter 4.5, figure 4.16). It can be suggested that the observed reduction of the biosynthesis of higher gangliosides in neuronal cells by **5b** might be a consequence of the interruption of intracellular membrane flow, but we did not investigate the morphological studies in nerve cells. We cannot distinguish, whether Golgi vesiculation is responsible for the block in the biosynthesis of complex GSLs, or if the accumulation of GSLs leads to the change of the Golgi structure. Further experiments are required to identify the molecular target and to clarify the mechanism of action that leads to the metabolic and morphological effects in cell culture, and how they are related.

As mentioned above, we observed that in the presence of **5b** in culture medium, the incorporation of L-[3-^{14}C]serine into ceramide is increased. Therefore, we cannot distinguish whether the observed effect on Golgi morphology is caused by **5b** directly, or results from the elevated ceramide content in the cell in a certain cellular compartment. Many examples are found in the literature, that decribe the change of the Golgi morphology in the presence of drugs that interfere with sphingolipid metabolism (Table 5.1). In addition, in a variety of human diseases, including amyotrophic lateral sclerosis, corticobasal degeneration,

Alzheimer's and Creutzfeld-Jacob disease, spinocerebellar ataxia type 2, and in Niemann-Pick type C disease, the Golgi apparatus is fragmented (Gonatas et al., 2006). However, there is no plausible mechanism described, that explains the connection between sphingolipids and the constitution of the Golgi apparatus. Therefore, several aspects are briefly discussed.

Hu and coworkers have reported, that the exogenous addition of 2.5 µM cell permeable C_6-ceramide to the culture medium leads to a vesiculation of the Golgi in HeLa cells (Hu et al., 2005). They also showed that this treatment leads to a 50-fold increase in the levels of sphingosine, and that also the presence of 2,5 µM sphingosine causes Golgi fragmentation. However, also these authors provide no evidence about how ceramide or sphingosine induces the morphological change of the Golgi. To exclude the possibility that the disruption of these organelle results from unspecific factors, e. g. by altering the physicochemical properties of the membrane, they also tested L-erythro-ceramide, which failed to alter the morphology of the Golgi apparatus. Stereoisomers of naturally configured ceramide are often used as a control to rule out physico-chemical factors. However, since the discovery of the ceramide-transporter CERT by Hanada and coworkers (Hanada et al., 2003) and the studies about its substrate-specifity (Kumagai et al., 2005), we know that the intermembrane transfer of unnatural stereoisomers of ceramide is very low compared to that of natural ceramide. Therefore, there is no information available about the local concentration of the different ceramide-derivatives in the Golgi or ER, when applied to the culture medium.

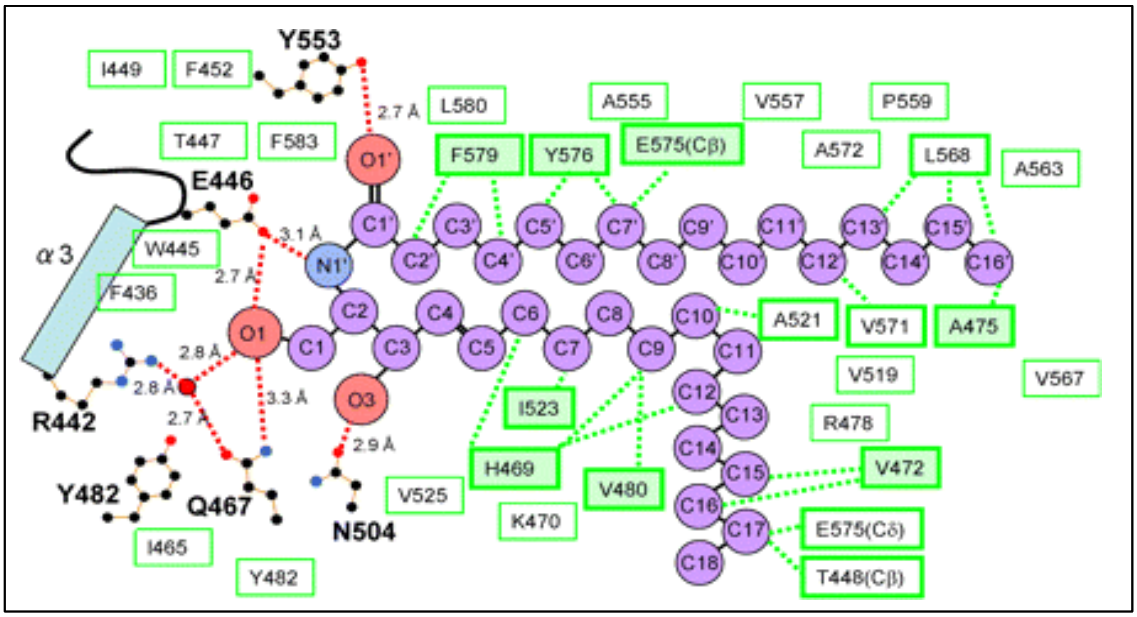

Figure 5.2: **Schematic representation of C_{16}-ceramide recognition by the CERT START domain (Kudo et al., 2008).** Residues lining the amphiphilic cavity are shown. Red dashed lines, hydrogen bonds; red circles, water molecules; black, blue, and red dots, C, N, and O atoms, respectively, of the residues involved in the hydrogen bond network. Green boxes indicate residues contributing to the hydrophobicity of the cavity in general, whereas green boxes with thick borders indicate those with direct hydrophobic interactions, which are represented as green dashed lines.

In this context, inactivation of CERT by a point mutation (Hanada et al., 2003) or by use of the stereospecific CERT inhibitor (1*R*,3*R*)*N*-(3-hydroxy-1-hydroxymethyl-3-phenylpropyl)dodecamide (HPA-12; Fig. 5.3; Yasuda et al., 2001) causes an increased ceramide content in the ER without vesiculation of the Golgi apparatus. Inhibition of this protein in drug-resistant cancer cell lines has also been shown to sensitize these cells to several cytotoxic agents (Swanton et al., 2007; Kolesnick et al., 2007). In addition, inactivation of CERT together with an inhibition of SMSr (sphingomyelin synthase related protein), which transforms ceramide to ceramidephosphoethanolamine, are proposed to cause an increase of ceramide content in the ER of HeLa cells, and leads to the fragmentation of the Golgi apparatus (J. Holthuis, personal communication).

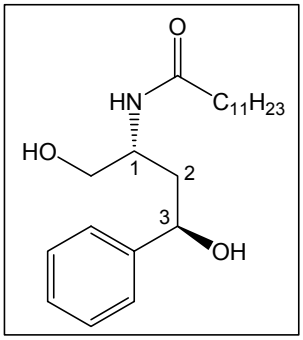

Figure 5.3: HPA-12

It can be expected that the synthetic ceramide-derivatives accumulate in the ER and induce the same effect as endogenous ceramide, or they can act as an agonist of CERT and elevate the endogenous ceramide content in the ER, or they do this by inhibiting SMSr, which can be expected for a ceramide analog. However, the mechanism of how ceramide, or sphingosine, induce Golgi vesiculation, is still unknown. Analysis of the crystal structure of the START (steroidogenic acute regulatory protein-related) domain of CERT demonstrated that the binding pocket forms a hydrogen bond network with the hydroxyl-groups and the amide-group of ceramide, and that there is no space for additional bulky groups (Kudo et al., 2008).
In addition to CERT, the lipid-binding protein FAPP2 (four-phosphate adaptor protein) is reported to be required for the non-vesicular transport of glucosylceramide to the distal Golgi compartments (D'Angelo et al., 2007). Knockdown of FAPP2 leads to a reduction of the biosynthesis of glycosphingolipids (Halter et al., 2007). In addition, FAPPs are decribed to be required for the formation of transport vesicles from the *trans*-Golgi to the plasma membrane (Godi et al., 2004). It is therefore not unlikely that the ceramide derivatives **5a** and **5b** can affect glycosphingolipid biosynthesis through the inhibition of CERT or FAPP2.

The group of Brindley investigated the effect of ceramide on membrane trafficking (Abousalham et al., 2002). They showed that C_2-ceramide, but not dihydro-C_2-ceramide, can block the association of ARF1 (ADP-ribosylation factor) with Golgi-enriched membranes. The ARF family represents a group of several small G-proteins that play a central role in the organization of the secretory and endocytic pathways (Gillingham and Munro, 2007, Figure 5.2). In COP-coated (COP = coat protein) vesicle formation, the GDP-bound form of ARF associates with the donor Golgi membrane, where guanine nucleotide exchange factors (GEFs) promote the exchange of the bound GDP for GTP. In its GTP-bound state, ARF promote the binding of the coatomer (COPI coat protein), leading to vesicle budding. The Golgi-disturbing drug Brefeldin

A specifically binds to the usually transient ARF*GDP-GEF complex, which cannot proceed to nucleotide dissociation, resulting in a block of vesicular traffic (Renault et al., 2003). It can be expected that the ceramide derivatives **5a** and **5b** interfere with this vesicle budding in the same way as it is proposed for C_2-ceramide.

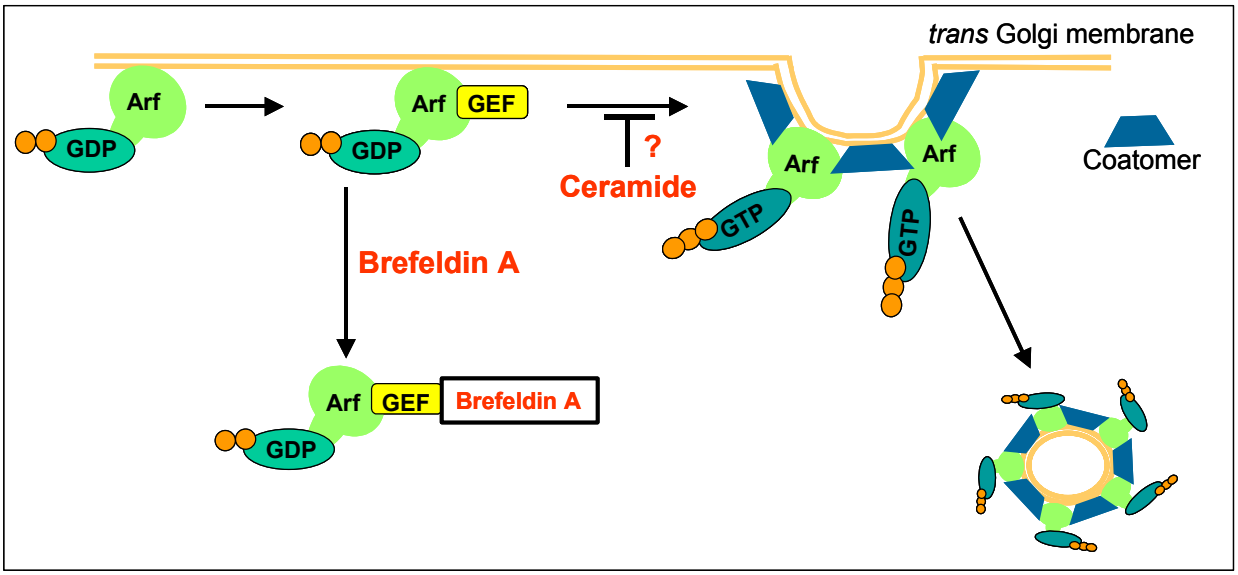

Figure 5.6: Mechanism of COP-coated vesicle formation from the trans Golgi network modified from (Kirchhausen, 2000). Inhibition step for Brefeldin A and the hypothetical influence of ceramide are indicated.

Many other factors contribute to the formation and maintenance of the structure of the Golgi apparatus including the cytoskeleton (Lázaro-Diéguez et al., 2006), regulatory kinases (PKC and PKA), calcium ion concentration within the Golgi lumen, or in the adjacent cytosol (Dolman and Tepikin, 2006). Several drugs that are unrelated to each other in their structure and reported mode of action have been described to disturb the integrity of the Golgi apparatus (Table 5.1). Further experiments are required to analyze the exact mechanism of how ceramide and ceramide-derivatives influence the morphology of this organell.

Compound (concentration applied to cultured cells)	**Reference**
Arachidonyltrifluoromethyl ketone (40 µM)	Kuroiwa et al., 2001
Brefeldin A (1 µg/ml)	van Echten and Sandhoff, 1989
Cetaben (100 µM)	Kovacs et al., 2004
Cyclofenil diphenol (40-100 µg/ml)	Mason and Lancaster 1992
Clofibrate (500 µM)	Figueiredo and Brown 1999
C_6-ceramide (2,5 µM)	Hu et al., 2005
Cholesterol (5 µM as mβCD/Chol-Complex)	Ying et al., 2003
Colcemid (1 µM)	Sandoval et al., 1984
CI-976 (25 µM)	Chambers et al., 2005
2,4-Dichlorophenoxyacetic acid (1 mM)	Rosso et al., 2000
Dicumarol (200 µM)	Mironov et al., 2004
Methyl 2-(4-fluorophenylcarbamoyl)benzoate (100 µM)	Feng et al., 2003
Ilimaquinone (30 µM)	Veit et al., 1993
Isotetrandrine (25 µM)	Chan et al., 2004
Monensin (1 µM)	Tartakoff, 1983
Nocodazole (5 µM)	Minin, 1997
Norrisolide (40 µM)	Guizzunti et al., 2006
Nordihydroguaiaretic acid (NDGA, 25 µM)	Nakamura et al., 2001
Okadaic acid (1 µM)	Lococq et al., 1991
PDMP (100 µM)	Nakamura et al., 2002
Retinoic acid (10 µM)	Wu et al., 1994
Vinblastine (50 µM)	Wehland et al., 1983

Table 5.1: Golgi-disturbing agents

5.3. A Benzazepinone as conformationally restricted ceramide derivative

Previous cell culture studies indicated that benzazepinone **24** (chapter 4.8; Figure 4.23) acts as an inhibitor of sialyltransferase II at a concentration of 10 µM in the culture medium, and as an inhibitor of GalNAc-transferase at higher concentrations of 25 µM. The molecular bases for this inhibition are not known; even, if the effect is a direct or indirect one. In this work, the labeling experiments have been repeated in cultured neurons with D-[^{14}C]galactose in the presence of benzazepinone **24** at a concentration of 25 µM (chapter 4.8.2, Figure 4.24). The results were similar to the effects described in presence of 10 µM by Sawatzki (2003a). To investigate, if the conformational restriction or the presence of the bulky aromatic group within the benzazepinone **24** is responsible for the observed effects in cell culture, we synthesized the open chain analog **25** (chapter 4.8.1, figure 4.23) and tested **24** and **25** in cultured neuronal cells on its influence of glycosphingolipid biosynthesis. We have shown that the *N*-phenylacetylceramide derivative **25** has the same effect on sphingolipid biosynthesis, but additionally showed cytotoxic effects. It can be expected that the compound **25** behaves like a short-chain ceramide (C_2- and C_6-ceramide). It has been described that exogenous addition of short-chain ceramides to cultured cells leads to apoptotic responses, while the saturated form dihydroceramide has no effect (Bielawska et al., 1993). Hydrogenation of the double bond in **25** should lead to a less toxic compound that should be even more comparable to compound **24**.
Ceramide and ceramide derivatives have been described as modulators of PKC activity, although their mechanism of action is controversially discussed. The Benzolactames **35** and **36** have been described as activators of Protein Kinase C (PKC) (Nakagawa et al., 2006; Mach et al., 2006; Endo et al., 1999).

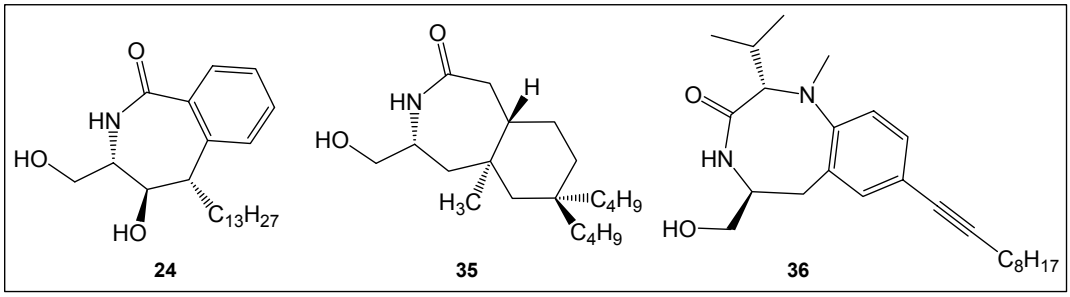

Figure 5.3: Structures of ceramide derivative **24** and PKC activators **35** and **36**

To verify, if the enhancement of the relative amount of a-series gangliosides (e. g. GM3, GM2, GD1a and GT1b) can result from the stimulation of an intracellular phosphorylation of sialyltransferase II (Bieberich et al., 1998), we first wanted to analyze the influence of ceramide derivative **24** on PKC activity in a micellar assay. We observed that in the presence of 50 µM ceramide derivative **24** in the assay buffer, no activation of PKC occurs. From this result, we exclude the possibility that the ceramide derivative directly binds to PKC. Moreover, the activity of PKCs is regulated by many other factors, such as phosphatidylserine, calcium ions, and lipid mediators such as diacylglycerol, fatty acids, cholesterol sulfate, and lysophospholipids (Shirai and Saito, 2002). As discussed above for the oxazinones **5a** and **5b**, several other mechanisms exist that might account for the influence of the synthetic ceramide derivative on GSL metabolism.

6. Material and Methods

6.1. Material

6.1.1. Analytical Techniques and Instruments

Autoclave	FVS3, Fedegari/Integra, Fernwald, Germany
Blotter	Mini-TransBlot, BioRad, München, Germany
Centrifuges	Eppendorf, Hamburg, Germany
	L 8-80, mit SW-28-Ti-Rotor, Beckmann, Palo Alto, USA
C, H, N Analysis: CHNO-Rapid	Heraeus
Centrifuge tubes	12 ml: Costar, Cambridge, USA
	15 ml: Greiner, Nürtingen, Germany
	50 ml: Falcon/BectonDickinson, Bedford, USA
FAB-mass spectrometer	H1, Kratos, Manchester
Fluoroscanner	Fluoroscan II, Labsystems
Gel chamber	Mini-TransBlot, BioRad, München, Germany
Glass tools	Schott-Duran, Jenaglas, Mainz, Germany
Hot air gun	Regulator 2000, Rapid, Hestra, Sweden
Incubator	Heraeus-Christ, Hanau, Germany
IR: 1600 FT-IR spectrometer	Perkin-Elmer, Boston, Massachusetts, USA
Microscope	Flourescence microscope Zeiss Axiovert 35 with filters (Bp 485, Ft 510, 515-565), Oberkochen, Germany
NMR: DPX300 and DPX400	Bruker, Karlsruhe, Germany
Polarimeter: P341	Perkin-Elmer, Boston, Massachusetts, USA
Overhead mixer	Gesellschaft für Labortechnik, Burgwedel, germany
PH-meter	pH 537, WTW, Weinheim, Germany
Phosphoimager	Fuji BAS 1000 Bio Imaging Analyzer, Raytest, Straubenhardt, Germany
Phosphoimaging plates	^{14}C-screen BAS MS 2040, ^{3}H-Screen BAS Tr 2040, Raytest, Straubenhardt, Germany
Scintillation counter	Tri-Carb 1900CA, Packard Instruments Co., Inc, Downers Grove, USA
Shaker water bath	Gesellschaft für Labortechnik, Burgwedel, Germany
SigmaPlot software	SPSS science, Erkrath, Germany
Sterilbenches	LaminAirHA 2472 GS, Heraeus, Düsseldorf, Germany
Thermomixers	Komfort, Eppendorf, Hamburg, Germany
TLC-tank	Desaga, Heidelberg, Germany
TLC-heater	TLC-Plate Heater III, Camag, Berlin, Germany
Ultra centrifuge	L8-70M, Beckman Instruments, München, Germany
Ultrasound bath	Sonorex RK 100, Bandelin, Berlin, Germany

Ultrasound	Cap horn, Sonifer B-12, Branson Ultrasonic Corp., Danbury, USA
Vortex	MS Minishaker, IKA-Werk, Staufen, Germany
Water purification	Millipore-Pelicon filtration device with polysulfone filter cassette, Millipore, Molsheim, France

6.1.2. Consumables and Chemicals

Agarose	Invitrogen Life Technologies, Bethesda, USA
AraC (cytosine arabinose)	Sigma, Taufenkirchen, Germany
Barrycidal-36	Biohit, Köln, Germany
BCA	Sigma, Taufkirchen, Germany
BSA	Sigma, Taufenkirchen, Germany
CDP-Cholin	Sigma, Taufkirchen, Germany
Cell flask	Costar, Bodenheim, Germany
Chemiluminescence reagent	Perkin Elmer Life Sciences, Rodgau-Jügesheim, Germany
Coomassie brilliant blue	Serva Feinbiochemika, Heidelberg, Germany
DEAE Sephadex A-25	GE Healthcare, Uppsala, Sweden
Deuterated solvents	d_1-Chloroform Uvasol®, Merck, Darmstadt, Germany d_4-Methanol, Euriso-Top, Saint-Aubin Cedex, France
Dry solvents (Crown-Cap)	Fluka, Buchs, Switzerland
Ganglioside GM3	Fidia Research Laboratories, Abano, Italy
DNase	Roche, Mannheim, Germany
E-64	Serva, Heidelberg, Germany
Glycerol	Merck, Darmstadt, Germany
HEPES	Merck, Darmstadt, Germany
Imaging plates	^{14}C-Screen (BAS MS 2040), ^{3}H-Screen (BAS Tr 2040), Raytest, Straubenhardt, Germany
LiChroprep® RP18 (40-63 µM)	Merck, Darmstadt, Germany
Leupeptin	Sigma, Deisenhofen, Germany
Lipid standards	Sigma, Taufenkirchen, Germany
Nonidet P-40	Fluka, Buchs, CH
Octyl-β-D-glucopyranoside	Glycon, Luckenwalde, Germany
Pepstatin A	Boehringer, Mannheim, Germany
Phytosphingosine (isolated from Sacharomyces cerevisiae)	Cosmoferm B.V., Delft, Netherlands
PMSF	Sigma, Deisenhofen, Germany
Reaction vessel	Eppendorf, Hamburg, Germany
Silica gel 60 F254 (40-63 µM)	Merck, Darmstadt, Germany
Screw cap glass	Pyrex, Bibby Sterlin Ltd, Stone, Great Britain

Sterile filters	Sarorius, Göttingen, Germany
Szintillation vials	Packard Biosciences, Gronigen, Netherlands
TLC plates (aluminium coated with silica gel 60 F254 (40-63 µM)	Merck, Darmstadt, Germany
Triton X-100	Sigma, Taufkirchen, Germany
Tween 20	Sigma, Taufkirchen, Germany
Ultima Gold	Packard, Frankfurt a.M., Germany

6.1.3. Radiolabeled Chemicals

D-[1-^{14}C]Galactose	Amersham Pharmacia, Freiburg, Germany
L-[3-^{14}C]Serine	Amersham Pharmacia, Freiburg, Germany
UDP[^{3}H]GalNAc	American Radiolabeled Chemicals (obtained through Biotrend, Cologne, Germany)

6.2. Biological materials

6.2.1. Cells and additives

Human fibroblasts	Kinderklinik St. Augustin, Germany
NMRI mice	Animal house of the University of Bonn
SF9 insect cells	Invitrogen, Karlsruhe, Germany
Baculovirus stock	Michaela Wendeler
DMEM, MEM	Gibco, Eggenstein, Germany
Glutamine	
Foetal calf serum (FCS)	Cytogen, Berlin, Germany
Leupeptin hemisulfate	Sigma, Taufkirchen, Germany
Horse serum	Cytogen, Berlin, Germany
streptomycin	Sigma, Deisenhofen, Germany
Trypsin	Cytogen, Berlin, Germany
N-Acetyl-L-Alanine-L-Glutamine	Seromed, Biochrom, Berlin, Germany
TNM-FH medium	Sigma, Deisenhofen, Germany

6.3. Methods

6.3.1. General Conditions for synthesis

All reactions were carried out with magnetic stirring and, if involving moisture– or air-sensitive reagents involved, were performed under nitrogen using syringe-septum cap techniques. All glassware was flame-dried under vacuum and purged with argon prior to use.

6.3.2. Chromatographic methods

TLC (Thin layer chromatography) was carried out with aluminium plates coated with SiO_2 to control the completion of a reaction or to analyze the profile of column chromatography. The chromatograms were examined under UV light (λ = 254 nm bzw. 366 nm) and by treatment of the TLC plate with one of the solutions given below, followed by heating with a heat gun.

Column chromatography was performed using silica gel 60 (0.040-0.063 mm).

Visualizing reagents:

4-anisaldehyde/acetic acid/sulfuric acid	2:500:10 (v/v/v)	(Miescher, 1946)
Ninhydrin/ethanol	1:10 (w/v)	(Patton and Chism, 1951)
Phosphomolybdic acid/ $Ce(SO_4)_2/H_2SO_4/H_2O$	5:2:12:230 (w/w/v/v)	
2,4-Dinitrophenylhydrazine/ethanol/ H_2SO_4/H_2O	2:50:10:15 (w/v/v/v)	(Behforant et al., 1985)
$CuSO_4$ x 5 H_2O/H_3PO_4 (85 %)/H_2O	15.6:9.4:75 (w/v/v)	(Yao and Rastetter, 1985)

6.4. Instrumental Analytic

^{1}H- and ^{13}C-NMR-spectra were recorded on a Bruker spectrometer in deuterated solvent at room temperature. Chemical shifts δ are relative to solvent and given in ppm. The coupling constants (J) are given in Hz. The following abbreviations are used for multiplicities: s = singlet, d = doublet, t = triplet, q = quartet, m = multiplet, br = broad.

FAB (All Fast Atom Bombardment spectra) were recorded in meta-nitrobenzoic acid in the analytical laboratories of the department of Chemistry, University of Bonn.
EI (electron impact ionization) spectra were recorded on a Kratos MS50, ThermoQuest Finnigin MAT 95 XL.
HR (High-resolution) masses were determined by EI.
ESI (electrospray ionization) mass spectra were measured on Q-TOF-2-mass spectrometer equipped with a nanospray source. Lipid samples to be analyzed were dissolved in methanol (100 pmol/µl).

IR (Infrared spectra) were recorded on a FT-IR 1600 spectrometer. Samples were measured either as a film on KBr plates or (for solids) as KBr tablets. The absorption bands are given in wave numbers (cm^{-1}). For the band characterization the following abbreviations were used: br (broad), s (strong), m (medium), vs (very strong), w (weak).

MPs (melting points) were determined with a capillary instrument SMP 20 and are uncorrected.

Elemental analyses were performed in the microanalytical laboratories of the department ofChemistry, University of Bonn.

Optical rotations were measured at rt on a P341 polarimeter with monochromatic light (λ = 589.3 nm). The samples with a concentration of 0.1-1.0g/100ml were measured in quarz glass cuvets (vol. 1 ml).

6.5. Biological and biochemical experiments

6.5.1. Cell culture

All procedures with cells were carried out under sterile conditions.

Granule cells were cultured from cerebella of 6-day-old mice as described before (van Echten et al., 1998). Briefly, cells were isolated by mild trypsinization (0.05%, w/v) and dissociated by repeated passage through a constricted Pasteur pipette in a DNAse solution (0.1%, w/v). The cells were then suspended in DMEM containing 10% heat-inactivated horse serum and plated onto poly-L-lysine-coated 8 cm^2 Petri dishes. Twenty-four hours after plating, 40 µM cytosine arabinoside (AraC) was added to the medium to arrest the division of nonneuronal cells. After 5 or 6 days in culture, cells were used for metabolic studies. Cells were incubated at 35.5 °C in a 5% CO_2 atmosphere.

Fibroblasts and **B104 cells** were routinely cultured in 75 cm^2 flasks in DMEM, supplemented with 2 mM glutamine, 10% heat-inactivated fetal calf serum, and streptomycin 100 mg/L. Cells were incubated at 37°C in a 5% CO_2 atmosphere. After reaching a confluent state, the cells were subcultered 1:2 in culture flasks or seeded in plates for experiments. For passaging of cells, the medium was removed and the cells were washed with PBS. After addition of 2 mL trypsin/EDTA, the cells were incubated for 1-2 min at 37°C. Cells were carefully detached by gently tapping and the digestion was stopped by addition of 3 mL DMEM containing 10% FCS. The cells were centrifuged with 300 g for 10 min at 4°C, the supernatant was discarded and the cells were resuspended in growth medium. For experiments, cells were grown until confluence in 21 cm^2 petri dishes or flasks.

Sf9 Insect cells were cultured in TNM-FH medium containing 10% FCS in a shaking incubator at 28°C.

6.5.2. Metabolic studies with cultured fibroblasts and cerebellar granule cells

Metabolic studies were performed with confluent cells in 8 cm^2 (cerebellar neurons) or 21 cm^2 (fibroblasts) plastic culture dishes. Growth medium was removed and the cells were rinsed two times with MEM. The cells were preincubated with synthetic lipid analogues in concentrations of 5-50 µM in the culture medium, together with 0.3% heat-inactivated calf serum (fibroblasts) or 0.3% heat-inactivated horse serum (cerebellar neurons) for 24 h. The stock solution (5 mM) of synthetic ceramide analogs in methanol was stored at –20°C. The sphingolipids of cultivated cells were metabolically labeled by addition of either L-[3-^{14}C]-Serine (1 µCi/mL) or D-[^{14}C]-Galactose (2.5 µCi/mL). After 24 h, medium was removed, cells were washed twice with 1 mL of PBS, and harvested after addition of trypsin in screw cap glasses. After washing with PBS, cells were stored at –20°C.

6.5.3. Protein determination

Cell protein was quantified as described by Bradford (Bradford, 1976) using BSA as standard. The Bradford reagent (5 mg Coomasie Blue G250, 5 mL methanol, 10 mL H_3PO_4 (85%), 85 mL H_2O) was stored at 4°C. Prior to lipid extraction, cell pellets were homogenized in 400 µl of water and aliquots were used for protein determination. 5 µL of cell homogenate were filled to 20 µL with water in a multiwell plate. 200 µL of Bradford reagent working solution were added. After 20 min incubation at rt, the absorbtion of samples was measured at 595 nm. Protein content was calculated on the basis of a standard curve, obtained by diluting the BSA standard (0.25-5 µg BSA/20 µL).

6.5.4. Lipid extraction

Cell pellets were suspended in 1 mL water and homogenized 3 times (30 s) by ultrasonic treatment (120 W). Aliquots for protein determination and radioactivity determination were issued and 4 mL methanol was added to the cell homogenate. The solution was vortexed, sonificated for 15 min and 2 mL of chloroform-methanol-water (10:3:1, v/v/v) were added and incubated for 24 h at 50°C. Insoluble cellular components were separated by filtritation through wadding. The screw cap glass was rinsed with 2 mL of chloroform-methanol-water (70:30:3, v/v/v), and the extract was dried under a stream of nitrogen.

6.5.5. Anion-exchange chromatography

The separation of acidic and neutral lipids was carried out by ion exchange chromatography with a weak anion exchanger, DEAE Sephadex A-25. To obtain maximum affinity of acidic lipids, the medium was converted first from the chloride to the acetate form. 500 g of ion exchanger was first slurred with 1 L methanol for 12 hours to allow the resin to swell. Then it was suspended in 0.5 L water and allowed to stand for 24 hours. Then the resin was transferred into a glass column and suspended in 0.5 L 1 M Sodium acetate solution. To eliminate almost all chloride, the resin had to be washed several times with 1 M Sodium

acetate solution, until no chloride was detectable by silver nitrate test. Then the acetate form was washed first with 1 L water and then with 1 L methanol and was stored as 1:1 suspension in methanol at 4°C before use.

Small pieces of silanized glass fiber wadding were introduced into glass Pasteur pipettes and 1 mL of DEAE-Sephadex A-25/methanol suspension (1:1) in acetate form was added and equilibrated with 3 mL of chloroform-methanol-water (3:7:1, v/v/v). Samples were dissolved in 2 mL of the same solvent, sonicated for 1 min, and applied to the column. The column was washed with 6 mL of the same solvent. This pass-through fraction contained the neutral sphingolipids. Acidic lipids were eluted with 8 mL of chloroform-methanol-0.8 M potassium acetate (30:60:5, v/v/v). The lipid fractions were evaporated to dryness under a nitrogen stream.

6.5.6. Alkaline hydrolysis

Phospholipids were removed by mild alkaline hydrolysis. Samples were dissolved in 1 mL of chloroform-methanol (1:1, v/v), vortexed, and the glass of the reaction vessel was rinsed with 1.5 mL of the same solvent. After 5 min ultrasonic treatment, addition of 62 µL 4 N NaOH, and additional 5 min ultrasound, the solution was incubated for 120 min at 37°C in a water bath. After the reaction mixture was cooled and neutralized with 10 µL glacial acetic acid, the lipids were evaporated under nitrogen to dryness.

6.5.7. Reversed-Phase Chromatography (RP18)

Desaltment of lipid samples was performed according to literature (Williams and McCluer, 1980).

Small pieces of silanized glass fiber wadding were introduced into glass Pasteur pipettes and 1.5 mL of LiCroprep (1:1) was added and washed with 1 mL methanol, 2 mL water, 1 mL methanol, 2 mL of chloroform/methanol (1:1 (v/v)), 1 mL methanol and 2 mL of chloroform/methanol/0.1M KCl in water (3:48:47 (v/v/v)). Lipid samples were dissolved in 1 mL methanol, sonicated for 5 min, and 1 mL ammonium acetate (300mM in water) was added. The mixture was directly applied to the column. The probe glass was rinsed two times with 1 mL ammonium acetate (200 mM in methanol/water 1:1 (v/v)), and the solution was added to the column. The column was washed with 6 mL of water. Lipids were eluted with 1 mL methanol and 8 mL of chloroform/methanol (1:1 (v/v)). The lipid fractions were evaporated to dryness under a stream of nitrogen.

6.5.8. Thin-layer chromatography

Lipid samples corresponding to the same amounts of all protein were dissolved in 1 ml chloroform-methanol (1:1, v/v), transferred to eppendorf tubes, and evaporated to dryness under nitrogen stream. The residues were dissolved in 40 µL chloroform-methanol (1:1, v/v) and applied with glass capillaries to Silica gel 60-precoated glass plates. The Eppendorf vessels were rinsed with 25 µL and 10 µL of the same solvent. The TLC-plates were dried under vacuum over sodiumhydroxid. The chromatography tank was lined with filter

paper and filled with 200 mL of mobile phase. For the separation of different lipids, the following mixtures were used:

Neutral lipids	chloroform/methanol/water	60:35:8 (v/v/v)
Neutral lipids	first: chloroform/methanol/glacial acetic acid second: chloroform	70:30.8 (v/v/v); 2 times 2/3
Acidic lipids	chloroform/methanol/0.22% $CaCl_2$	60:35:8 (v/v/v)
Ceramides	chloroform/methanol/water	190:9:1 (v/v/v)

After drying, lipid bands were visualized by Phosphoimaging and treatment with cupric sulfate pentahydrate phosphoric acid reagent at 180 °C for 10 min. Data are analyzed using the TINA software.

6.5.9. Preparation of lipid extracts for quantification by mass spectrometry

Lipids were extracted according to the procedure of Bligh and Dyer (1959). Lipids were extracted for 12h at rt in 2.8 mL of a nonpolar solvent mixture with the composition: methanol/chloroform/water (2:1:0.8 (v/v/v)). Then a double-phase system was obtained by adding 1 mL chloroform and 1 mL water (final ratio: methanol/chloroform/water = 2:2:1.8 (v/v/v)). After the mixture was centrifuged at 2500 rpm for 10 min, 90% of the lower phase containing less polar lipids (ceramide, PC, PS, GlcCer, LacCer, Gb3, Gb4, SM) was separated from the upper phase and dried under a stream of nitrogen. The upper phase together with the interphase (containing gangliosides) was dried under a stream of nitrogen, redissolved in 100 mL methanol, and desalted as described under 6.5.7. For mass spectrometric analysis, the lipid probes were dissolved in methanol (lower phase in 50 µL MeOH, upper phase in 200 µL MeOH) and analyzed by ESI-MS in both positive and negative ion modes.

6.5.10. Expression and membrane preparation of GM2 synthase (GalNAc-transferase)

GM2 synthase was expressed using the baculovirus/Sf9 expression system as described previously (Wendeler, 2004). Cells were infected with a viral stock containing the expression vector pVL1393-$GM2S_M$ (Wendeler, 2004) at a multiplicity of infection of 1. After 72 h, insect cells were harvested by centrifugation with 1800 rpm for 5 min at 4°C. Cells were washed twice with ice-cold PBS and then resuspended in 50 mM HEPES (pH 7.3) containing 1mM $MnCl_2$ to a cell density of 15 x 10^6 cells/mL, frozen in liquid nitrogen, and stored at –80°C. The cells were thawed on ice, and the same volume of lysis buffer (50 mM HEPES, pH 7.3, 1 mM $MnCl_2$, 0.3 M NaCl, 2mM PMSF, 10 µg/ml leupeptin, 10 µg/mL E-64) was added. Cells were disrupted by ultrasound (4 x 30s, 50% intensity, 60W), centrifugated at 800g, and the resulting supernatant was centrifugated at 100000 g for 1 h at 4°C. Then, the pellet was resuspended in extraction buffer (20 mM HEPES, pH 7.3, 1 mM $MnCl_2$, 150 mM NaCl, 0.04 % PG) and homogenized by ultrasound (2 x 30s). Aliquots of the membrane fractions are frozen in liquid nitrogen and then stored at –80°C.

6.5.11. Glycosyltransferase Assay

Enzyme activity was determined according to the *in vitro*-assay described by Pohlentz (Pohlentz *et al.*, 1988). This assay is based on the transfer of [^{3}H]-GalNAc from UDP-[^{3}H]GalNAc and quantification of the resulting ganglioside GM2 by scintillation counting. The assay volume was 50 µL, consisting of 40 µL assay buffer and 10 µL cell homogenate. The required amounts of UDP-[^{3}H]GalNAc (100 000 cpm/nmol) and GM3 (0-7 nmol) were applied to the test tubes, and organic solvent was removed under a stream of nitrogen. 40 µL of assay buffer (125 mM HEPES, pH 7.3, 12.5 mM $MnCl_2$, 0.5% w/v *N*-Octyl-beta-D-glucopyranoside, 12.5 mM CDP-choline (immediately added before use)) was added and each tube was sonicated for 30 sec. in a cup horn sonicator at 100 W. The transferase preparation was added, and the tubes were incubated at 37°C for 30 min. The reaction was stopped by adding 134 µL methanol and 150 µL water on ice. The samples were applied to RP18 chromatography. The assay samples were applied to the column and the reaction vial was rinsed with 0.5 mL methanol-water (4:6, v/v). After washing the column with water the [^{3}H]-GM2 was eluted with 3 x 1 mL methanol and 3 x 1 mL chloroform-methanol (1:1, v/v). The eluate was evaporated to dryness under a stream of nitrogen. The residue was dissolved in 1 mL chloroform-methanol (1:1, v/v), and 0.5 mL were used for scintillation counting. Data were analyzed with the Enzyme Kinetics module of the SigmaPlot software.

6.5.12. Fluorescence microscopy

Human fibroblasts (10^4-10^5) were plated into each well of an 8-well Lab-Tek TM II chambered cover slide coated with 10% FCS and cultured in 200 µl DMEM, supplemented with 2 mM glutamine, 10% heat-inactivated fetal calf serum, and streptomycin 100 mg/L, at 37°C, 5% CO_2. Drugs were added to the medium to a final concentration of 1µg/ml BFA, or 25 µM ceramide derivative **5b**, repectively. The Golgi was labeled in the absence (control) or presence of drugs with C_6-NBD-ceramide/BSA complex (1 µM) for 1h at 4°C according to literature (Puetz and Schwarzmann, 1995). Then, the cells were washed twice with HMEM, warmed to 37°C for 1h, and observed by live imaging using a fluorescence microscope (Zeiss Axiovert 35, filter: BP 485, FT 510, 515-565). Images were collected with the AxioCam MRc, and the images were visualized with the AxioVision 3.1. The C_6-NBD-ceramide/BSA-complex was kindly provided by Dr. Günter Schwarzmann.

6.5.13. PKC activity assay

The PKC activity assay was obtained from Promega and the experiment was made according to the manufacturer's instructions. The assay is based on a rhodamine-labeled fluorescent peptide that is phosphorylated by PKC according to a literature protocol (Isbell et al., 1995). In agarose gel electrophoresis, the phosphorylated peptide migrates toward the anode, while the non-phosphorylated peptide migrates toward the cathode.

The assay volume was 25 µL and the reactions were carried out in 500 µL test tubes. The required amounts of Phorbolic ester ($5 \cdot 10^{-3}$ nmol), ceramide derivative **5b** (1,25 nmol), and ceramide derivative **24**

(1,25 nmol) were applied to the test tubes, and organic solvent was removed under a stream of nitrogen. The tubes were kept on ice and for each sample, 5 µL of fivefold concentrated assay buffer, 5 µL (20 µg) PepTag®C1Peptide, 5 µL of fivefold concentrated PKC activator solution, 1 µL peptide protection solution were added. At time zero, the tubes were removed from ice and incubated in a water bath at 30°C for 2 minutes. Then, 4 µL (10 ng) of Protein Kinase C was added to each tube (with the exception of the negative control) and incubated at 30°C for 30 minutes. The reaction was stopped by submerging the reaction tube in a boiling water bath. The samples were stored at –20°C in the dark until ready to load on the agarose gel.

6.5.14. Agarose Gel

Separation of non-phosphorylated substrate (PepTagC1petide) and phosphorylated product was carried out by Agarose gel electrophoresis. The samples were loaded to an agarose gel (0.8% agarose in 50 mM Tris-HCl, pH 8.0). Electrophoresis was performed at 70 V for 3 h. The gel was examined under UV light (λ = 365 nm) and photographed.

6.5.15. Quantification by Spectrophotometry

The negatively charged phosphorylated bands were excised from the gel and placed into a 1.5 mL tube. After melting the gel by heating to 95°C, 125 µL of the hot agarose was added to a tube containing 75 µL Solubilization Solution and 50 µL glacial acetic acid. The probes were quickly vortexed and transferred to a well in a 96-well plate and and the absorbance was measured at 544 nm.

7. Synthetic section

7.1. Synthesis of Garner aldehydes 2a and 2b

(*S*)-*tert*-Butyl 4-(*N*-methoxy-*N*-methylcarbamoyl)-2,2-dimethyloxazolidine-3-carboxylate (1a)

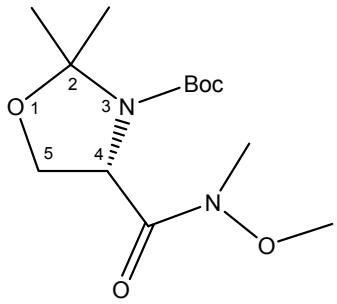

The synthesis was carried out according to literature (Campbell et al. 1998). The analytical data are in agreement with those reported in the literature. Yield: 63-81% over 3 steps, white solid, $C_{13}H_{24}N_2O_5$, M = 288.34 g/mol, R_f (petroleum ether/ethyl acetate, 1:1 (v/v)) = 0.41.

^{1}H-NMR (400 MHz, $CDCl_3$, mixture of rotamers) δ [ppm]: 1.43 (s, 9H, $C(CH_3)_3$), 1.50 (s, 3H, $C(CH_3)_2$), 1.64 (s, 3H, $C(CH_3)_2$), 3.14 (s, 3H, NCH_3), 3.68 (s, 3H, OCH_3), 3.90 (dd, 1H, $^2J_{HH}$ = 9.1 Hz, $^3J_{HH}$ = 3.4 Hz, H-5$_A$), 4.13 (dd, 1H, $^2J_{HH}$ = 9.1 Hz, $^3J_{HH}$ = 7.2 Hz, H-5$_B$), 4.74 (dd, 1H, $^3J_{HH}$ = 3.4 Hz, $^3J_{HH}$ = 7.2 Hz, H-4). ^{13}C-NMR (100 MHz, $CDCl_3$, mixture of rotamers) δ [ppm]: 24.7, 25.7 and 28.5 ($C(\underline{C}H_3)_2$ and $C(\underline{C}H_3)_3$), 32.6 (NCH_3), 57.9 (OCH_3), 61.2 (C-4), 66.2 (C-5), 80.6 ($\underline{C}(CH_3)_3$), 95.1 ($\underline{C}(CH_3)_2$, 152.2 (CO), 171.4 (CO). FAB-MS: *m/z* (%): 289.2 ([M+H]$^+$, 40%). Elemental analysis: [$C_{13}H_{24}N_2O_5$] calc.: C 54.15, H 8.39, N 9.72; found.: C 54.23, H 8.36, N 9.76.

(*S*)-*tert*-Butyl 4-formyl-2,2-dimethyloxazolidine-3-carboxylate (2a)

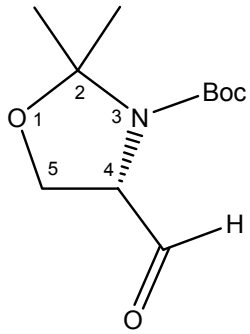

The synthesis was carried out according to literature (Garner, 1984). **1a** (2 eq.) was dissolved in anhydrous THF, cooled to 0°C, Lithiumaluminiumhydride (1M in THF, 1.5 eq.) was added dropwise, and then the mixture was stirred for 30 min. The mixture was cooled to –15°C, and potassium hydrogensulfate (saturated aqueous solution, 100 mL) was added slowly. The product was extracted with diethylether, dried over sodium sulfate, filtered, and the solvent was removed under reduced pressure. To avoid racemization of the

aldehyde, it was directly used as a raw product without further purification. Raw yield: 83 – 95 %, yellow oil, $C_{11}H_{19}NO_4$, M = 229.27 g/mol, R_f (cyclohexane/ethyl acetate, 1:1 (v/v)) = 0.81.
^{1}H-NMR (300 MHz, $CDCl_3$) δ [ppm]: 1.41 (s, 9H, $C(CH_3)_3$), 1.48 (s, 6H, $C(CH_3)_2$), 4.05 (t, 1H, $^3J_{HH}$ = 5.2 Hz, H-4), 3.90 (m, 2H, H-5), 9.55 (s, 1H, CHO). ^{13}C-NMR (75 MHz, $CDCl_3$) δ [ppm]: 23.8 ($C(\underline{C}H_3)_2$), 28.3 ($C(\underline{C}H_3)_3$), 63.9 and 64.7 (C-5 and C-4), 81.1 ($\underline{C}(CH_3)_3$), 95.1 ($\underline{C}(CH_3)_2$), 152.0 (C=O), 199.3 (C=O). FAB-MS: *m/z* (%) : 230.1 ($[M+H]^+$, 30%).

(4*S*,5*R*)-*tert*-Butyl 4-(*N*-methoxy-*N*-methylcarbamoyl)-2,2,5-trimethyloxazolidine-3-carboxylate (1b)

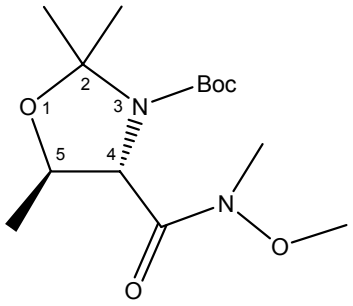

The synthesis was conducted according to the preparation of compound **1a** (Campbell et al., 1998). Yield: 4.17 g (13.8 mmol) = 55 % over 3 steps, white solid, $C_{14}H_{26}N_2O_5$, M = 302.37 g/mol, R_f (cyclohexane/ethyl acetate, 1:1 (v/v)) = 0.64, α_D = -11.3° (c = 0.577, $CHCl_3$).
^{1}H-NMR (400 MHz, $CDCl_3$, mixture of rotamers) δ [ppm]: 1.33 (d, 3H, $^3J_{HH}$ = 7.3 Hz, CH_3), 1.36 (s, 9H, $C(CH_3)_3$), 1.43 (s, 6H, $C(CH_3)_2$), 3.18 (s, 3H, NCH_3), 3.69 (s, 3H, OCH_3), 4.06 (dq, 1H, $^3J_{HH}$ = 4.8 Hz, $^3J_{HH}$ = 7.3 Hz, H-5), 4.46 (d, 1H, CHN, $^3J_{HH}$ = 4.8 Hz, H-4). ^{13}C-NMR (100 MHz, $CDCl_3$, mixture of rotamers) δ [ppm]: 19.5 (CH_3), 24.2 ($C(\underline{C}H_3)_2$), 28.6 ($C(\underline{C}H_3)_3$), 32.6 (NCH_3), 61.3 and 63.5 (OCH_3 and C-4), 74.6 (C-5), 80.6 ($\underline{C}(CH_3)_3$), 95.2 ($\underline{C}(CH_3)_2$), 151.4 (CO), 152.2 (CO). ESI-MS (positive mode): *m/z* (%) = 303.18 ($[M+H]^+$, 45%), 325.16 ($[M+Na]^+$, 8%). Elemental analysis:[$C_{14}H_{26}N_2O_5$] calc.: C 55.61, H 8.67, N 9.26; found.:C 55.22, H 8.59, N 9.10.

(4*S*,5*R*)-*tert*-Butyl 4-formyl-2,2,5-trimethyloxazolidine-3-carboxylate (2b)

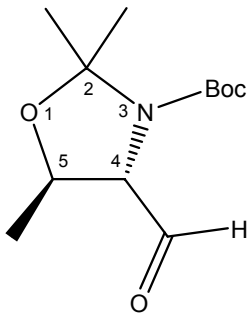

The synthesis was conducted according to the synthesis of compound **2a** (Garner, 1984). To a solution of Weinreb amide **1b** (3.69 g, 12.8 mmol) in dry THF (70 mL), Lithiumaluminiumhydride (1M solution in THF,

12.8 mL, 12.8 mmol) was slowly added at 0°C. The aldehyde was used directly without further purification to avoid racemization. Colorless oil, $C_{12}H_{21}NO_4$, M = 243.30 g/mol, R_f (cyclohexane/ethyl acetate, 1:1 (v/v) = 0.64.

7.2. Synthesis of iodine-containing heterocycles 5a, 5b, and 8a

(*R*)-*tert*-Butyl 2,2-dimethyl-4-(pentadec-1'-enyl)oxazolidine-3-carboxylate (3a)

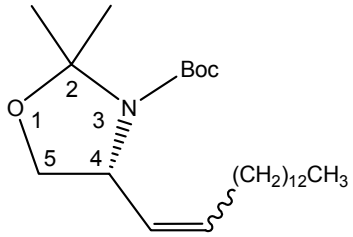

The alkene was synthesized according to literature (Campbell et al., 1998). To a suspension of tetradecyltriphenylphosphonium bromide (9.81 g, 18.19 mmol) in dry tetrahydrofuran under an argon atmosphere cooled to –78°C, n-Butyllithium (1.6 M solution in hexane, 11.38 mL, 18.21 mmol) was added dropwise. The mixture was stirred for 15 min, allowing the temperature to reach 0°C, and the resulting dark red solution was stirred for an additional hour. After cooling to –78°C, *tert*-Butyl 4(*S*)-formyl-2,2-dimethyloxazolidin-3-carboxylate **2a** (2.88 g, 12.56 mmol) dissolved in dry THF (30 mL), was added dropwise over a 10 min period. The reaction mixture was stirred until the temperature reached rt, and then for additional 3 h. The mixture was quenched with saturated aqueous ammonium chloride (100 mL) and extracted with ethyl acetate (3x 120 mL). The combined organic phases were washed with water and dried with Na_2SO_4. After evaporation of the solvent under reduced pressure, the residue was purified by chromatography on silica gel (cyclohexane/ethyl acetate, 10:1 (v/v)) to give alkene as colorless oil. Combined yield: mixture of *Z/E*-isomers = 8:1; 3.76 g (9 mmol) = 73%. The (*Z*)-alkene was isolated in 43% of total product. Colorless oil, $C_{26}H_{49}NO_3$, M = 409.36 g/mol, R_f (petroleum ether/ethyl acetate = 10:1 (v/v)) = 0.36 (*E*-alkene) and 0.41 (*Z*-alkene).

^{1}H-NMR (400 MHz, $CDCl_3$) δ [ppm]: 0.81 (t, 3H, $^3J_{HH}$ = 6.9 Hz, CH_3), 1.19 (m, 22H, CH_2), 1.37 (m, 17H, CH_2, $C(CH_3)_3$ and $C(CH_3)_2$), 1.95 (dt, 2H, $^3J_{HH}$ = 7.0 Hz, $^3J_{HH}$ = 7.0 Hz, CH_2), 3.56 (dd, 1H, $^3J_{HH}$ = 3.3 Hz, $^2J_{HH}$ = 8.6 Hz, H-5_A), 3.98 (dd, 1H, $^3J_{HH}$ = 6.2 Hz, $^2J_{HH}$ = 8.6 Hz, H-5_B), 4.56 (m, 1H, H-4), 5.34 (m, 2H, CH).

^{13}C-NMR (100 MHz, $CDCl_3$) δ [ppm]: 14.1 (CH_3), 22.9 (CH_2), 28.7 ($C(\underline{C}H_3)_3$), 29.3-29.9 (CH_2, $C(\underline{C}H_3)_2$), 32.1 (CH_2), 32.3 (CH_2), 54.7 (C-4), 69.2 (C-5), 79.7 ($\underline{C}(CH_3)_3$), 94.1 ($\underline{C}(CH_3)_2$, 128.7 and 134.0 (CH), 152.0 (C=O). FAB-MS: *m/z* (%) = 410.4 (11%, $[M+H]^+$)

(1*R*,7a*S*)-Dihydro-1-(1'(*R*)-iodotetradecyl)-5,5-dimethyl-1*H*-oxazolo[3,4-*c*]oxazol-3(5*H*)-one (4b)

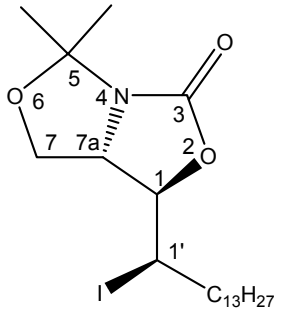

The oxazolidinone **4b** was prepared according to the literature method (Jordá-Gregori et al., 2000). To a solution of *Z*-alkene **3a** (1.3 g, 3.07 mmol) in dichloromethane (15 mL), *N*-iodosyccinimide (NIS, 1.54 g, 6.87 mmol) was added at room temperature and was stirred for 48 h. The reaction was quenched with aqueous sodium thiosulfate (10% solution) and was extracted three times with CH_2Cl_2 (50 mL). The extracts were washed with $NaHCO_3$ (10% aqueous solution, 100 mL) dried over Na_2SO_4, and evaporated to dryness under reduced pressure. The residue was purified by column chromatography on silica gel (cyclohexane/ethyl acetate, 9:1 (v/v)). Yield: 382 mg (770 µmol) = 26 %, white solid, $C_{21}H_{38}INO_3$, M = 479.43 g/mol, R_f (cyclohexane/ethyl acetate, 9:1 (v/v)) = 0.46.

^{1}H-NMR (400 MHz, $CDCl_3$) δ [ppm]: 0.85 (t, 3H, $^3J_{HH}$ = 6.8 Hz, CH_3), 1.23 (m, 20H, CH_2), 1.33 (m, 2H, CH_2), 1.44 (s, 3H, $C(CH_3)_2$), 1.69 (s, 3H, $C(CH_3)_2$), 1.77 (td, 2H, $^3J_{HH}$ = 6.3 Hz, $^3J_{HH}$ = 2.1 Hz, CH_2), 3.67 (ddd, 1H, $^3J_{HH}$ = 11.6 Hz, $^3J_{HH}$ = 6.8 Hz, $^3J_{HH}$ = 4.3 Hz, H-7a), 4.18 (m, 3H, H-1' and H-$7_{A,B}$), 4.42 (dd, 1H, $^3J_{HH}$ = 5.4 Hz, $^3J_{HH}$ = 3.8 Hz, H-1). ^{13}C-NMR (100 MHz, $CDCl_3$) δ [ppm]: 14.2 (CH_3), 22.7 – 32.3 (CH_2 and $C(\underline{C}H_3)_2$), 35.2 (CH_2 and CHI), 61.9 (C-8), 70.0 (C-1), 76.8 (C-7), 95.1 ($C(CH_3)_2$), 156.3 (C-5). FAB-MS: *m/z* (%) = 480.2 (41%, $[M+H]^+$)

(7*S*,8*S*,8a*S*)-Dihydro-8-iodo-3,3-dimethyl-7-tridecyl-oxazolo[3,4-*c*][1,3]oxazin-5(1*H*,3*H*,7*H*)-one(4a)

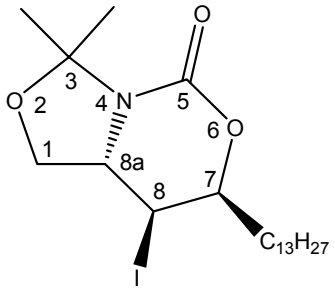

Compound **4a** was obtained as by-product in the synthesis of **4b**. Yield: 128 mg (267 µmol) = 10%, yellow solid, $C_{21}H_{38}INO_3$, M = 479.43 g/mol, R_f (cyclohexane/ethylacetate, 9:1 (v/v)) = 0.49.

^{1}H-NMR (400 MHz, $CDCl_3$) δ [ppm]: 0.86 (t, 3H, $^3J_{HH}$ = 7.0 Hz, CH_3), 1.24 (m, 20H, CH_2), 1.35 (m, 1H, CH_2), 1.56 (s, 3H, $C(CH_3)_2$), 1.59 (s, 3H, $C(CH_3)_2$), 1.63 (m, 1H, CH_2), 2.08 (m, 2H, CH_2), 3.53 (dd, 1H, $^2J_{HH}$ = $^3J_{HH}$ = 9.3 Hz, $^3J_{HH}$ = 9.3 Hz, H-1_A), 3.95 (dd, 1H, $^3J_{HH}$ = 11.3 Hz, $^3J_{HH}$ = 4.5 Hz, H-8), 4.02 (ddd, 1H, $^3J_{HH}$ = 11.3 Hz, $^3J_{HH}$ = 9.3 Hz, $^3J_{HH}$ = 5.2 Hz, H-8a), 4.26 (dd, 1H, $^3J_{HH}$ = 8.6 Hz, $^3J_{HH}$ = 5.2 Hz, H-1_B), 4.36 (ddd, 1H,

$^3J_{HH}$ = 10.6 Hz, $^3J_{HH}$ = 4.5 Hz, $^3J_{HH}$ = 2.1 Hz, H-7). ^{13}C-NMR (100 MHz, $CDCl_3$) δ [ppm]: 13.1 (CH_3), 20.6 (CH_2), 21.7 - 32.5 (CH_2 and C($\underline{C}H_3)_2$), 60.5 (C-8a), 69.3 (C-4), 76.3 (C-7), 81.4 (C-3), 96.1 ($\underline{C}(CH_3)_2$), 147.8 (C-5). ESI-MS (positive mode): *m/z* (%) = 480.2 (100%, $[M+H]^+$).

(4*S*,5*R*)-4-Hydroxymethyl-5-[1'(*R*)-iodotetradecyl]-1,3-oxazolidin-2-one (5b)

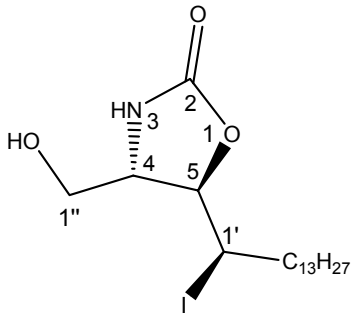

Carbamate **4b** (144 mg, 300 µmol) was dissolved in THF (3 ml). Hydrochloric acid (1M solution, 3 mL) was added and the reaction mixture was stirred for 16 h. The reaction mixture was diluted with water (10 mL), extracted three times with dichloromethane (20 mL), and the combined organic phases were dried with Na_2SO_4. After removal of the solvent under pressure, the residue was purified by silica gel chromatography (chloroform/methanol, 10:1 (v/v)). Yield : 128 mg (291.5 µmol) = 97%, white solid, $C_{18}H_{34}INO_3$, M = 439.37 g/mol, R_f (chloroform/methanol, 10:1 (v/v)). = 0.49.

^{1}H-NMR (400 MHz, $CD_3OD/CDCl_3$ = 6:1) δ [ppm]: 0.74 (t, 3H, $^3J_{HH}$ = 7.0 Hz, CH_3), 1.07 (d, 2H, $^3J_{HH}$ = 6.5 Hz, CH_2), 1.15 (m, 20H, CH_2), 1.22 (m, 1H, CH_2), 1.45 (m, 1H, CH_2), 3.51 (dd, 1H, $^3J_{HH}$ = 5.1 Hz, $^2J_{HH}$ = 11.5 Hz, H-1''$_A$), 3.63 (dd, 1H, $^3J_{HH}$ = 3.5 Hz, $^2J_{HH}$ = 11.5 Hz, H-1''$_B$), 3.69 (ddd, 1H, $^3J_{HH}$ = 5.2 Hz, $^3J_{HH}$ = 3.5 Hz, $^3J_{HH}$ = 3.5 Hz, H-4), 4.06 (ddd, 1H, $^3J_{HH}$ = 10.5 Hz, $^3J_{HH}$ = 4.3 Hz, $^3J_{HH}$ = 3.0 Hz, H-1'), 4.21 (dd, 1H, $^3J_{HH}$ = 4.1 Hz, $^3J_{HH}$ = 3.0 Hz, H-5). ^{13}C-NMR (100 MHz, $CD_3OD/CDCl_3$ = 6:1) δ [ppm]: 14.1 (CH_3), 18.8 – 35.4 (CH_2), 39.0 (CHI), 63.2 (C-4), 68.2 (C-1), 80.5 (C-5), 159.9 (C-2). IR: $\tilde{\nu}$ [cm^{-1}] = 1698.4 (C=O). ESI-MS (positive mode): *m/z* (%) = 440.2 (87%, $[M+H]^+$), 268 (100%, $[C_6H_7INO_3]^+$), 238 (82%, $[C_5H_5INO_2]^+$).

(4S,5S,6S)-4-Hydroxymethyl-5-iodo-6-tridecyl-1,3-oxazinan-2-one (5a)

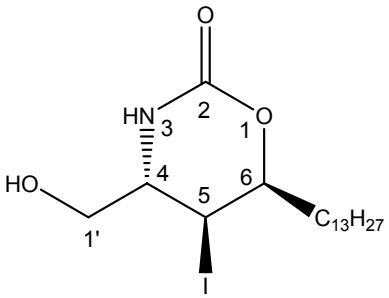

Carbamate **4b** (128 mg, 267 µmol) was dissolved in THF (3 mL) and hydrochloric acid (1M solution, 3 mL), and the mixture was stirred for 12 h at 60°C. The reaction was diluted with water (10 mL), extracted three

times with dichloromethane (20 mL) and the combined organic phases were dried with Na_2SO_4. After removal of the solvent under pressure, the residue was purified by silica gel chromatography (chloroform/methanol, 10:1 (v/v)). Yield: 30 mg (68 µmol) = 26%, white solid, $C_{18}H_{34}INO_3$, M = 439.37 g/mol, R_f (chloroform/methanol, 10:1 (v/v)) = 0.49.

^{1}H-NMR (400 MHz, $CDCl_3$) δ [ppm]: 0.86 (t, 3H, $^3J_{HH}$ = 7.1 Hz, CH_3), 1.24 (m, 20H, CH_2), 1.33 (m, 1H, CH_2), 1.57 (m, 1H, CH_2), 1.72 (m, 1H, CH_2), 1.81 (m, 1H, CH_2), 3.64 (m, 1H, H-1'$_A$), 3.80 (m, 2H, H-6, H-1'$_B$), 4.10 (m, 1H, H-4), 4.34 (m, 1H, H-5), 6.60 (br, 1H, OH), 9.10 (m, 1H, NH). ^{13}C-NMR (100 MHz, $CDCl_3$) δ [ppm]: 14.2 (CH_3), 22.7 (CH_2), 28.7 (CH_2), 29.4 (CH_2), 29.6 (CH_2), 29.7 (CH_2), 32.0 (CH_2), 34.0 (CH_2), 58.1 (C-4), 64.3 (C-1'), 80.3 (C-6), 154.7 (C-2). IR: $\tilde{\nu}$ [cm^{-1}] = 1634.0 (C=O). ESI-MS (positive mode): *m/z* (%) = 462.10 (100%, $[M+Na]^+$), 901.24 (10%, $[2M+Na]^+$).

(4*S*,5*S*,6*S*)-5-Iodo-2-oxo-6-tridecyl-1,3-oxazinane-4-carbaldehyde (8a)

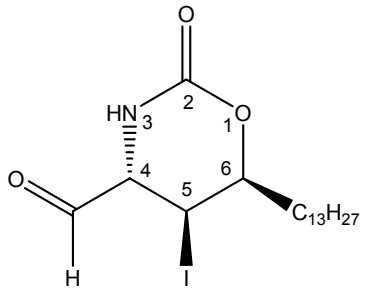

A solution of pyridinium chlorochromate (17 mg, 78.9 µmol) and oxazinanone **5a** (15 mg, 34.1 µmol) in dichloromethane (2 mL) was stirred for 12h at rt. The product was extracted with ether and purified by column chromatography with silica gel (hexane/ethyl acetate, 2:1 (v/v)). Yield: 13 mg (29.7 µmol) = 87 %, colorless solid, $C_{18}H_{32}INO_3$, M = 437.36 g/mol, R_f (hexane/ethyl acetate, 2:1(v/v)) = 0.42.

^{1}H-NMR (400 MHz, $CDCl_3$) δ [ppm]: 0.86 (t, 3H, $^3J_{HH}$ = 7.0 Hz), 1.24 (m, 22H, CH_2), 1.82 (m, 2H, CH_2), 5.18 (ddd, 1H, $^3J_{HH}$ = 6.6 Hz, $^3J_{HH}$ = 6.1 Hz, $^3J_{HH}$ = 3.3 Hz, H-6), 5.88 (dd, 1H, $^3J_{HH}$ = 3.3 Hz, $^3J_{HH}$ = 1.4 Hz, H-5), 6.96 (dd, 1H, $^3J_{HH}$ = 3.3 Hz, $^3J_{HH}$ = 1.3 Hz, H-4), 9.27 (s, 1H, CHO). ^{13}C-NMR (100 MHz, $CDCl_3$) selected peaks δ [ppm]: 14.15 (CH_3), 22.7, 29.7, 76.7 (C-6). ESI-MS (positive mode): *m/z* (%) = 438.18 (8%, $[M+H]^+$).

7.3. Synthesis of bromine-containing heterocycles 7.2a and 7.2b

(1*R*,7a*S*)-Dihydro-1-((1'*R*)-bromotetradecyl)-5,5-dimethyl-1*H*-oxazolo[3,4-*c*]oxazol-3(5*H*)-one (7.1b)

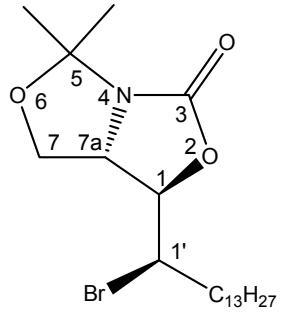

To a solution of *Z*-alkene **3a** (512.2 µmol, 217 mg) in CH_2Cl_2 (1 mL) was added *N*-bromosuccinimide (NBS, 1.21 mmol, 215 mg) at room temperature. The mixture was stirred at the same temperature for 3d. The reaction was quenched with aqueous sodium thiosulfate (10% solution) and was extracted three times with CH_2Cl_2 (50 mL). The extracts were washed with $NaHCO_3$ (10% aqueous solution, 100 mL), dried over Na_2SO_4, and evaporated to dryness under reduced pressure. The residue was purified by column chromatography on silica gel (cyclohexane/ethyl acetate, 4:1 (v/v)). Yield: 46 mg (106.7 µmol) = 21%, yellow solid, $C_{21}H_{38}BrNO_3$, M = 431.20 g/mol, R_f (cyclohexane/ethyl acetate, 5:1 (v/v)) = 0.46.

^{1}H-NMR (400 MHz, $CDCl_3$) δ [ppm]: 0.86 (t, 3H, $^3J_{HH}$ = 6.8 Hz, CH_3), 1.24 (s, 22H, CH_2), 1.43 (s, 3H, $C(CH_3)_2$), 1.70 (s, 3H, $C(CH_3)_2$), 1.72 (m, 1H, CH_2), 1.90 (m, 1H, CH_2), 3.67 (dd, $^3J_{HH}$ = $^2J_{HH}$ = 8.1 Hz, H-7$_A$), 4.10 (dt, 1H, $^3J_{HH}$ = 10.8 Hz, $^3J_{HH}$ = 3.7 Hz, H-1'), 4.14 (dd, 1H, $^2J_{HH}$ = 8.4 Hz, $^3J_{HH}$ = 6.8 Hz, H-7$_B$), 4.25 (ddd, 1H, $^3J_{HH}$ = 6.5 Hz, $^3J_{HH}$ = 7.8 Hz, $^3J_{HH}$ = 5.4 Hz, H-7a), 4.47 (dd, 1H, $^3J_{HH}$ = 5.3 Hz, $^3J_{HH}$ = 3.9 Hz, H-1).

^{13}C-NMR (100 MHz, $CDCl_3$) δ [ppm]: 14.1 (CH_3), 22.7 – 32.0 (CH_2 and $C(\underline{C}H_3)_2$), 43.1(C-1'), 61.0 (C-7a), 68.8 (C-7), 79.1 (C-1), 95.1 (C-5), 156.1 (C-3). ESI-MS (positive scan): *m/z* (%) = 432.27 and 434.23 (20%, $[M+H]^+$).

(4*S*,5*R*)-4-Hydroxymethyl-5-[1'(*R*)-bromotetradecyl]-1,3-oxazolidin-2-one (7.2b)

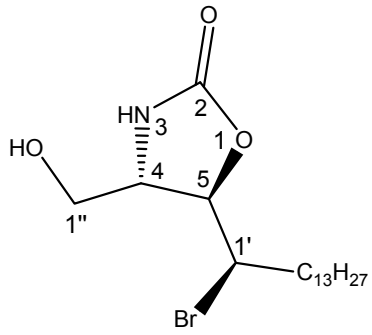

Compound **7.1b** (40 mg, 92.8 µmol) was dissolved in THF (2 mL). Hydrochloric acid (1M solution, 2 mL) was added and the reaction mixture was stirred for 16 h at rt. The reaction was diluted with water (10 mL), extracted three times with dichloromethane (20 mL), and the combined organic phases were dried with

Na_2SO_4. After removal of the solvent under pressure, the residue was purified by silica gel chromatography (chloroform/methanol, 10:1 (v/v)). Yield: 23 mg (58.6 µmol) = 63%, white solid, $C_{18}H_{34}BrNO_3$, M = 392.37 g/mol, R_f (chloroform/methanol, 10:1 (v/v)) = 0.49

^{1}H-NMR (400 MHz, $CD_3OD/CDCl_3$ = 10:1) δ [ppm]: 0.70 (t, 3H, $^3J_{HH}$ = 7.1 Hz, CH_3), 1.09 (m, 20H, CH_2), 1.15 (m, 1H, CH_2), 1.43 (m, 1H, CH_2) 1.52 (m, 2H, CH_2), 3.79 (dd, 1H, $^3J_{HH}$ = 4.5 Hz, $^2J_{HH}$ = 11.5 Hz, H-1''$_A$), 3.83 (dd, 1H, $^3J_{HH}$ = 4.7 Hz, $^2J_{HH}$ = 11.5 Hz, H-1''$_B$), 4.02 (ddd, 1H, $^3J_{HH}$ = 4.7 Hz, $^3J_{HH}$ = 4.7 Hz, $^3J_{HH}$ = 4.5 Hz, H-4), 4.34 (ddd, 1H, $^3J_{HH}$ = 7.8 Hz, $^3J_{HH}$ = 6.5 Hz, $^3J_{HH}$ = 2.7 Hz, H-1'), 4.74 (dd, 1H, $^3J_{HH}$ = 4.6 Hz, $^3J_{HH}$ = 2.7 Hz, H-5). ^{13}C-NMR (100 MHz, $CD_3OD/CDCl_3$ = 10:1) δ [ppm]: 14.3 (CH_3), 23.8 – 33.2 (CH_2), 43.3 (C-4), 64.3 (C-1'), 69.6 (C-1''), 79.6 (C-5), 159.1 (C-2). ESI-MS (positive mode): *m/z* (%) = 392.2 and 394.2 (20%, $[M+H]^+$),

(4*S*,5*S*,6*S*)-4-Hydroxymethyl-5-bromo-6-tridecyl-1,3-oxazinan-2-one (7a)

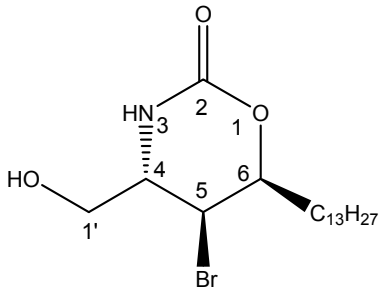

The oxazinanone **7a** was obtained from *Z*-alkene **3a** over 2 steps. Yield: 10 mg (25.5 µmol) = 5% over two steps, white solid, $C_{18}H_{34}BrNO_3$, M = 392.37 g/mol, R_f (chloroform/methanol, 10:1 (v/v)) = 0.49.

^{1}H-NMR (400 MHz, $CDCl_3/CD_3OD$ = 10:1) δ [ppm]: 0.72 (t, 3H, $^3J_{HH}$ = 7.0 Hz, CH_3), 1.11 (s, 22H, CH_2), 1.60 (m, 1H, CH_2), 1.72 (m, 1H, CH_2), 3.20 (dt, $^3J_{HH}$ = 3.1 Hz, $^3J_{HH}$ = 1.6 Hz, H-6), 3.43 (dd, 1H, $^2J_{HH}$ = 11.5 Hz, $^3J_{HH}$ = 5.1 Hz, H-1'$_A$), 3.51 (dd, 1H, $^2J_{HH}$ = 11.5 Hz, $^3J_{HH}$ = 4.2 Hz, H-1'$_B$), 3.58 (m, 1H, H-4), 4.08 (dd, 1H, $^3J_{HH}$ = 4.6 Hz, $^3J_{HH}$ = 3.1 Hz, H-5).

7.4. Synthesis of alkyne oxazinanones 10.2a-c and 11

3-Decyne-1-methanesulfonate

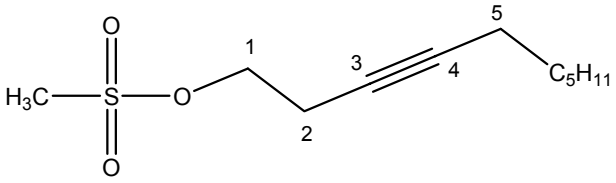

3-Decyne-1-ol (2.9 mL, 16.49 mmol) was dissolved in pyridine (70 mL) and cooled to -10°C. Methanesulfonyl chloride (1.5 mL, 19.4 mmol) was added dropwise over a period of 10 min, and solution

was stirred for 1h at –10°C, and for 3h at rt. The solvent was removed under reduced pressure and the residue was purified with silica gel by column chromatography (toluene/ethyl acetate, 17:3 (v/v)). Yield: 3.29 g (14.17 mmol) = 86%, colorless oil, $C_{11}H_{20}O_3S$, M = 232.34 g/mol, R_f (toluene/ethyl acetate, 17:3 (v/v)) = 0.54.

^{1}H-NMR (400 MHz, CD_3OD) δ [ppm]: 0.82 (t, 3H, $^3J_{HH}$ = 7.0 Hz), 1.17-1.33 (m, 6H, CH_2), 1.40 (dd, 2H, $^3J_{HH}$ = 7.7 Hz, $^3J_{HH}$ = 7.4 Hz, 6-CH_2), 2.06 (dt, 1H, $^2J_{HH}$ = 7.1 Hz, $^3J_{HH}$ = 2.4 Hz, 5-H_A), 2.08 (dt, 1H, $^2J_{HH}$ = 7.0 Hz, $^3J_{HH}$ = 2.4 Hz, 5-H_B), 2.54 (dt, 1H, $^2J_{HH}$ = 7.0 Hz, $^3J_{HH}$ = 2.4 Hz, 2-H_A), 2.56 (dt, 1H, $^2J_{HH}$ = 6.9 Hz, $^3J_{HH}$ = 2.4 Hz, 2-H_B), 2.97 (s, 3H, CH_3), 4.19 (t, 2H, 1-$H_{A,B}$). ^{13}C-NMR (100 MHz, CD_3OD) δ [ppm]: 14.1 (10-CH_3), 18.7 (5-CH_2), 20.1 (2-CH_2), 22.6 (9-CH_2), 28.6 and 28.8 (C-6 and C-7), 37.6 (CH_3), 68.2 (1-CH_2), 74.2 (4-C), 83.2 (3-C). FAB-MS: *m/z* (%) = 233.1 ($[M+H]^+$, 100%), 464.2 ($[2M+H)]^+$, 4%), Elemental analysis: [$C_{11}H_{20}O_3S$] calc.: C 56.86, H 8.68; found: C 55.93, H 8.23.

1-Iodo-3-decyne

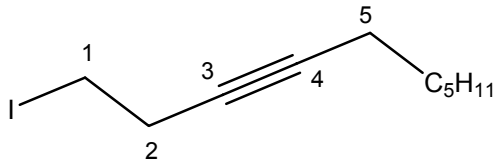

Method A: To a solution of sodiumiodide (12.41 g, 82 mmol) in acetone (230 mL), 3-Decin-1-methansulfonate (3.84 g, 16.54 mmol) was added and stirred for 2h at 60°C, and for 12h at rt. The reaction was diluted with water (200 mL), extracted with ethyl acetate (3x 100 mL) and the combined organic phases were dried with Na_2SO_4. After removal of the solvent under reduced pressure, the residue was purified by silica gel chromatography (toluene/ethyl acetate, 85:15 (v/v)). Method B: 3-Decin-1-ol (2.28 ml, 12.96 mmol) was suspended in THF (60 ml), cooled to –70°C, and methyltriphenoxyphosphonium iodide (5.9 g, 13.05 mmol) was added. After 30 min of stirring, the reaction mixture was allowed to warm to rt and stirred for another 4 h. Then, methanol (12 ml) was added and the solvent was removed under reduced pressure. The residue was purified by silica gel chromatography (toluene/ethyl acetate, 85:15 (v/v)). Yield: Method A: 4.04 g (15.3 mmol) = 93%, Method B: 3.14 g (11.89 mmol) = 92 %, colorless oil, $C_{10}H_{17}I$, M = 264.04 g/mol, R_f (cyclohexane) = 0.51.

^{1}H-NMR (400 MHz, CD_3OD) δ [ppm]: 0.82 (t, 3H, $^3J_{HH}$ = 6.9 Hz, CH_3), 1.23 (m, 6H, CH_2), 1.32 (m, 2H, CH_2), 1.40 (m, 2H, CH_2), 2.05 (dt, 1H, $^2J_{HH}$ = 6.9 Hz, $^3J_{HH}$ = 2.3 Hz, 5-H_A), 2.07 (dt, 1H, $^2J_{HH}$ = 6.8 Hz, $^3J_{HH}$ = 2.4 Hz, 5-H_B), 2.64 (dt, 1H, $^2J_{HH}$ = 7.5 Hz, $^3J_{HH}$ = 2.3 Hz, 2-H_A), 2.67 (dt, 1H, $^2J_{HH}$ = 7.4 Hz, $^3J_{HH}$ = 2.3 Hz, 2-H_B), 3.13 (t, 2H, $^3J_{HH}$ = 7.4 Hz, 1-$H_{A,B}$). ^{13}C-NMR (100 MHz, CD_3OD) δ [ppm]: 2.7 (C-2), 14.2 (C-10), 18.8 (C-5), 22.7 (C-9), 24.3 (C-1), 28.6 and 28.9 (C-6 und C-7), 31.4 (C-8), 78.9 (C-4), 82.5 (C-3). ESI-MS (positive mode): *m/z* (%) = 265.06 ($[M+H]^+$). IR: $\bar{\nu}$ [cm^{-1}] = 2926.2 ν(-CH_2-), 2250 ν(-C≡C), 1465.2 δ(-CH_2-), 1377.7 δ(-CH_3). Elemental analysis: [$C_{10}H_{17}I$] calc.: C 45.47, H 6.49; found.: C 45.06, H 6.62.

3-Decynyl-1-triphenylphosphonium iodide

In toluene (160 mL), 1-Iodo-3-Decyne (16.17 g, 61.23 mmol) and triphenylphosphine (16.04 g, 61.23 mmol) were dissolved and stirred for 12h at 110°C. The solvent was decanted, and the product was washed with ether. Yield: 9.92 g (18.28 mmol) = 30%, colorless solid, $C_{28}H_{32}IP$, M = 526.43 g/mol.

^{1}H-NMR (400 MHz, CD_3OD) δ [ppm]: 0.85 (t, 3H, CH_3), 1.22 (m, 8H, CH_2), 1.85 (m, 2H, CH_2), 2.72 (tt, 1H, $^3J_{HH}$ = 6.9 Hz, $^4J_{HH}$ = 2.4 Hz, 2-H_A), 2.76 (tt, 1H, $^3J_{HH}$ = 6.9 Hz, $^4J_{HH}$ = 2.4 Hz, 2-H_B), 4.12 (dt, 2H, $^2J_{PH}$ = 12.3 Hz, $^3J_{HH}$ = 6.9 Hz, H-1), 7.79 (dd, 6H, $^3J_{HH}$ = 7.7 Hz, $^4J_{PH}$ = 3.4 Hz, H_{arom}), 7.93 (dm, 3H, $^3J_{HH}$ = 7.5 Hz, H_{arom}), 8.03 (ddd, 6H, $^3J_{PH}$ = 12.8 Hz, $^3J_{HH}$ = 7.3 Hz, $^4J_{HH}$ = 0.9 Hz, H_{arom}). ^{13}C-NMR (100 MHz, CD_3OD) δ [ppm]: 13.7 (C-1), 14.4 (CH_3), 19.0, 21.5, 23.0, 23.2 and 32.1(CH_2), 77.5 and 85.3 (C-3 and C-4), 119.1 and 126.1 (qC_{arom}), 131.0 – 135.9 (C_{arom}). IR: $\bar{\nu}$ [cm^{-1}] = 3100 ν(CH_{arom}), 2922.5 ν(-CH_2-), 2120 ν(-C≡C-), 1435.8 δ(-CH_2-). ESI-MS (positive mode): *m/z* (%) = 399.2 (100%, $[C_{28}H_{32}P]^+$), 527.1 (2%, $[M+H]^+$).

(*R*)-*tert*-Butyl 2,2-dimethyl-4-(undec-1-en-4-ynyl)oxazolidine-3-carboxylate (9)

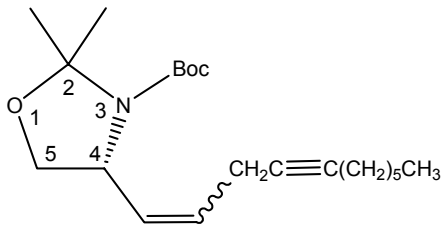

The alkene (**9**) was synthesized according to the synthesis of alkene **3a** (Campbell et al., 1998): Weinreb amide **1a** (3.52 g, 12.8 mmol), Lithiumaluminium hydride (1M solution in THF, 12.8 ml, 12.8 mmol), Dec-3-ynyltriphenyl-phosphonium iodide (6.07 g, 11.18 mmol), and n-Butyllithium (1.6 M solution in hexane, 6.4 mL, 10.2 mmol). The product was purified by chromatography on silica gel (cyclohexane/ethyl acetate, 10:1 (v/v)). Yield: 1.99 g (5.69 mmol) = 44 % over 2 steps, yellow oil, $C_{21}H_{35}NO_3$, M = 349.51 g/mol,

R_f (chloroform/methanol, 20:1 (v/v)) = 0.33 (*E*-alkene), 0.29 (*Z*-alkene).

^{1}H-NMR (400 MHz, $CDCl_3$) δ [ppm]: 0.82 (t, 3H, $^3J_{HH}$ = 7.0 Hz), 1.21 (m, 4H, CH_2), 1.29 (m, 5H, CH_2 and $C(CH_3)_2$), 1.44 (s, 9H, $C(CH_3)_3$), 1.49 (s, 3H, $C(CH_3)_2$), 1.52 (m, 2H, CH_2), 2.05 (dt, 2H, $^3J_{HH}$ = 7.0 Hz, $^3J_{HH}$ = 2.1 Hz, CH_2), 2.90 (m, 2H, CH_2), 3.61 (dd, 1H, $^2J_{HH}$ = 8.6 Hz, $^3J_{HH}$ = 2.8 Hz, H-5_A), 4.00 (dd, 1H, $^2J_{HH}$ = 8.6 Hz, $^3J_{HH}$ = 6.4 Hz, H-5_B), 4.54 (m, 1H, H-4), 5.77 (dt, 1H, $^3J_{HH}$ = 15.6 Hz, $^3J_{HH}$ = 8.4 Hz, CH), 6.21 (dd, 1H, $^3J_{HH}$ = 15.6 Hz, $^3J_{HH}$ = 2.1 Hz). ^{13}C-NMR (100 MHz, $CDCl_3$) δ [ppm]: 14.0 (CH_3), 17.3 (CH_2), 18.7 (CH_2), 22.5 (CH_2), 26.9 ($C(\underline{C}H_3)_2$), 28.4 (CH_2), 28.5 ($C(\underline{C}H_3)_3$), 28.9 (CH_2), 31.3 (CH_2), 54.3 (C-4), 68.6 (C-5), 85.3 and 85.9 (C-2 and $\underline{C}(CH_3)_3$), 127.4 (CH), 131.3 (CH), 151.9 (CO). IR: $\bar{\nu}$ [cm^{-1}] = 3445.4 ν($C(CH_3)_2$), 2930.1 ν(-CH_2-), 2450 ν(-C≡C-), 1760.3 ν(C=O), 1465.2, 1371.9 δ(-CH_3). FAB-MS: *m/z* (%) = 350.2 (18 %, $[M+H]^+$), 250.2 (50 %, $[M+H-C_5H_9O_2]^+$).

(7*S*,8*S*,8a*S*)-Dihydro-8-iodo-3,3-dimethyl-7-(non-2-inyl)oxazolo[3,4-*c*][1,3]oxazin-5(1*H*,3*H*,7*H*)-one (10.1a)

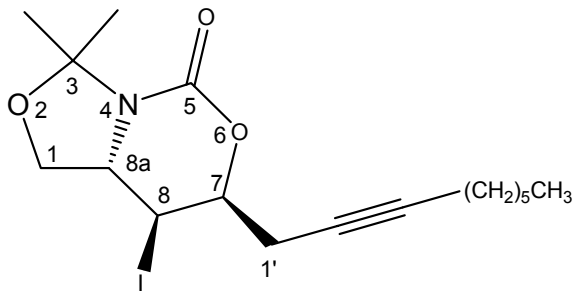

The compound (**10.1a**) was obtained as by-product within the synthesis of **10.1b**. Yield: 4 mg (9.5 µmol) = 3%, white solid, $C_{17}H_{26}INO_3$, M = 419.30 g/mol, R_f (cyclohexane/ethyl acetate = 5:1 (v/v)) = 0.31.

^{1}H-NMR (400 MHz, CD_3Cl_3) δ [ppm]: 0.82 (t, 3H, $^3J_{HH}$ = 7.0 Hz, CH_3), 1.21-1.40 (m, 8H, CH_2), 1.52 (s, 3H, $C(CH_3)_2$), 1.55 (s, 3H, $C(CH_3)_2$), 2.10 (m, 2H, CH_2), 2.81 (dd, 1H, $^2J_{HH}$ = 17.5 Hz, $^3J_{HH}$ = 3.7 Hz, CH_2), 2.87 (dd, 1H, $^2J_{HH}$ = 17.5 Hz, $^3J_{HH}$ = 3.5 Hz, CH_2), 3.56 ("t", 1H, $^3J_{HH}$ = $^2J_{HH}$ = 9.1 Hz, H-1_A), 3.85 ("t", 1H, $^3J_{HH}$ = 10.7 Hz, H-8), 3.99 (ddd, 1H, $^3J_{HH}$ = 10.9 Hz, $^3J_{HH}$ = 9.4 Hz, $^3J_{HH}$ = 5.9 Hz, H-8a), 4.19 (dd, 1H, $^2J_{HH}$ = 9.0 Hz, $^3J_{HH}$ = 5.7 Hz, H-1_B), 4.39 (ddd, 1H, $^3J_{HH}$ = 10.5 Hz, $^3J_{HH}$ = 3.6 Hz, $^3J_{HH}$ = 3.5 Hz, H-7).

^{13}C-NMR (100 MHz, CD_3OD) δ [ppm]: 14.1 (CH_3), 18.8 (CH_2), 19.7 (C-5), 22.6 (CH_2), 23.8 ($C(\underline{C}H_3)_2$), 24.3 (CH_2) 26.2 ($C(\underline{C}H_3)_2$), 28.8 (CH_2), 28.6 (CH_2), 31.4 (CH_2), 60.7 (C-8a), 70.3 (C-1), 72.4 (qC), 80.5 (C-4), 84.6 (qC), 97.2 (C-3), 148.5 (C-5). FAB-MS: *m/z* (%) = 420.1 ($[M+H]^+$, 64%).

(1*R*,7a*S*)-Dihydro-1-(1'(*R*)-iododec-3-inyl)-dihydro-5,5-dimethyl-1*H*-oxazolo[3,4-*c*]oxazol-3(5*H*)-one (10.1b)

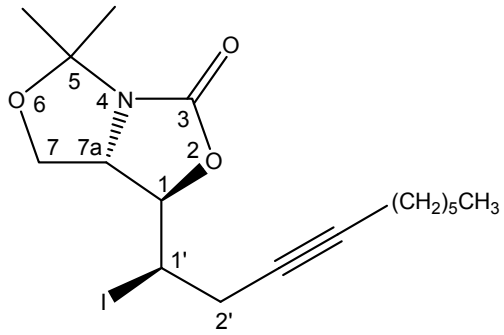

The compound was prepared according to synthesis of **4b**. Alkene **9** (*E*/*Z*-isomeres, 980.2 mg, 2.80 mmol) was dissolved in dichloromethane (10 ml) and *N*-iodosuccinimide (1.26 g, 5.6 mmol) was added. The reaction was stirred for 48 h at rt. The residue was purified by column chromatography with silica gel (hexane/ethyl acetate, 10:1 (v/v)). Yield: 370.1 mg (882 µmol) = 32 %, white solid, $C_{17}H_{26}INO_3$, M = 419.30 g/mol, R_f (hexane/ethyl acetate = 5:1 (v/v)) = 0.31.

^{1}H-NMR (400 MHz, CD_3Cl_3) δ [ppm]: 0.82 (t, 3H, $^3J_{HH}$ = 7.2 Hz, CH_3), 1.26 (m, 4H, CH_2), 1.35 (m, 2H, CH_2), 1.42 (s, 3H, $C(CH_3)_2$), 1.47 (m, 2H, CH_2), 1.69 (s, 3H, $C(CH_3)_2$), 2.07 (tt, 2H, $^3J_{HH}$ = 7.0 Hz, $^5J_{HH}$ = 2.4 Hz, CH_2), 2.79 (ddt, 1H, $^2J_{HH}$ = 17.2 Hz, $^3J_{HH}$ = 7.1 Hz, $^5J_{HH}$ = 2.3 Hz, H-2'$_A$), 2.88 (ddt, 1H, $^2J_{HH}$ = 17.2 Hz, $^3J_{HH}$

= 7.2 Hz, $^5J_{HH}$ = 2.4 Hz, H.2'$_B$), 3.64 (dd, 1H, $^2J_{HH}$ = $^3J_{HH}$ = 7.2 Hz, H-7$_A$), 4.13 (m, 3H, H-1' and H-7$_B$ and H-7a), 4.29 (dd, 1H, $^3J_{HH}$ = 5.2 Hz, $^3J_{HH}$ = 3.7 Hz, H-1). ^{13}C-NMR (100 MHz, CD_3OD) δ [ppm]: 14.2 (CH_3), 18.9 (CH_2), 22.7 (CH_2), 23.5 (C-1'), 26.2 (CH_2), 27.6 (C($\underline{C}H_3)_2$), 28.7 (CH_2), 28.8 (CH_2), 31.0 (C($\underline{C}H_3)_2$), 31.5 (CH_2), 63.3 (C-7a), 68.7 (C-7), 76.8 and 79.0 (C-3' and C-4'), 84.3 (C-1), 95.2 (C-5), 156.1 (C-3). IR: $\overline{\nu}$ [cm^{-1}] = 3378.0 ν(C($CH_3)_2$), 2930.0 ν(-CH_2-), 2250 ν(-C≡C-), 1694.0 ν(C=O), 1455.3 δ(-CH_2-), 1384.0 δ(-CH_3). FAB-MS: *m/z* (%) = 420.1 (64 %, $[M+H]^+$).

(4*S*,5*R*)-4-Hydroxymethyl-5-(1'(*R*)-iododec-3-inyl)oxazolidin-2-one (10.2b)

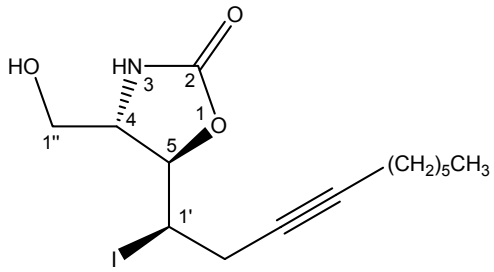

The compound **10.2b** was obtained according to the synthesis of oxazolidinone **5b**. Carbamate **10.1b** (144 mg, 300 µmol) was dissolved in THF (3 mL), and hydrochloric acid (1M solution, 3 mL) was added and stirred for 16 h at rt. The reaction was diluted with water (10 mL), extracted three times with dichloromethane (20 mL) and the combined organic phases were dried with Na_2SO_4. After removal of the solvent under pressure, the residue was purified by silica gel chromatography (chloroform/methanol, 10:1 (v/v)). Yield: 81 mg (213.6 µmol) = 71%, white solid, $C_{14}H_{22}INO_3$, M = 379.23 g/mol, R_f (chloroform/methanol = 10:1 (v/v)) = 0.19.

^{1}H-NMR (400 MHz, $CD_3OD/CDCl_3$ = 1:1 (v/v)) δ [ppm]: 0.82 (t, 3H, $^3J_{HH}$ = 7.0 Hz, CH_3), 1.23 (m, 6H, CH_2), 1.42 (m, 2H, CH_2), 2.15 (t, 2H, $^3J_{HH}$ = 7.0 Hz, CH_2), 2.79 (ddt, 1H, $^2J_{HH}$ = 17.2 Hz, $^3J_{HH}$ = 7.3 Hz, $^5J_{HH}$ = 2.3 Hz, H-2'$_A$), 2.87 (ddt, 1H, $^2J_{HH}$ = 17.2 Hz, $^3J_{HH}$ = 7.5 Hz, $^5J_{HH}$ = 2.3 Hz, H-2'$_B$), 3.57 (dd, 1H, $^2J_{HH}$ = 12.1 Hz, $^3J_{HH}$ = 5.7 Hz, H-1'$_A$), 3.72 (m, 2H, H-1'$_B$ and H-4), 4.08 (td, 1H, $^3J_{HH}$ = 7.3 Hz, $^3J_{HH}$ = 3.0 Hz, H-1'), 4.30 (dd, 1H, $^3J_{HH}$ = 4.4 Hz, $^3J_{HH}$ = 3.0 Hz). ^{13}C-NMR (100 MHz, $CD_3OD/CDCl_3$ = 1:1 (v/v)) δ [ppm]: 13.1 (CH_3), 18.0 (CH_2), 22.2 (CH_2), 28.4 (CH_2), 31.4 (CH_2), 34.2 (CH_2), 36.2 (CH_2), 48.3 (CH_2), 59.8 (CH_2), 50.9 (CH_2), 62.6 (CH_2), 77.0 (CH_2), 79.0 (qC), 79.4 (qC), 83.0 (C-5), 159.5 (C-2). FAB-MS: *m/z* (%) = 380.1 (100%, $[M+H]^+$).

(7*R*,8*S*,8a*S*)-Dihydro-8-iodo-3,3-dimethyl-7-(non-2-inyl)oxazolo[3,4-*c*][1,3]oxazin-5(1*H*,3*H*,7*H*)-one (10.1c)

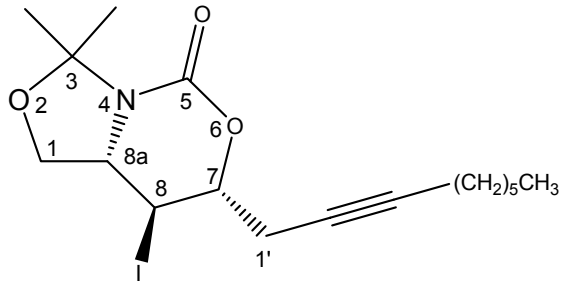

The compound (**10.1c**) was obtained as major product within the synthesis of **10.1b**. Yield: 697.6 mg (1.84 mmol) = 66%, white solid, $C_{17}H_{26}INO_3$, M = 419.30 g/mol, R_f (chloroform/methanol = 10:1 (v/v)) = 0.81.

^{1}H-NMR (400 MHz, CD_3Cl_3) δ [ppm]: = 0.70 (t, 3H, $^3J_{HH}$ = 7.3 Hz, CH_3), 1.07 (m, 6H, CH_2), 1.24 (m, 2H, CH_2), 1.42 (s, 3H, $C(CH_3)_2$), 1.46 (s, 3H, $C(CH_3)_2$), 1.85 (tt, 2H, $^3J_{HH}$ = 7.0 Hz, $^5J_{HH}$ = 2.4 Hz, CH_2), 2.34 (ddt, 1H, $^2J_{HH}$ = 17.2 Hz, $^3J_{HH}$ = 6.4 Hz, $^5J_{HH}$ = 2.3 Hz, CH_2), 2.62 (ddt, 1H, $^2J_{HH}$ = 17.2 Hz, $^3J_{HH}$ = 4.7 Hz, $^5J_{HH}$ = 2.3 Hz, CH_2), 2.92 (dd, 1H, $^3J_{HH}$ = 9.6 Hz, $^2J_{HH}$ = 8.5 Hz, H-1_A), 3.04 (dd, 1H, $^3J_{HH}$ = 11.1 Hz, $^3J_{HH}$ = 5.1 Hz, H-8), 3.81 (ddd, 1H, $^2J_{HH}$ = 8.4 Hz, $^3J_{HH}$ = 5.4 Hz, H-1_B), 3.94 (ddd, 1H, $^3J_{HH}$ = 11.1 Hz, $^3J_{HH}$ = 9.7 Hz, $^3J_{HH}$ = 5.4 Hz, H-8a), 4.00 (ddd, 1H, $^3J_{HH}$ = 6.4 Hz, $^3J_{HH}$ = 4.7 Hz, $^3J_{HH}$ = 4.7 Hz, H-7). ^{13}C-NMR (100 MHz, CD_3OD) δ [ppm]: 14.6 (CH_3), 19.5 (CH_2), 19.9 (C-8), 23.3 (CH_2), 24.4 ($C(\underline{C}H_3)_2$), 24.5 (CH_2), 27.0 ($C(\underline{C}H_3)_2$), 29.3 (CH_2), 29.4 (CH_2), 32.0 (CH_2), 57.5 (C-8a), 71.0 (C-2'), 75.4 (C-3'), 78.0 (C-1), 84.5 (C-7), 97.4 (C-3), 147.9 (C-5). ESI-MS (positive mode): *m/z* (%) = 420.07 (100 %, $[M+H]^+$), 839.20 (31 %, $[2M+H]^+$), 861.20 (6 %, $[2M+Na]^+$)

(4*S*,5*S*,6*R*)-4-Hydroxymethyl-5-iodo-6-(non-2-inyl)-1,3-oxazinan-2-one (10.2c)

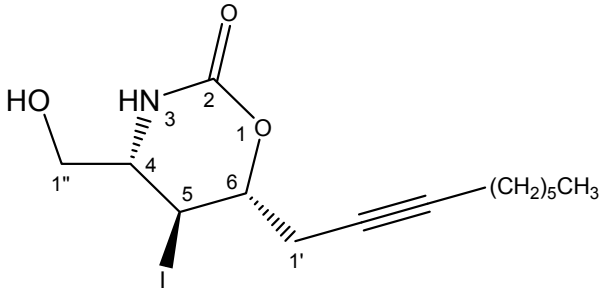

The oxazinanone **10.2c** was synthesized according to the synthesis of oxazinanone **5a**. Oxazinanone **10.1c** (226.4 mg, 597 µmol) and THF/1M HCl (1:1 (v/v), 5 mL). Yield: 60 mg (158 µmol) = 27%, white solid, $C_{14}H_{22}INO_3$, M = 379.23 g/mol, R_f (chloroform/methanol = 10:1 (v/v)) = 0.23.

^{1}H-NMR (400 MHz, $CD_3OD/CDCl_3$ = 1:1 (v/v)) δ [ppm]: 0.82 (t, 3H, $^3J_{HH}$ = 7.0 Hz, CH_3), 2.08 (tt, 2H, $^3J_{HH}$ = 7.0 Hz, $^3J_{HH}$ = 2.3 Hz), 2.79 (ddt, 1H, $^2J_{HH}$ = 17.2 Hz, $^3J_{HH}$ = 7.3 Hz, $^3J_{HH}$ = 2.3 Hz, CH_2), 2.87 (ddt, 1H, $^2J_{HH}$ = 17.1 Hz, $^3J_{HH}$ = 7.5 Hz, $^3J_{HH}$ = 2.3 Hz, CH_2), 3.58 (dd, 1H, $^3J_{HH}$ = 12.6 Hz, $^3J_{HH}$ = 5.7 Hz, H-1''$_A$), 3.77 (m, 2H, H-1''$_B$ and H-4), 4.08 (td, 1H, $^3J_{HH}$ = 7.3 Hz, $^3J_{HH}$ = 3.0 Hz, H-6), 4.30 (dd, 1H, $^3J_{HH}$ = 4.4 Hz, $^3J_{HH}$ = 3.0 Hz, H-5). ^{13}C-NMR (100 MHz, $CD_3OD/CDCl_3$ = 1:1 (v/v)) δ [ppm]: 14.1 (CH_3), 18.8 (CH_2), 22.6 (CH_2), 27.1

(CH_2), 28.6 (CH_2), 28.7 (CH_2), 31.4 (CH_2), 33.0 (C-5), 59.2 (C-4), 63.6 (CH_2), 78.9 (C-6), 84.1 (qC), 159.3 (C-2). ESI-MS (positive mode): *m/z* (%) = 380.05 (49 %, $[M+H]^+$), 402.04 (20 %, $[M+Na]^+$).

(4*S*,5*S*,6*R*)-4-Hydroxymethyl-5-iodo-6-(non-2-enyl)-1,3-oxazinan-2-one (11)

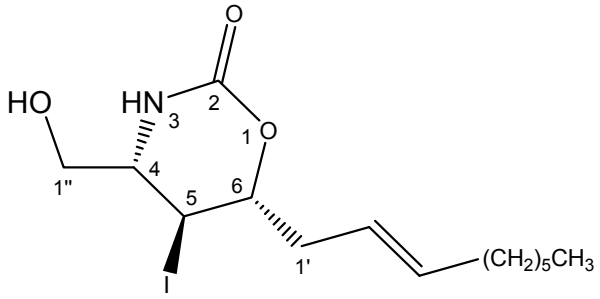

Oxazinanone **10.2c** (53 mg, 139.7 µmol) was dissolved in dichloromethane (1 mL), and trifluoroacetic acid (25 µL, 194 µmol) and triethylsilane (89 µL, 558.8 µmol) were added. The mixture was stirred for 16 h at room temperature. The reaction was diluted with ethyl acetate (100 mL), washed with water (2x 50 mL), sodium hydrogencarbonate (50 mL), and brine (50 mL), and the organic layer was dried with Na_2SO_4. Then the solvent was removed under reduced pressure and the residue was purified by column chromatography on silica gel (chloroform/methanol, 10:1 (v/v)). The product (**11**) could only be isolated in a mixture with alkyne **10.2c**. White solid, $C_{14}H_{24}INO_3$, M = 381.25 g/mol R_f (chloroform/methanol = 10:1 (v/v)) = 0.12. Yield: 17 mg (mixture of **10.2c** and **11** ((1:10)).

^{1}H-NMR (400 MHz, CD_3OD) δ [ppm]: = 0.81 (t, 3H, $^3J_{HH}$ = 7.1 Hz, CH_3), 1.10 (m, 8H, CH_2), 1.96 (m, 2H, CH_2), 2.66 (dd, 2H, $^3J_{HH}$ = 7.0 Hz, $^3J_{HH}$ = 6.7 Hz, H-1'$_{A,B}$), 3.62 (dd, 1H, $^2J_{HH}$ = 12.5 Hz, $^3J_{HH}$ = 5.5 Hz, H-1''$_A$), 3.78 (m, 2H, H-1''$_B$ and H-4), 4.02 (ddd, 1H, $^3J_{HH}$ = 8.2 Hz, $^3J_{HH}$ = 6.7 Hz, $^3J_{HH}$ = 2.8 Hz, H-6), 4.22 (dd, 1H, $^3J_{HH}$ = 4.6 Hz, $^3J_{HH}$ = 2.8 Hz, H-5), 5.26 (ddt, 1H, $^3J_{HH}$ = 18.0 Hz, $^3J_{HH}$ = 7.2 Hz, $^4J_{HH}$ = 1.6 Hz, CH_{alkene}), 5.52 (ddt, 1H, $^3J_{HH}$ = 18.0 Hz, $^3J_{HH}$ = 7.4 Hz, $^4J_{HH}$ = 1.5 Hz, CH_{alkene}). ESI-MS (positive mode): *m/z* (%) = 404.7 (93%, $[M+Na]^+$).

7.5. Synthesis of ω-azido-oxazinanone (12)

(*R*)-*tert*-Butyl 2,2-dimethyl-4-ethenyloxazolidine-3-carboxylate (14)

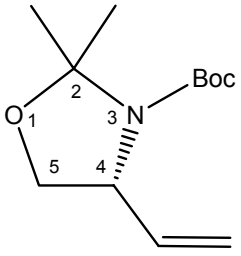

The alkene was synthesized according to literature (Campbell et al., 1998). To a suspension of Methyltriphenylphosphonium bromide (7.47 g, 20.9 mmol) in dry tetrahydrofuran (150 mL), KHMDS (potassium bis(trimethylsilyl)amide, 0.5 M solution in toluene, 41.84 mL, 20.9 mmol) was added dropwise in argon atmosphere, and the mixture was stirred for 1 hour at rt. After cooling to –78°C, *tert*-Butyl 4(S)-formyl-2,2-dimethyloxazolidin-3-carboxylate (**1a**, 2 g, 8.7 mmol) dissolved in dry THF (30 mL) was added dropwise over a 10 min period. The reaction mixture was stirred until the temperature reached rt and then for further 12h. After addition of methanol (20 ml), the mixture was quenched with saturated aqueous ammonium chloride (100 mL) and extracted with ethyl acetate (3x 120 mL). The combined organic phases were washed with water and dried with Na_2SO_4. After evaporation of the solvent under reduced pressure, the residue was purified by chromatography on silica gel (cyclohexane/ethyl acetate, 20:1 (v/v)) to give alkene as colorless oil. Yield: 1.82 g (8.01 mmol) = 92%, colorless oil, $C_{12}H_{21}NO_3$, M = 227.3 g/mol, R_f (hexane/ethyl acetate, 7:1 (v/v)) = 0.38.

^{1}H-NMR (400 MHz, $CDCl_3$) δ [ppm]: 1.43 (s, 9H, $C(CH_3)_3$), 1.50 (s, 3H, $C(CH_3)_2$), 1.59 (s, 3H, $C(CH_3)_2$), 3.68 (dd, 1H, $^2J_{HH}$ = 8.8 Hz, $^3J_{HH}$ = 2.4 Hz, H-5_A), 3.97 (dd, 1H, $^2J_{HH}$ = 8.8 Hz, $^3J_{HH}$ = 6.2 Hz, H-5_B), 4.25 (m, 1H, H-4), 5.14 (m, 2H, H-2'), 5.80 (m, 1H, H-1´). ^{13}C-NMR (100 MHz, $CDCl_3$) δ [ppm]: 23.9 ($C(\underline{C}H_3)_2$), 25.1 ($C(\underline{C}H_3)_2$), 28.6 ($C(\underline{C}H_3)_3$), 59.9 (C-4), 68.4 (C-5), 80.4 ($\underline{C}(CH_3)_3$), 93.9 (C-2), 116.0 (C-2'), 137.7 (C-1'), 152.3 (CO). ESI-MS (positive mode): *m/z* (%) = 250.1 ($[M+Na]^+$, 100%).

(*R*)-*tert*-Butyl 4-((*E*)-11-hydroxy-undec-1-enyl)-2,2-dimethyloxazolidine-3-carboxylate (15)

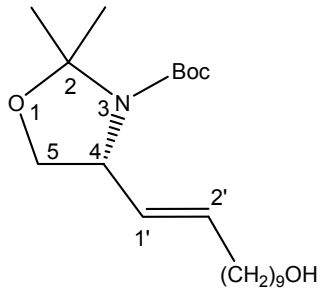

Alkene **14** (282.3 mg, 1.26 mmol) was dissolved in dichloromethane (30 mL), and undec-10-enol (363.6 µL, 2.52 mmol) and Grubbs second-generation catalyst (10 mg, 11.7 µmol) were added. The reaction mixture was refluxed for 4 hours, during which the color of the solution turned from red into brown. After evaporation of the solvent under reduced pressure, the residue was purified by chromatography on silica gel (cyclohexane/ethyl acetate, 8:1 (v/v)) to give alkene **15** as colorless oil. Yield: 279 mg (756 µmol) = 60%, colorless oil, $C_{21}H_{39}NO_4$, M = 369.54 g/mol, R_f (hexane/ethyl acetate, 8:1 (v/v)) = 0.14.

^{1}H-NMR (400 MHz, $CDCl_3$) δ [ppm]: 1.25 (m, 14H, CH_2), 1.42 (s, 9H, $C(CH_3)_3$), 1.48 (s, 3H, $C(CH_3)_2$), 1.57 (s, 3H, $C(CH_3)_2$), 2.00 (dt, 2H, $^3J_{HH}$ = 7.0 Hz, $^3J_{HH}$ = 7.1 Hz, CH_2), 3.60 (t, 2H, $^3J_{HH}$ = 6.7 Hz, CH_2), 3.69 (dd, 1H, $^2J_{HH}$ = 8.8 Hz, $^3J_{HH}$ = 2.0 Hz, H-5_A), 3.99 (dd, 1H, $^2J_{HH}$ = 8.8 Hz, $^3J_{HH}$ = 6.0 Hz, H-5_B), 4.15 (m, 1H, OH), 4.28 (m, 1H, H-4), 5.29 (dt, 1H, $^3J_{HH}$ = 15.3 Hz, $^3J_{HH}$ = 5.6 Hz, H-2'), 5.34 (dd, 1H, $^3J_{HH}$ = 15.1 Hz, $^3J_{HH}$ = 7.6 Hz, H-1').

^{13}C-NMR (100 MHz, $CDCl_3$) δ [ppm]: 22.3 (CH_2), 25.9 ($C(\underline{C}H_3)_2$), 27.6 (CH_2), 28.7 ($C(\underline{C}H_3)_3$), 29.3-33.0 (CH_2), 44.1 (CH_2), 59.4 (CH_2), 63.2 (C-4), 68.7 (C-5), 79.6 ($\underline{C}(CH_3)_3$), 93.9 (C-2), 130.5 and 132.9 (C-1' and C-2'), 152.2 (CO). ESI-MS (positive mode): *m/z* (%) = 370.29 ($[M+H]^+$, 13%), 392.26 ($[M+Na]^+$, 100%).

(*R*)-*tert*-Butyl 4-((*E*)-11-azido-undec-1-enyl)-2,2-dimethyloxazolidine-3-carboxylate (16)

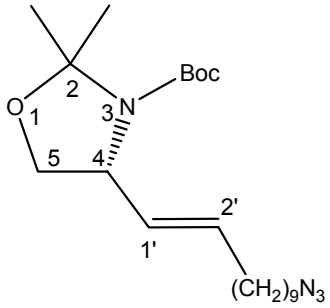

Method A: Alcohol **15** (217 mg, 587 µmol) and pyridine (1 mL) were dissolved in dichloromethane (10 mL) and cooled to –20°C. Methanesulfonyl chloride (54 µL, 704.6 µmol) was added slowly and the reaction was stirred for 1h at 0°C and additional 4h at rt. After addition of $NaHCO_3$-solution (10 ml), the methane sulfonate was extracted with dichloromethane (3x 50 mL) and dried with Na_2SO_4. After evaporation of the solvent under reduced pressure, the residue was dissolved in dimethylformamide (10 mL), and sodium azide (4.76 g, 73 mmol) was added. The reaction mixture was stirred for 12 hours, quenched with water (100 mL), and the product was extracted with ethylacetate (4x 50 mL). After evaporation of the solvent under reduced pressure, alkene **16** was purified by chromatography on silica gel (cyclohexane/ethyl acetate, 20:1 (v/v)).

Method B: Alkene **14** (400 mg, 1.76 mmol) was dissolved in dichloromethane (50 mL), and 11-azido-undec-1-ene (1.72 g, 8.81 mmol) and Grubbs second-generation catalyst (10 mg, 11.7 µmol) were added. The reaction mixture was refluxed for 12 hours. After evaporation of the solvent under reduced pressure, the residue was purified by chromatography on silica gel (cyclohexane/ethyl acetate, 20:1 (v/v)). Yield: Method A: 53 mg (134 µmol) = 23 % over 2 steps, Method B: 373 mg (945 µmol) = 54 %, colorless oil, $C_{21}H_{38}N_4O_3$, M = 394.55 g/mol, R_f (hexane/ethyl acetate, 5:1 (v/v)) = 0.75.

^{1}H-NMR (400 MHz, $CDCl_3$) δ [ppm]: 1.26 (m, 14H, CH_2), 1.42 (s, 9H, $C(CH_3)_3$), 1.48 (s, 3H, $C(CH_3)_2$), 1.57 (s, 3H, $C(CH_3)_2$), 2.0 (dt, 2H, $^3J_{HH}$ = 6.9 Hz, $^3J_{HH}$ = 6.9 Hz, CH_2), 3.23 (t, 2H, $^3J_{HH}$ = 6.9 Hz, CH_2), 3.68 (dd, 1H, $^2J_{HH}$ = 8.7 Hz, $^3J_{HH}$ = 2.1 Hz, H-5_A), 3.99 (dd, 1H, $^2J_{HH}$ = 8.7 Hz, $^3J_{HH}$ = 6.0 Hz, H-5_B), 4.28 (m, 1H, H-4), 5.29 (dt, 1H, $^3J_{HH}$ = 15.4 Hz, $^3J_{HH}$ = 7.7 Hz, H-2'), 5.30 (dd, 1H, $^3J_{HH}$ = 15.4 Hz, $^3J_{HH}$ = 5.4 Hz, H-1').

^{13}C-NMR (100 MHz, $CDCl_3$) δ [ppm]: 22.3 (CH_2), 26.9 ($C(\underline{C}H_3)_2$), 27.6 (CH_2), 28.6 ($C(\underline{C}H_3)_3$), 29.0-32.3 (CH_2), 44.1 (CH_2), 51.7 (CH_2), 59.4 (C-4), 68.7 (C-5), 79.5 ($\underline{C}(CH_3)_3$), 93.9 (C-2), 129.3 and 132.8 (C-1' and C-2'), 152.2 (CO). ESI-MS (positive mode): *m/z* (%) = 417.3 ($[M+Na]^+$, 100%).

11-Azido-undec-1-ene

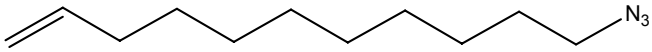

10-Undecenol (2.95 mL, 14.65 mmol) and pyridine (15 mL) were dissolved in dichloromethane (50 mL) and cooled to –20°C. Methanesulfonyl chloride (2.74 mL, 17.6 mmol) was added slowly and the reaction was stirred for 1h at 0°C and for additional 8h at rt. After addition of $NaHCO_3$-solution (30 ml), the methane sulfonate was extracted with dichloromethane (4x 100 mL) and dried with Na_2SO_4. After evaporation of the solvent under reduced pressure, the residue was dissolved in dimethylformamide (30 mL) and sodium azide (14.3 g, 220 mmol) was added. The reaction mixture was stirred for 12 hours, quenched with water (100 mL) and the product was extracted with ethylacetate (4x 100 mL). After evaporation of the solvent under reduced pressure, the azide was purified by chromatography on silica gel (cyclohexane/ethyl acetate, 20:1 (v/v)). Yield: 2.317 g (11.86 mmol) = 81 % over 2 steps, colorless oil, $C_{11}H_{21}N_3$, M = 195.31 g/mol,
R_f (hexane/ethyl acetate 20:1 (v/v)) = 0.58.
^{1}H-NMR (400 MHz, $CDCl_3$) δ [ppm]: 1.20 (m, 12H, CH_2), 1.59 (m, 2H, CH_2), 2.04 (m, 2H, CH_2), 3.24 (t, 2H, $^3J_{HH}$ = 7.0 Hz, H-10), 4.92 (ddt, 1H, $^3J_{HH}$ = 10.2 Hz, $^4J_{HH}$ = 2.2 Hz, $^2J_{HH}$ = 1.8 Hz, H-1a), 4.99 (ddt, 1H, $^3J_{HH}$ = 17.1 Hz, $^2J_{HH}$ = 3.7 Hz, $^2J_{HH}$ = 1.6 Hz, H-1b), 5.80 (ddt, 1H, $^3J_{HH}$ = 17.0 Hz, $^3J_{HH}$ = 10.3 Hz, $^3J_{HH}$ = 6.7 Hz, H-2). ^{13}C-NMR (100 MHz, $CDCl_3$) δ [ppm]: 26.9-29.6 (CH_2), 34.0 (C-3), 51.6 (C-11), 114.3 (C-1), 139.3 (C-2). EI-MS: *m/z* (%) = 194.1 ([M-H]$^+$, 37%).

(7*S*,8*S*,8a*S*)-7-(9-Azidononyl)-dihydro-8-iodo-3,3-dimethyloxazolo[3,4-c][1,3]oxazin (1H,3H,7H)-one (17)

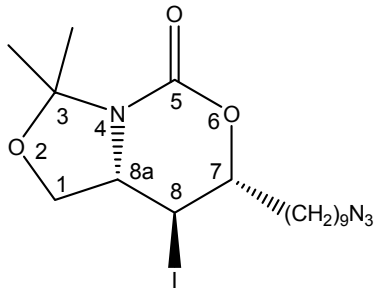

Oxazolidinone **17** was prepared according to the synthesis of compound **4b**. To a solution of alkene **16** (300 mg, 760 µmol) in dichloromethane (30 mL), *N*-iodosuccinimide (342 mg, 1.52 mmol) was added at room temperature. After stirring for 24 h, the reaction was diluted with dichloromethane (20 mL), the organic phase washed with 10% aqueous sodiumthiosulfate (20 mL), and then extracted with dichloromethane (4x 50 mL). The combined organic layers were washed with 10% aqueous $NaHCO_3$ and dried with Na_2SO_4. After removal of the solvent under pressure, the residue was purified by silica gel chromatography (cyclohexane/ethyl acetate, 5:1 (v/v)). Yield: 124 mg (267 µmol) = 35 %, white solid, $C_{17}H_{29}IN_4O_3$, M = 464.34 g/mol, R_f (cyclohexane/ethyl acetate, 5:1 (v/v)) = 0.50. ^{1}H-NMR (400 MHz, CD_3OD) δ [ppm]: 1.30 (m, 14H, CH_2), 1.58 (s, 3H, $C(CH_3)_2$), 1.60 (s, 3H, $C(CH_3)_2$), 1.72 (m, 1H, CH_2), 2.11 (m, 1H, CH_2), 3.23 (t, 2H, $^3J_{HH}$ = 7.0 Hz, CH_2), 3.58 (dd, 1H, $^3J_{HH}$ = 8.8 Hz, $^3J_{HH}$ = 9.6 Hz, H-1_A), 3.65 (t, 1H, $^3J_{HH}$ = 10.7 Hz, H-7),

4.01 (ddd, 1H, $^3J_{HH}$ = 10.6 Hz, $^3J_{HH}$ = 9.6 Hz, $^3J_{HH}$ = 5.5 Hz H-8a), 4.31 (dd, 1H, $^2J_{HH}$ = 8.8 Hz, $^3J_{HH}$ = 5.5 Hz, H-1_B), 4.34 (dd, 1H, $^3J_{HH}$ = 10.7 Hz, $^3J_{HH}$ = 8.1 Hz, H-8). ^{13}C-NMR (100 MHz, CD_3OD) δ [ppm]: 21.7 - 29.6 (CH_2 and C($\underline{C}H_3)_2$), 33.7 (C-8), 51.7 (CH_2), 61.8 (C-8a), 70.5 (C-1), 82.6 (C-7), 97.4 (C-3), 149.1 (C-5). FAB-MS: *m/z* (%) = 465.1 (1%, $[M+H]^+$), 487.1 (100%, $[M+Na]^+$).

(4S,5S,6R)-6-(9-Azidononyl)-4-hydroxymethyl-5-iodo-1,3-oxazinan-2-one (12)

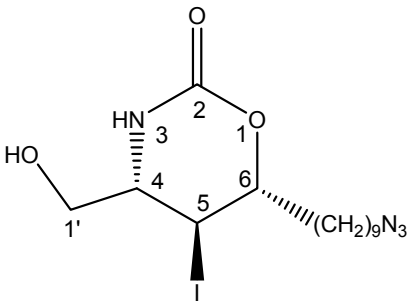

The compound **12** was obtained according to the synthesis of oxazolidinone **5b**. Carbamate **17** (124 mg, 300 µmol) was dissolved in THF (5 mL), hydrochloric acid (1M solution, 5 mL) was added, and the reaction mixture was stirred for 12 h under reflux. The reaction was neutralized with sodium hydrogencarbonate (5 mL), extracted three times with dichloromethane (20 mL), and the combined organic phases were dried with Na_2SO_4. After removal of the solvent under reduced pressure, the residue was purified by silica gel chromatography (chloroform/methanol, 10:1 (v/v)). Yield: 90 mg (212.1 µmol) = 71%, colorless wax, $C_{14}H_{25}IN_4O_3$, M = 424.28 g/mol, R_f (chloroform/methanol = 10:1 (v/v)) = 0.29.

^{1}H-NMR (400 MHz, $CDCl_3$) δ [ppm]: 1.18 (m, 14H, CH_2), 1.23 (m, 1H, CH_2), 1.50 (m, 1H, CH_2), 3.19 (t, 2H, $^3J_{HH}$ = 6.9 Hz, CH_2), 3.67 (dd, 1H, $^2J_{HH}$ = 12.4 Hz, $^3J_{HH}$ = 6.4 Hz, H-$1'_A$), 3.69 (dd, 1H, $^2J_{HH}$ = 12.4 Hz, $^3J_{HH}$ = 4.8 Hz, H-$1'_B$), 3.97 (dd, 1H, $^3J_{HH}$ = 9.2 Hz, $^3J_{HH}$ = 9.9 Hz, H-5), 4.25 (ddd, $^3J_{HH}$ = 9.4 Hz, $^3J_{HH}$ = 6.4 Hz, $^3J_{HH}$ = 4.8 Hz, H-4), 4.25 (dt, $^3J_{HH}$ = 10.1 Hz, $^3J_{HH}$ = 3.4 Hz, H-6). ^{13}C-NMR (100 MHz, $CDCl_3$) δ [ppm]: 21.7-37.5 (CH_2), 51.7 (C-1'), 58.2 and 64.6 (CH_2 and C-4), 77.5 (CH_2) 80.6 (C-5), 161.8 (C-2). FAB-MS: *m/z* (%) = 425.1 (25%, $[M+H]^+$), 447.1 (6%, $[M+Na]^+$).

7.7. Synthesis of 1'C Methyl-oxazinanones 23.2a and 23.2b

(4R,5R)-*tert*-Butyl 2,2,5-trimethyl-4-(pentadec-1'-enyl)oxazolidine-3-carboxylate (3b)

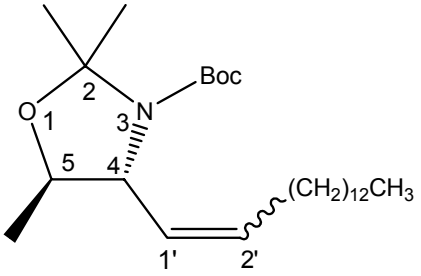

To a solution of Weinreb amide **1b** (1.67 mmol, 480.7 mg) in dry THF (12 mL), lithiumaluminiumhydride (1M solution in THF, 1.7 mL, 1.7 mmol) was added slowly at 0°C. The reaction was stirred for 1 h, cooled to –15°C, and a saturated aqueous solution of potassium hydrogensulfate (10 mL) was added slowly. After dilution with ether (10 mL), the solution was stirred for 30 min. The aqueous layer was extracted three times with diethyl ether (20 mL) and the combined organic layers were dried with sodiumsulfate. The solvent was removed and the residue was dried under reduced pressure. Dry tetradecyltriphenylphosphoniumbromide (2.92 mmol, 1.57 g) was suspended in dry THF (20 ml), cooled to –78°C, and n-butyllithium (1.6 M in Hexan, 3.03 mmol, 1.82 mL) was added dropwise while stirring. The dark red solution was stirred for 30 min at 0°C and cooled down again to -78°C. A solution of the aldehyde **2b** in dry THF (10 mL) was added dropwise. The reaction was stirred for 3h at room temperature. Then, the reaction was quenched with an saturated aqueous ammonium chloride solution (20 mL) and the aqueous layer was extracted three times with ethyl acetate (3x 20 mL). The combined organic layers were washed with water (50 mL), dried with sodiumsulfate, and the solvent was removed under reduced pressure. The residue was purified by column chromatography with silica gel (cyclohexane/ethyl acetate, 10:1). Both isomers were obtained in a ratio of E/Z = 1: 5. Yield: 565.00 mg (1.33 mmol) = 97 % over 2 steps, colorless oil, $C_{26}H_{49}NO_3$, M = 423.37 g/mol, R_f (cyclohexane/ethyl acetate, 5:1 (v/v)) = 0.58 (*Z*-alkene), 0.52 (*E*-alkene).

^{1}H-NMR (400 MHz, CD_3OD) δ [ppm]: 0.81 (t, 3H, CH_3, $^3J_{HH}$ = 7.0 Hz), 1.20 (m, 22H, CH_2), 1.21 (m, 3H, CH_3), 1.36 (s, 9H, $C(CH_3)_3$), 1.44 (s, 3H, $C(CH_3)_2$), 1.53 (s, 3H, $C(CH_3)_2$), 2.03 (m, 2H, CH_2), 3,68 (dd, 1H, $^3J_{HH}$ = 7.9 Hz, $^3J_{HH}$ = 6.9 Hz, H-4), 4.06 (m, 1H, H-5), 5.10 (*Z*-alkene: dd, 1H, $^2J_{HH}$ = 10.8 Hz, $^3J_{HH}$ = 9.2 Hz), 5.18 (*E*-alkene: dd, 1H, , $^2J_{HH}$ = 15.3 Hz, $^3J_{HH}$ = 8.1 Hz). ^{13}C-NMR (100 MHz, CD_3OD) δ [ppm]: 14.3 (CH_3), 17.8 (CH_3), 22.9 (CH_2), 28.0 ($C(\underline{C}H_3)_2$), 28.6 ($C(\underline{C}H_3)_3$, 28.4 - 31.9 (CH_2), 61.6 (C-4), 75.8 (C-5), 79.8 ($\underline{C}(CH_3)_3$), 94.1 ($\underline{C}(CH_3)_2$), 125.7 and 130.1 (C-1' and C-2'), 152.4 (CO). FAB-MS: *m/z* = 424.3 ($[M+H]^+$, 7%), 322.3 $[(M-C_5H_{10}O_2+H)]^+$, 45%). IR: $\overline{\nu}$ [cm^{-1}] = 721.6 and 980.5 δ(C-H), 1061.3, 1090.2, 1176.5 and 1254.2 (C-O), 1384.5 ($C(CH_3)_3$ and $C(CH_3)_2$), 1456.0 (s), 643.9 (C=C), 1698.4 (C=O), 2052.9 and 2920.6 v (CH_2 and CH_3). EI-HR-MS:[$C_{26}H_{49}NO_3$] *m/z* = calc.: 423.3711, found: 423.3705.

(1*R*,7*R*,7a*S*)-Dihydro-1-[1'(*R*)iodotetradecyl]-5,5,7-trimethyl-1*H*-oxazolo[3,4-*c*]oxazol-3(5*H*)-one (23.1b)

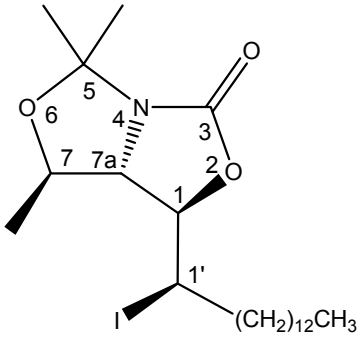

To a solution of *E*/*Z*-alkene **3b** (409 mg, 0.97 mmol) in dichloromethane (12 mL), *N*-iodosyccinimide (NIS, 437 mg, 1.94 mmol) was added at room temperature. After stirring for 48 h, the reaction was diluted with dichloromethane (10 mL), the organic phase washed with 10% aqueous sodiumthiosulfate (10 mL), and then extracted with dichloromethane (4x 20 mL). The combined organic layers were washed with 10% aqueous $NaHCO_3$ and dried with Na_2SO_4. After removal of the solvent under pressure, the residue was purified by silica gel chromatography (cyclohexane/ethyl acetate, 10:1 (v/v)). Yield: 274.2 mg (556 µmol) = 57 %, white solid, $C_{22}H_{40}INO_3$, M = 493.46 g/mol, R_f (cyclohexane/ethyl acetate, 5:1 (v/v)) = 0.25.
^{1}H-NMR (400 MHz, CD_3OD) δ [ppm]: 0.84 (t, 3H, $^3J_{HH}$ = 7.1 Hz, CH_3), 1.23 (m, 24H, CH_2), 1.46 (s, 3H, $C(CH_3)_2$), 1.68 (s, 3H, $C(CH_3)_2$), 1.33 (d, 1H, $^3J_{HH}$ = 5.9 Hz, CH_3), 3.65 (dd, 1H, $^3J_{HH}$ = 8.7 Hz, $^3J_{HH}$ = 3.9 Hz, H-7a), 3.81 (dq, 1H, $^3J_{HH}$ = 8.6 Hz, $^3J_{HH}$ = 5.9 Hz, H-7), 4.10 (ddd, 1H, $^3J_{HH}$ = 9.0 Hz, $^3J_{HH}$ = 5.3 Hz, $^3J_{HH}$ = 3.7 Hz, H-1'), 4.38 (dd, 1H, $^3J_{HH}$ = 3.8 Hz, $^3J_{HH}$ = 3.8 Hz, H-1). ^{13}C-NMR (100 MHz, CD_3OD) δ [ppm]: 14.4 (CH_3), 22.9 (CH_2), 24.0 (CH_2), 26.6 (CH_2), 28.9 (CH_2), 29.5 - 29.9 (CH_2, $C(\underline{C}H_3)_2$ und C-1'), 32.1 (CH_2), 32.4 (CH_2), 36.1 (CH_2), 67.8 (C-7a), 76.5 and 78.0 (C-1 and C-7), 95.0 (C-5), 156.4 (C-3). FAB-MS: *m/z* (%) = 494.2 (100%, $[M+H]^+$), 987.5 (3%, $[2M+H]^+$).

(1*R*,7*S*,8*S*,8a*S*)-Dihydro-8-iodo-1,3,3-trimethyl-7-tridecyloxazolo[3,4-*c*][1,3]oxazin-5(1*H*,3*H*,7*H*)-one (23.1a)

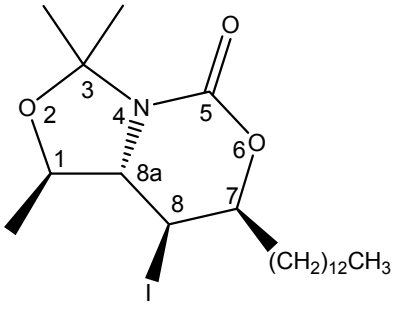

The compound was obtained as by-product within the reaction of *Z*-alkene **3b** with NIS. Yield: 173 mg (351 µmol) = 36 %, white solid, $C_{22}H_{40}INO_3$, M = 493.46 g/mol, R_f (cyclohexane/ethyl acetate = 10:1) = 0.19.
^{1}H-NMR (400 MHz, CD_3OD) δ [ppm]: 0.86 (t, 3H, $^3J_{HH}$ = 7.0 Hz), 1.23 (m, 24H, CH_2), 1.48 (d, 3H, $^3J_{HH}$ = 5.9 Hz, CH_3), 1.58 (s, 6H, $C(CH_3)_2$), 1.64 (m, 1H, CH_2), 2.12 (m, 1H, CH_2), 3.44 (dd, 1H, $^3J_{HH}$ = 10.7 Hz, $^3J_{HH}$ = 8.7 Hz, H-8a), 3.74 (dq, 1H, $^3J_{HH}$ = 8.6 Hz, $^3J_{HH}$ = 5.9 Hz, H-1), 3.97 (dd, 1H, $^3J_{HH}$ = 10.7 Hz, $^3J_{HH}$ =

4.5 Hz, H-8), 4.23 (ddd, 1H, $^3J_{HH}$ = 10.5 Hz, $^3J_{HH}$ = 4.4 Hz, $^3J_{HH}$ = 1.8 Hz, H-7). ^{13}C-NMR (100 MHz, CD_3OD) δ [ppm]: 14.2 (CH_3), 20.1 and 24.1 (C($\underline{C}H_3$)$_2$), 18.9 (CH_3), 26.2 (C-8), 22.7-32.0 (CH_2), 62.6 (C-8a), 76.7 (C-1), 80.6 (C-7), 94.6 (C-3), 148.8 (C-5). FAB-MS: *m/z* (%) = 494.2 ([M+H]$^+$, 100 %), 987.4 ([2M+H]$^+$, 6%), Elemental analysis: [$C_{22}H_{40}INO_3$] calc.: C 53.55, H 8.17, N 2.84; found.:C 53.13, H 8.12, N 2.79.

(1*R*,7*R*,8*S*,8a*S*)-Dihydro-8-iodo-1,3,3-trimethyl-7-tridecyloxazolo[3,4-*c*][1,3]oxazin-5(1*H*,3*H*,7*H*)-one (23.1c)

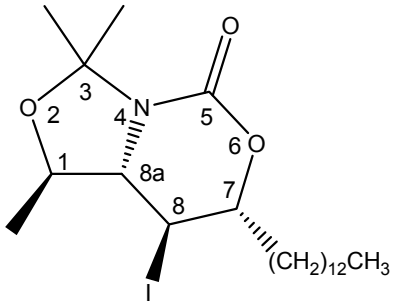

The oxazolidinone was obtained in a mixture with the oxazolidinone and oxazinanone as by-product within the reaction of *E*-alkene **3b** with NIS. $C_{22}H_{40}INO_3$, M = 493.46 g/mol, R_f (cyclohexane/ethyl acetate, 10:1 (v/v)) = 0.19.

^{1}H-NMR (400 MHz, CD_3OD) δ [ppm]: 0.84 (t, 3H, $^3J_{HH}$ = 7.1 Hz, CH_3), 1.23 (m, 24H, CH_2), 1.33 (d, 1H, $^3J_{HH}$ = 5.9 Hz, CH_3), 1.54 (s, 3H, (CH_3)$_2$), 1.58 (s, 3H, (CH_3)$_2$), 3.49 (dd, 1H, $^3J_{HH}$ = 10.5 Hz, $^3J_{HH}$ = 8.4 Hz, H-8a), 3.58 (dd, 1H, $^3J_{HH}$ = 10.6 Hz, $^3J_{HH}$ = 10.6 Hz, H-8), 3.73 (dq, 1H, $^3J_{HH}$ = 8.4 Hz, $^3J_{HH}$ = 5.9 Hz, H-1), 4.31 (ddd, 1H, $^3J_{HH}$ = 10.6 Hz, $^3J_{HH}$ = 7.7 Hz, $^3J_{HH}$ = 2.6 Hz, H-7). ^{13}C-NMR (100 MHz, CD_3OD) δ [ppm]: 14.3 (CH_3), 19.9 (CH_3), 22.6 - 33.7 (CH_2, C($\underline{C}H_3$)$_2$ and C-8), 66.3 (C-8a), 77.0 (C-1), 82.4 (C-7), 94.1 (C-3), 149.0 (C-5). FAB-MS: *m/z* (%) = 494.2 ([M+H]$^+$, 100 %), 987.4 ([2M+H]$^+$, 6%).

(4*S*,5*R*)-4-(1''(*R*)-Hydroxyethyl)-5-(1'(*R*)-iodotetradecyl)oxazolidin-2-one (23.2b)

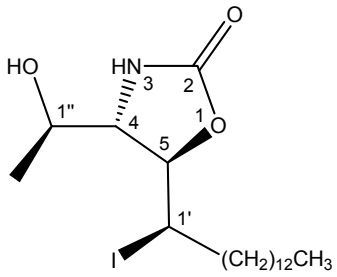

Compound **23.2b** was made according to the synthesis of compound **5b**. Oxazolidinone **23.1b** (371 µmol, 183 mg) was dissolved in a solution of 1N HCl in THF (1:1, 5 mL), stirred for 5 h at rt. After the volume was reduced under reduced pressure, the product was extracted with ethyl acetate and dried with sodiumsulfate. The solvent was removed under reduced pressure and the residue was purified by chromatography on silica gel (cyclohexane/ethyl acetate = 10:1 (v/v)). Yield: 62.1 mg (13.7 mmol) = 37 %,

white solid, $C_{19}H_{36}INO_3$, M = 453.40 g/mol, R_f (chloroform/methanol, 20:1 (v/v)) = 0.16, α_D = -33.1° (c = 0.39, $CHCl_3$/MeOH, 1:1 (v/v)).

^{1}H-NMR (400 MHz, $CDCl_3$) δ [ppm]: 0.89 (t, 3H, $^3J_{HH}$ = 6.5 Hz, CH_3), 1.24 (d, 3H, $^3J_{HH}$ = 6.4 Hz, CH_3), 1.28 (m, 24H, CH_2), 3.44 (dd, 1H, $^3J_{HH}$ = 4.5 Hz, $^3J_{HH}$ = 4.5 Hz, H-4), 3.66 (qd, 1H, $^3J_{HH}$ = 6.3 Hz, $^3J_{HH}$ = 4.8 Hz, H-1''), 3.9 (ddd, 1H, $^3J_{HH}$ = 10.1 Hz, $^3J_{HH}$ = 4.1 Hz, $^3J_{HH}$ = 2.8 Hz, H-1'), 4.50 (dd, $^3J_{HH}$ = 3.5 Hz, $^3J_{HH}$ = 2.4 Hz, H-5), 7.59 (m, 1H, NH). ^{13}C-NMR (100 MHz, $CDCl_3$) δ [ppm]: 13.9 (CH_3), 18.6 (CH_3), 22.6 (CH_2), 28.6 – 29.6 (CH_2), 31.9 (CH_2), 35.2 (CH_2), 38.8 (C-1'), 63.0 (C-4), 68.0 (C-1''), 80.3 (C-5), 159.7 (C-2). IR: $\bar{\nu}$ [cm^{-1}] = 2536.3 ν(-CH_2), 1651.9 ν(C=O), 1457.9 δ(-CH_3). FAB-MS: *m/z* (%) = 454.18 (100%, $[M+H]^+$).

(4*S*,5*S*,6*S*)-4-(1'(*R*)-Hydroxyethyl)-5-iodo-6-tridecyl-1,3-oxazinan-2-one (23.2a)

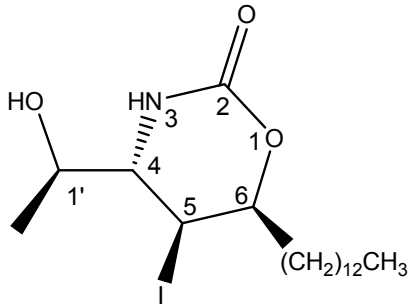

Synthesis and purification of **23.2a** was done according to the preparation of lipid **5a**. Oxazinanone **23.1a** (351 µmol, 137 mg) was dissolved in 1N HCl in THF (1:1, 5 mL) and the reaction mixture was stirred for 24 h at 60 °C. Yield: 21 mg (46 µmol) = 13%, white solid, $C_{19}H_{36}INO_3$, M = 453.40 g/mol, R_f(chloroform/ methanol, 20:1 (v/v)) = 0.19.

^{1}H-NMR (400 MHz, $CDCl_3$/CD_3OD = 5:1) δ [ppm]: 0.72 (t, 3H, $^3J_{HH}$ = 7.0 Hz, CH_3), 1.26 (d, 3H, $^3J_{HH}$ = 6.6 Hz, CH_3), 1.31 (m, 21H, CH_2), 1.65 (m, 1H, CH_2), 1.81 (m, 1H, CH_2), 1.95 (m, 1H, CH_2), 3.36 (t, 1H, $^3J_{HH}$ = 4.5 Hz, H-4), 3.66 (qd, 1H, $^3J_{HH}$ = 6.4 Hz, $^3J_{HH}$ = 4.6 Hz, H-1'), 3.93 (ddd, 1H, $^3J_{HH}$ = 10.2 Hz, $^3J_{HH}$ = 4.1 Hz, $^3J_{HH}$ = 2.7 Hz, H-6), 4.04 (dd, 1H, $^3J_{HH}$ = 4.3 Hz, $^3J_{HH}$ = 2.7 Hz, H-5). ^{13}C-NMR (100 MHz, $CDCl_3$/CD_3OD = 5:1) δ [ppm]: 14.6 (CH_3), 20.5 (CH_3), 23.5 (CH_2), 28.6 (CH_2), 30.2 (CH), 30.4 (CH_2), 32.7 (CH_2), 67.1 (CH), 70.7 (CH), 77.2 (CH_2), 155.5 (C-2). IR: $\bar{\nu}$ [cm^{-1}] = 2932.4 ν(-CH_2-), 1722.3 ν(C=O), 1456.1 δ(-CH_3). FAB-MS: *m/z* (%) = 454.2 (68%, $[M+H]^+$), 476.1, (74%, $[M+Na]^+$).

7.8. Synthesis of oxazinanones 18a and 18b

(2S,3S,4R)*tert*-Butyl 1,3,4-trihydroxyoctadecane-2-ylcarbamate (19)

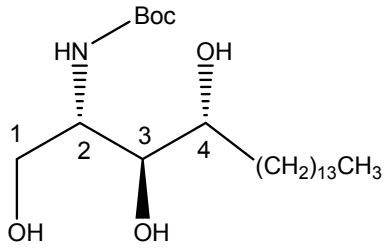

Triethylamine (7.21 mmol, 1.0 mL was added to a solution of phytosphingosine (4.72 mmol, 1.50 g) in tetrahydrofurane (15 ml) at 0°C. Then di-*tert*-butyl-dicarbonate (7.08 mmol, 1.55 g) was added to, and the mixture was stirred for 24 h at room temperature. The solvent was removed under reduced pressure and the crude product was purified by chromatography on silica gel (chloroform/methanol, 10:1 (v/v)). Yield: 1.47 g (mmol) = 75 %, white solid, $C_{23}H_{47}NO_5$, M = 417.62 g/mol, R_f (chloroform/ methanol, 10:1 (v/v)) = 0.54.

^{1}H-NMR (400 MHz, $CD_3OD/CDCl_3$ = 1:1) δ [ppm]: 0.84 (t, 3H, $^3J_{HH}$ = 7.2 Hz, CH_3), 1.19 (m, 24H, CH_2), 1.23 (m, 2H, CH_2), 1.37 (s, 9H, $C(CH_3)_3$), 3.58 (m, 2H, H-2 and H-4), 3.65 (dd, 1H, $^2J_{HH}$ = 11.0 Hz, $^3J_{HH}$ = 5.2 Hz, H-1_A), 3.74 (m, 1H, H-4), 3.80 (dd, 1H, $^2J_{HH}$ = 10.8 Hz, $^3J_{HH}$ = 3.2 Hz, H-1_B), 3.93 (m, 1H, H-3), 5.43 (d, 1H, $^3J_{HH}$ = 8.6 Hz, NH). ^{13}C-NMR (100 MHz, $CD_3OD/CDCl_3$ = 1:1) δ [ppm]: 14.3 (CH_3), 22.9 (CH_2), 26.2 (CH_2), 28.6 ($C(\underline{C}H_3)_3$), 28.5 – 32.1 (CH_2), 53.1 (C-2), 62.1 (C-1), 73.2 (C-4), 76.2 (C-3), 80.3 ($\underline{C}(CH_3)_3$), 156.7 (CO). FAB-MS: *m/z* (%) = 418.4 (20%, $[M+H]^+$). Elemental analysis: [$C_{23}H_{47}INO_5$] calc.: C 66.15, H 11.34, N 3.35; found: C 66.10, H 11.43, N 3.30.

(4S,5S)*tert*-Butyl 2,2-di-*tert*-butyl-4-(1'(R)-hydroxypentadecyl)-1,3,2-dioxasilinan-5-ylcarbamate (20)

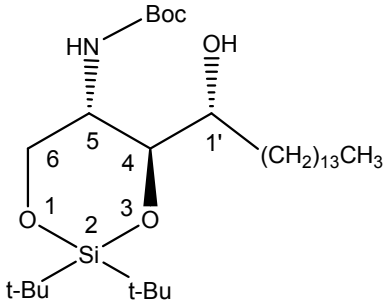

The synthesis of **20** followed (Hoberg, 1997). Di-*tert*-butylsilylbis(trifluoromethane)sulfonate (2.83 mmol, 1.03 mL) was added dropwise over 30 min to a solution of compound **19** (2.85 mmol, 1.19 g) in *N*,*N*-Dimethylformamide (20 mL) at –40°C. The solution was stirred for 1 h at rt, pyridine (7.37 mmol, 600 µL) was added and stirred for 5 min. The solution was diluted with ether (20 mL) and washed once with saturated $NaHCO_3$ (70 mL), twice with water (70 mL), and dried over Na_2SO_4. Solvents were removed under reduced pressure and the residue was purified by chromatography with silica gel (cyclohexane/ethyl

acetate, 5:1 (v/v)). Yield: 986.8 mg (1.77 mmol) = 62 %, white solid, $C_{31}H_{63}NO_5Si$, M = 557.92 g/mol, R_f (cyclohexane/ethyl acetate, 5 :1 (v/v)) = 0.51. ^{1}H-NMR (400 MHz,$CDCl_3$) δ [ppm]: 0.85 (t, 3H, $^3J_{HH}$ = 6.4 Hz), 0.99 (s, 9H, $C(CH_3)_3$), 1.01 (s, 9H, $C(CH_3)_3$), 1.23 (m, 24H, CH_2), 1.40 (m, 10H, $C(CH_3)_3$ und CH_2), 1.46 (m, 1H, CH_2), 2.16 (dt, 1H, $^3J_{HH}$ = 9.1 Hz, $^3J_{HH}$ = 2.1, H-1'), 3.63 (m, 1H, H-4), 3.64 (dd, 1H, $^2J_{HH}$ = 10.2 Hz, $^3J_{HH}$ = 10.2 Hz, H-6_A), 3.81 (m, 1H, OH), 3.86 (dd, 1H, $^3J_{HH}$ = 9.6 Hz, $^3J_{HH}$ = 3.7 Hz, H-5), 4.03 (dd, 1H, $^2J_{HH}$ = 10.4 Hz, $^3J_{HH}$ = 4.3 Hz, H-6_B), 4.39 (d, 1H, $^3J_{HH}$ = 9.2 Hz, NH). ^{13}C-NMR (100 MHz,$CDCl_3$) δ [ppm]: 14.3 (CH_3), 20.5 ($\underline{C}(CH_3)_3$, 22.9 (CH_2), 23.0 (CH_2), 26.0 (CH_2), 27.3 (CH_2), 27.8 ($C(\underline{C}H_3)_3$), 28.5 (CH_2), 29.6, 29.8 – 29.9 (CH_2), 49.9 (C-5), 67.8 (C-6), 73.2 (C-1'), 80.7 (C-4), 155.2 (CO). ESI-MS (positive mode): *m/z* (%) = 558.46 (100%, $[M+H]^+$), 580.45 (70%, $[M+Na]^+$).

(4*S*,5*S*)*tert*-Butyl 2,2-di-*tert*-butyl-4-(1'(*R*)-methanesulfonyloxypentadecyl)-1,3,2-dioxa-silinan-5-ylcarbamate (21)

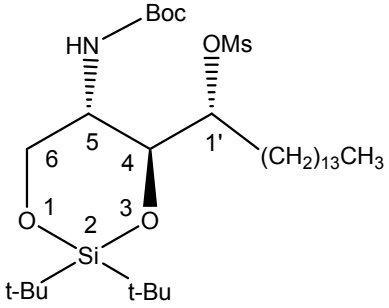

A solution of compound **20** (0.78 mmol, 454.2 mg) in pyridine (4.5 mL) was cooled to –10°C. Then, methanesulfonylchloride (1.29 mmol, 100 µL) was added slowly, and the mixture stirred for 30 min at the same temperature. The mixture was warmed to rt and stirred for 12 h. After evaporation of the solvent, the residue was purified by column chromatography (cyclohexane/ethyl acetate, 2:1(v/v)). Yield: 391.85 mg (0.63 mmol) = 81 %, colorless solid, $C_{32}H_{65}NO_7SSi$, M = 636.01 g/mol, R_f (cyclohexane/ethyl acetate, 5:1 (v/v)) = 0.58.

^{1}H-NMR (400 MHz, $CDCl_3$) δ [ppm]: 0.85 (t, 3H, $^3J_{HH}$ = 7.1 Hz), 0.99 (s, 9H, $C(CH_3)_3$), 1.02 (9H, $C(CH_3)_3$), 1.23 (m, 24H, CH_2), 1.41 (s, 9H, $(C(CH_3)_3$), 1.46 (m, 2H, CH_2), 3.00 (s, 3H, CH_3), 3.70 (m, 1H, H-5), 3.75 (dd, 1H, $^2J_{HH}$ = 10.0 Hz, $^3J_{HH}$ = 4.1 Hz, H-6_A), 4.06 (dd, 1H, $^2J_{HH}$ = 9.7 Hz, $^3J_{HH}$ = 4.0 Hz, H-6_B), 4.33 (dd, 1H, $^2J_{HH}$ = 10.0 Hz, $^3J_{HH}$ = 2.0 Hz, H-4), 4.41 (d, 1H, $^3J_{HH}$ = 9.5 Hz, NH), 4.79 (dt, 1H, $^3J_{HH}$ = 10.4 Hz, $^3J_{HH}$ = 2.0 Hz, H-1'). ^{13}C-NMR (100 MHz, $CDCl_3$) δ [ppm]: 14.3 (CH_3), 20.5 (CH_3), 22.9 (CH_2), 23.0 (CH_2), 25.7 (CH_2), 27.3 (CH_2), 27.7 (CH_2), 27.8 ($C(\underline{C}H_3)_3$), 27.9 ($C(\underline{C}H_3)_3$), 28.0 (CH_2), 28.5 ($C(\underline{C}H_3)_3$), 29.4 (CH_2), 29.6 (CH_2), 29.8 (CH_2), 29.9 (CH_2), 32.1 (CH_2), 38.9 (CH_2), 49.4 (C-5), 67.8 (C-6), 79.2 (C-4), 80.6 ($\underline{C}(CH_3)_3$), 83.8 (C-1'), 155.1 (CO). IR: ν [cm^{-1}] = 2919.6 and 2850.5 ν(-CH_2-), 1670.9 ν(C=O), 1468.6 δ(-CH_3). ESI-MS (positive mode): *m/z* (%) = 658.41 (76 %, $[M+Na]^+$), 1293.84 (4 %, $[2M+Na]^+$).

(4a*S,8R,8aS*)-2,2-Di-*tert*-Butyl-8-tetradecyl-tetrahydro-1,3,7-trioxa-5-aza-2-sila-naphtalen-6-one (22b)

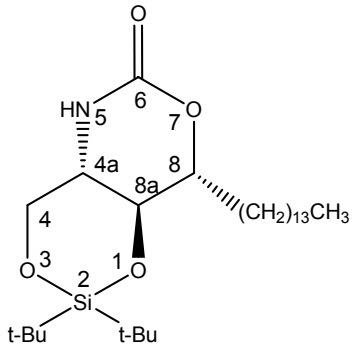

Compound **20** (0.17 mmol, 104.7 mg) was dissolved in tetrahydrofurane (1 mL) and cooled to 0°C. Lithiumdiisopropylamine (189 µmol, 97.5 µL) was added to the mixture and stirred for 1h at room temperature. After evaporation of the solvent under vacuum, the residue was purified by column chromatography (cyclohexane/ethyl acetate, 4:1 (v/v)). Yield: 71.36 mg (147.5 µmol) = 82 %, colorless solid, $C_{27}H_{53}NO_4Si$, M = 483.80 g/mol, R_f (cyclohexane/ethyl acetate/trietylamine = 3:1:0,001 (v/v/v)) = 0,17, $[\alpha]_D$ = +39.5° (c = 0.4, $CHCl_3$).

^{1}H-NMR (400 MHz, $CDCl_3$): δ [ppm] = 0.81 (t, 3H, $^3J_{HH}$ = 6.7 Hz, CH_3), 0.90 (s, 9H, $C(CH_3)_3$), 0.97 (s, 9H, $C(CH_3)_3$), 1.19 (m, 24H, CH_2), 1.39 (m, 1H, CH_2), 1.54 (m, 2H, CH_2), 1.83 (m, 1H, CH_2), 3.38 (ddd, 1H, $^3J_{HH}$ = 10.6 Hz, $^3J_{HH}$ = 9.3 Hz, $^3J_{HH}$ = 4.5 Hz, H-4a), 3.68 (dd, 1H, $^2J_{HH}$ = 10.1 Hz, $^3J_{HH}$ = 9.3 Hz, H-4_A), 3.74 (dd, 1H, $^2J_{HH}$ = 10.1 Hz, $^3J_{HH}$ = 10.5 Hz, H-4_B), 4.01 (ddd, 1H, $^3J_{HH}$ = 9.4 Hz, $^3J_{HH}$ = 7.2 Hz, $^3J_{HH}$ = 5.6 Hz, H-8), 4.06 (dd, 1H, $^2J_{HH}$ = 10.1 Hz, $^3J_{HH}$ = 5.6 Hz, H-8a), 6.50 (m, 1H, NH). ^{13}C-NMR (100 MHz, $CDCl_3$) δ [ppm] = 13.1 (CH_3), 18.9 ($C(\underline{C}H_3)_3$), 21.7 (CH_2), 21.8 (CH_2), 23.1 (CH_2), 25.9 (CH_2), 26.4 ($\underline{C}(CH_3)_3$), 28.4 (CH_2), 28.5 (CH_2), 28.6 (CH_2), 28.7 (CH_2), 29.2 (CH_2), 29.8 (CH_2), 30.9 (CH_2), 52.5 (C-4a), 66.3 (C-4), 71.0, 79.7 (C-8 and C-8a), 154.2 (C-6). ESI-MS: *m/z* (%) = 484.4 ($[M+H]^+$, 100%), 506.3 ($[M+Na]^+$, 12%), 968.7 ($[2M+H]^+$, 11%). ESI-HR-MS: $[C_{27}H_{53}NO_4Si+Na]^+$ *m/z* = calcd.: 506.36359, found: 506.36520

(4*S*,5*S*,6*R*)-5-Hydroxy-4-hydroxymethyl-6-tetradecyl-1,3-oxazinan-2-one (18b)

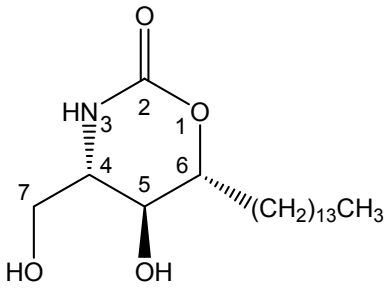

tert-Butylammoniumfluoride (1 M solution in THF, 500 µmol, 500 µL) was added dropwise to a solution of tetrahydronaphtalene **22b** (124 µmol, 60.0 mg) in THF (5 mL) at 0°C. The reaction was stirred for 1 h at 0°C and then for additional 30 min at room temperature. After removal of the solvent under reduced pressure, the residue was purified by chromatography on silica gel (toluene/ethanol, 5:1 (v/v)). Yield: 12 mg (34.9

µmol) = 26 %, white solid, F_P = 123°C, $C_{19}H_{37}NO_4$, M = 343.50 g/mol, R_f (toluene/ethanol, 5:1 (v/v)) = 0.26, $[\alpha]_D$ = +17.0° (c = 0.19, $CHCl_3$/MeOH, 5:1 (v/v)).

^{1}H-NMR (400 MHz, $CDCl_3/CD_3OD$ = 5:1 (v/v)): δ [ppm] = 0.80 (t, 3H, $^3J_{HH}$ = 6.7 Hz, CH_3), 1.18 (m, 22H, CH_2), 1.30 (m, 1H, CH_2), 1.50 (m, 2H, CH_2), 1.83 (m, 1H, CH_2), 3.18 (ddd, 1H, $^3J_{HH}$ = 9.2 Hz, $^3J_{HH}$ = 6.3 Hz, $^3J_{HH}$ = 3.2 Hz, H-4), 3.33 (pt, 1H, $^3J_{HH}$ = 9.2 Hz, H-5), 3.47 (dd, 1H, $^2J_{HH}$ = 11.5 Hz, $^3J_{HH}$ = 6.3 Hz, H-7_A), 3.72 (dd, 1H, $^2J_{HH}$ = 11.5 Hz, $^3J_{HH}$ = 3.2 Hz, H-7_B), 3.95 (m, 1H, H-6). ^{13}C-NMR (100 MHz, $CDCl_3/CD_3OD$ = 5:1 (v/v)): δ [ppm] = 14.9 (CH_3), 23.8 (CH_2), 25.7 (CH_2), 30.6 (CH_2), 30.7 (CH_2), 30.8 (CH_2), 30.9 (CH_2), 32.4 (CH_2), 33.1 (CH_2), 59.6 (C-4), 63.2 (C-7), 66.1 (C-5), 81.3 (C-6), 156.9 (C-2).

IR: v [cm^{-1}] = 3282 (OH), 2918 (CH_2), 2851 (CH_2), 1682 (CO), 1472 (CH_3). FAB-MS: *m/z* (%) = 344.3 ($[M+H]^+$, 4%). ESI-HR-MS: $[C_{19}H_{37}NO_4+Na]^+$ *m/z* = calcd.: 366.26147, found: 366.26208

(4a*S*,8*S*,8a*S*)-2,2-Di-*tert*-Butyl-8-tetradecyltetrahydro-1,3,7-trioxa-5-aza-2-sila-naphtalen-6-one (22a)

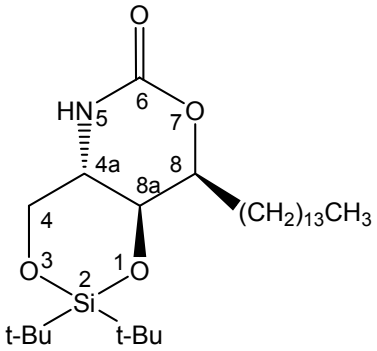

Compound **21** (170 µmol, 104.7 mg) was dissolved in THF and refluxed for 8 h. The solvent was removed under reduced pressure and the residue was purified by column chromatography with silica gel (cyclohexane/ethyl acetate, 3:1 (v/v)). Yield: 65.7 mg (135.8 µmol) = 75 %, colorless solid, $C_{27}H_{53}NO_4Si$, M = 483.80 g/mol, R_f (cyclohexane/ethyl acetate, 3:1(v/v)) = 0.25.

^{1}H-NMR (500 MHz, $CDCl_3$): δ [ppm] = 0.90 (t, 3H, $^3J_{HH}$ = 6.9 Hz, CH_3), 1.02 (s, 9H, $C(CH_3)_3$), 1.09 (s, 9H, $C(CH_3)_3$), 1.28 (m, 22H, CH_2), 1.59 (m, 2H, CH_2), 1.73 (m, 1H, CH_2), 1.89 (m, 1H, CH_2), 3.59 (ddd, 1H, $^2J_{HH}$ = $^3J_{HH}$ = 10.3 Hz, $^3J_{HH}$ = 4.68 Hz, H-4a), 3.88 (dd, 1H, $^2J_{HH}$ = $^3J_{HH}$ = 10.3 Hz, H-4_A), 4.12 (dd, 1H, $^3J_{HH}$ = 10.0 Hz, $^3J_{HH}$ = 4.6 Hz, H-4_B), 4.26 (dd, 1H, $^3J_{HH}$ = 9.6 Hz, $^3J_{HH}$ = 5.2 Hz, H-8a), 4.39 (ddd, 1H, $^3J_{HH}$ = 7.6 Hz, $^3J_{HH}$ = 5.3 Hz, $^3J_{HH}$ = 2.4 Hz, H-8), 5.19 (m, 1H, NH). ^{13}C-NMR (125 MHz, $CDCl_3$): δ [ppm] = 13.1 (CH_3), 19.0 ($\underline{C}(CH_3)_3$), 21.7 (CH_2), 21.9 (CH_2), 24.6 (CH_2), 25.9 ($C(\underline{C}H_3)_3$), 26.0 ($C(\underline{C}H_3)_3$), 27.5 (CH_2), 28.4 (CH_2), 28.5 (CH_2), 28.6 (CH_2), 28.7 (CH_2), 30.9 (CH_2), 48.5 (C-4a), 66.8 (C-4), 69.7 and 78.2 (C-8 and C-8a), 151.3 (C-6). FAB-MS: *m/z* (%) = 484.4 ($[M+H]^+$, 7%).

(4*S*,5*S*,6*S*)-5-Hydroxy-4-hydroxymethyl-6-tetradecyl-1,3-oxazinan-2-one (18a)

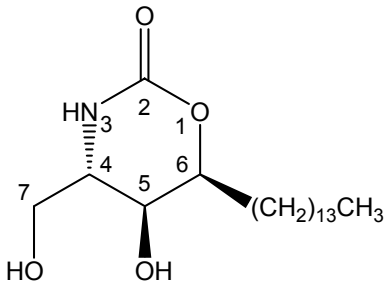

Compound **18a** was prepared according to synthesis of compound **18b**. A solution of tetrahydronaphtalen **22a** (134.4 μmol, 65 mg) in THF (5 mL) was cooled to 0°C and *tert*-butylammoniumfluoride (1 M solution in THF, 500 μmol, 500 μL) was added. The reaction was stirred for 1 h at 0°C, warmed to rt and stirred for additional 30 min. After evaporation of the solvent under reduced pressure, the residue was purified by column chromatography with silica gel (toluene/ethanol, 5:1 (v/v)). Yield: 3.1 mg (9.0 μmol) = 93%, white solid, $C_{19}H_{37}NO_4$, M = 343.50 g/mol, R_f (toluene/ ethanol, 5:1 (v/v)) = 0.16.

^{1}H-NMR (400 MHz, $CDCl_3/CD_3OD$ = 5:1 (v/v)): δ [ppm] = 0.80 (t, 3H, $^3J_{HH}$ = 6.7 Hz, CH_3), 1.18 (m, 24H, CH_2), 1.44 (m, 2H, CH_2), 3.33 (ddd, 1H, $^3J_{HH}$ = 2.4 Hz, $^3J_{HH}$ = 5.7 Hz, $^3J_{HH}$ = 8.3 Hz, H-6), 3.46 (d, 2H, $^3J_{HH}$ = 6.1 Hz, H-7_A and H-7_B), 3.75 (pt, 1H, $^3J_{HH}$ = 2.4 Hz, H-5), 4.13 (ddd, 1H, $^3J_{HH}$ = 2.0, $^3J_{HH}$ = 5.2, $^3J_{HH}$ = 7.2 Hz, H-4). ^{13}C-NMR (125 MHz, $CDCl_3/CD_3OD$ = 5:1 (v/v)): δ [ppm] = 13.7 (CH3), 19.5 (CH_2), 22.5 (CH_2), 23.6 (CH_2), 25.1 (CH_2), 26.9 (CH_2), 27.5 (CH_2), 29.2 (CH_2), 29.3 (CH_2), 29.4 (CH_2), 29.5 (CH_2), 29.8 (CH_2), 31.8 (CH_2), 58.1 and 63.0 (C-4 and C-5), 63.3 (CH_2), 77.6 (C-6), 155.3 (C-2). IR: $\bar{\nu}$ [cm^{-1}] = 3423 (OH), 2920 (CH_2), 1654 (CO). ESI-MS (positive mode): *m/z* (%) = 344.3 ($[M+H]^+$, 60 %), 366.25 ($[M+Na]^+$, 100 %)

7.9. Synthesis of *N*-Phenylacetylsphingosine (25)

(4*S*)-*tert*-Butyl 4-(1'(*R*)-hydroxyhexadec-2-ynyl)-2,2-dimethyloxazolidine-3-carboxylate (3c)

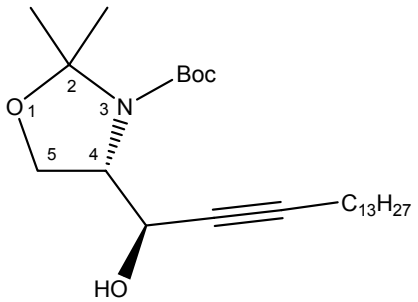

Compound **3c** was prepared according to a described method (Garner et al., 1988). Pentadecyne (3.97 mL, 15.13 mmol), nButyllithium (2.7 M solution in heptane, 5.09 ml, 13.76 mmol) and Garner aldehyde (3.16 g, 13.76 mmol). The reaction mixture was stirred for 3 h at –20°C. The product was purified by column chromatography with silica gel (petroleum ether/ethyl acetate, 7:1, (v/v)). Yield: 1.45 g (3.32 mmol) = 24 %, white solid, $C_{26}H_{47}NO_4$, M = 437.66 g/mol, R_f (petroleum ether/ethyl acetate, 7:1, (v/v)) = 0.25.

^{1}H-NMR (400 MHz, $CDCl_3$): δ [ppm] = 0.86 (t, 3H, $^3J_{HH}$ = 6.9 Hz, CH_3), 1.24 (m, 14H, CH_2), 1.48 (s, 9H, $C(CH_3)_3$), 1.49 (s, 3H, $C(CH_3)_2$), 1.54 (s, 3H, $C(CH_3)_2$), 2.17 (td, 2H, $^3J_{HH}$ = 7.0 Hz, $^4J_{HH}$ = 1.8 Hz, CH_2), 3.89 (m, 1H, H-5_A), 4.05 (m, 1H, H-5_B), 4.11 (m, 1H, H-4), 4.71 (m, 1H, H-1'). FAB-MS: *m/z* (%) = 438.3 ($[M+H]^+$, 13 %).

(4*S*)-*tert*-Butyl (1'(*R*)-Hydroxyhexadec-2(*E*)-enyl)-2,2-dimethyloxazolidine-3-carboxylate (27)

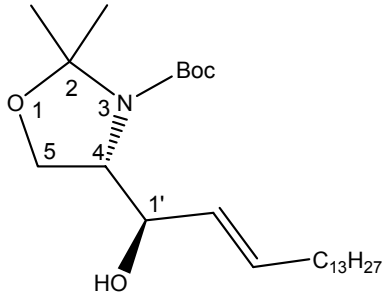

Compound **27** was prepared and purified according to a described method (Nyangulu et al., 2006). Alkyne **26** (896.7 mg, 2.04 mmol), RedAl (2.91 mL, 10.2 mmol) and diethylether (30 mL). The reaction mixture was stirred for 12h at rt. The product was purified by column chromatography with silica gel (cyclohexane/ethyl acetate, 5:1, (v/v)). Yield: 70 mg (159 µmol) = 8 %, white solid, $C_{26}H_{49}NO_4$, M = 439.67 g/mol,
R_f (cyclohexane/ ethyl acetate, 5:1, (v/v)). = 0.23.
^{1}H-NMR (400 MHz, $CDCl_3$): δ [ppm] = 0.85 (t, 3H, $^3J_{HH}$ = 7.1 Hz, CH_3), 1.24 (m, 20H, CH_2), 1.40 (m, 2H, CH_2), 2.02 (s, 15H, $C(CH_3)_2$ and $C(CH_3)_3$), 2.19 (m, 2H, CH_2), 3.61 ("t", 1H, $^3J_{HH}$ = 6.6 Hz), 3.81 (m, 1H, CH_2), 4.01 (m, 1H), 4.10 (m, 1H), 5.37 (dd, 1H, $^3J_{HH}$ = 15.4 Hz, $^3J_{HH}$ = 6.3 Hz, H-2'), 5.67 (dt, 1H, $^3J_{HH}$ = 15.4 Hz, $^3J_{HH}$ = 6.8 Hz, H-3'). ^{13}C-NMR (100 MHz, $CDCl_3$): δ [ppm] = 14.1 (CH_3), 22.9 (CH_2), 24.9 ($C(\underline{C}H_3)_2$), 26.5 (CH_2), 28.6 (CH_2), 29.4 (CH_2), 29.5 (CH_2), 29.7 (CH_2), 29.8 (CH_2), 29.9 (CH_2), 31.0 ($C(\underline{C}H_3)_3$), 32.1 (CH_2), 32.6 (CH_2), 62.3 (C-4), 74.1 (C-1'), 81.2 ($\underline{C}(CH_3)_3$), 94.7 (C-2), 133.3 and 133.5 (C-2' and C-3'), 166.7 (C=O). FAB-MS: *m/z* (%) = 440.3 (7 %, $[M+H]^+$).

***N*-((2*S*,3*R*,*E*)-1,3-dihydroxyoctadec-4-en-2yl)phenylacetamide (25)**

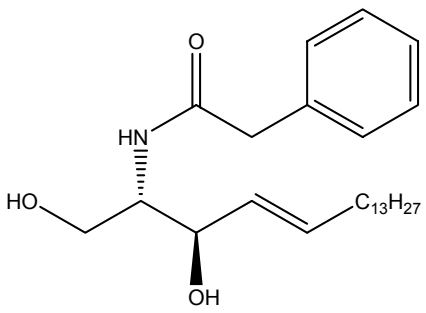

Compound **27** (70 mg ,159 µmol) was dissolved in THF (5 ml) and hydrochloric acid (1M solution, 5 mL) was added, and the solution was stirred for 24 h at rt. The reaction was diluted with water (10 mL),

extracted three times with dichloromethane (20 mL) and the combined organic phases were dried with Na_2SO_4. After removal of the solvent under reduced pressure, the residue was dissolved in methanol (5 mL), cooled to 0°C and triethylamine and benzoyl chloride (45 µL, 340 µmol) were added. The reaction mixture was stirred for 12 h and the solvent was evaporated under vacuum. The product was purified by column chromatography with silica gel (chloroform/methanol, 20:1, (v/v)). Yield: 7 mg (17 µmol) = 11 % over 2 steps, white solid, $C_{26}H_{43}NO_3$, M = 417.63 g/mol, R_f (chloroform/methanol, 20:1, (v/v)) = 0.3.
^{1}H-NMR (400 MHz, $CDCl_3$): δ [ppm] = 0.81 (t, 3H, $^3J_{HH}$ = 7.0 Hz, CH_3), 1.93 (m, 2H, CH_2), 3.59 (dd, 1H, $^2J_{HH}$ = 10.8 Hz, $^3J_{HH}$ = 2.9 Hz), 3.82 (dd, 1H, $^2J_{HH}$ = 12.8 Hz, $^3J_{HH}$ = 4.0 Hz), 4.18 (dd, 1H, $^3J_{HH}$ = 5.2 Hz, $^3J_{HH}$ = 4.6 Hz), 5.37 (ddt, 1H, $^3J_{HH}$ = 15.4 Hz, $^3J_{HH}$ = 6.5 Hz, $^5J_{HH}$ = 1.4 Hz, H-5), 5.63 (dtd, 1H, $^3J_{HH}$ = 15.4 Hz, $^3J_{HH}$ = 6.8 Hz, $^5J_{HH}$ = 1.2 Hz, H-4). ^{13}C-NMR (125 MHz, $CDCl_3$): δ [ppm] = 14.3 (CH_3), 22.9 (CH_2), 29.3 (CH_2), 29.5 (CH_2), 29.6 (CH_2), 29.7 (CH_2), 29.9 (CH_2), 32.2 (CH_2), 32.5 (CH_2), 44.1 (CH_2), 55.2 (C-2), 62.6 (C-1), 74.5 (C-3), 127.6, 128.8, 129.2, 129.6, 134.7 and 134.8 (C_{arom} and C_{alkene}), 172.0 (CO). FAB-MS: *m/z* (%) = 418.2 (32%, $[M+H]^+$).

7.11. Synthesis of glycolipid standards 30 and 34

O-(5-Acetamino-3,5-dideoxy-D-glycero-α-D-galacto-2-nonulopyranosylonic acid)-(2,3)-O-β-D-galactopyranosyl-(1,4)-O-β-D-glucopyranosyl-(1,1)-(2*S*,3*R*,4*E*)-2-hexanoylamino-4-oktadecen-1,3 diol (30)

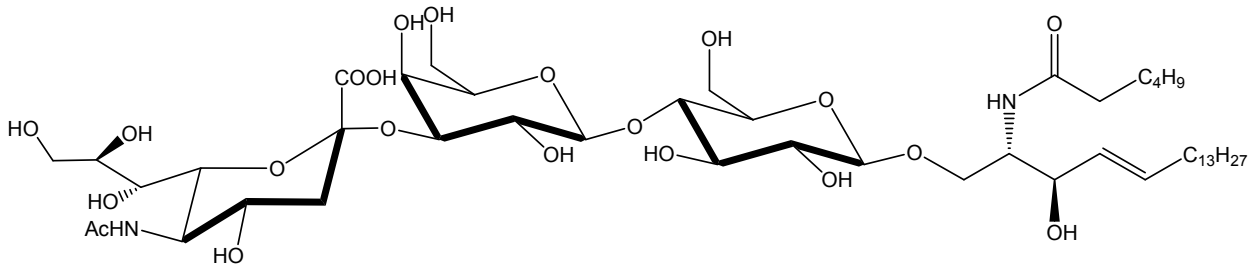

Acetylated GM3-C_6 **29** (67.9 mg, 44.21 µmol) was dissolved in methanol (5 mL) and cooled to 0°C. Sodium methylate (0.5 M solution in methanol, 500 µL, 250 µmol) was added and the reaction mixture was stirred for 12h at rt. Then, the reaction mixture was cooled to 0°C, water (500 µL) was added, and the reaction mixture was stirred for 5h. After Amberlyst 15 was added to the reaction mixture, the product was filtrated, the solvent was removed under reduced pressure. The product was purified by reverse phase chromatography with RP18 (Elution: chloroform/methanol = 1:1 (v/v)). Yield: 37.1 mg (36.64 µmol) = 84%, white solid, $C_{47}H_{84}N_2O_{21}$, M = 1013.17 g/mol, R_f (nbutanol/ethanol/water = 2:1:1 (v/v/v)) = 0.5. ESI-MS (positive mode): *m/z* (%) = 1057.53 ($[M+2Na]^+$, 100%), 1035.56 ($[M+Na]^+$, 18%). EI-HR-MS:$[C_{47}H_{83}N_2Na_2O_{21}]^+$ *m/z* = calcd.: 1057.5278, found: 1057.5258

Lyso-sulfatide (32)

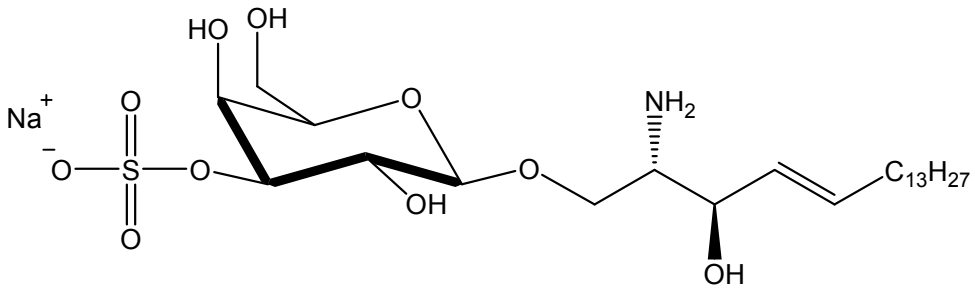

Lysosulfatide **32** was prepared according to a described method (Koshy et al., 1982). Sulfatide (49 mg, 60.4 µmol) was dissolved in a mixture of sodium hydroxide (0.5 M aqueous solution) in methanol/water (9:1 (v/v), 2 mL) and stirred at 80°C for 6d. The solvent was removed under a stream of nitrogen and the residue was purified by column chromatography with silica gel (chloroform/methanol/triethylamine, 3:1:0.001 (v/v/v)). Yield: 4.7 mg (8.34 µmol) = 14%, white solid, $C_{24}H_{46}NNaO_{10}S$, M = 563.27 g/mol, R_f (chloroform/methanol/triethylamine, 3:1:0.001 (v/v/v)) = 0.24. ESI-MS (negative mode): *m/z* (%) = 540.31 ($[M]^-$, 53%), ESI-MS (positive mode): *m/z* (%) = 564.84 ($[M+Na]^+$, 58).

Heptadecanoicacid-2,5-Dioxopyrrolidine-1-ylester (33)

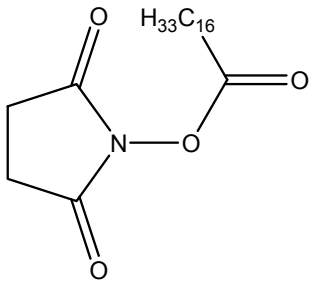

Ester **33** was prepared according to a described method (Kim et al., 2004). Heptadecanoic acid (500 mg, 1.85 mmol), EDC (389.2 mg, 2.03 mmol) and *N*-hydroxy-succinimide (255.5 mg, 2.22 mmol) were dissolved in dichloromethane (20 mL) and stirred at 40°C. The reaction mixture was diluted with water (20 mL) and the product was extracted with ether (3x 60 mL). The combined organic layers were dried with sodium sulfate, filtered and solvent was removed under reduced pressure. Yield: 462.7 mg (1.26 mmol) = 68%, white solid, $C_{21}H_{37}NO_4$, M = 367.27 g/mol.

^{1}H-NMR (300 MHz, $CDCl_3$) δ [ppm]: 0.81 (t, 3H, $^3J_{HH}$ = 6.2 Hz, CH_3), 1.19 (m, 26H, CH_2), 1.66 (m, 2H, CH_2), 2.52 (t, 2H, $^3J_{HH}$ = 7.4 Hz, CH_2), 2.74 (s, 4H, CH_2). ^{13}C-NMR (100 MHz, $CDCl_3$) δ [ppm]: 14.1 (CH_3), 22.7 (CH_2), 24.6 (CH_2), 25.6 (CH_2), 28.8 (CH_2), 29.1 (CH_2), 29.3 (CH_2), 29.4 (CH_2), 29.5 (CH_2), 29.6 (CH_2), 29.7 (CH_2), 30.9 (CH_2), 31.9 (CH_2), 34.0 (CH_2), 168.7 (C=O), 169.3 (C=O).

C_{17}-sulfatide (34)

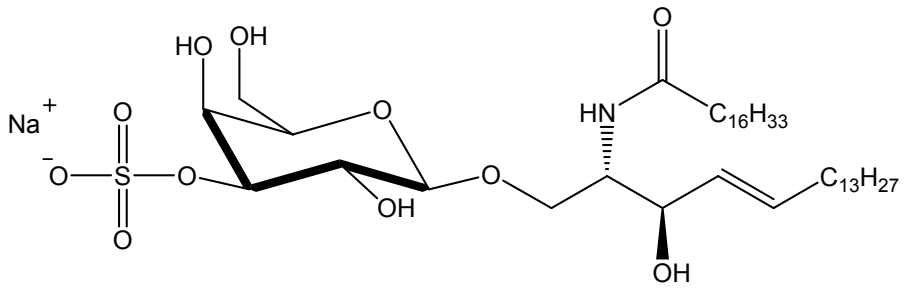

Amide **34** was prepared according to a described method (Kim et al., 2004). Ester **33** (34.4 µmol, 12.66 mg) was dissolved in tetrahydrofurane (0.5 mL) and lysosulfatide (**32**, 4.7 mg, 8.34 µmol) and triethylamine (28.8 µL, 103.4 µmol) were added. The reaction mixture was stirred for 14h at 50°C, water (5 mL) was added and the product was extracted with ethyl acetate (3x 10 mL). The combined organic layers were dried with Na_2SO_4, filtered and solvent was removed under reduced pressure. The residue was purified by column chromatography with silica gel (chloroform/methanol = 3:1 (v/v)). Yield: 1.17 mg (1.43 µmol) = 17%, white solid, $C_{41}H_{78}NNaO_{11}S$, M = 815.52 g/mol, R_f (chloroform/methanol, 3:1 (v/v)) = 0.28. ESI-MS (negative mode): *m/z* (%) = 792.49 ($[M]^-$, 100 %), ESI-MS (positive mode): *m/z* (%) = 816.69 ($[M+Na]^+$, 100%).

8. References

Abe, A.; Inokuchi, J.; Jimbo, M.; Shimeno, H.; Nagamatsu, A.; Shayman, J. A.; Shukla, G. S.; Radin, N. S. (**1992**) Improved inhibitors of glucosylceramide synthase. *J Biochem., 111*: 191-196.

Abousalham, A.; Hobman, T. C.; Dewald, J.; Garbutt, M.; Brindley, D. N. (**2002**) Cell-permeable ceramides preferentially inhibit coated vesicle formation and exocytosis in Chinese hamster ovary compared with Madin-Darby canine kidney cells by preventing the membrane association of ADP-ribosylation factor. *Biochem J., 361*: 653-661.

Agard, N. J.; Baskin, J. M.; Prescher, J. A.; Lo, A.; Bertozzi, C. R. (**2006**) A comparative study of bioorthogonal reactions with azides. *ACS Chem Biol.*, 1: 644-648.

Alvi, K. A.; Jaspars, M.; Crews, P. (**1994**) Penazetidine A, an alkaloid inhibitor of protein kinase C. *Bioorg Med Chem Lett.*, *4*: 2447-2450.

Ariga, T.; Kobayashi, K.; Hasegawa, A.; Kiso, M.; Ishida, H.; Miyatake, T. (**2001**) Characterization of high-affinity binding between gangliosides and amyloid beta-protein, *Arch Biochem Biophys.*, *388*: 225-230.

Baer, T.; Kratzer, B.; Wild, R.; Sandhoff, K.; Schmidt, R. R. (**1993**) Synthesis of sphingosines. Part 8. Synthesis of methyl-branched sphingosines. *Liebigs Ann. Chem.:* 419-426.

Bajjalieh, S.; Batchelor, R. (**2000**) Ceramide kinase. *Methods Enzymol., 311*: 207-215.

Barranger, J. A.; O'Rourke, E. (**2001**) Lessons learned from the development of enzyme therapy for Gaucher disease. *J Inherit Metab Dis., 24*: 89-96.

Barrish J. C.; Spergel S. H.; Moreland S.; Grover G.; Hedberg S. A.; Pudzianowski A. T.; Gougoutas J. Z.; Malley M. F. (**1993**) Conformationally constrained calcium channel blockers: novel mimics of 1-benzazepin-2-ones, *Bioorg Med Chem., 1*: 309-25.

Behforouz, M.; Bolan, J. L.; Flynt, M. S. (**1985**) 2,4-Dinitrophenylhydrazones: a modified method for the preparation of these derivatives and an explanation of previous conflicting results, *J Org Chem., 50*: 1186-1189.

Beaulieu, P. L.; Duceppe, J. S.; Johnson, C. (**1991**) Synthesis of chiral vinylglycines. *J Org Chem., 56*: 4196-4204.

Bieberich, E.; Freischutz, B.; Liour, S. S.; Yu, R. K. (**1998**) Regulation of ganglioside metabolism by phosphorylation and dephosphorylation, *J Neurochem., 71*: 972-9.

Bieberich, E.; MacKinnon, S.; Silva, J.; Li, D. D.; Tencomnao, T.; Irwin, L.; Kapitonov, D.; Yu, R. K. (**2002**) Regulation of Ganglioside Biosynthesis by Enzyme Complex Formation of Glycosyltransferases, *Biochemistry, 41*: 11479-11487.

Bielawska, A.; Crane, H. M.; Liotta, D.; Obeid, L. M.; Hannun, Y. A. (**1993**) Selectivity of ceramide-mediated biology. Lack of activity of erythro-dihydroceramide. *J Biol Chem., 268*: 26226-32.

Bligh, E. G.; Dyer, W. J. (**1959**) A rapid method of total lipid extraction and purification. *Can J Biochem Physiol., 37*: 911-917.

Bourbon, N. A.; Yun J.; Kester, M. (**2000**) Ceramide directly activates protein kinase C zeta to regulate a stress-activated protein kinase signaling complex. *J Biol Chem.*, *275*: 35617-23.

Bradford, M. M. (**1976**) A rapid and sensitive method for the quantification of microgramm quantitation of microgram quantities of protein utilizing the principle of protein-dye binding, *Anal. Biochem., 72*: 248-254.

Brady, R. O. (**1997**) Gaucher's disease: past, present and future. *Bailliere's clinical haematology, 10*: 621-634.

Braendli, A. W.; Hansson, G. C.; Rordriguez-Boulan, E.; Simons, K. A (**1988**) Polarized epithelial cell mutant deficient in translocation of UDP-galactose into the Golgi complex. *J Biol Chem., 263*: 16283-16290.

Braulke, T.; Geuze, H. J.; Slot, J. W.; Hasilik, A.; Von Figura, K. (**1987**) On the effects of weak bases and monensin on sorting and processing of lysosomal enzymes in human cells. *Eur J Cell Biol., 43*: 316-321.

Braun, P. E.; Snell, E. E. (**1968**) Biosynthesis of sphingolipid bases. II. Keto intermediates in synthesis of sphingosine and dihydrosphingosine by cell-free extracts of Hansenula ciferri, *J Biol Chem.*, *243*: 3775-83.

Brodesser, S. (**2007**) Der Stoffwechsel der Sphingolipide (Einfluss von Substratanaloga der Dihydroceramid-Desaturase auf den Sphingolipidstoffwechsel humaner Keratinozyten und Untersuchungen zum Lipidstoffwechsel bei Spinocerebellärer Ataxie Typ 2). Dissertation, Universität Bonn.

Brodesser, S.; Sawatzki P.; Kolter, T. (**2003**) Bioorganic chemistry of ceramide. *Eur. J. Org. Chem. 11*: 2021-2034.

Brown, D. A.; London, E. (**2000**) Structure and function of sphingolipid- and cholesterol-rich membrane rafts. *J Biol Chem.*, *275*: 17221-17224.

Buschard, K.; Hoy, M.; Bokvist, K.; Olsen, H. L.; Madsbad, S.; Fredman, P.; Gromada, J. (**2002**) Sulfatide controls insulin secretion by modulation of ATP-sensitive K(+)-channel activity and Ca(2+)-dependent exocytosis in rat pancreatic beta-cells. *Diabetes, 51*: 2514-2521.

Chalfant, C. E.; Szulc, Z.; Roddy, P.; Bielawska, A.; Hannun, Y. A. (**2004**) The structural requirements for ceramide activation of serine-threonine protein phosphatases. *J Lipid Res., 45*: 496-506.

Conzelmann, E.; Sandhoff, K. (**1983-1984**) Partial enzyme deficiencies: residual activities and the development of neurological disorders. *Dev Neurosci., 6*: 58-71.

Campbell, A. D.; Raynham, T. M.; Taylor, R. J. K. (**1998**) A simplified route to the (R)-Garner aldehyde and (S)-vinylglycinol. *Synthesis*, 12: 1707-1709.

Casado-Bellver, F. J.; Gonzalez-Rosende, M. E.; Asensio, A.; Jorda-Gregori, J. M.; Alvarez-Sorolla, A.; Sepulveda-Arques, J.; Orena, M.; Galeazzi, R. (**2002**) Synthesis of chiral oxazolidin-2-ones from N-alkoxycarbonyl amino epoxides: a computational study. *J Chem Soc., 14*: 1650-1654.

Chalfant, C. E.; Szulc, Z.; Roddy, P.; Bielawska, A.; Hannun, Y. A. (**2004**) The structural requirements for ceramide activation of serine-threonine protein phosphatases. *J Lipid Res.* 45: 496-506.

Chambers, K.; Judson, B.; Brown, W. J. (**2005**) A unique lysophospholipid acyltransferase (LPAT) antagonist, CI-976, affects secretory and endocytic membrane trafficking pathways. *J Cell Sci., 118*: 3061-3071.

Chan, D.; Strang, M.; Judson, B.; Brown, W. J. (**2004**) Inhibition of membrane tubule formation and trafficking by isotetrandrine, an antagonist of G-protein-regulated phospholipase A2 enzymes. *Mol Biol Cell., 15*: 1871-1880.

Chung, N.; Mao, C.; Heitman, J.; Hannun, Y. A.; Obeid, L. M. (**2001**) Phytosphingosine as a specific inhibitor of growth and nutrient import in Saccharomyces cerevisiae. *J Biol Chem., 276*: 35614-35621.

Clasen, K. (**1994**) Synthese von Sphingosin und Sphingosinderivaten (Synthese des Gangliosids C_6-GM3) Dissertation, Universität Bonn.

Coderch, L.; Lopez O.; de la Maza, A.; Parra, J. L. (**2003**) Ceramides and skin function. *Am J Clin Dermatol.,* 4: 107-129.

Colina, C.; Flores, A.; Rojas, H.; Acosta, A.; Castillo, C.; Garrido, M. del R.; Israel, A.; DiPolo, R.; Benaim, G. (**2005**) Ceramide increase cytoplasmic Ca2+ concentration in Jurkat T cells by liberation of calcium from intracellular stores and activation of a store-operated calcium channel. Arch Biochem Biophys., 436: 333-345.

Colombo, I.; Sottocornola, E.; Moretti, S.; Meloni, M. A.; Pippia, P.; Berra, B. (**2000**) Modifications of glycosphingolipid profile and synthesis in normal rat fibroblasts and in syngeneic neoplastic cells at different subculture stages. *Biochim Biophys Acta.,* 1485: 214-224.
Cruciani, V.; Mikalsen, S.-O. (**2005**) Ilimaquinone inhibits gap junctional communication in a connexin isotype-specific manner. *Exp Cell Res., 304*: 136-148.

Csala, M.; Marcolongo, P.; Lizak, B.; Senesi, S.; Margittai, E.; Fulceri, R.; Magyar, J. E.; Benedetti, A.; Banhegyi, G. (**2007**) Transport and transporters in the endoplasmic reticulum. *Biochim Biophys Acta., 1768*: 1325-1341.

Corey, E. J.; Hopkins P. B. (**1982**) Diisopropylsilyl ditriflate and di-*tert*-Butylsilyl ditriflate: New reagents for the protection of diols. *Tetradedron Lett., 23*: 4871-4874.

Dawkins, J. L.; Hulme, D. J.; Brahmbhatt, S. B.; Auer-Grumbach, M.; Nicholson, G. A. (**2001**) Mutations in SPTLC1, encoding serine palmitoyltransferase, long chain base subunit-1, cause hereditary sensory neuropathy type I. *Nat Genet., 27*: 309-312.

D'Angelo, G.; Polishchuk, E.; Di Tullio, G.; Santoro, M.; Di Campli, A.; Godi, A.; West, G.; Bielawski, J.; Chuang, C.-C.; van der Spoel, A. C.; Platt, F. M.; Hannun, Y. A.; Polishchuk, R.; Mattjus, P. De Matteis, M. A. (**2007**) Glycosphingolipid synthesis requires FAPP2 transfer of glucosylceramide. *Nature, 449*: 62-67.

Dawson, G.; Matalon, R.; Dorfman, A. (**1972**) Glycosphingolipids in cultured human skin fibroblasts. I. Characterization and metabolism in normal fibroblasts. *J Biol Chem., 247*: 5944-50.

Delgado, A.; Casas, J.; Llebaria, A.; Abad, J. L.; Fabrias, G. (**2007**) Chemical tools to investigate sphingolipid metabolism and functions. *ChemMedChem, 2*: 580-606.

De Rosa, M. F.; Sillence, D.; Ackerley, C.; Lingwood, C. (**2004**) Role of Multiple Drug Resistance Protein 1 in Neutral but Not Acidic Glycosphingolipid Biosynthesis. *J Biol Chem., 279*: 7867-7876.

Dinter, A.; Berger, E. G. (**1998**) Golgi-disturbing agents. *Histochem Cell Biol., 109*: 571-590.

Dolman, N. J.; Tepikin, A. V. (**2006**) Calcium gradients and the Golgi. Cell Calcium, 40, 505-512.

Dougherty, Ann M.; McDonald, Frank E.; Liotta, Dennis C.; Moody, Steven J.; Pallas, David C.; Pack, Carrie D.; Merrill, Alfred H. (**2006**) Synthesis of 1-Deoxysphingosine Derivatives with Conformationally Restricted Pyrrolidinediol Head Groups. *Org Lett., 8*: 649-652.

Dugger, H. A.; Schwarz, Hans J. (**1967**) Preparation of tritiated water, sulfuric acid, and trifluoroacetic acid. *J Labelled Compd., 3*: 251-256.

Ekroos, K.; Chernushevich, I. V.; Simons, K.; Shevchenko, A. (**2002**) Quantitative profiling of phospholipids by multiple precursor ion scanning on a hybrid quadrupole time-of-flight mass spectrometer. *Anal. Chem., 74*: 941-949.

Elojeimy, S.; Holman, D. H.; Liu, X.; El-Zawahry, A.; Villani, M.; Cheng, J. C.; Mahdy, A.; Zeidan, Y.; Bielwaska, A.; Hannun, Y. A.; Norris, J. S. (**2006**) New insights on the use of desipramine as an inhibitor for acid ceramidase. *FEBS Lett., 580*: 4751-4756.

Endo, Y.; Shimazu, M.; Fukasawa, H.; Driedger, P. E.; Kimura, K.; Tomioka, N.; Itai, A.; Shudo, K. (**1999**) Synthesis, computer modeling and biological evaluation of novel protein kinase C agonists based on a 7-membered lactam moiety. *Bioorg Med Chem Lett., 9:* 173-178.

Eskelinen, E.-L.; Tanaka, Y.; Saftig, P. (**2003**) At the acidic edge: emerging functions for lysosomal membrane proteins. *Trends Cell Biol., 13*: 137-145.

Fan, J.-Q.; Ishii, S. (**2007**) Active-site-specific chaperone therapy for Fabry disease Yin and Yang of enzyme inhibitors. *FEBS J., 274*, 4962-4971.

Feng, Y.; Yu, S.; Lasell, T. K. R.; Jadhav, A. P.; Macia, E.; Chardin, P.; Melancon, P.; Roth, M.; Mitchison, T.; Kirchhausen, T. (**2003**) Exo1: A new chemical inhibitor of the exocytic pathway. *Proc Nat Acad Sci USA*, *100*: 6469-6474.

Feng, J. (**2006**) Microtubule: a common target for parkin and Parkinson's disease toxins. *Neuroscientist, 12*: 469-476.

Fernandis, A. Z.; Wenk, M. R. (**2007**) Membrane lipids as signaling molecules. *Curr Opin Lipidol., 18*: 121-128.

Fischer, E. (**1894**) Influence of configuration on the action of enzymes. *Chem Ber., 27*: 3479-83.

Fürst, W.; Sandhoff, K. (**1992**) Activator proteins and topology of lysosomal sphingolipid catabolism. *Biochim Biophys Acta., 1126*: 1-16.

Futerman, A. H.; Hannun, Y. A. (**2004**) The complex life of simple sphingolipids. *EMBO Reports, 5*: 777-782.

Futerman, A. H.; Riezman, H. (**2005**) The ins and outs of sphingolipid synthesis. *Trends Cell Biol., 15*: 312-318.

Futerman A. H; van Meer G. (**2004**) The cell biology of lysosomal storage disorders. *Nat Rev Mol Cell Biol., 5:* 554-565.

Garner, P. (**1984**) Stereocontrolled addition to a penaldic acid equivalent: an asymmetric synthesis of threo-α -hydroxy-L-glutamic acid. *Tetrahedron Lett., 25*: 5855-5858.

Giannis, A.; Kolter, T. (**1993**) Peptide mimetics for receptor ligands: discovery, development, and medicinal perspectives *Angew. Chem.,105*: 1303-1326; *Angew. Chem. Int. Ed. Engl., 32*: 1244-1267.

Gieselmann, V. (**1995**) Lysosomal storage diseases. *Biochim Biophys Acta., 1270*: 103-136.

Gieselmann, V.; Pohlmann, R.; Hasilik, A.; Von Figura, K. (**1983**) Biosynthesis and transport of cathepsin D in cultured human fibroblasts. *J Cell Biol., 97*: 1-5.

Gillingham, A. K.; Munro, S. (**2007**) The small G proteins of the Arf family and their regulators. *Annu Rev Cell Dev Biol., 23*: 579-611.

Giraudo, C. G.; Maccioni, H. J. F. (**2003**) Ganglioside Glycosyltransferases Organize in Distinct Multienzyme Complexes in CHO-K1 Cells. *J Biol Chem., 278*: 40262-40271.

Godi, A.; Di Campli, A.; Konstantakopoulos, A.; Di Tullio, G.; Alessi, D. R.; Kular, G. S.; Daniele, T.; Marra, P.; Lucocq, J. M.; De Matteis, M. A. (**2004**) FAPPs control Golgi-to-cell-surface membrane traffic by binding to ARF and PtdIns(4)P. *Nat Cell Biol., 6*: 393-404.

Goni, F. M.; Alonso, A. (**2002**) Sphingomyelinases: enzymology and membrane activity. *FEBS Letters, 531*: 38-46.

Goni, F. M.; Alonso, A. (**2006**) Biophysics of sphingolipids I. Membrane properties of sphingosine, ceramides and other simple sphingolipids. *Biochim Biophys Acta., 1758*: 1902-1921.

Gonatas, N. K.; Stieber, A.; Gonatas, J. O. (**2006**) Fragmentation of the Golgi apparatus in neurodegenerative diseases and cell death. *J Neurol Sci., 246*: 21-30.

Griffiths, G. M. (**2007**) Gaucher disease: forging a new path to the lysosome. *Cell, 131*: 647-649.

Grimmer, S.; Ying, M.; Waelchli, S.; van Deurs, B.; Sandvig, K. (**2005**) Golgi vesiculation induced by cholesterol occurs by a dynamin- and cPLA2-dependent mechanism. *Traffic, 6*: 144-156.

Guengerich, F. P. (**2005**) Activation of alkyl halides by glutathione transferases. *Methods Enzymol., 401*: 342-353.

Guillerm, G.; Frappier, F.; Tabet, J.-C.; Marquet, A. (**1977**) Deuterium or tritium labeling by ionic hydrogenation. A convenient route to specifically labeled dethiobiotin. *J Org Chem., 42*: 3776-3778.

Guizzunti, G.; Brady, T. P.; Malhotra, V.; Theodorakis, E. A. (**2006**) Chemical Analysis of Norrisolide-Induced Golgi Vesiculation. *J Am Chem Soc.*, *128*: 4190-4191.

Guzikowski, A. P.; Cai, S. X.; Espitia, S. A.; Hawkinson, J. E.; Huettner, J. E.; Nogales, D. F.; Tran, M.; Woodward, R. M.; Weber, E.; Keana, J. F. (**1996**) Analogs of 3-hydroxy-1H-1-benzazepine-2,5-dione: structure-activity relationship at N-methyl-D-aspartate receptor glycine sites. *J Med Chem., 39*: 4643-4653.

Ha, H.-J.; Hong, M. C.; Ko, S. W.; Kim, Y. W.; Lee, W. K.; Park, J. (**2006**) Synthesis of constrained ceramide analogs and their potent antileukemic activities. *Bioorg Med Chem Lett., 16*: 1880-1883.

Hakomori, S. (**2005**) Organization and function of glycosphingolipids in membrane. *Proc Jpn Acad., 81*: 189-203.

Halter, D.; Neumann, S.; van Dijk, S. M.; Wolthoorn, J.; de Maziere, A. M.; Vieira, O. V.; Mattjus, P.; Klumperman, J.; van Meer, G.; Sprong, H. (**2007**) Pre- and post-Golgi translocation of glucosylceramide in glycosphingolipid synthesis. *J Cell Biol., 179*: 101-115.

Halter, D.; Neumann, S.; van Dijk, S. M.; Wolthoorn, J.; de Maziere, A. M.; Vieira, O. V.; Mattjus, P.; Klumperman, J.; van Meer, G.; Sprong, H. (**2007**) Pre- and post-Golgi translocation of glucosylceramide in glycosphingolipid synthesis. *J Cell Biol., 179*: 101-115.

Han, X.; Cheng, H. (**2005**) Characterization and direct quantitation of cerebroside molecular species from lipid extracts by shotgun lipidomics. *J. Lipid Res., 46*: 163-175.

Hanada, K. (**2005**) Sphingolipids in infectious diseases. *Jpn J Infect Dis., 58*: 131-148

Hanada, K. (**2003**) Serine palmitoyltransferase, a key enzyme of sphingolipid metabolism. *Biochim Biophys Acta., 1682*:16-30.

Hanada, K.; Kumagai, K.; Yasuda, S.; Miura, Y.; Kawano, M.; Fukasawa, M.; Nishijima, M. (**2003**) Molecular machinery for non-vesicular trafficking of ceramide. *Nature, 426*: 803-809.

Hanada, K. (**2006**) Discovery of the molecular machinery CERT for endoplasmic reticulum-to-Golgi trafficking of ceramide. *Mol Cell Biochem., 286*: 23-31.

Hang, H. C.; Geutjes, E.-J.; Grotenbreg, G.; Pollington, A. M.; Bijlmakers, M. J.; Ploegh, H. L. (**2007**) Chemical Probes for the Rapid Detection of Fatty-Acylated Proteins in Mammalian Cells. *J Am Chem Soc., 129*: 2744-2745.

Hannun, Y. A. (**1996**) Functions of ceramide in coordinating cellular responses to stress. Science, 274: 1855-1859.

Hannun, Y. A.; Obeid, L. M. (**2008**) Principles of bioactive lipid signalling: lessons from sphingolipids. *Nat Rev Mol Cell Biol., 9*: 139-150.

Hanzal-Bayer, M. F.; Hancock, J. F. (**2007**) Lipid rafts and membrane traffic. *FEBS Letters, 581*: 2098-2104.

Harrold, M. W. (**1996**) The influence of conformational isomerism on drug action and design. *Am J Pharm Educ., 60*: 192-197.

Heerklotz, H.; Szadkowska, H.; Anderson, T.; Seelig, J. (**2003**) The Sensitivity of Lipid Domains to Small Perturbations Demonstrated by the Effect of Triton. *J Mol Biol., 329*: 793-799.

Heinrich, M.; Wickel, M.; Winoto-Morbach, S.; Schneider-Brachert, W.; Weber, T.; Brunner, J.; Saftig, P.; Peters, C.; Kronke, M.; Schutze, S. (**2000**) Ceramide as an activator lipid of cathepsin D. *Adv Exp Med Biol., 477*: 305-315.

Herold, P. (**1988**) Synthesis of D-erythro- and D-threo-sphingosine derivatives from L-serine. Helv Chim Acta., 71; 354-62.

Heung, L. J.; Luberto, C.; Del Poeta M. (**2006**) Role of Sphingolipids in Microbial Pathogenesis. *Infect Immun.*, *74*: 28–39.

Hoberg, J. O. (**1997**) Synthesis and chemistry of 4,6-O-di-(*tert*-butyl)silanediyl-D-glucal. *Carbohydr Res*., *300*: 365-367.

Holland, W. L.; Brozinick, J. T.; Wang, L.-P.; Hawkins, E. D.; Sargent, K. M.; Liu, Y.; Narra, K.; Hoehn, K. L.; Knotts, T. A.; Siesky, A.; Nelson, D. H.; Karathanasis, S. K.; Fontenot, G. K.; Birnbaum, M. J.; Summers, S. A. (**2007**) Inhibition of ceramide synthesis ameliorates glucocorticoid-, saturated-fat-, and obesity-induced insulin resistance. *Cell Metabol., 5*: 167-179.

Holleran, W. M.; Takagi, Y.; Uchida, Y. (**2006**) Epidermal sphingolipids: Metabolism, function, and roles in skin disorders. *FEBS Letters, 580*: 5456-5466.

Houjou, T.; Yamatani, K.; Nakanishi, H.; Imagawa, M.; Shimizu, T.; Taguchi, R. (**2004**) Rapid and selective identification of molecular species in phosphatidylcholine and sphingomyelin by conditional neutral loss scanning and MS3. *Rapid Commun Mass Spectrom., 18*: 3123-3130.

Hu, W.; Xu, R.; Zhang, G.; Jin, J.; Szulc, Z. M.; Bielawski, J.; Hannun, Y. A.; Obeid, L. M.; Mao, C. (**2005**) Golgi fragmentation is associated with ceramide-induced cellular effects. *Mol Biol Cell., 16*: 1555-1567.

Hüsken, N. (**2006**) Mechanistische Untersuchungen einer neuartigen anionotropen 1,2-Umlagerung. Diplomarbeit, Universität Bonn.

Huitema K.; van den Dikkenberg J.; Brouwers J. F. H. M.; Holthuis J. C. M. (**2004**) Identification of a family of animal sphingomyelin synthases. *EMBO J., 23*: 33-44.

Hurwitz, R.; Ferlinz, K.; Sandhoff, K. (**1994**) The tricyclic antidepressant desipramine causes proteolytic degradation of lysosomal sphingomyelinase in human fibroblasts. *Biol Chem Hoppe Seyler., 375*: 447-450.

Hurwitz, R.; Ferlinz, K.; Vielhaber, G.; Moczall, H.; Sandhoff, K. (**1994**) Processing of human acid sphingomyelinase in normal and I-cell fibroblasts. *J Biol Chem., 269*: 5440-5445.

Huwiler, A.; Fabbro, D.; Pfeilschifter, J. (**1998**) Selective ceramide binding to protein kinase C-α and -δ isoenzymes in renal mesangial cells. *Biochem., 37*: 14556-14562.

Iber, H.; van Echten, G.; Klein, R. A.; Sandhoff, K. (**1990**) pH-dependent changes of ganglioside biosynthesis in neuronal cell culture. *Eur J Cell Biol., 52*: 236-240.

Iber, H.; Van Echten, G.; Sandhoff, K. (**1991**) Substrate specificity of α2,3-sialyltransferases in ganglioside biosynthesis of rat liver Golgi. *Eur J Biochem., 195*: 115-120.

Ishizuka, I. (**1997**) Chemistry and functional distribution of sulfoglycolipids. *Prog Lipid Res., 36*: 245-319.

Isbell, J. C.; Christian, S. T.; Mashburn, N. A.; Bell, P. D. (**1995**) A non-radioactive fluorescent method for measuring protein kinase C activity. *Life Sciences, 57*: 1701-1707.

IUPAC-IUB Joint Commision on Biochemical Nomenclature (JCBN) (**1998**) Nomenclature of glycolipids. Recommendations (**1997**). *Eur. J Biochem., 257*: 293-298.

Jaskiewicz, E.; Zhu, G.; Bassi, R.; Darling, D. S.; Young, W. W. Jr (**1996**) Beta1,4-N-acetylgalactosaminyltransferase (GM2 synthase) is released from Golgi membranes as a neuraminidase-sensitive, disulfide-bonded dimer by a cathepsin D-like protease. *J Biol Chem., 271*: 26395-26403.

Johnson, C. D. (**1993**), Stereoelectronic effects in the formation of 5- and 6-membered rings: the role of Baldwin's rules. *Acc Chem Res., 26*: 476-482.

Jorda-Gregori, J. M.; Gonzalez-Rosende, M. E.; Cava-Montesinos, P.; Sepulveda-Arques, J.; Galeazzi, R.; Orena, M. (**2000**) 1,3-Oxazin-2-ones vs tetrahydrofurans by iodocyclisation of 2-alkoxycarbonylamino-3-alken-1-ols. *Tetrahedron: Asymmetry, 11*: 3769-3777.

Jurczak, J.; Golebiowski, A. (**1989**) Optically active N-protected α-amino aldehydes in organic synthesis. *Chem Rev., 89*: 149-164.

Kang, J.-H.; Kim, S. Y.; Lee, J.; Marquez, V. E.; Lewin, N. E.; Pearce, L. V.; Blumberg, P. M. (**2004**) Macrocyclic diacylglycerol-bis-lactones as conformationally constrained analogues of diacylglycerol-lactones. Interactions with protein kinase C. *J Med Chem., 47*: 4000-4007.

Kho, Y.; Kim, S. C.; Jiang, C.; Barma, D.; Kwon, S. W.; Cheng, J.; Jaunbergs, J.; Weinbaum, C.; Tamanoi, F.; Falck, J.; Zhao, Y. (**2004**) A tagging-via-substrate technology for detection and proteomics of farnesylated proteins. *Proc Natl Acad Sci U S A, 101*: 12479-12484.

Kurita, T.; Izu, H.; Sano, M.; Ito, M.; Kato, I. (**2000**) Enhancement of hydrolytic activity of sphingolipid ceramide N-deacylase in the aqueous-organic biphasic system. *J Lipid Res., 41:* 846-851.

Kyrklund, T. (**1987**) Two procedures to remove polar contaminants from a crude brain lipid extract by using prepacked reversed-phase columns. *Lipids, 22*: 274-277.

Kemp, S. J.; Bao, J.; Pedersen, S. F. (**1996**) Selective Inversion of the Proximal or Distal Hydroxyl Groups in syn,syn-3-[(Alkoxycarbonyl)amino] 1,2-Diols via Cyclic Sulfates. *J Org. Chem., 61*: 7162-7167.

Kim, S.; Song, S.; Lee, T.; Jung, S.; Kim, D. (**2004**) Practical Synthesis of KRN7000 from Phytosphingosine. *Synthesis, 6:* 847-850.

Kirchhausen, T. (**2000**) Three ways to make a vesicle. *Nat Rev Mol Cell Biol., 1*: 187-198.

Klein, T. R.; Kirsch, D.; Kaufmann, R.; Riesner, D. (**1998**) Prion rods contain small amounts of two host sphingolipids as revealed by thin-layer chromatography and mass spectrometry. *Biol Chem., 379*: 655-666.

Klein, D.; Pohlentz, G.; Schwarzmann, G.; Sandhoff, K. (**1987**) Substrate specificity of GM2 and GD3 synthase of Golgi vesicles derived from rat liver. *Eur J Biochem., 167*: 417-424.
Koshy, K. M.; Boggs, J. M. (**1982**) A high-yield saponification of galactosylceramide 3-sulfate. *Lipids, 17*: 998-1000.

Kobayashi, T.; Kobayashi, S. (**2000**) Swern oxidation of bicyclo[2.2.1]hept-5-ene-2,3-diol and its pyrazine-fused derivatives: An improved synthesis of bicyclo[2.2.1]hept-5-ene-2,3-dione and an unexpected ring-opening reaction. *Molecules [online computer file], 5*: 1062-1067.

Koelzer, M.; Werth, N.; Sandhoff, K. (**2004**) Interactions of acid sphingomyelinase and lipid bilayers in the presence of the tricyclic antidepressant desipramine*. FEBS Lett., 559*: 96-98.

Kolesnick, R.; Altieri, D.; Fuks, Z. (**2007**) A CERTain role for ceramide in taxane-induced cell death. *Cancer Cell, 11*: 473-475.

Kolter, T. (**2004**) Glycosphingolipids. In: Bioactive Lipids. (Editors: A. Nicolau, G. Kokotos) Oily Press Lipid Library*, 17*:169-196.

Kolter, T. (**2004**) Conformational restriction of sphingolipids. In: Highlights in Bioorganic Chemistry, (Editors: C. Schmuck, H. Wennemers) Wiley-VCH: 48-60.

Kolter, T.; Sandhoff, K. (**2000**) Lysosomal degradation of glycolipids. *Carbohydrates in Chemistry and Biology, 3*: 455-472.

Kolter, T.; Proia, R. L.; Sandhoff, K. (**2002**) Combinatorial ganglioside biosynthesis. *J Biol Chem., 277*: 25859-25862.

Kolter, T.; Sandhoff, K. (**1999**) Sphingolipids - their metabolic pathways and the pathobiochemistry of neurodegenerative diseases. *Angew. Chem., 111*: 1633-1670; *Angew. Chem. Int. Ed. 38*: 1532-1568.

Kolter, T.; Sandhoff, K. (**2006**) Sphingolipid metabolism diseases. *Biochim Biophys Acta., 1758*: 2057-2079.

Kolter, T.; Sandhoff, K. (**2005**) Principles of lysosomal membrane digestion: Stimulation of sphingolipid degradation by sphingolipid activator proteins and anionic lysosomal lipids. *Annu Rev Cell Dev Biol., 21*: 81-103.

Kovacs, W. J.; Schrader, M.; Walter, I.; Stangl, H. (**2004**) The hypolipidemic compound cetaben induces changes in Golgi morphology and vesicle movement. *Histochem Cell Biol., 122*: 95-109.

Kudo, N.; Kumagi, K.; Tomishige, T.; Wakatsuki, S.; Nishijima, M.; Hanada, K.; Kato, R. (**2008**) Structural basis for specific lipid recognition by CERT responsible for nonvesicular trafficking of ceramide. *Proc Natl Acad Sci U S A., 105*: 488-493.

Kulkarni, Y. S. (**1999**) Serine derivatives in organic synthesis. *Aldrichimica Acta, 32*: 18-27.

Kumagai, K.; Yasuda, S.; Okemoto, K.; Nishijima, M.; Kobayashi, S.; Hanada, K. (**2005**) CERT Mediates Intermembrane Transfer of Various Molecular Species of Ceramides. *J Biol Chem., 280*: 6488-6495.

Kursanov, D. N.; Parnes, Z. N.; Loim, N. M. (**1974**) Applications of ionic hydrogenation to organic synthesis. *Synthesis, 9*: 633-651.

Kwon, Y. B.; Kim, C. D.; Youm, J.-K.; Gwak, H. S.; Park, B. D.; Lee, S. H.; Jeon, S.; Kim, B. J.; Seo, Y.-J.; Park, J.-K.; Lee, J.-H. (**2007**) Novel synthetic ceramide derivatives increase intracellular calcium levels and promote epidermal keratinocyte differentiation. J Lipid Res., 48: 1936-1943.

Ladisch, S.; Li, R. (**2000**) Purification and analysis of gangliosides. *Methods Enzymol., 312*: 135-145.

Lammers, Gwen; Jamieson, James C. (**1989**) Studies on the effect of lysosomotropic agents on the release of Galβ1-4GlcNAcα-2,6-sialyltransferase from rat liver slices during the acute-phase response. *Biochem J*., *261*: 389-893.

Lapidot, Y., S. R.; Wolman, Y. (**1967**) Use of esters of N-hydroxysuccinimide in the synthesis of N-acylaminoacids. *J. Lipid Res. 8*: 142-145.

Lazaro-Dieguez, F.; Jimenez, N.; Barth, H.; Koster, A. J.; Renau-Piqueras, J.; Llopis, J. L.; Burger, K. N. J.; Egea, G. (**2006**) Actin filaments are involved in the maintenance of Golgi cisternae morphology and intra-Golgi pH. *Cell Motil Cytoskeleton., 63*: 778-791.

Lee, K. Y.; Kim, J. N. (**2000**) Facile synthesis of phosphonium salts from alcohols *Bull Kor Chem Soc., 21*: 763-764.

Leeson, P. D.; Iversen, L. L. (**1994**) The glycine site on the NMDA receptor: structure-activity relationships and therapeutic potential. *J Med Chem., 37*: 4053-67.

Leinekugel, P.; Michel, S.; Conzelman, E.; Sandhoff, K. (**1992**) Quantitative correlation between the residual activity of β-hexosaminidase A and arylsulfatase A and the severity of the resulting lysosomal storage disease. Hum Genet., 88: 513-523.

Leoni, L. M.; Shih, H. C.; Deng, L.; Tuey, C.; Walter, G.; Carson, D. A.; Cottam, H. B. (**1998**) Modulation of ceramide-activated protein phosphatase 2A activity by low molecular weight aromatic compounds. *Biochem Pharmacol., 55*: 1105-1111.

Leurs, R.; Blandina, P.; Tedford, C.; Timmerman, H. (**1998**) Therapeutic potential of histamine H3 receptor agonists and antagonists. *Trends Pharmacol Sci., 19*: 177-183.

Liang, X.; Andersch, J.; Bols, M. (**2001**) Garner 's aldehyde. *J Chem Soc., 18*: 2136-2157.

Lipsky, N. G.; Pagano, R. E. (**1985**) A vital stain for the Golgi apparatus. *Science, 228*: 745-747.

Liu, G.; Kleine, L.; Hebert, R. L. (**1999**) Advances in the signal transduction of ceramide and related sphingolipids. *Crit Rev Clin Lab Sci., 36*: 511-73.

Liu, Y.; Wada, R.; Kawai, H.; Sango, K.; Deng, C.; Tai, T.; McDonald, M. P.; Araujo, K.; Crawley, J. N.; Bierfreund, U.; Sandhoff, K.; Suzuki, K.; Proia, R. L. (**1999**) A genetic model of substrate deprivation therapy for a glycosphingolipid storage disorder. *J Clin Invest., 103*: 497-505.

Macala, L. J.; Yu, R.; Ando S. (**1983**) Analysis of brain lipids by high performance thin-layer chromatography. *J Lipid Res., 24*: 1243-1250.

Macchia, M.; Barontini, S.; Bertini, S.; Di Bussolo, V.; Fogli, S.; Giovannetti, E.; Grossi, E.; Minutolo, F.; Danesi, R. (**2001**) Design, Synthesis, and Characterization of the Antitumor Activity of Novel Ceramide Analogues. *J Med Chem., 44*: 3994-4000.

Mach, U. R.; Lewin, N. E.; Blumberg, P. M.; Kozikowski, A. P. (**2006**) Synthesis and pharmacological evaluation of 8- and 9-substituted benzolactam-V8 derivatives as potent ligands for protein kinase C, a therapeutic target for Alzheimer's disease. *ChemMedChem, 1*: 307-314.

Malolanarasimhan, K.; Kedei, N.; Sigano, D. M.; Kelley, J. A.; Lai, C. C.; Lewin, N. E.; Surawski, R. J.; Pavlyukovets, V. A.; Garfield, S. H.; Wincovitch, S.; Blumberg, P. M.; Marquez, V. E. (**2007**) Conformationally Constrained Analogues of Diacylglycerol (DAG). 27. Modulation of Membrane Translocation of Protein Kinase C (PKC) Isozymes α and δ by Diacylglycerol Lactones (DAG-Lactones) Containing Rigid-Rod Acyl Groups. *J Med Chem., 50*: 962-978.

Mandon, E. C.; Van Echten, G.; Birk, R.; Schmidt, R. R.; Sandhoff, K. (**1991**) Sphingolipid biosynthesis in cultured neurons. Down-regulation of serine palmitoyltransferase by sphingoid bases. *Eur J Biochem., 198*: 667-74.

Mandon, E. C.; Ehses, I.; Rother, J.; Van Echten, G.; Sandhoff, K. (**1992**) Subcellular localization and membrane topology of serine palmitoyltransferase, 3-dehydrosphinganine reductase, and sphinganine N-acyltransferase in mouse liver. *J Biol Chem., 267*: 11144-11148.

Mann, A.; Le Chatelier, H.-L. (**2003**) Conformational restriction and/or steric hindrance in medicinal chemistry. In: The Practice of Medicinal Chemistry, 2nd Edition (Editor: Wermuth, C. M), Elsevier: 233-250.

Mason, R. M.; Lancaster, C. A. (**1992**) Effects of cyclofenil diphenol, an agent which disrupts Golgi structure, on proteoglycan synthesis in chondrocytes. *Biochem J., 281*: 525-531.

Mateo, C.; Alvarez, R.; Perez-Melero, C.; Pelaez, R.; Medarde, M. (**2007**) Conformationally restricted macrocyclic analogues of combretastatins. Bioorg Med Chem Lett., 17: 6316-6320.

Mathias, S.; Dressler, K. A.; Kolesnick, R. N. (**1991**) Characterization of a ceramide-activated protein kinase: stimulation by tumor necrosis factor alpha. *Proc Natl Acad Sci U S A, 88*: 10009-10013.

McCaffrey, G.; Jamieson, J. C. (**1993**) Evidence for the role of a cathepsin D-like activity in the release of Galβ1-4GlcNAcα2-6sialyltransferase from rat and mouse liver in whole-cell systems. *Comp Biochem Physiol B Biochem Mol Biol.*, 104B: 91-94.

McKillop, A.; Taylor, R. J. K.; Watson, R. J.; Lewis, N. (**1994**) An improved procedure for the preparation of the Garner aldehyde and its use for the synthesis of N-protected 1-halo-2-(R)-amino-3-butenes. *Synthesis*: 31-33.

Merrill, A. H., Jr. (**2002**) De novo sphingolipid biosynthesis: a necessary, but dangerous, pathway. *J Biol Chem., 277*: 25843-25846.

Meier, E. M.; Schwarzmann, G.; Fuerst, W.; Sandhoff, K. (**1991**) The human GM2 activator protein. A substrate specific cofactor of β-hexosaminidase A. *J Biol Chem., 266*: 1879-1887.

Milstien, S.; Gude, D.; Spiegel, S. (**2007**) Sphingosine 1-phosphate in neural signalling and function. *Acta Paediatr Suppl., 96*: 40-43.

Miescher, K., (**1946**) Steroids. XLIX. Color reactions, 29: 743-752 .

Munro, S. (**2003**) Lipid rafts: elusive or illusive? *Cell, 115*: 377-388.

Nakagawa, Y.; Irie, K.; Yanagita, R. C.; Ohigashi, H.; Tsuda, K.-I.; Kashiwagi, K.; Saito, N. (**2006**) Design and Synthesis of 8-Octyl-benzolactam-V9, a Selective Activator for Protein Kinase Cε and η. *J Med Chem., 49*: 2681-2688.

Nakamura, M.; Nakazawa, J.; Usui, T.; Osada, H.; Kono, Y.; Takatsuki, A. (**2000**) Nordihydroguaiaretic acid, of a new family of microtubule-stabilizing agents, shows effects differentiated from paclitaxel. *Biosci Biotechnol Biochem., 67*, 151-157.

Nakamura, M.; Kuroiwa, N.; Kono, Y.; Takatsuki, A. (**2001**) Glucosylceramide synthesis inhibitors block pharmacologically induced dispersal of the Golgi and anterograde membrane flow from the endoplasmic reticulum: implication of sphingolipid metabolism in maintenance of the Golgi architecture and anterograde membrane flow. *Biosci Biotechnol Biochem., 65*: 1369-1378.

Naetzker, S.; Heinemann, T.; Figueroa-Perez, S.; Schnieders, B.; Schmidt, R. R.; Sandhoff, K.; van Echten-Deckert, G. (**2002**) Cis-4-methylsphingosine phosphate induces apoptosis in neuroblastoma cells by opposite effects on p38 and ERK mitogen-activated protein kinases. Biol Chem., 383: 1885-94.

Neuenhofer, S.; Schwarzmann, G.; Egge, H.; Sandhoff K. (**1985**) Synthesis of lysogangliosides, *Biochem., 24*: 525-532.

Nixon, G. F.; Mathieson, F. A.; Hunter, I. (**2008**) The multi-functional role of sphingophosphorylcholine. *Prog Lipid Res., 47*: 62-75.

Nyangulu, J. M.; Nelson, K. M.; Rose, P. A.; Gai, Y.; Loewen, M.; Lougheed, B.; Quail, J. W.; Cutler, A. J.; Abrams, S. R. (**2006**) Synthesis and biological activity of tetralone abscisic acid analogues. *Org Biomol Chem., 4*: 1400-1412.

Ogretmen, B.; Pettus, B. J.; Rossi, M. J.; Wood, R.; Usta, J.; Szulc, Z.; Bielawska, A.; Obeid, L. M.; Hannun, Y. A. (**2002**) Biochemical mechanisms of the generation of endogenous long chain ceramide in response to exogenous short chain ceramide in the A549 human lung adenocarcinoma cell line: role for endogenous ceramide in mediating the action of exogenous ceramide. *J. Biol. Chem.*,277: 12960–12969.

Pan, B.; Fromholt, S. E.; Hess, E. J.; Crawford, T. O.; Griffin, J. W.; Sheikh, K. A.; Schnaar, R. L. (**2005**) Myelin-associated glycoprotein and complementary axonal ligands, gangliosides, mediate axon stability in the CNS and PNS: Neuropathology and behavioral deficits in single- and double-null mice. *Exp Neurol., 195*: 208-217.

Patton, A. R.; Chism, P. (**1951**) Quantitative paper chromatography of amino acids. *Anal. Chem., 23*: 1683-1685.

Perez, M.; Hirschberg, C. B. (**1985**) Translocation of UDP-N-acetylglucosamine into vesicles derived from rat liver rough endoplasmic reticulum and Golgi apparatus. *J Biol Chem., 260*, 4671-4678.

Pewzner-Jung, Y.; Ben-Dor, S.; Futerman, A. H. (**2006**) When do lasses (longevity assurance genes) become CerS (ceramide synthases)?: Insights into the regulation of ceramide synthesis. *J Biol Chem., 281*: 25001-25005.

Pfitzner, K. E.; Moffatt, J. G. (**1963**) A new and selective oxidation of alcohols. *J Am Chem Soc., 85*: 3027-3028.

Garner, P.; Park, J. M.; Malecki, E. (**1988**) A stereodivergent synthesis of D-erythro-sphingosine and D-threo-sphingosine from L-serine. *J Org Chem., 53*: 4395-4398.

Pfefferkorn, J. A.; Song, Y.; Sun, K.-L; Miller, S. R.; Trivedi, B. K.; Choi, C.; Sorenson, R. J.; Bratton, L. D.; Unangst, P. C.; Larsen, S. D.; Poel, T.-J.; Cheng, X.-M.; Lee, C.; Erasga, N.; Auerbach, B.; Askew, V.; Dillon, L.; Hanselman, J. C.; Lin, Z.; Lu, G.; Robertson, A.; Olsen, K.; Mertz, T.; Sekerke, C.; Pavlovsky, A.; Harris, M. S.; Bainbridge, G.; Caspers, N.; Chen, H.; Eberstadt, M. (**2007**) Design and synthesis of hepatoselective, pyrrole-based HMG-CoA reductase inhibitors. *Bioorg Med Chem. Letters, 17*: 4538-4544.

Platt, F. M.; Butters, T. D. (**2000**) Substrate deprivation: a new therapeutic approach for the glycosphingolipid lysosomal storage diseases. *Expert Reviews in Molecular Medicine [online computer file]*

Platt, F. M.; Neises, G. R.; Reinkensmeier, G.; Townsend, M. J.; Perry, V. H.; Proia, R. L.; Winchester, B.; Dwek, R. A.; Butters, T. D. (**1997**) Prevention of lysosomal storage in Tay-Sachs mice treated with N-butyldeoxynojirimycin. *Science, 276*: 428-431.

Pohlentz, G.; Klein, D.; Schmitz, D.; Schwarzmann, G.; Peter-Katalinic, J.; Sandhoff, K. (**1988**) Biosynthesis of gangliosides from asialogangliosides in rat liver Golgi vesicles. *Biol Chem Hoppe Seyler, 369*: 55-63.

Puri, V.; Watanabe, R.; Dominguez, M.; Sun, X.; Wheatley, C. L.; Marks, D. L.; Pagano, R E. (**1999**) Cholesterol modulates membrane traffic along the endocytic pathway in sphingolipid-storage diseases. *Nat Cell Biol., 1*: 386-388.

Pütz, U.; Schwarzmann, G. (**1995**) Golgi staining by two fluorescent ceramide analogs in cultured fibroblasts requires metabolism. *Eur J Cell Biol., 68*: 113-121.

Purpura, D. P.; Suzuki, K. (**1976**) Distortion of neuronal geometry and formation of aberrant synapses in neuronal storage disease. *Brain Res., 116*: 1-21.

Radin, N. S. (**1996**) Treatment of Gaucher disease with an enzyme inhibitor. *Glycoconj J., 13*: 153-157.

Reetz, M. T. (**1991**) New methods to use amino acids as chiral synthons in organic synthesis. *Angew Chem., 103*: 1559-1573; *Int. Ed. Engl., 30*: 1531-1546.

Renault, L.; Guibert, B.; Cherfils, J. (**2003**) Structural snapshots of the mechanism and inhibition of a guanine nucleotide exchange factor. *Nature*, *426*: 525-530.

Richardson, K.; Jamieson, J. C. (**1995**) Release of sialyltransferases from rat liver Golgi membranes by a cathepsin D-like proteinase: comparison of the release of Galβ1-4GlcNAcα2-6 sialyltransferase, Galβ1-3(4)GlcNAcα2-3 sialyltransferase and lactosylceramide α2-3 sialyltransferase (SAT-1). *Comp Biochem Physiol B Biochem Mol Biol.*, 110B: 445-450.

Ron, D.; Kazanietz, M. G. (**1999**) New insights into the regulation of protein kinase C and novel phorbol ester receptors. *FASEB Journal, 13:* 1658-1676.

Roseman, S. (**1970**) The synthesis of complex carbohydrates by multiglycosyltransferase systems and their potential function in intracellular adhesion. *Chem. Phys Lipids, 5*: 270-297.

Rosenwald, A. G.; Pagano, R. E. (**1993**) Inhibition of glycoprotein traffic through the secretory pathway by ceramide. *J Biol Chem., 268*: 4577-4579.

Rosso, S. B.; Caceres, A. O.; De Duffard, A. M. E.; Duffard, R. O.; Quiroga, S. (**2000**) 2,4-Dichlorophenoxyacetic acid disrupts the cytoskeleton and disorganizes the Golgi apparatus of cultured neurons. *Toxicol Sci., 56*: 133-140.

Rother, J.; Van Echten, G.; Schwarzmann, G.; Sandhoff, K. (**1992**) Biosynthesis of sphingolipids: dihydroceramide and not sphinganine is desaturated by cultured cells. *Biochem Biophys Res Commun., 189*, 14-20.

Ruvolo, P. P. (**2003**) Intracellular signal transduction pathways activated by ceramide and its metabolites. *Pharmacol Res., 47*: 383-92.

Ryves, W. J.; Evans, A. T.; Olivier, A. R.; Parker, P. J.; Evans, F. J (**1991**) "Activation of the PKC-isotypes alpha, beta 1, gamma, delta and epsilon by phorbol esters of different biological activities" *FEBS Lett. 288*: 5-9

Sandhoff, K.; Kolter, T. (**1996**) Topology of glycosphingolipid degradation. *Trends Cell Biol., 6*: 98-103.

Sangiorgio, V.; Pitto, M.; Palestini, P.; Masserini, M. (**2004**) GPI-anchored proteins and lipid rafts. *Ital J Biochem., 53*: 98-111.

Sawatzki, P. (**2003a**) Ceramid-Analoga als Werkzeuge in der Bioorganischen Chemie von Glykolipiden. Dissertation, Universität Bonn.

Sawatzki, P.; Kolter, T. (**2004**) Syntheses of 3-C-methylceramides. *Eur J Org Chem.,* 17: 3693-3700.

Sawatzki, P.; Mikeska, T.; Nieger, M.; Bolte, M.; Kolter, T. (**2003b**) (4S,5S)-4-[(1R)-1,2-Dihydroxyethyl]-5-tridecyl-1,3-oxazolidin-2-one. *Acta Crystallogr C, C59*: o225-o227.

Saxon, E.; Bertozzi, C. R. (**2000**) Cell surface engineering by a modified Staudinger reaction. *Science, 287*: 2007-2010.

Saxon, E.; Luchansky, S. J.; Hang, H. C.; Yu, C.; Lee, S. C.; Bertozzi, C. R. (**2002**) Investigating Cellular Metabolism of Synthetic Azidosugars with the Staudinger Ligation. *J Am Chem Soc., 124*, 14893-14902.

Scheel, G.; Acevedo, E.; Conzelmann, E.; Nehrkorn, H.; Sandhoff, K. (**1982**) Model for the interaction of membrane-bound substrates and enzymes. Hydrolysis of ganglioside GD1a by sialidase of neuronal membranes isolated from calf brain. *Eur J Biochem., 127*: 245-253.

Scheel, J.; Matteoni, R.; Ludwig, T.; Hoflack, B.; Kreis, T. E. (**1990**) Microtubule depolymerization inhibits transport of cathepsin D from the Golgi apparatus to lysosomes. *J Cell Sci., 96*: 711-720.

Schenck, M.; Carpinteiro, A.; Grassme, H.; Lang, F.; Gulbins, E (**2007**) Ceramide: Physiological and pathophysiological aspects. *Arch Biochem Biophys., 462*: 171-175.

Schnaar, R.L. (**2004**) Glycolipid-mediated cell-cell recognition in inflammation and nerve regeneration. *Arch Biochem Biophys., 426*: 163-172.

Sciannamblo, M.; Chigorno, V.; Passi, A.; Valaperta, R.; Zucchi, I.; Sonnino, S. (**2003**) Changes of the ganglioside pattern and content in human fibroblasts by high density cell population subculture progression. *Glycoconj J.,* 19:181-186.

Shaw, A. S. (**2006**) Lipid rafts: now you see them, now you don't. *Nat Immunol., 7*: 1139-1142.

Shier, W. T.; Shier, A. C. (**2000**) Sphingosine- and ceramide-analog toxins-an update. *J Toxicol*., 19: 189-246.

Shirai, Y.; Saito, N. (**2002**) Activation mechanisms of protein kinase C: maturation, catalytic activation, and targeting. *J Biochem.,* 132: 663-668.

Sims, K. J.; Alvarez-Vasquez, F.; Voit, E. O.; Hannun, Y. A. (**2007**) A guide to biochemical systems modeling of sphingolipids for the biochemist. *Methods Enzymol., 432*: 319-350.

Simons, K.; Ikonen, E. (**1997**) Functional rafts in cell membranes. *Nature, 387*: 569-572.

Simpson, M. A.; Cross, H.; Proukakis, C.; Priestman, D. A.; Neville, D. C. A.; Reinkensmeier, G.; Wang, H.; Wiznitzer, M.; Gurtz, K.; Verganelaki, A.; Pryde, A.; Patton, M. A.; Dwek, R. A.; Butters, T. D.; Platt, F. M.; Crosby, A. H. (**2004**) Infantile-onset symptomatic epilepsy syndrome caused by a homozygous loss-of-function mutation of GM3 synthase. *Nat Genet., 36*: 1225-1229.

Silence, D.J.; Platt, F.M. (**2003**) Storage diseases: new insights into sphingolipid functions. *Trends Cell Biol. 13*: 195-203.

Siskind, L. J.; Kolesnick, R. N.; Colombini, M. (**2006**) Ceramide forms channels in mitochondrial outer membranes at physiologically relevant concentrations. *Mitochondrion, 6*: 118-125.

Sonnino, S.; Mauri, L.; Chigorno, V.; Prinetti, A. (**2006**) Gangliosides as components of lipid membrane domains. *Glycobiology, 17*: 1R-13R.

Spiegel, S.; Milstien, S. (**2003**) Sphingosine-1-phosphate: an enigmatic signalling lipid. *Nat Rev Mol Cell Biol., 4*: 397-407.

Suzuki, K. (**1998**) Twenty five years of the 'psychosine hypothesis': a personal perspective of its history and present status. *Neurochem. Res. 23*: 251-259.

Suzuki, E.; Handa, K.; Toledo, M. S.; Hakomori, S. (**2004**) Sphingosine-dependent apoptosis: A unified concept based on multiple mechanisms operating in concert. *Proc Natl Acad Sci U S A., 101*: 14788-14793.

Stoffel, W.; LeKim, D.; Sticht, G. (**1968**) Biosynthesis of dihydrosphingosine *in vitro*. *Hoppe Seylers Z Physiol Chem., 349*: 664-70.

Svennerholm, L. (**1963**) Chromatographic separation of human brain gangliosides. *J Neurochem., 10*: 613-623.

Swanton, C.; Marani, M.; Pardo, O.; Warne, P. H.; Kelly, G.; Sahai, E.; Elustondo, F.; Chang, J.; Temple, J.; Ahmed, A. A.; Brenton, J. D.; Downward, J.; Nicke, B. (**2007**) Regulators of mitotic arrest and ceramide metabolism are determinants of sensitivity to paclitaxel and other chemotherapeutic drugs. *Cancer Cell, 11*: 498-512.

Tafesse, F. G.; Ternes, P.; Holthuis, J. C. M. (**2006**) The multigenic sphingomyelin synthase family. *J Biol Chem., 281*: 29421-29425.

Tartakoff, A. M. (**1983**) Perturbation of vesicular traffic with the carboxylic ionophore monensin. *Cell, 32*: 1026-1028.

Tifft, C.J.; Proia, L. (**2000**), Stemming the tide: glycosphingolipid synthesis inhibitors as therapy for storage diseases. *Glycobiology, 10*: 1249-1258.

Toma, L.; Pinhal, M. A.; Dietrich, C. P.; Nader, H. B.; Hirschberg, C. B. (**1996**) Transport of UDP-galactose into the Golgi lumen regulates the biosynthesis of proteoglycans. *J Biol Chem., 271*: 3897-901.

Toshinori, S.; Kenichi, H.; Hironobu, H.; Tatsuya, Y. (**2007**) Syntheses of oligosaccharides using cell function. *TIGG*, *19*: 1-17

Townsend, L. E.; Benjamins, J. A.; Skoff, R. P. (**1984**) Effects of monensin and colchicine on myelin galactolipids. *J Neurochem., 43*: 139-45.

Tropak, M. B.; Mahuran, D. (**2007**) Lending a helping hand, screening chemical libraries for compounds that enhance β-hexosaminidase A activity in GM2 gangliosidosis cells. *FEBS J., 274*: 4951-4961.

Uliana, A. S.; Giraudo, C. G.; Maccioni, H. J. F. (**2006**) Cytoplasmic tails of SialT2 and GalNAcT impose their respective proximal and distal Golgi localization. *Traffic, 7*: 604-612.

van Echten-Deckert, G.; Giannis, A.; Schwarz, A.; Futerman, A. H.; Sandhoff, K. (**1998**) 1-Methylthiodihydroceramide, a novel analog of dihydroceramide, stimulates sphinganine degradation resulting in decreased de novo sphingolipid biosynthesis. *J Biol Chem., 273*: 1184-1191.

van Echten, G.; Iber, H.; Stotz, H.; Takatsuki, A.; Sandhoff, K. (**1990**) Uncoupling of ganglioside biosynthesis by Brefeldin A. *Eur J Cell Biol., 51*: 135-139.

van Echten, G.; Sandhoff, K. (**1989**) Modulation of ganglioside biosynthesis in primary cultured neurons. *J Neurochem., 52*: 207-14.

van Echten, G.; Birk, R.; Brenner-Weiss, G.; Schmidt, R. R.; Sandhoff, K. (**1990**) Modulation of sphingolipid biosynthesis in primary cultured neurons by long chain bases. *J Biol Chem., 265*: 9333-9999.

van Blitterswijk, W. J.; van der Luit, A. H.; Veldman, R. J.; Verheij, M.; Borst, J. (**2003**) Ceramide: second messenger or modulator of membrane structure and dynamics? *Biochem J., 369*: 199-211.

van Meer, G. (**1998**) Lipids of the Golgi membrane. *Trends Cell Biol., 8*: 29-33.

van Meer, G.; Sprong, H. (**2004**) Membrane lipids and vesicular traffic. *Curr Opin Cell Biol., 16*: 373-378.

von Figura, K.; Gieselmann, V.; Jaeken, J. (**2001**) Metachromatic Leukodystrophy. In: The Metabolic and Molecular Bases of Inherited Disease, McGraw Hill (Editors: C.R. Scriver, A.L. Beaudet, W.S. Sly, D.Valle), 8th Ed.: 3695-3724.

Vyas, A. A.; Schnaar, R. L. (**2001**) Brain gangliosides: Functional ligands for myelin stability and the control of nerve regeneration. *Biochimie, 83*: 677-682.

Wang, G.; Silva, J.; Krishnamurthy, K.; Tran, E.; Condie, B. G.; Bieberich, E. (**2005**) Direct Binding to Ceramide Activates Protein Kinase Cξ before the Formation of a Pro-apoptotic Complex with PAR-4 in Differentiating Stem Cells. *J Biol Chem., 280*: 26415-26424.

Waschołowski, V.; Giannis, A. (**2006**) Sphingolactone: selective and irreversible inhibitors of neutral sphingomyelinase. *Angew Chem., Int. Ed., 45*: 827-830.

Watanabe, M.; Kazuta, Y.; Hayashi, H.; Yamada, S.; Matsuda, A.; Shuto, S. (**2006**) Stereochemical Diversity-Oriented Conformational Restriction Strategy. Development of Potent Histamine H3 and/or H4 Receptor Antagonists with an Imidazolylcyclopropane Structure. *J Med Chem., 49*: 5587-5596.

Watson, A. D. (**2006**) Lipidomics: a global approach to lipid analysis in biological systems. *J Lipid Res., 47*: 2101-2111.

Wehland, J.; Henkart, M.; Klausner, R.; Sandoval, I. V. (**1983**) Role of microtubules in the distribution of the Golgi apparatus: effect of taxol and microinjected anti-alpha-tubulin antibodies. *Proc Natl Acad Sci U S A., 80:* 4286-4290.

Weitz, G.; Lindl, T.; Hinrichs, U.; Sandhoff, K. (**1983**) Release of sphingomyelin phosphodiesterase (acid sphingomyelinase) by ammonium chloride from CL 1D mouse L-cells and human fibroblasts. Partial purification and characterization of the exported enzymes. *Hoppe Seylers Z Physiol Chem., 364*: 863-871.

Wendeler, M. (**2004**) Biosynthese und Abbau des Gangliosids GM2 (Expression und Charakterisierung von GM2-Synthase und GM2-Aktivator. Dissertation, Universität Bonn.

Wendeler, M.; Wirtz, J.; Kolter, T. (**2005**) Sphingolipids as emerging drug targets: Therapeutic applications of ceramide analogs. *Drug Design Reviews-Online, 2*: 53-65.

Wendeler, M.; Reilaender, H.; Hoernschemeyer, J.; Schwarzmann, G.; Kolter, T.; Sandhoff, K. (**2003**) Recombinant ganglioside GM2 synthase-expression in insect cells and enzyme assay. *Methods Enzymol., 363*: 476-489.

Whitfield, P.; Johnson, A. W.; Dunn, K. A.; Delauche, A. J. N.; Winchester, B. G.; Franklin, R. J. M. (**2000**) GM1-gangliosidoses in a cross-bred dog confirmed by detection of GM1-ganglioside using electrospray ionisation-tandem mass spectrometry. *Acta Neuropathol., 100*: 409-414.

Wilkening, G.; Linke T.; Sandhoff K. (**1998**) Lysosomal degradation on vesicular membrane surfaces. Enhanced glucosylceramide degradation by lysosomal anionic lipids and activators. *J. Biol. Chem. 273*: 30271-30278.

Wilkening, G.; Linke, T.; Uhlhorn-Dierks, G.; Sandhoff, K. (**2000**), Degradation of membrane-bound ganglioside GM1. Stimulation by bis(monoacylglycero)phosphate and the activator proteins SAP-B and GM2-AP. *J Biol Chem. 275*: 35814-35819.

Williams, M. A.; McCluer, R. H. (**1980**) The use of Sep-Pak C18 cartridges during the isolation of gangliosides. *J Neurochem.*, *35*: 266-269.

Wirtz, J. (**2003**) Synthese und Untersuchung konformativ fixierter Ceramidanaloga, Diplomarbeit, Universität Bonn.

Wirtz, J.; Kolter, T. (**2007**) Novel tools for the proteomic identification of acylated proteins. *ChemBioChem, 8*: 1631-1635.

Wu, Y. N.; Gadina, M.; Tao-Cheng, J. H.; Youle, R. J. (**1994**) Retinoic acid disrupts the Golgi apparatus and increases the cytosolic routing of specific protein toxins. *J Cell Biol., 125*: 743-753.

Yamamoto, A.; Haraguchi, M.; Yamashiro, S.; Fukumoto, S.; Furukawa, K.; Takamiya, K.; Atsuta, M.; Shiku, H.; Furukawa, K. (**1996**) Heterogeneity in the expression pattern of two ganglioside synthase genes during mouse brain development. *J Neurochem., 66*: 26-34.

Yamashita, T.; Wada, R.; Sasaki, T.; Deng, C.; Bierfreund, U.; Sandhoff, K.; Proia, R. L. (**1999**) A vital role for glycosphingolipid synthesis during development and differentiation. *Proc Natl Acad Sci U S A., 96*: 9142-9147.

Yamashita, T.; Hashiramoto, A.; Haluzik, M.; Mizukami, H.; Beck, S.; Norton, A.; Kono, M.; Tsuji, S.; Daniotti, J.L.; Werth, N.; Sandhoff, R.; Sandhoff, K.; Proia, R.L. (**2003**) Enhanced insulin sensitivity in mice lacking ganglioside GM3. *Proc Natl Acad Sci U S A. 100*: 3445-3449.

Yao, J. K.; Rastetter, G M. (**1985**) Microanalysis of complex tissue lipids by high-performance thin-layer chromatography. *Anal Biochem., 150*: 111-116.

Yusuf, H. K.; Schwarzmann, G.; Pohlentz, G.; Sandhoff, K. (**1987**) Oligosialogangliosides inhibit GM2- and GD3-synthesis in isolated Golgi vesicles from rat liver. *Biol Chem Hoppe Seyler., 368*: 455-62.

Young, W. W., Jr.; Allende, M. L.; Jaskiewicz, E. (**1999**) Reevaluating the effect of brefeldin A (BFA) on ganglioside synthesis: the location of GM2 synthase cannot be deduced from the inhibition of GM2 synthesis by BFA. *Glycobiology, 9*: 689-695.

Yu, Z.; Sawkar, A. R.; Kelly, J. W. (**2007**) Pharmacologic chaperoning as a strategy to treat Gaucher disease. *FEBS J., 274*: 4944-4950.

Ying, M.; Grimmer, S.; Iversen, T. G.; Van Deurs, B.; Sandvig, K. (**2003**) Cholesterol loading induces a block in the exit of VSVG from the TGN. *Traffic, 4*: 772-784.

Zhao, H.; Przybylska, M.; Wu, I.-H.; Zhang, J.; Siegel, C.; Komarnitsky, S.; Yew, N. S.; Cheng, S. H. (**2007**) Inhibiting glycosphingolipid synthesis improves glycemic control and insulin sensitivity in animal models of type 2 diabetes. *Diabetes, 56:* 1210-1218.

Zimmermann, P.; Schmidt, R. R. (**1988**) Synthese von erytro-Sphingosinen über Azidoderivate. *Liebigs Ann. Chem.:* 663-667.

Zimmermann, P.; Bommer, R.; Bär, T.; Schmidt, R. R. (**1988**) Azidosphingosine Glycosylation in Glycosphingolipid Synthesis. *J Carbohydr Chem., 7*: 435-452.

9. Abbreviations

$[\alpha]_D$	optical rotation
δ	chemical shifts (relative to the solvent) of ^{1}H or ^{14}C-NMR signal
λ	wave length
Ac	acetyl
Bu	butyl
CHAPS	3-[(3-cholamidopropyl)dimethylammonio]-1-propanesulfonate
DEAE	diethylaminoethyl
DMF	dimethylformamide
DMEM	Dulbecco's modified Eagle's medium
ESI-MS	electrospray ionization mass spectrometry
ER	Endoplasmic reticulum
F_P	melting point
FAB-MS	fast atom bombardement mass spectrometry
Gal	galactose
GalNAc	*N*-Acetyl-D-galactosamine
GalNAc-T	*N*-Acetyl-D-galactosaminyl transferase
Glc	glucose
GSL	glycosphingolipids
HEPES	*N*-2-Hydroxyethylpiperazine-*N*-2-ethansulfoic acid
Hz	Hertz
$^{x}J_{y,z}$	coupling constant
MEM	minimal essential medium
mNBA	meta-nitrobenzyl alcohol
MS	mass spectrometry
NMR	nuclear magnetic resonance
NMRI	Navy Marine Research Institute
PBS	phosphate buffered saline
THF	tetrahydrofuran
tBu	*Tert*-Butyl
TLC	thin layer chromatography

Triton	TritonX-100 (polyethylene glycol p-(1,1,3,3-tetramethylbutyl)-phenyl ether)
UDP	Uridine 5'-(trihydrogen diphosphate)
GlcT	Glucosyltransferase
GalT I	Galactosyltransferase I
GalT II	Galactosyltransferase II
SAT I	Sialyltransferase I, ST3Gal V
SAT II	Sialyltransferase II, ST8Sia I
SAT III	Sialyltransferase III, ST3Sia V
SAT IV	Sialyltransferase IV, ST3Gal I
SAT V	Sialyltransferase V, ST8Sia III
SAT X	Sialyltransferase X, ST8Sia II

10. Nomenclature of glycosphingolipids

Glycosphingolipids are named according to commonly used nomenclature that is introduced by Svennerholm (Svennerholm, 1963; IUPAC-IUB, 1998).

Cer	ceramide, *N*-Acylsphingosine
GlcCer	Glcβ1Cer
GalCer	Galβ1Cer
LacCer	Galβ1,4Glcβ1Cer
Gb3	Galα1,4Galβ1,4Glcβ1Cer
Gb4	GalNAcβ1,3Galα1,4Galβ1,4Glcβ1Cer
GA2	GalNAcβ1,4Galβ1,4Glcβ1Cer
GA1	Galβ1,3GalNAcβ1,4Galβ1,4Glcβ1Cer
GM1b	NeuAcα2,3Galβ1,3GalNAcβ1,4Galβ1,4Glcβ1Cer
GD1c	NeuAcα2,8NeuAcα2,3Galβ1,3GalNAcβ1,4Galβ1,4Glcβ1Cer
GD1α	NeuAcα2,3Galβ1,3(NeuAcα2,6)GalNAcβ1,4Galβ1,4Glcβ1Cer
GM3	NeuAcα2,3Galβ1,4Glcβ1Cer
GM2	GalNAcβ1,4(NeuAcα2,3)Galβ1,4Glcβ1Cer
GM1a	Galβ1,3GalNAcβ1,4(NeuAcα2,3)Galβ1,4Glcβ1Cer
GD1a	NeuAcα2,3Galβ1,3GalNAcβ1,4(NeuAcα2,3)Galβ1,4Glcβ1Cer
GT1a	NeuAcα2,8NeuAcα2,3Galβ1,3GalNAcβ1,4(NeuAcα2,3)Galβ1,4Glcβ1Cer
GT1α	NeuAcα2,3Galβ1,3(NeuAcα2,6)GalNAcβ1,4(NeuAcα2,3)Galβ1,4Glcβ1Cer
GD3	NeuAcα2,8NeuAcα2,3Galβ1,4Glcβ1Cer
GD2	GalNAcβ1,4(NeuAcα2,8NeuAcα2,3)Galβ1,4Glcβ1Cer
GD1b	Galβ1,3GalNAcβ1,4(NeuAcα2,8NeuAcα2,3)Galβ1,4Glcβ1Cer
GT1b	NeuAcα2,3Galβ1,3GalNAcβ1,4(NeuAcα2,8NeuAcα2,3)Galβ1,4Glcβ1Cer
GQ1b	NeuAcα2,8NeuAcα2,3Galβ1,3GalNAcβ1,4(NeuAcα2,8NeuAcα2,3)Galβ1,4Glcβ1Cer
GQ1bα	NeuAcα2,3Galβ1,3(NeuAcα2,6)GalNAcβ1,4(NeuAcα2,8NeuAcα2,3)Galβ1,4Glcβ1Cer
GT3	NeuAcα2,8NeuAcα2,8NeuAcα2,3Galβ1,4Glcβ1Cer
GT2	GalNAcβ1,4(NeuAcα2,8NeuAcα2,8NeuAcα2,3)Galβ1,4Glcβ1Cer
GT1c	Galβ1,3GalNAcβ1,4(NeuAcα2,8NeuAcα2,8NeuAcα2,3)Galβ1,4Glcβ1Cer
GQ1	NeuAcα2,3Galβ1,3GalNAcβ1,4(NeuAcα2,8NeuAcα2,8NeuAcα2,3)Galβ1,4Glcβ1Cer
GP1c	NeuAcα2,8NeuAcα2,3Galβ1,3GalNAcβ1,4(NeuAcα2,8NeuAcα2,8NeuAcα2,3)Galβ1,4Glcβ1Cer
GP1cα	NeuAcα2,3Galβ1,3(NeuAcα2,6)GalNAcβ1,4(NeuAcα2,8NeuAcα2,8NeuAcα2,3)Galβ1,4Glcβ1Cer
GM4	NeuAcα2,3Galβ1Cer